How Manipulating Oxygen and Iron Availability Affects Tregs and the Immune System

Marie Sion

Supervised by Fadi Issa and Joanna Hester

Thesis submitted for the degree of Doctor of Philosophy
Vacation Term 2023

TABLE OF CONTENTS

ABSTRACT

Regulatory T cells (Tregs) are essential for maintaining immune balance, failure of which can result in infections, cancer, autoimmunity, or chronic inflammation. Hypoxia and hypoferremia are common features of inflammatory microenvironments, but their effect on Tregs is poorly understood. In this thesis, I investigate how manipulating oxygen and iron availability affects Tregs and the immune system. Firstly, I examine how hypoxia and HIF signalling affects Treg and immune biology using hypoxia-treated mice lacking specific genes of the hypoxia pathway to reveal a complex interplay between different HIF isoforms and subunits. I also investigate how hypoxia signalling alters Treg transcription using single cell and bulk RNA sequencing, revealing a role for the p38 MAPK-NFkB signalling pathway and an association between CD25 loss and increased CD22-Notch1 signalling in Tregs. To examine how iron biology impacts Tregs, I use an *in vitro* iron deprivation model to show that Tregs appear more resistant to hypoferremia than conventional T cells. I show that cell-intrinsically iron-deprived Tregs are suppressive *in vitro* but not *in vivo*, and that the Treg:Teff ratio favours Tregs (and consequently tolerance) in models using mixed bone marrow chimeras and malaria infection. Finally, I investigate how iron limitation impacts graft survival in a skin transplantation model, showing that iron deprivation can restrain alloresponses and rejection. The work presented here provides a deeper understanding of the mechanisms that regulate Treg function and uncovers areas for potential therapeutic applications in all diseases arising from immune imbalance.

GLOSSARY

ADP	Adenosine diphosphate
AHR	Aryl hydrocarbon receptor
AICD	Activation-induced cell death
AIRE	Autoimmune regulator
ALS	Autoimmune lateral sclerosis
AMP	Adenosine monophosphate
ANA	Antinuclear antibodies
APC	Antigen presenting cell
ARNT	Aryl hydrocarbon receptor nuclear translocator
ATP	Adenosine triphosphate
BCR	B cell receptor
BMP	Bone morphogenic protein
CAD	C-terminal transactivator domain
CAR	Chimeric antigen receptor
cAMP	Cyclic adenosine monophosphate
CBP	CREB binding protein
CREB	cAMP response element binding protein
ChIPseq	Chromatin immunoprecipitation sequencing
CODDD	C terminal of oxygen dependent degradation domain
CTLs	Cytotoxic T lymphocytes
CTLA-4	Cytotoxic T lymphocyte-associated protein 4
DAMPs	Damage-associated molecular patterns
DC	Dendritic cell
DCYTB	Duodenal cytochrome B
DKO	Double knock out
DMT	Divalent metal transporter
EAE	Experimental autoimmune encephalitis
EPO	Erythropoietin
FBLX5	F-box leucine-rich repeat protein 5
FIH	Factor inhibiting HIF
Foxp3	Forkhead box P3
GC	Germinal centre
GDF15	Growth differentiation factor 15
GITR	Glucocorticoid-induced TNFR related
GMP	Good manufacturing protocol
GM-CSF	Granulocyte/macrophage colony stimulating factor

Gstm5	Glutathione S-transferase mu 5
GVHD	Graft versus host disease
HAF	Hypoxia associated factor
HIF	Hypoxia inducible factor
HFE	High Fe^{2+}
HRE	Hypoxia responsive element
Hsp	Heat shock protein
IBS	Inflammatory bowel syndrome
ICOS	Inducible T cell co-stimulator
IDO	Indoleamine 2,3 dioxygenase
IFN	Interferon
Ig	Immunoglobulin
IKK	Ikappa B kinase
IL	Interleukin
IPEX	Immune dysregulation, polyendocrinopathy, enteropathy, X-linked
IRE	Iron responsive element
IRI	Ischaemia reperfusion injury
IRP	Iron regulatory protein
Itk	IL-2-inducible T cell kinase
iTreg	Induced Treg
JAK	Janus kinase
KD	Knockdown
KIR	Killer Ig-like
KO	Knock out
LAG3	Lymphocyte activation gene 3
LAP	Latency associated peptide
LDH	Lactate dehydrogenase
LPS	Lipopolysaccharide
LSP1	Lymphocyte specific protein 1
MAPK	Mitogen-activated protein kinase
MDSCs	Myeloid-derived suppressor cells
MHC	Major histocompatibility complex
MS	Multiple sclerosis
mTEC	Medullary thymic epithelial cells
mTOR	Mechanistic target of rapamycin
mTORC	Mammalian target of rapamycin complex
NFAT	Nuclear factor of activated T cells
NFkB	Nuclear factor kappa-light-chain-enhancer of activated B cells
NIK	NFkB inducing kinase

NK cell	Natural killer cell
NODDD	N terminal of oxygen dependent degradation domain
PAMPs	Pathogen-associated molecular patterns
PAS	Period-ARNT-Single minded
PBMC	Peripheral blood mononuclear cells
PDK1	3-phosphoinositide-dependent protein kinase 1
PHD	Prolyl hydroxylase domain
PhD	Permanent head damage
PI3K	Phosphoinositide 3 kinase
PTEN	Phosphatase and tensin homologue deleted on chromosome 10
pTreg	Peripheral Tregs
RACK1	Receptor of activated protein C kinase 1
REDD1	Regulated in development and DNA damage response 1
RORγT	Receptor-related organ nuclear receptor γ T
ROS	Reactive oxygen species
scRNAseq	Single cell RNA sequencing
shRNA	Short hairpin RNA
SLE	Systemic lupus erythematosus
SMAD	Small mothers against decapentaplegic
STAT	Signal transducer and activator of transcription
TCR	T cell receptor
TGF	Transforming growth factor
TIM3	T cell immunoglobulin 3
TLR	Toll-like receptor
Tconv	Conventional T cells
Teff	Effector T cells
Tfrc	Transferrin receptor
Th cells	Helper T cells
TIGIT	T cell immunoglobulin and immunoreceptor tyrosine-based inhibitory motif
TNF	Tumour necrosis factor
TRAIL	TNF-related apoptosis inducing ligand
Treg	Regulatory T cells
TSDR	Treg-specific demethylation region
tSNE	t-distributed stochastic neighbour embedding
UMAP	Uniform manifold approximation and projection
VEGF	Vascular endothelial growth factor
VHL	Von Hippel Lindau
VPD	Violet proliferation dye

1 – INTRODUCTION

1.1 – BALANCE IN IMMUNITY

1.1a – CANCER AND INFECTIONS

The immune system evolved over many millennia to protect us from pathogens and malignant mutations. Many redundancies are built into it at a huge energetic cost: 10^9 new immune cells are created from the bone marrow daily, many of which do not survive due to the randomness of VDJ recombination producing non-functional B and T cell receptors which must then be deleted. Even the redundancy of creating two parallel adaptive systems which are antigen-specific alongside the broader approach of the adaptive system is very energetically demanding. And yet, the existence of this expensive complexity demonstrates its importance and reflects the evolutionary pressure placed on us by equally adaptable pathogens and cellular dysfunctions. Unsurprisingly, those with either primary (inherited) or secondary (caused by disease, immunosuppressive drugs, or environmental factors) immunodeficiencies often face lethality without intervention.

The innate immune system is adept at recognising abnormal patterns such as tissue damage and barrier organ breakdown that could open the door for invading pathogens, and patterns more specific to pathogens themselves such as cytosolic DNA, lipopolysaccharides (LPS), and other proteins found in bacterial cell walls and flagella through damage- and pathogen-associated molecular patterns (DAMPs and PAMPs)[1]. Cytokine release and complement activation as well as antigen presentation help alert the adaptive immune system to potential danger, and these then contribute antigen-specific cellular and humoral killing alongside the phagocytic activities of the innate system. Phagocytosis, complement-induced membrane attack complexes, granzyme and perforin production, and apoptosis induction via Fas/FasL signalling are just some of the powerful weapons the immune system wields against pathogenic and malignant threats[1]. NK cells recognise and eliminate both infected and malignant cells through their expression of killer Ig-like receptors (KIRs) that bind major histocompatibility complex (MHC) class I and provide inhibitory signals, and thus MHC shedding in abnormal cells is recognised by NK cells as an important part of immunosurveillance[2,3].

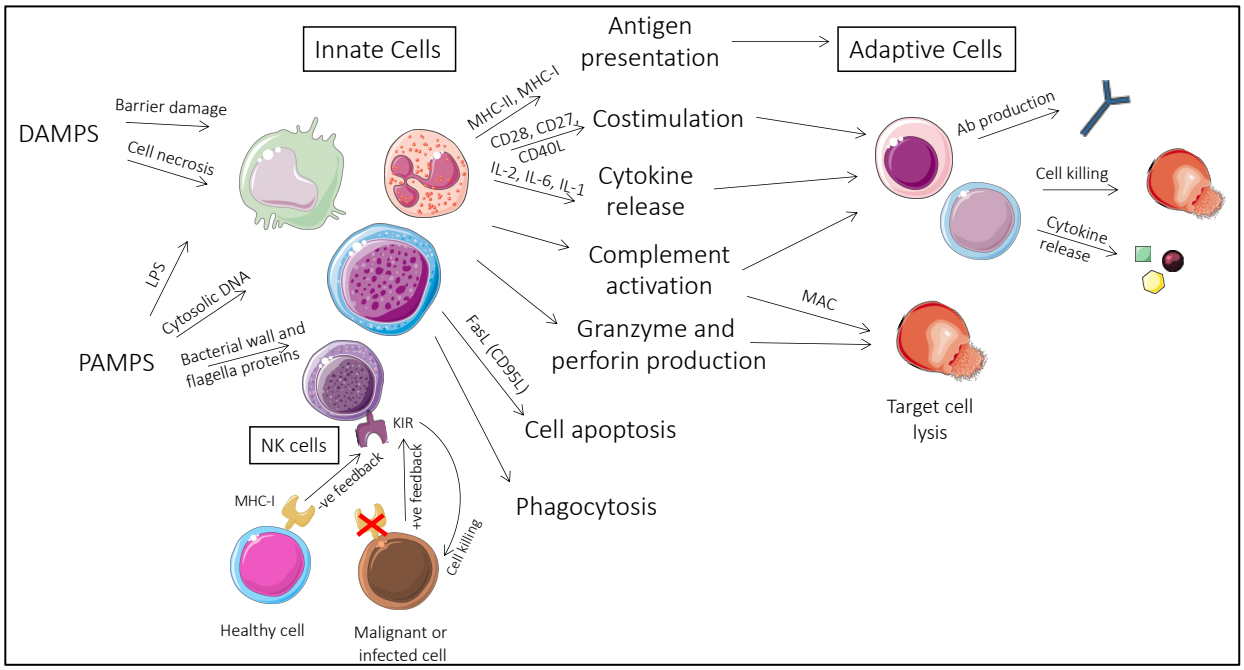

Fig 1.1 – Overview of innate immunity. DAMPs such as barrier damage and cell death, and PAMPS specific to bacterial and viral structures activate innate immune cells. In turn, these present antigens on MHC (signal 1), provide costimulation (signal 2), produce cytokines (signal 3), and produce complement that activate adaptive cells. Complements leading to membrane attack complex (MAC), and granzyme and perforin release lead to lysis of target cells, as does expression of FasL for apoptosis, and phagocytosis of extracellular bacteria and infected cells. NK cells also detect lack of MHC-I on infected and malignant cells which don't provide inhibitory signals to KIRs on NK cells.

The concept of immunosurveillance was first proposed in 1957[4], and as cancerous cells cannot be recognised by non-self characteristics in the same way invading pathogens can, they provide additional challenge to the immune system. Nonetheless, the immune system is quite adept at killing malignant cells; immunoediting is a hallmark of cancer[5], and most successful tumours either recruit suppressive cells such as Tregs and myeloid-derived suppressor cells (MDSCs), or express co-inhibitory checkpoints and soluble anti-inflammatory cytokines to inhibit and exhaust infiltrating leukocytes[6]. Immune checkpoint therapy has been the biggest advance in cancer therapy[7] and much of ongoing cancer research focuses on immunotherapy, which is unsurprising when considering how powerful the immune system is in fighting both cancer and infections.

1.1b – Immunopathology and Allergy

While the immune system's cytotoxic capabilities are essential to survival and provide crucial protection, the mechanisms that allow it to kill dangerous cells and pathogens can sometimes also unnecessarily damage healthy tissues. An example of this collateral damage is immunopathology, where the inflammatory and cytotoxic responses to a pathogen cause damage to the surrounding tissue. This happens in infections, and sometimes the immune response rather than the infectious agent is responsible for the main symptoms of the disease. This is the case in infections such as West Nile, Dengue, and polio viruses[8]. The damage can be cell-mediated, such as the deadly vascular leakage that occurs in the small minority of 50 million people infected with Dengue virus, which is thought to be caused by cross-reactive T cells, or by cytokine damage which is central to much immunopathology[8]. This was also the case in COVID-19 infections, where much of the pathology of severe cases was driven by cytokine storm and exuberant IL-6 production[9–11], which is congruent with observing severe cases in otherwise young and healthy patients with active immune systems. Other infections have similar phenomena where most suffer mild disease, but rare cases of severe infection are caused by immunopathology when appropriate tolerance mechanisms are not upheld[8].

Normal infections are met with acute expansion of the immune compartment and cytokine production, but regulatory cell compartments expand alongside this to control these responses. Tregs expand dynamically at early and later timepoints in cytotoxic T lymphocyte (CTL)

expansion in order to keep up with and control initial inflammation, and later to induce resolution[12], and IL-10 production by Tregs has also been shown to induce memory cell formation[13]. Resolution requires inhibiting neutrophil extravasation to stop leukocyte accumulation in tissues, and macrophage reprogramming toward efferocytosis to clear apoptotic debris[14]. The resolution phase of inflammation requires soluble mediators such as lipoxins, resolvins, and protectins, as well as anti-inflammatory cytokines such as IL-10 and transforming growth factor ß (TGFβ)[14]. Failure to initiate this resolution programme can cause acute infections to persist and morph into chronic inflammation[15], and diseases such as colitis and Crohn's disease are associated with impaired production of such mediators like annexin A1 and lipoxin A4[16–18].

The main symptoms of chronic inflammation are often driven by immunopathological damage. These low-grade inflammatory diseases are becoming more common, especially in affluent countries where sedentary lifestyles, obesity, and high-fat diets are prevalent, as this contributes to ROS production in diseases such as atherosclerosis[19,20]. Irritable bowel syndrome (IBS) is another disease characterised by chronic inflammation, and although its aetiology is complex and poorly understood, a strong immunopathology component is suspected[21], with links to increased T cell activation in the bowel established[22]. Other complex diseases with unknown causes such as Alzheimers[23] and cardiovascular disease[24] have immune contributions as well, so immunopathology is likely to be an active participant in a wide range of diseases.

Aberrant immune-driven damage is also seen in the context of allergies, which are inappropriate responses to innocuous antigen that can sometimes be life-threatening. Most allergies are driven by IgE linking to already sensitised mast cells and basophils, causing degranulation and the release of histamines and prostaglandins responsible for liquid discharge and muscle contraction which, in serious cases, can lead to anaphylaxis. Despite being inconvenient at best and fatal at worst, IgE is highly evolutionarily conserved, and has been suggested to have evolved to protect us from ancient and dangerous allergens that we no longer face[25], although it is still useful against parasites. Despite having little evolutionary advantage, allergies remain on the rise in line with the hygiene hypothesis[26], especially with increased urbanisation which is seeing a rise in allergy and autoimmunity[27].

1.1c – Autoimmunity and Loss of Tolerance

A consequence of unresolved infections and a friend to chronic inflammation is autoimmunity, whereby the immune system is autoreactive and treats the body's own cells to the same damage intended for harmful pathogens. Many diseases such as rheumatoid arthritis and type I diabetes which were both first identified in the 1800s[28,29] have been recently discovered to have autoimmune drivers. Autoimmunity can be driven by humoral factors (B cell production of autoantibodies that target self-antigens), or cellular factors, driven by aberrant T or myeloid cell pathogenicity. Autoimmune diseases are often driven by Th17 cells, which are also important in neutrophil recruitment in infections[30], but seem to have a special association with autoimmunity[31,32]. It is unclear why they drive this propensity to autoimmunity, but inhibiting their IL-17 production seems to curb autoimmune induction and disease[33–35], and IL-17 production is generally restricted to Th17 cells. Another odd association of autoimmunity is with sex-restriction, in that women are up to four times more likely than men to develop autoimmune disease[36]. The reasons behind this are still obscure, and factors such as X chromosome gene expression and hormonal differences have been proposed, as have higher levels of baseline circulating antibody in women which may have evolved to protect offspring during pregnancy and breastfeeding[36], but these reasons are still unclear.

While autoimmunity is not uncommon, and we are finding autoimmune components to more and more diseases that traditionally were not suspected to be of immune origin, there are many systems in place to prevent it; these are essentially tolerance, which informs the immune system of what constitutes the self – which is not to be harmed – so that this important distinction can be made. The breakdown of tolerance is what leads to autoimmunity. Educating the immune system in tolerance is crucial to counteract the equally essential randomness built into the adaptive immune system, which allows us the adaptability to co-evolve with equivalently versatile pathogens.

1.1d – Mechanisms of Tolerance

As T and B cell receptors are created randomly, many of them have the capacity to recognise self-antigen and initiate autoimmunity. Tolerance is the process that prevents this, and can be split into central and peripheral arms, although it is increasingly recognised that these responses exist on a spectrum. Central tolerance oversees T and B cell development at early stages of their maturation, and peripheral tolerance is a longer standing process in the peripheral and lymphoid tissues that helps maintain it and contend with any possible slips into autoimmunity that, as discussed above, can arise from infection and inflammation. Receptor editing of immature B cells in the bone marrow[37] and negative selection of autoreactive developing T cells in the thymus[38] make up the core of central tolerance, and during development both cell types also undergo positive selection to ensure that the randomly assorted B and T cell receptors (BCR and TCRs) are capable of tonic signalling (and MHC binding, in the case of TCRs).

Any antigens that developing B cells encounter in the bone marrow are bound to be self-antigens, but instead of deleting any self-reactive BCRs, receptor editing allows them to be recycled and try editing remaining available light chain segments to try to produce a non-autoreactive BCR[37,39]. Failure to achieve this leads to clonal deletion or anergy. T cells do not have such editing flexibility, so they are exposed to a much wider selection of self-antigen thanks to expression of the transcription factor AIRE on medullary thymic epithelial cells (mTECs) and dendritic cells (DCs) in the thymic medulla, which allows promiscuous expression of self-antigens. Excessive thymocyte binding strength leads to apoptosis of the potentially self-reactive T cells, while intermediate strength of binding induces Tregs[38], which play an important role in maintaining peripheral tolerance.

Peripheral tolerance recovers any cells that slipped through the cracks of central tolerance. T cells require costimulation and cytokine signalling during TCR ligation, absence of which leads to anergy. This ensures that they only respond as part of a concerted immune response in which the cells around them have also identified a discernible threat, which forms the basis of peripheral tolerance. CD28 signalling represses Foxp3 expression[40], and lack of it and

other costimulation induces anergy. Enhanced coinhibitory signalling from regulatory cell populations such as Tregs and tolerogenic DCs, which also produce anti-inflammatory cytokines, also lead to anergy and can induce apoptosis via Fas and Bim signalling[41]. TGFβ in the periphery can also induce peripheral Tregs by inducing Foxp3 expression in an IL-4 dependent manner[40], and thymic Tregs are capable of orchestrating infectious tolerance by delivering surface TGFβ to surrounding T cells[42]. Thus, autoreactive T cells acting without appropriate backup can be converted to pTregs, whereby the self-reactive TCR that could have been pathogenic instead becomes protective.

Central tolerance reduces the percentage of autoreactive B cells from ~75% down to ~40%, and this drops down to 20% when immature B cells first encounter the periphery and are very sensitive to activation-induced cell death (AICD), ensuring that autoreactive B cells that react to tissue antigens they encounter as soon as they emerge from the bone marrow are deleted[43]. However, new autoreactive clones can be created *de novo* in the periphery via somatic hypermutation: upon activation in germinal centres, the activation induced deaminase enzyme creates individual C:G → U:G substitutions in the variable region of the BCR gene[44], which allows low-affinity BCRs to acquire better specificity for antibody affinity finetuning in real time. This does run the risk of mutating a safe BCR clone into an autoreactive one, and this is associated with antinuclear antibody production in systemic lupus erythematosus (SLE)[45]. Consequently, peripheral tolerance must control autoreactive B cells of both germline and mutational origin[45]. In line with two-signal activation, remaining autoreactive B cells that escape Fas and Bim-mediated apoptosis but who do not receive T cell help will become anergic, and persist but remain functionally unresponsive[43]. While reversibly dysfunctional self-reactive B cells may seem like a liability, their cross-reactivity to potential pathogens makes them worthwhile[43], and they also play a role in maintaining T cell tolerance as well, as anergic B cells have been shown to promote Tregs in the periphery[46].

1.2 – REGULATORY T CELLS

1.2a – PHENOTYPE AND MARKERS

Considering the possible danger that excessive immune activation poses, especially in light of its great flexibility, having a dedicated cell population to police immunity is advantageous. A suppressive T cell population was first theorised in the late 1960s when thymectomy and adoptive transfer experiments indicated that a T cell population existed that conferred tolerance[47,48], but it remained elusive for another quarter of a century. The seminal discovery of CD25 by Sakaguchi allowed us to identify this suppressive T cell population. They found that antibody depletion of $CD25^+$ cells induced autoimmunity[49], and subsequent studies further confirmed suppressive function to define Tregs, usually based on *in vitro* suppression or autoimmune consequences of their depletion[50–52]. Absence of Tregs in humans also leads to autoimmunity in a fatal disease called immune dysregulation, polyendocrinopathy, enteropathy, X-linked (IPEX)[53].

The discovery of the transcription factor Foxp3 as the master regulator of Tregs[54,55] allowed further forays into Treg research. Forced retroviral expression into naïve T cells can confer a suppressive phenotype onto them[56], indicating that Foxp3 is sufficient for Treg function. Foxp3 can activate genes responsible for Treg signature and function such as CD25, cytotoxic T lymphocyte-associated protein 4 (CTLA-4), and transforming growth factor ß (TGFβ), while repressing others such as IL-2 and interferon gamma (IFNγ), and transcription factors associated with other T helper phenotypes[57]. Chromatin immunoprecipitation sequencing (ChIPseq) in human Tregs identified Foxp3 interaction with other transcription factors important for T cell development, including AP-1, nuclear factor of activated T cells (NFAT), Runx family transcription factors, and a specially enriched interaction with signal transducer and activator of transcription (STAT)5[58]. Interestingly, only 23% of human Foxp3 targets were shared by mice[58], indicating species-specific functions of Foxp3 despite very similar phenotypes observed when it is lost in IPEX patients or Scurfy mice[53,54].

Foxp3 is the best marker for identifying Tregs, as although CD25 is very useful for identifying Tregs in mice, it is transiently upregulated on Tconvs during activation in humans[59], making it difficult to identify Tregs on the basis of CD25 alone in humans. Nevertheless, Foxp3 too can be transiently upregulated upon activation without conferring suppressive function in humans[60–62], so it remains context and activation dependent and may be similar to Tconv acquisition of coinhibitory markers during activation. These differences between mice and men may be reflective of the differences observed in Foxp3 transcription targets and control between these species[58]. The observation that Tregs express lower levels of the IL-7 receptor CD127[63] made it much easier to isolate human Tregs using surface markers, and $CD4^{+}CD25^{+}CD127^{lo}$ is a good surface phenotype for Tregs that correlates well with Foxp3 expression and function.

There are a multitude of other markers that are commonly expressed on Tregs, and which correlate with various aspects of their function in different ways. Most of these are coinhibitory surface markers, but Helios is a transcription factor which is quite important for Tregs. It was originally thought to differentiate natural (nTregs) from peripheral (pTregs)[64], and although this hasn't been supported, Helios is correlated with Treg suppression and stability[65], although it does not seem to drive these[66]. Interestingly, CD4 or Foxp3-restricted knockout of Helios did not affect development, but $Foxp3^{Cre}Helios^{fl/fl}$ mice developed late onset autoimmunity after several months of age[66,67]. ChIPseq of Helios knockout Tregs revealed decreased Foxp3, CD25, and IL-2-driven STAT5, and an increase in Caspase3 in $Helios^{-}$ Tregs[67], and it was proposed that Helios might contribute to Treg stability in a STAT5-dependent manner[66].

Surface coinhibitory markers are important for immune regulation and especially for controlling T cells; their expression is usually upregulated on Tconvs as part of their activation which helps moderate activation responses, and coinhibitory markers are also associated with exhaustion and anergy, especially in the context of cancer. Although coinhibitor expression is not restricted to Tregs, it can be used to help identify and define them. On Tregs, lymphocyte activation gene 3 (LAG3) inhibition abrogates their suppressive function, and ectopic transfer of it confers suppression onto Tconvs[68]. LAG3 also represses Myc expression which is normally kept low in Tregs to suppress anabolism[69]. T cell immunoglobulin 3 (TIM3) is associated with controlling type I and Th1-driven immune responses[70], and is associated with peripheral tissue infiltration[68]. Coinhibitory markers such as these are built into the control of T cell activation and

provide balance to counteract the costimulation they may receive, so expression of such molecules is often associated with activated Tregs as it correlates with their suppressive function and even helps stabilise them[71]. Tregs also constitutively express costimulatory molecules such as OX40, glucocorticoid-*i*nduced TNFR related (GITR), and 4-1BB at much higher levels than Tconvs, and these are often used to help define Tregs, but they also allow them to outcompete Tconvs for costimulatory ligands and thus contribute to Treg suppressive function[72]. However, excessive signalling through these costimulatory molecules indicates that strong costimulation is being presented by antigen presenting cells (APCs) and may reflect a genuine threat requiring immune intervention, so signalling downstream of such molecules is detrimental to Treg suppressive function[73,74] in order to allow appropriate placation of Tregs when immune responses are genuinely required.

1.2b – Mechanisms of Regulation

Tregs employ a diverse selection of approaches in their suppression, which allows for multi-faceted immune regulation and finetuning of their suppression to adapt to contextual cues. Their suppression is usually categorised as either contact-dependent, which is mediated via expression of surface markers and their interaction with their ligands, or contact independent, which relies on the release of soluble factors and cytokines. Some of the co-inhibitory markers discussed above are directly responsible for Treg suppression, and other classic coinhibitory ligands such as PD-L1 expressed on Tregs can directly ligate PD-1 on Tconvs to suppress them[72,75]. However, most of their contact-dependent suppression actually involves interaction with DCs and APCs: CTLA-4 has up to 100-fold higher affinity for costimulatory ligands CD80/86 than CD28 due to its kinetics[76], so high expression of CTLA-4 on Tregs effectively robs Tconvs of the CD28-mediated signal 2 they require and thus impair their activation. Not only that, but the frequent endocytosis of CTLA-4 can allow it to actually remove CD80/86 off the surface of APCs and internalise them within Tregs[77], so that these costimulatory molecules are not simply kept occupied and unavailable for Tconvs but actively absent. Treg-specific knockout of CTLA-4 induces fatal autoimmunity[78]. TIGIT acts similarly to outcompete CD226 for its ligand CD155 and trogocytose CD155[68]. LAG3 is also a high-affinity competitor for MHC-II and thus can outcompete CD4 binding, but it also negatively affects other cell types by impairing DC maturation[68,79].

Contact-dependent mechanisms of suppression from Tregs can also include cytolysis, which is not normally a feature of $CD4^+$ helper cells. Expression of TNF-related apoptosis inducing ligand (TRAIL) on Tregs can induce apoptosis on target cells expressing its receptor death receptor 5[80], and apoptosis can also be instigated through Fas-FasL signalling[81]. Tregs can also kill target cells via perforin and granzyme A/B mechanisms commonly associated with CD8 and NK cell cytotoxicity[79].

Tregs can suppress in contact-independent ways by acting as metabolic disruptors. The surface-expressed ectoenzyme CD39 can hydrolyse adenosine triphosphate (ATP) to adenosine di- or monophosphate (ADP or AMP), thus depriving cells of extracellular ATP for energy[82]. Furthermore, CD73 on Tregs can further degrade AMP to adenosine which signals through the A2A receptor to raise intracellular cyclic AMP levels in DCs and T cells, thus repressing IL-2 and IL-4 signalling via activation of the inducible cAMP early repressor[82]. Signalling via A2A receptors has been shown to induce new peripheral Tregs[83], and Tregs can also deliver cyclic AMP to cells directly via gap junctions[82]. Tregs can induce DC expression of Indoleamine 2,3 dioxygenase (IDO), a potent immunosuppressive enzyme that catabolises tryptophan to deplete amino acid availability and conveniently produces suppressive pro-apoptotic metabolites[84].

Regarding contact-independent suppression, the CD25 molecule so central to Treg discovery is also of importance: CD25 is the alpha chain of the IL-2 receptor, and although not required for signalling, its inclusion in the trimeric form of the receptor greatly increases its affinity for IL-2[68]. This is thought to allow Tregs to rob Tconvs of their IL-2 by acting as an IL-2 sink[79], which is reminiscent of some of the other mechanisms described above. The role of CD25 as a mechanism of suppression rather than survival has been questioned, as Tregs are heavily reliant on IL-2 for survival and do not produce it themselves, but its role in cytokine deprivation-mediated apoptosis favours CD25 as a mediator of Treg function[79,85]. Additionally, Tregs have been known to produce soluble CD25 which is immunosuppressive[86] and does not provide the Tregs with any import or survival advantage, suggesting that it is more than just a survival mechanism. When considering the importance of IL-2 as a “signal 3” factor for T cell activation and Tregs’ tendency to hoard other sources of costimulation, it is hard to imagine that the first defining marker of Tregs – by nature mostly restricted to them – would not lead to IL-2 starvation and hence suppression.

As well as cytokine hoarding, Tregs also produce anti-inflammatory cytokines, namely TGFβ, IL-10, and IL-35. The IL-10 receptor signals downstream through Jak/STAT signalling pathways to inhibit NFkB signalling, IFNγ and chemokine production, and MHC-II and CD80/86 on APCs[87]; T cell activation in the presence of IL-10 can also induce anergy[87]. TGFβ tends to signal via small mothers against decapentaplegic (SMADs) and can inhibit proliferation via inhibition of growth promoting transcription factor Myc, as well as induce apoptosis, autophagy, and senescnence[88]. Loss or inhibition of TGFβ leads to loss of suppressive function *in vitro* and autoimmunity *in vivo*[82,89]. TGFβ can also be tethered to latency associated peptide (LAP) on the cell surface of activated Tregs, and thus be used contact-dependently too[79], which has been shown to be important in suppressing NK cells[90] and also involved in contact-dependent induction of infectious tolerance[82]. IL-35, although more recently discovered and less intently studied, has been shown to suppress proliferation and cytokine production but also to play a key role in infectious tolerance[82,91].

As well as being directly suppressive, IL-10, TGFβ, and IL-35 can also induce pTregs under the right circumstances, which is essential to maintaining peripheral tolerance and adds a layer of ingeniousness to Treg suppression; indeed, not only does this recruit new Tregs for backup, but it also reduces the population of active Tconvs needing to be suppressed, a very efficient two-fold tactic also seen in their use of adenosine and tryptophan. TGFβ-induced SMAD3 can complex with other transcription factors to form an enhanceosome in the promoter of Foxp3[92] and has epigenetic effects in the SMAD region as well[92]. Although commonly used for inducing Tregs *in vitro*, TGFβ is not able to induce the transcriptional signatures and Foxp3 stability of true Tregs, and their suppression is variable, which makes iTregs a suboptimal choice for therapies[93]. IL-10 and TGFβ help maintain the stability of tTregs, especially in the presence of other polarising and proinflammatory cytokines like IFNγ and IL-4[79], but Treg phenotype and stability *in vivo* is incredibly context dependent.

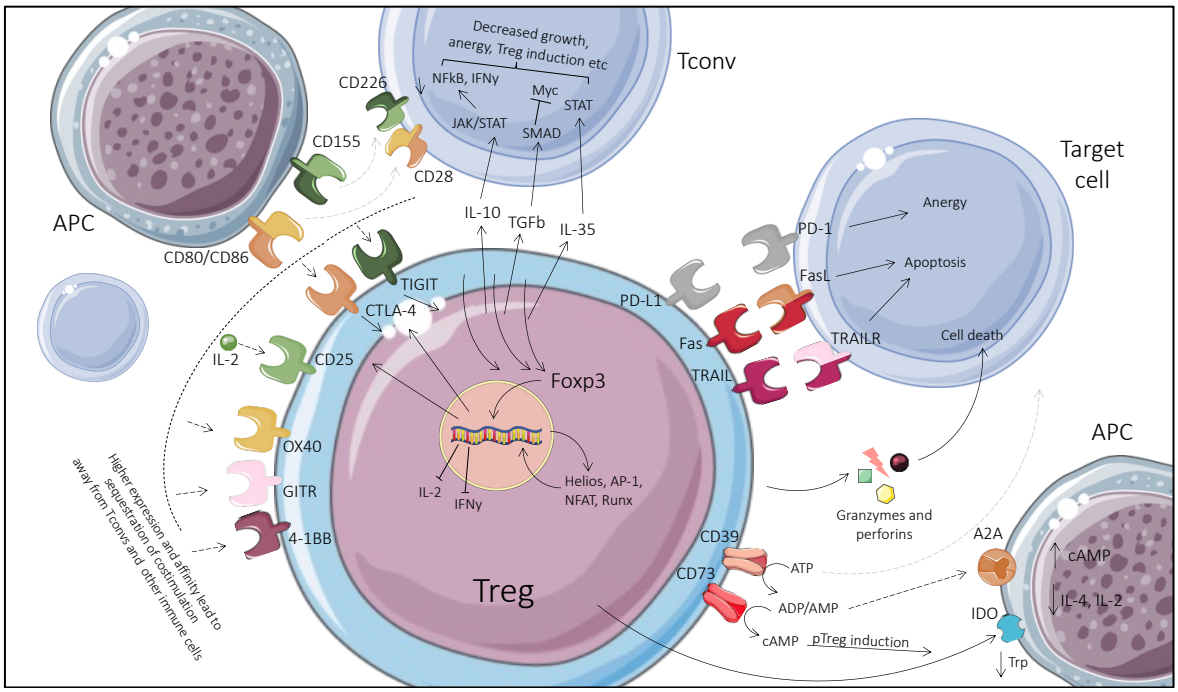

Fig 1.2 – Schematic overview of Treg expression and suppression mechanisms. As shown by the curved dotted line, other cells are preferentially deprived of costimulation due to Tregs' higher expression of costimulatory markers OX40, GITR, 4-1BB, and CD25 which hoards IL-2 away from other immune cells. Additionally, CTLA-4 and TIGIT have higher affinity for costimulatory ligands CD80/CD86 and CD155 on APCs than their native, lower affinity receptors CD28 and CD226 respectively, expressed on Tconvs, and can even trogocytose them off the surface of APCs to remove them as costimulation for other cells. Tregs also secrete anti-inflammatory cytokines TGFβ, IL-10, and IL-35, which result in SMAD signalling and decreased Myc-induced proliferation, Jak/STAT inhibition of NFkB signalling, IFNγ and chemokine production, and MHC-II and CD80/86 on APCs[87], and STAT-induced inhibition of proliferation and cytokine production, respectively. These cytokines can also promote Foxp3 expression to induce new pTregs and maintain Treg stability. Tregs also use PD-L1, TRAIL, and Fas, and granzymes and perforins, to induce anergy and apoptosis of activated cells. CD39 deprives cells of extracellular ATP and produces tolerising ADP/AMP for APCs, and CD73 produces cAMP which can induce pTregs. Tregs can also induce IDO on APCs to lower extracellular tryptophan and disrupt cells' metabolic needs.

1.2c – Treg Stability and Polarisation to Other Th Cell Types

Although Tregs have a special functional role and a signature quite distinct to other $CD4^+$ T cell subsets, they could be considered just another specialised T helper subset. Indeed, Th subsets also have their own transcription factors, cytokines of choice, and specialisations[94] (*Table 1*), which one could argue are equivalent to Tregs' Foxp3, TGFβ/IL-10/IL-35, and suppressive function. However, Tregs are developmentally distinct and arise in the thymus in response to particular stimuli that differentiate them from regularly developing Tconvs, whereas other Th subtypes typically develop later in the periphery from $Foxp3^-$ Tconvs. Nonetheless, Tregs do have the flexibility to acquire varying degrees of characteristics from the other Th subsets, and even lose their Treg identity entirely and commit to another Th lineage[95].

Table 1 – T helper subsets:

T HELPER	TRANSCRIPTION FACTOR	CYTOKINES PRODUCED	INDUCED BY	IMMUNE SPECIALISATION	RECRUITS
Th1	T-bet	IFNγ	IFNγ, IL-12	Intracellular pathogens	Macrophages
Th2	GATA-3	IL-4, IL-5, IL-13	IL-4	Parasites, helminths	Eosinophils
Th17	RORγT	IL-17, IL-22	TGFβ, IL-6	Extracellular bacteria	Neutrophils

It has been proposed that acquiring semblance of other Th subsets may help Tregs become functionally specialised to control immune responses driven by that type of polarisation, and even enhance their suppression[95,96]. The acquisition of co-expressed Th transcription factor expression (alongside Foxp3) and Th-like characteristics allows Tregs to express the same chemokine receptors and colocalise to the same sites of inflammation as the helper T cells they are suppressing[95–97]. There seems to be a greater propensity for Tregs to favour Th17 over other Th lineages[98,99], which perhaps might be related to TGFβ's role in Th17 induction, and provides a very interesting balancing act between tolerance and autoimmunity.

Even temporarily losing suppressive function might be important for allowing necessary inflammatory responses, as we know from immunosuppressive drug regimens that inflexible immune suppression can lead to dangerous infections of malignancies, so Tregs integrate subtle context cues to refine their responses as needed. Various inflammatory signals can induce loss of suppressive function with or without loss of Foxp3 expression[100]. Methylation of conserved non-coding sequences (CNS) in the Foxp3 promoter are very important in maintaining its stability, namely CNS2, the Treg-specific demethylation region (TSDR)[101]. TGFβ-induced Tregs often lack TSDR demethylation[100], which contributes to their instability. Additionally, Foxp3 itself can form a complex to stabilise the TSDR, thus acting as a lineage-affirming feedforward loop[100]. Many factors can contribute to this variability in Treg plasticity, including mTOR signalling[102], retinoic acid[103], and STAT4[104], amongst others[105], so the role of Foxp3 and suppressive function is incredibly context dependent and the magnitude of all these signals likely dictates the extent to which Tregs maintain various aspects of their identity. This malleability is very important to the adaptability and duality that helps Tregs allow necessary responses to take place when needed, while also overseeing resolution and tolerance.

1.3 – Therapeutic Uses of Tregs

1.3a – Cellular Therapy

As discussed, the mechanisms that balance protective immune responses and tolerance are complex and delicate, and their dysregulation in either direction leads to disease. Intolerance in autoimmunity or the less natural scenarios of transplant rejection and graft versus host disease (GVHD) involve immune responses which can be life-threatening. In fairness, immune responses to allotransplants are completely appropriate as the immune system did not evolve to accept artificially introduced organs, which is a very recent medical practice. Current therapies try to hamper these immune responses via immunosuppressive drugs, which pharmaceutically inhibit various pathways essential to inflammation. However, these pharmacological approaches do not differentiate between rejection of self (or artificially extended self in the case of allotransplantation) and rejection of potentially dangerous pathogens and tumours, so patients on life-long immunosuppression are extremely prone to cancer and opportunistic infections[59]. This is a better alternative than complete destruction of one's vital organs in the short term, but still rather bleak in the long term.

One promising effort to reduce the long-term morbidity associated with pharmaceutical immune suppression is to use cellular therapy. In essence, this involves isolating and expanding, and perhaps also improving, a patient's own cells *ex vivo* and re-infusing them to re-establish tolerance. Various immunosuppressive and tolerogenic cell populations are candidates of interest, including myeloid-derived suppressor cells (MDSCs), tolerogenic dendritic cells (DCs), and regulatory B cells, but we will limit our focus to Tregs. The flexibility of Tregs discussed above allows for them to suppress immune damage but also respond to the cues that allow them to take a backseat during important infections and cancer. So far, clinical trials have not been running long enough for effects on malignancies to be assessed, but infections post-transplantation were significantly reduced in Treg-transfused patients compared to the standard immunosuppression arm[106]. The goal is to develop cellular therapy to the point where patients can be weaned off pharmacological suppression in part or even entirely, which is possible in some liver recipients as the liver is naturally tolerogenic and was achieved in up to 70% of recipients[107], although this depends on timing[108].

As well as infusing Tregs to promote tolerogenic balance, there is opportunity to manipulate them during expansion to boost their effectiveness or try to better track them. There is little understanding about the fate or localisation of Tregs once they are infused. Some efforts have been made to track infused Tregs *in vivo* so that their migration patterns can be traced, especially in transplantation where homing to the graft is of importance. Even though genetic engineering with bioluminescent approaches is not suitable for patients, some success has been achieved with radionuclide labelling which was compatible with good manufacturing practice (GMP) manufacture[109].

1.3b – Human Clinical Trials

Cell immunotherapy approaches include polyclonally expanded Tregs, antigen-specific Tregs stimulated by donor cells or antigen, or chimeric antigen receptor (CAR) Tregs engineered for specific antigens. There has been success in mouse preclinical models infusing Tregs[59,110–112] that has led to clinical trials in patients with various diseases (*Table 2*).

Table 2 – Clinical trials using Treg cell therapy

Disease	Specificity	Clinical Trial	Outcome
Crohn's disease	OVA-specific Tr1	NCT02327221	Terminated
Crohn's disease	Polyclonal $CD45RA^+$	NCT03185000	Ongoing
Type I diabetes	Polyclonal	ISRCTN06128462	50% remission w/ 2 doses Tregs[113]
Type I diabetes	Polyclonal	NCT01210664	Phase I success but 75% decline in Tregs[114]
Type I diabetes	Polyclonal + IL-2	NCT02772679	Increased Tregs & cytotoxic cells[114]
Type I diabetes	Umbilical cord derived	NCT02932826	Ongoing
Cutaneous SLE	Polyclonal	NCT02428309	Single patient, ↓ skin IL-17[115]
Pemphigus vulgaris	Polyclonal	NCT03239470	Unpublished
Autoimmune hepatitis	Polyclonal	NCT02704338	Ongoing
ALS	Polyclonal	NCT03241784	Phase I success, progression slowed[116]

ALS	Polyclonal	NCT04055623	Phase II ongoing
GVHD	Polyclonal iTreg	NCT01634217	Phase I success[117]
GVHD	Fucosylated	NCT02423915	Phase I safe, no GVHD but high fevers[118]
GVHD	Polyclonal Tregs + Tconvs	NCT01660607	Phase I safe, chimerism achieved but Tac prophylaxis better[119]
GVHD	Polyclonal	2012-002685-12	Terminated
GVHD	Polyclonal Tregs + Tconvs	NCT04678401	Unpublished
GVHD	Polyclonal Tregs + Tconvs	NCT01818479	Terminated
GVHD	Donor Tregs	NCT00602693	Phase I success[120]
GVHD	Polyclonal	NCT04013685	Improved acute/chronic GVHD and survival[121]
GVHD	Polyclonal	NCT01903473	95% full engraftment, 15% grade 2 aGVHD[122]
GVHD	Polyclonal	NCT01937468	Phase I safe, preferential donor Treg clone expansion[123]
GVHD	Polyclonal	NCT02385019	Ongoing
GVHD	Donor Tregs	NCT02749084	Ongoing
GVHD	Polyclonal	NCT03683498	Results awaited
GVHD	Polyclonal	NCT01453140	Terminated
GVHD	Umbilical cord Tregs	NCT00376519	Terminated
Liver transplant	Polyclonal	NCT02166177	Phase I safe, reduced T cell responses[124]
Liver transplant	Donor-specific	NCT03654040	Ongoing
Liver transplant	Donor-specific	NCT03577431	Results awaited
Liver transplant	Donor-specific	NCT02474199	2/5 patients dosed reached 1^{ary} endpoint but not enough patients to assess efficacy[125]
Liver transplant	Polyclonal	NCT01624077	Status unknown
Liver transplant	IL-17 producing	NCT01117077	Terminated
Liver transplant	CAR Treg (HLA-A2)	NCT05234190	Ongoing

Kidney transplant	Donor stem and T cells + recipient polyclonal Tregs	NCT03943238	Ongoing
Kidney transplant	Polyclonal	NCT02129881	Phase I success, fewer infections in Treg arm[106]
Kidney transplant	Polyclonal	ISRCTN: 11038572	Ongoing
Kidney transplant	Polyclonal	NCT02371434	Phase I success[126]
Kidney transplant	CAR Treg (HLA-A2)	NCT04817774	Ongoing
Kidney transplant	Polyclonal	NCT02145325	Phase I success, circulating Tregs amplified[127]
Kidney transplant	Donor BM + recipient Tregs	NCT03867617	Ongoing
Kidney transplant	Polyclonal	NCT01446484	Status unknown
Cardiac transplant	Thymic polyclonal	NCT04924491	Ongoing
Islet transplant	Polyclonal	NCT04820270	Ongoing
Islet transplant	Polyclonal	NCT03444064	Ongoing
Islet transplant	Polyclonal	NCT05349591	Ongoing
Islet transplant	Polyclonal + IL-2	NCT02772679	Increased Tregs but also cytotoxic cells[114]
COVID	Off-the-shelf cord blood Tregs	NCT04468971	Phase I success[128]

While most of these studies demonstrate the safety, feasibility, and efficacy of Treg infusion, there are significant limitations: as always, time and money limit everything, and indeed the expansion protocols often take many weeks, as does the rigorous quality controls to phenotype and assess suppression of the product before infusion. This is of course expensive, mainly because autologous Tregs must be made for each patient, and while personalised medicine is an attractive concept, an off-the-shelf product that could be administered universally would be much more efficient and economical. Additionally, Tregs make up only 5-10% of circulating $CD4^+$ T cells, so it is difficult to reach the millions of cells required for infusion, and low cell yield does unfortunately disqualify some patients from participating in clinical trials. Therefore, any efforts to improve Treg function which might lower the required yield might help include more patients and make cellular therapy more attainable.

1.3c – Tipping the Balance Toward Tregs

In an effort to supplement cellular therapy protocols and reduce some of the practical limitations of Treg therapy, giving Tregs an extra boost is an attractive solution that could help reduce the cell yield requirements for infusion or even improve endogenous Tregs within the patient without need for *ex vivo* cell expansion. To achieve this, mechanisms that differentiate Tregs from Tconvs must be identified and exploited, as these allow us to tip the balance between them in whichever direction is required. Control of this balance could help in cases ranging from infections and cancer to autoimmunity and transplantation, covering a rather significant proportion of human disease. In many situations, the two functional subsets act as mirrors, where the same signals activate both cell types causing suppression in one and inflammation in the other, but these are not ideal targets as they risk aggravating already problematic inflammatory responses if the Tconvs were to be boosted too. Tregs are also at a disadvantage both numerically and in terms of proliferative proficiency. Preferably, a mechanism that improves Tregs while impairing Tconvs would be ideal, but as there is such a fundamental overlap in what governs their activation – for Tregs are at the end of the day still T cells, and thus what activates Tregs nearly always also activates their dangerous counterparts – there are precious few options available.

One popular candidate for endogenous Treg expansion is low dose IL-2, which takes advantage of the increased CD25 expression on Tregs to try to deliver a low enough dose to be preferentially bound to Tregs but not by other cell types. This risks activating effector T cells, but ultra-low dose therapies have been used safely in autoimmune and transplantation settings[59,129] but have not yet been effective in extending graft survival[130]. In Treg infusion trials combined with IL-2, Tregs were successfully expanded but so were cytotoxic cells such as CTLs and NK cells[114], highlighting the need for Treg-targeted approaches. IL-2 is very short lived so several modified forms have been generated to try and improve half-life and specificity, such as combining it with a specific anti-IL-2 mAb which was shown to be Treg-specific and protect against autoimmunity[131]. Further work engineering antibody fusion proteins takes this a step further and several mutein IL-2s have been created to be CD25-specific and more Treg selective to reduce undesirable off-target effects[132,133].

Another differential pathway that sets Tregs apart from other T cells is the PI3K-mTOR-Akt signalling axis, which is important for cell growth, respiration, and migration[134]. mTOR signalling is accepted to impair Treg formation by via Akt-Foxo signalling and repression of Treg transcriptional programme[135–137], but it was shown that of the 2 complexes that mTOR forms, mTORC1 is actually required for Treg suppression *in vitro* and *in vivo* and upregulates CTLA-4 and ICOS expression while repressing mTORC2 signalling which is responsible for Treg deregulation[138]. Rapamycin (clinically, sirolimus) inhibits mTOR signalling and has been shown to improve Treg proportion, Foxp3 expression, and suppressive function *in vitro* and *in vivo*, and is commonly used therapeutically as an immunosuppressant and in Treg cell therapy cultures *ex vivo*[59,106,139–141]. mTOR controls metabolism, which also differentiates Tregs who favour oxidative phosphorylation and fatty acid oxidation while activated Tconvs prefer glycolysis[142,143].

Similarly, the Itk kinase has been shown to repress Tregs, and knocking it out in $CD4^+$ T cells polarised cells toward Tregs even in Th17-inuducing conditions, which was mediated by a reduction in PI3K-mTOR signalling and increased expression of PTEN, normally repressed by Itk[134]. PTEN can be repressed by strong TCR signalling which favours Teffs over Tregs[134], and PTEN KO in Tregs impaired suppression and stability and increased glycolysis[144,145]. Myc can repress PTEN and regulate cell metabolism, and its expression is finetuned by TCR and IL-2 signalling strength[146] and Itk signalling[134]. These interwoven pathways regulate T cell compartment balance, which is already being utilised therapeutically, so identifying new mechanisms that could help achieve this would be beneficial.

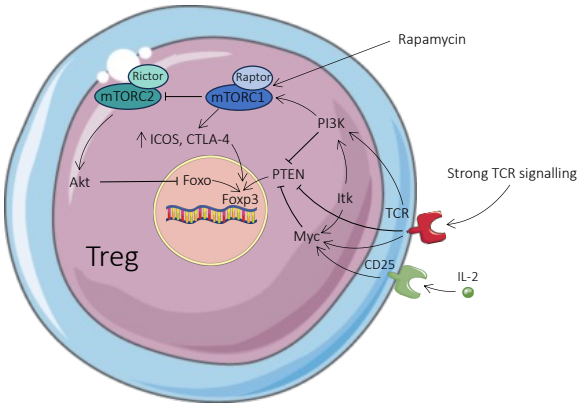

Fig 1.2 – Overview of Akt-PI3K-mTOR pathway in Tregs. mTORC1 induces ICOS and CTLA-4 which promote Foxp3, and represses mTORC2 which impairs Tregs via Akt repression of Foxo, a Foxp3 enhancer. Itk, strong TCR signalling, and IL-2 induce Myc and PI3K which repress PTEN, another Foxp3 stabiliser. Together, these pathways rule the Treg/Tconv balance.

1.4 – How Physiological Context Affects Immune Responses

1.4a – Immune Cells Face Various Microenvironments

While nutrient and molecule availability can shape immune responses, so too can immune responses shape the molecular landscape they exist in. Immune cells are some of the most metabolically active, and fast-responding neutrophil's oxidative burst consumes much of the oxygen and nutrient pool in a local tissue, leaving a very depleted buffet for cells arriving late to the scene. Furthermore, pathogens or tumours responsible for the immune response are often highly metabolically active themselves and can deplete local environments of nutrients even before inflammation. Tumours especially are known for creating microenvironments, which are often immunosuppressive and usually very much nutrient depleted and inadequately irrigated by hastily and shoddily constructed blood vessels. Additionally, any wounds or lesions are usually associated with blood loss and more chronically, fibrosis, further limiting blood and nutrient supply. Cellular damage, apoptosis, and necrosis secondary to local trauma further change the composition of local microenvironments and interact with immune cells.

Even without inflammation, immune cells patrol and reside all over the body, and must adapt to a plethora of nutrient and oxygen gradients across various tissue niches, from oxygen-filled lungs and nutrient-dense gut to the far recesses of the body's food deserts, as well as co-existing with various microbiomes residing in barrier organs. Most areas of the body are supplied with more oxygen than is required metabolically and thus form oxygen reserves, but some areas still have relatively low oxygen tensions, termed physiologically hypoxia[147]. The spleen and lymph nodes where most immune cells exist are separated into zones with distinct oxygen and nutrient availabilities, and their developmental journey through the specialised and highly active sites of the bone marrow and thymus represent further physiological niches, with the bone marrow and germinal centres of the lymph nodes representing some of the most physiologically hypoxic sites in the body[147]. There is also normal fluctuation in oxygen levels, which increase in the gut following a meal and decrease in germinal centres during clonal expansion[147]. Thus, understanding how these various nutritional landscapes, both physiological and pathological, can shape immune responses is critical to understanding how immune cells operate in these contexts to properly encompass the full nuance of immune function being studied in health and disease.

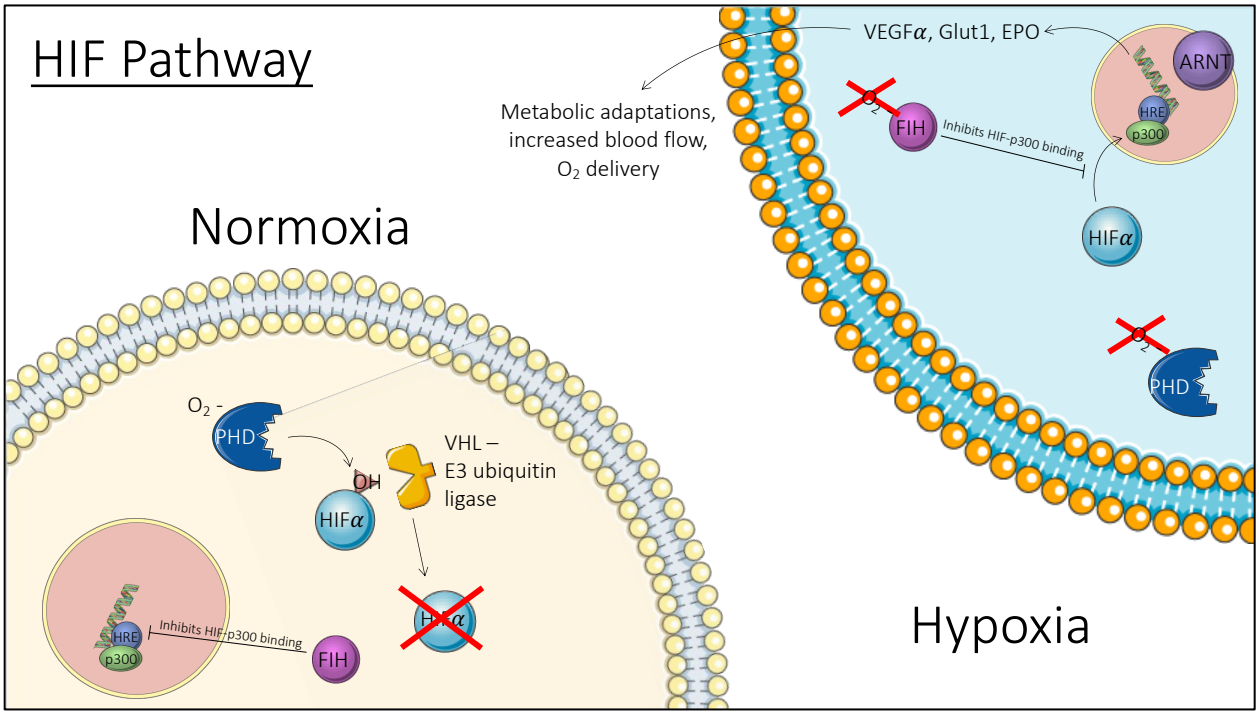

Fig 1.3 – Schematic overview of the HIF oxygen sensing pathway and regulation. In normoxia, oxygen-dependent 2-oxoglutarate enzymes PHD and FIH keep HIF degraded via hydroxylation for VHL recognition, and inhibit its binding to co-activator p300 which allows HIF to bind HREs. In hypoxia, HIF doesn't get degraded and is able to dimerise with ARNT and bind p300, inducing HIF target genes that help cells respond to the hypoxic conditions by switching to anabolic metabolism and increasing blood and oxygen delivery.

It has been known for quite some time that oxygen, or "fire air" as brilliantly coined by its discoverer[148], is capable of great explosive violence whilst also being essential to sustaining life. Early and small organisms could absorb it directly through their cell membrane and skin, but as more complex multicellular organisms evolved, oxygen availability became less direct, and mechanisms had to evolve to help cells respond to changes in oxygen tension. However, our understanding of these mechanisms was a mystery for quite some time, until George Semenza identified and isolated hypoxia inducible factor (HIF), binding partner to transcription cofactor aryl hydrocarbon receptor nuclear translocator (ARNT), as the factor that binds erythropoietin (EPO)[149,150].

A few years later, Eamonn Maher first cloned the von Hippel Lindau (VHL) gene[151] and the protein was then isolated in regard to tumour progression[152]. Peter Ratcliffe's lab then found that VHL was responsible for HIF's oxygen-dependent degradation[153]. The link between them was discovered simultaneously by Kaelin and Ratcliffe's labs, identifying prolyl hydroxylase enzymes (PHDs) as the missing oxygen-dependent factors that hydroxylate HIF[154,155], leading to its recognition by VHL and subsequent E3-ubiquitin ligase and proteasomal degradation. Thus, HIF is constitutively expressed but degraded at the protein level by an oxygen-dependent mechanism, which is disabled in times of hypoxia to allow HIF protein stabilisation and transcription factor activity, inducing genes that help cells adapt to low oxygen tension (*Fig 1.*). This work led to the award of a Nobel prize, on the very day that I started my PHD in fact.

We know of three HIF-α isoforms, 1, 2, and 3, which have overlapping and distinct transcriptional repertoires. HIF-1α is widely expressed whereas HIF-2α is more tissue-restricted and only found in vertebrates, and HIF-3α seems to be less similar to the other two forms and its regulation is less well understood[156]. HIF-3α has multiple splice variants and the best studied one dimerises with HIF-1α but is transcriptionally inactive, restricting HIF-1α signalling[156,157]. Additionally, splice variants lacking a transactivator domain still bind ARNT, limiting HIF-1/2α dimerisation opportunities and further restraining their activity[158]. HIF-2α also induces antisense HIF-1α RNA that can antagonise HIF-1α, but HIF-1α and 2α isoforms can also compensate for each other in one's absence and regulate genes they are not normally responsible for[159,160]. There is evidence that HIF-1α is expressed more acutely and during more severe hypoxia, while HIF-2α is hydroxylated less efficiently by PHDs and factor inhibiting HIF (FIH) and has a longer duration of expression, with a switch from the first to the second around 24 hours[160].

Structurally, HIF and ARNT belong to the PAS protein family and are both basic helix-loop-helix proteins that interact at their shared PAS domain[156]. HIF binds hypoxia responsive elements (HREs) in DNA of target genes such as erythropoietin, vascular endothelial growth factor (VEGF), and Glut1 that help cells import more blood and switch to anaerobic glycolysis for both cellular and systemic adaptation to hypoxia[156]. To initiate transcription, HIF recruits the coactivator p300 which allows HIFs to bind HREs, and is subject to the same oxygen-dependent inhibition as HIFs by another 2-oxoglutarate enzyme, FIH[161]; FIH hydroxylates an asparagine

residue in the C-terminal transactivator domain (CAD) domain of HIF and blocks its interaction with p300/CBP complex during normoxia[162]. HIF interaction with ARNT is also facilitated by Hsp90, which protects HIF from oxygen-independent degradation[163]. Oxygen-independent receptor of activated protein C kinase 1 (RACK1) competes with Hsp90 for HIF-1α binding and promotes its degradation[160], adding a further layer of regulation to the HIF machinery. Some of these modulators are isoform selective, such as hypoxia-associated factor (HAF) which promotes HIF-1α ubiquitination but enhances HIF-2α transactivation, and Hsp70 which degrades HIF-1α but not HIF-2α in prolonged hypoxia[160], promoting HIF-2α dominance in chronic hypoxia.

The PHD enzymes are also sensitive to iron chelators and cobalt ions, which can induce HIF activity in normoxia[156]. They bind HIFs at the N- and C-terminal oxygen-dependent degradation domains (NODDD and CODDD) to mediate their degradation[156]. Similarly to HIFs, there are 3 isoforms of PHD enzymes, and PHD1 and 3 are more tissue-restricted while PHD2 is the most ubiquitously expressed and is the main regulator of HIF[164]. PHD2 KO mice have placenta and heart defects, which is embryonically lethal, whereas mice with PHD1 or 3 KO develop normally[165]. PHD2 preferentially regulates HIF-1α over HIF-2α, whereas PHD3 has greater influence over HIF-2α[166]. PHD3 is also a HIF target which helps control HIF responses and acts as a negative feedback loop[167]. Mitochondrial reactive oxygen species (ROS) is also required for HIF stabilisation, and play a role in hypoxia sensing[168].

HIFα's binding partner ARNT is constitutively expressed and neither its RNA nor protein levels are affected by oxygen, although there is some evidence contradicting this that shows hypoxia induction of ARNT in certain cell lines[169]. ARNT is also the dimeric binding partner for aryl hydrocarbon receptor (AHR), another basic helix-loop-helix period-ARNT-single minded (PAS) protein which binds ecological pollutants such as dioxins that trigger conformation change to allow transcription of xenobiotic-responsive target genes[169]. There are also two ARNT paralogues, ARNT1 and 2, the second of which is more tissue restricted and does not bind AHR as efficiently[170] although it does dimerise with HIFs equivalently to ARNT1[171]. AHR is normally complexed with Src, and its activation leads to the release of Src which can induce downstream Erk signalling, as well as interacting with NFkB and Wnt-ß catenin signalling[172] so it can have immune implications, as can HIF and ARNT signalling.

1.4c – HIF AND IMMUNITY

As many inflammatory environments are hypoxic, HIF signalling is a common feature of immune cells operating in oxygen-depleted tissues, tumours, or tissues experiencing blood loss. Hypoxia is also a normal feature of physiological niches and plays a role in the normal functions of the immune system and its development[147]. Loss of HIF signalling in germinal centre T cells impairs B cell help and antibody responses[173], and in bone marrow, ARNT inhibition impairs haematopoietic stem cell function and viability[147]. The relationship between HIF and inflammation is bidirectional and as well as being induced by hypoxia, HIF can also be stabilised by multiple immune factors: TLR4 ligation with LPS in macrophages, TCR stimulation in T cells[174], ROS-induced PI3K-Akt signalling[175], mTOR signalling[176–178]. and various inflammatory cytokines such as TNFα[178,179] can stabilise HIF. HIF also alters cytokine production: PHD2 inhibition can promote TGFß production[180] and HIF-2α was shown to be essential for IL-12, IFNγ, TNFα, and IL-1ß production by macrophages[178], but results on CD8 cytokine production are mixed[181]. HIF-1α can also induce the CD39 and CD73 ectonucleases which convert ATP to adenosine[182] and can tolerise the immune landscape[183]. HIF also impacts metabolism by promoting a switch to glycolysis to help cells survive in anaerobic conditions, and this is associated with immune activation[147]. Interestingly, although HIF exhibits both pro- and anti-inflammatory effects, pharmacological PHD inhibition is reported to be mostly anti-inflammatory as a therapeutic option for inflammation[184].

Hypoxia has also been shown to induce the immunity and apoptosis regulator NFkB, which responds to inflammatory stimuli but can also be induced by hypoxia. HIF-1α can directly induce NFkB[185] and so can hypoxia-induced ROS[184]. PHD hydroxylation of the IKKß enzyme degrades canonical IkBα for canonical signalling[184,186] and FIH hydroxylation of domains may or may not also induce NFkB signalling[174,184,187]. Some of this induction is context-dependent, as PHD3 overexpression was shown to prevent NFkB[184], so there are some subtleties involved in this signalling induction. NFkB can also induce HIF expression, whereby the canonical NFkB subunits p50 and p65 can bind the HIF-1α promoter and overexpression of NFkB can induce normoxic HIF activity[184], so both pathways share a cyclical relationship and contribute to each other's hypoxic responsiveness. NFkB plays an important role as an immune transcription factor

that regulates proliferation, apoptosis, angiogenesis, and metastasis, and as it both responds to and induces cytokine and chemokine signalling, it is involved in many inflammatory diseases[187].

How HIF signalling contributes to immune and inflammatory disease is unclear, as it varies in various disease models and levels of hypoxia. In local infections, HIF appears to be mostly protective, while it is usually detrimental in systemic infections[188]. HIF-1α and HIF-2α can exacerbate sepsis and play a role in inflammatory cytokine release[189]. In IBS, HIF-1α could impair CD39 expression on Th17 cells and promote their autoimmune functions[189]. In hypoxic arthritic joints, HIF-2α but not HIF-1α was highly expressed and colocalised with inflammatory markers, and overexpression of HIF-2α induced arthritis while its inhibition was protective[190]. In cancer, hypoxia is a hallmark of tumours due to their high metabolic consumption and poor vascularisation, and hypoxia is associated with poor prognosis as it encourages an immunosuppressive environment by increasing PD-L1 expression and inducing suppressive populations such as Tregs, MDSCs, and tumour-associated macrophages[181,189]. Cytokines in the tumour microenvironment also inform whether HIF-1α or HIF-2α are predominant in regulating effector molecules[184], so both hypoxia and immunity shape each other and the tumour. Hypoxia is also often associated with other issues such as ischaemia and impaired blood supply from poor angiogenesis, thrombosis, or atherosclerosis, all of which also have inflammatory implications.

1.4d – How Iron Deprivation Impacts the Immune Response

Iron is forged in the heart of dying stars and is the most abundant element on our planet. Its uniquely reactive chemistry powers many essential cellular processes including ATP production and electron transport chain, lipid and fatty acid metabolism, and DNA synthesis and repair[191]. Iron-sulphur clusters are considered the most ancient catalyst[192], and take advantage of the energy released by oxidation and reduction of iron to power over 200 human enzymes[191]. And so, at the core of both the fundamental cell processes that sustain us and the planet we live on, as well as in the blood running through our veins, is stardust.

Because of iron's reactivity, it is kept carefully supervised across its journey through the gut, blood, and cells. Systemic iron levels are regulated not by controlling its export but its import, as there is no mechanism regulating its excretion[193]. Dietary iron is reduced by duodenal

cytochrome B (DCYTB) and about 1mg/day is taken up on the apical surface of the duodenum by divalent metal transporter 1 (DMT1), while the rest of the body's iron requirements (20-25mg/day) comes from recycling senescent erythrocytes[193,194] (*Fig 1.*). Iron is exported into the serum by ferroportin, the only known mammalian exporter of iron[194]. In the blood, iron is chaperoned by transferrin, which keeps it from wreaking havoc and oxidative damage, and the iron-transferrin complex is imported into cells via the transferrin receptor Tfrc, also known as CD71[193] (*Fig 1.*). Again, cellular damage and oxidative stress are avoided by sequestering iron within ferritin for intracellular storage[195] (*Fig 1.*).

Iron homeostasis is critical, as deficiency can lead to anaemia, poor oxygen delivery, and defects in the many cellular processes and enzymes that require iron, while iron overloading can cause cirrhosis, diabetes, arthritis, and cardiac and endocrine abnormalities[196] as seen in hereditary haemochromatosis. The key to systemic iron homeostasis is hepcidin, which internalises and degrades ferroportin on cells and in the duodenum to keep iron locked inside cells and out of the serum[197] (*Fig 1.*). Excessive systemic iron is sensed by bone morphogenic protein 6 (BMP6) signalling and the coreceptor gene hemojuvelin which signal via small mothers against decapentaplegic (SMAD) pathways to induce hepcidin gene expression in hepatocytes[198]. At the cellular level, iron homeostasis is maintained by iron regulatory proteins (IRPs), which are essentially to iron as HIFs are to oxygen. They bind genes containing iron regulatory elements (IREs) to stabilise genes such as transferrin receptor (Tfrc) and DMT1 that favour cellular and systemic iron import and repress ferritin and ferroportin[194] (*Fig 1.*). IRP1 contains an Fe-S cluster which it loses during iron deficiency, causing a structural change that favours RNA binding, while IRP2 lives a similar lifestyle to HIF by being kept ubiquitinated and degraded by the iron-dependent F-box leucine-rich repeat protein 5 (FBLX5), much akin to oxygen sensing by PHD[199]. Loss of both IRPs is embryonically lethal, while one at a time is quite mild, suggesting redundancy between them[200].

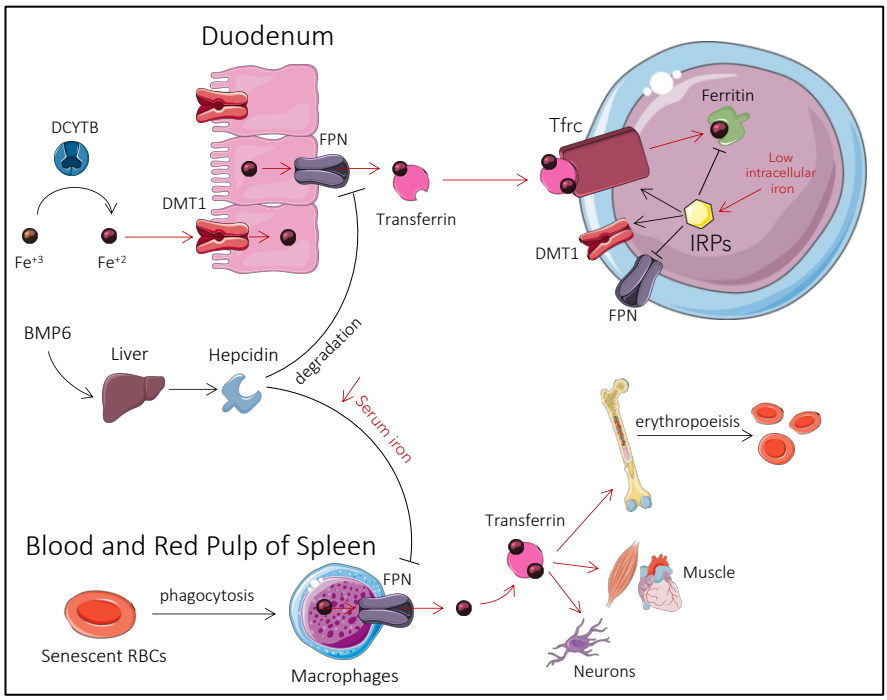

Fig 1.4 – Schematic overview of iron homeostasis. DCYTB reduces iron for import via DMT1 in the duodenum, where it's exported by ferroportin (FPN). In serum, transferrin transports iron and cells uptake it via Tfrc. Inside cells, ferritin stores iron and IRPs sense low iron levels to inhibit FPN and increase DMT1 and Tfrc to raise levels. Systematically, hepcidin degrades ferroportin to decrease serum iron.

Clearly, iron is necessary for many cellular functions and as immune cells tend to be highly metabolically active, they are very sensitive to changes in iron availability, but additional mechanistic links exist at various levels of iron and immune homeostasis to intertwine the two. In line with nutritional immunity, hepcidin-mediated inflammatory hypoferremia can starve extracellular bacteria of the iron they need to survive, and hepcidin is considered an acute phase protein in early immune responses, induced via IL-6 and STAT3 signalling in hepatocytes. Chronic low iron diet reduces IFNγ, IL-12, and IL-4 in mice[201,202] and IFNγ and TNFα in children[203], and iron supplementation could rescue IL-2 and IFNγ levels[204]. Iron also stimulates GM-CSF production by T cells to promote innate inflammation[205]. In cellular immunity, iron deficiency impairs adaptive responses, causing defects in IgG and maturity in GC B cells and reduced activation and granzyme B production by $CD8^+$ T cells[206]; iron loading also reduces $CD8^+$ T cell levels in hereditary haemochromatosis and β-thalassemia patients but they display a more effector phenotype[207,208]. CD71 is a hallmark of lymphocyte activation, which indicates a need for iron during cellular activation, and its inhibition impairs DNA synthesis and proliferation *in vitro*[209].

Clinically, iron deficiency impairs immune responses to infections[210–212] and vaccines[206,213–215] and is associated with worse outcomes. Its role in autoimmunity is seemingly more complex, with evidence showing both positive and negative correlations. Iron was shown to induce granulocyte macrophage colony stimulating factor (GM-CSF) production by T cells and drive disease in the autoimmune model experimental autoimmune encephalitis (EAE)[205]. Iron deposition in tissues has been noted to drive symptoms and neurodegeneration in multiple sclerosis (MS)[216], and systemic lupus erythmatosus (SLE) is associated with increased intracellular iron in $CD4^+$ T cells[199], indicating high intra-and extra-cellular iron levels are implicated in autoimmunity. In accordance with this, iron deprivation protects mice[217,218] and patients[219] from EAE/MS and SLE[220,221]. However, patients newly diagnosed with iron deficiency anemia were shown to have increased likelihood of developping subsequent autoimmune diseases[222], and deletion of the heme scavenger hemopoexin was shown to be similarly ambivalent by both enhancing Th17 responses and EAE disease progression[223] and also dampening mercury-induced autoimmunity[224]. Similarly, haptoglobin binds free haemoglobin and was found to be overexpressed in SLE patients[225].

Iron loading in thalassemia patients has been associated with an abormally low $CD8^+$ T cell compartment in a subset of patients, which exhibited poor activation and proliferation responses that were rescued by iron chelation[208], whereas others found that thalassemia was associated with low $CD4^+$ T cells instead and normal or high levels of $CD8^+$ T cells[226]. However, one of the studies that showed iron deficiency protected against EAE also included an iron overload arm which showed no change in disease progression[217]. Overall, the role of iron and iron loading in driving the symptoms of autoimmunity and in triggerring the loss of tolerance are unclear. Pregnancy is a nautural wonder of tolerance, and although iron deficiency has been associated with increased risk of infection during pregnancy[227], its role in fetal tolerance has not been explored despite the high prevalence of iron-deficient anemia during pregnancy.

In tranplantation, the role of iron deficiency in recipients is greatly complicated by its prevalence and association with anaemia pre-transplantation, various medications, surgical blood loss, and change in erythropoesis and EPO production[228]. While iron deficiency is associated with increased mortality after kidney transplantation, hepcidin/iron chelation (decreasing iron) and ferroportin/HFE knockout (promoting iron loading) were both shown to protect against ischaemia reperfusion injury (IRI) and oxidative stress which are drivers of early rejection[228]. Similarly, both iron loading and deficiency accelerated acute rejection in a cardiac allograft model[229]. Ferritin levels[230] and transferrin receptor expression on T cells[231] were noted to increase before and during rejection, and anti-Tfrc antibody prolonged graft survival in cardiac allograft model[232,233]. An important study by Bohne et al. investigated transcriptional signatures that differentiated operationally tolerant vs. non- tolerant patients with liver transplants and found that increased hepcidin and decreased Tfrc transcription were the most differentially expressed and the best predictors of operational tolerance[234], suggesting that decreased serum and cellular iron improves transplant outcomes. However, hepcidin and ferritin had no correlation with inflammatory markers in kidney recipients[235,236]. Overall, the jury is still out on the exact role of iron in autoimmunity and transplantation, and discrepancies between cellular vs serum/systemic iron limitation between studies are likely to be confounding things further.

Jabara et al. identified a mutation in Tfrc to be the cause of an observed familial immunodeficiency[237]. They observed normal circulating numbers of lymphocytes with intermittent neutropenia and thrombocytopenia, but fewer memory B cells and poor T cell proliferation *ex vivo*. Sequencing revealed a Tyr $\rightarrow$ His substitution that disrupts the Tfrc internalisation motif and leads to poor endocytosis and intracellular iron deficiency. This could be rescued with administraction of iron citrate, indicating that the Tfrc receptor is inefficient rather than completely incapable, which explains the health of the $Tfrc^{Y20H/Y20H}$ knockin mice they bred relative to the embryonically lethal $Tfrc^{-/-}$ knockout. The $Tfrc^{Y20H/Y20H}$ mice recapitulated the phenotype observed in human patients[237], and thanks to the much-appreciated generosity of the Drakesmith team, they were used extensively in my research.

1.4e – Interactions Between HIF and Iron Signalling

Although the work presented in this thesis does not have the scope to examine how iron and hypoxia signalling interact to affect Treg and immune function, the two pathways are intimately intertwined at multiple levels. Physiologically, they come together to fulfil our most fundamental biological needs via haemoglobin, the body's premier oxygen delivery carrier and largest iron requirement, with 70% of the body's iron stores found in erythrocytes[238]. There is also significant overlap in erythropoiesis, which requires iron to match haem construction requirements and is under the control of erythropoietin (EPO), a HIF target gene. Thus, hypoxia can increase erythropoiesis, but hypoferremia that would be aggravated by too much erythropoiesis signals via decreased hepcidin signalling to only allow erythropoiesis to take place in iron-replete conditions[239]. EPO is under the control of HIF-2α and interestingly, HIF-2α KO mice receiving wildtype bone marrow had impaired haematopoiesis but not the other way around, indicating that HIF-2α provides an environment for haematopoiesis but is not required in marrow cells themselves[238].

Hypoxia also greatly affects systemic iron homeostasis, as HIF-2α is very important in the gut iron import axis and responds to changes in hepatic hepcidin and ferroportin to balance dietary iron uptake; DCYTB and DMT1 are both HIF-2α targets and are induced by HIF-2α in response to hypoferremia to increase systemic iron accumulation[238]. Intriguingly, intestinal HIF-2α doesn't induce expression of VEGF or other normal hypoxia-responsive genes, and it is not clear how its intestinal activity is thus restricted[238]. HIF-1α represses the hepcidin promoter in the liver[240], and hypoxia is able to override inflammatory signals such as IL-6 that induce its expression[238]. HIF-2α also represses hepcidin expression but this is EPO-dependent, as EPO can repress hepcidin via both hepatocyte EPO receptors and erythroid-derived factors[238]. Together, HIF-1 and -2α cooperate to repress hepcidin via both systemic and cellular signalling.

The reason for HIF's functions as an iron sensor at the biochemical level is via the same mechanism as oxygen sensing, as the PHD enzymes are also dependent on iron as well as oxygen, and thus iron deficiency can disable them and stabilise HIF to induce expression of genes that help increase iron import[238]. HIF-2α is stabilised in DMT1 knockout but not

ferroportin knockout mice[239], indicating that it responds to intracellular and not serum iron levels. DMT1, DCYTB, and ferroportin promoters all contain an HRE[238], so intestinal HIF-2α activity helps promote iron accumulation. Iron and oxygen homeostasis are further interlinked at this cellular level through IRPs, and account for some of the IRP-independent control of iron homeostasis genes such as DCYTB, which is iron-responsive yet lacks an IRE[238]. Much as iron homeostasis genes contain an HRE, so too does the HIF-2α promoter contain an IRE, allowing it to be regulated by cellular iron deficiency[238]. In haematopoietic cells, IRP inhibits HIF translation to avoid overwhelming systemic iron demands, and IRP1 (but not IRP2) knockout mice develop polycythaemia due to high HIF-2α and EPO levels[241,242]. IRP1 seems to be the major regulator of HIF-2α's IRE[238], but IRP2 knockout in mouse embryonic fibroblasts induced both HIF-1α and HIF-2α, leading to metabolic switching[243]. However, intestinal HIF-2α is not regulated by IRPs, allowing PHD inhibition to increase iron import from the gut[238]. Additionally, HIF-2α can be activated by hepcidin, which acts cell-autonomously by inactivating PHD enzymes downstream of ferroportin activation[239]. Patients with Chuvash polycythaemia have a VHL mutation that systematically elevates HIF levels and is often treated with phlebotomy which results in iron deficiency, and this iron deficiency consistently increased HIF-1α protein stability but hypoferremia-induced degradation of HIF-2α mRNA via its IRE overrides the protein stabilisation[244].

In inflammation, less is known about how the interaction between iron and hypoxia affects immunity. Inflammatory microenvironments are often both hypoxic and iron depleted due to high nutrient consumption of invading immune cells such as neutrophils, and potentially by the tumour or pathogen that is inducing an immune response. Hypoxia is reciprocally associated with NFkB signalling[184,185], and can induce TNF and IL-1ß expression in certain iron-deprived intestinal cell lines, but either hypoxia or iron supplementation could also ameliorate hypoferremia-induced inflammation[245], so both iron and hypoxia can induce inflammatory signalling and their combined effects are highly cell-type specific, allowing for tissue-specific regulation. NFkB can also increase intracellular ferritin, which sequesters the labile iron pool and leads to further PHD inhibition[246]. As IL-6 induces hepcidin production, its expression is decreased in the intestine after exposure to environmental hypoxia in humans[245], thus allowing for erythropoiesis. In Covid, viral protein was suggested to infect erythrocytes and attack

haemoglobin, causing haemolysis and consequentially reduced oxygen transport leading to systemic hypoxia, and the haemolysis marker LDH was a an exceptionally accurate marker to differentiate mild from severe cases[247]. Additionally, severe hypoxaemia in Covid patients correlated with hypoferremia, despite high serum ferritin associated with inflammation[211]. Hypoxia can also induce autophagy that has been shown to reduce inflammation, but iron supplementation or overloading counteracted this by inducing mTOR activity[245]. Altogether, the interaction between the two varies clinically and is poorly understood.

Mechanistically, iron chelation has been shown to affect mTOR activity in various ways, with evidence that iron chelation consistently inhibits mTOR1 but has variable and tissue-specific effects on mTOR2, and HIF was shown to be partially responsible for the inhibition of mTOR via activation of REDD1[248,249]. mTOR coordinates cell growth and metabolic responses required for immune cell activation[248], and is an important player in adaptation to inflammation. In patients with Chuvash polycythaemia who often experience concurrent elevated HIF levels and iron deficiency, sequencing of PBMCs in iron-matched patients and controls revealed downregulation of *SMAD2* and *SMAD4* which indicate repressed TGFß activity, and genes related to TCR-CD3 signalling were also downregulated, including CD28; this is consistent with reports of lower CD4 T cell counts and lower CD4:CD8 ratio in these patients[244]. PI3K signalling was decreased, which would also suppress T cell proliferation, but inflammatory genes *TNF*, *IL1B, IL6* and *TLR4* were upregulated, as well as survival and anti-apoptotic genes[244]. Taken together, this indicates that the VHL mutation might induce inflammatory but less proliferative cell adaptations in humans. The addition of iron deficiency in these patients altered expression of genes related to mitochondria-mediated apoptosis, and HIF-2α-specific IRP-mediated degradation led to a HIF-1α-dominated response that favours genes relating to glycolysis and represses some of the HIF-2α-induced inflammatory genes[244]. Altogether, HIF and iron interact with several inflammatory genes, but little work has been done to investigate their joint effect on immunity and in specific cell types, despite their common combined prevalence in sites of inflammation and immune activity.

1.5 – HIF and Iron Signalling in Tregs

1.5a – HIF Signalling and Tregs

While the role of HIF and hypoxia in general immunity is fairly well studied, how they affect Tregs is much less understood. This is not due to a lack of studies but rather to inconsistency within the existing work in the field: some studies show opposite results *in vitro* and *in vivo* even with the same genetic models, and some papers directly contradict and fail to repeat other published results. The multitude of different approaches in manipulating HIF signalling (including environmental hypoxia, genetic, and pharmacological approaches), as well as different measurements of Treg fitness have led to great disparity in this field, as highlighted below.

Foxp3 Stabilisation

As Foxp3 is essential to Treg function and is the main basis of defining the Treg phenotype, signalling that increases or decreases its expression has profound effects on Tregs, so increases or decreases in its expression is a very common measurement of Tregs in research. The first report of hypoxia signalling being beneficial to Tregs is from Ben-Shoshan et al.[250], who investigated Tregs based on a few reports of HIF-1α signalling decreasing Tconv function[251–253]. They found that *in vitro* hypoxia induced *Foxp3* expression in Jurkat cells and human PBMCs, which was reversed by HIF-1α knockdown. They also used a VHL-resistant HIF-1α mutant to induce HIF-1α overexpression and found a dose-dependent correlation between HIF-1α and Foxp3; they then recreated this *in vivo* with hydrodynamic naked DNA injections to induce HIF-1α. This HIF-1α-dependent induction of Foxp3 was confirmed by Clambey et al., who also identified a HRE within the *Foxp3* promoter by ChIPseq analysis[254]. However, they also showed that TGFß neutralisation inhibited hypoxic induction of Foxp3 expression, which implies that HIF-1α's regulation of TGFß (which also has an HRE in its promoter) may control Foxp3 more than direct HIF-Foxp3 interaction[254]. Additionally, hypoxia and *in vivo* PHD inhibition were shown to increase Treg percentages and Foxp3 expression[254,255], as well as inducing *de novo* Treg induction from naïve Foxp3$^-$ cells *in vitro*, even without TGFß or other cytokines normally needed for iTreg differentiation[254].

Conversely, Westendorf et al. showed that hypoxic culture neither increased or decreased Foxp3 expression[256], and our group showed that PHD2 silencing did not affect demethylation of the TSDR which regulates Foxp3 stability[255]. Treg-restricted HIF-1α increase via knockout of *PHD2*[257] or *VHL*[258] decreased Foxp3 expression, which contradicts the above data. Two reports from Dang et al.[95] and Shi et al.[187] published within months of each other show that HIF-1α deficiency increases the number of Foxp3$^+$ cells even in Th17 skewing conditions which suggests that Tregs are impaired in the presence of HIF-1α. Hypoxic culture was shown to reduce Foxp3 expression[99,259] and decrease iTreg differentiation in a HIF-1α-dependent and HIF-2α-independent manner[260]. Additionally, Dang et al. showed that although HIF-1α deficiency wasn't reducing *Foxp3* mRNA, HIF-1α was binding Foxp3 at the protein level and causing its proteasomal degradation via ubiquitination[99]. However, Clambey et al. could not reproduce these results, and showed a direct correlation between Foxp3 mRNA and protein in both normoxia and hypoxia, opposing the notion of Foxp3 protein degradation[254]. Shi et al. also found that HIF-1α deficiency did increase Foxp3 at the mRNA level[261], opposing the theory of proteasomal degradation despite showing the same trends as Dang et al. However, a few years later, Hsiao et al.[257] were able to show the same trade-off between HIF-1α and Foxp3 protein expression as Dang et al., although they did not investigate mRNA levels.

It seems that HIF-1α is capable of direct and indirect interaction with Foxp3, both at the gene and at the protein level, but whether this interaction leads to its stabilisation or degradation is unclear. The studies employing VHL or PHD knockout may reasonably have effects outside of increasing HIFs that could play a role as yet unknown as they do have other targets, and the hypoxic cultures could have other effects on cellular stress responses or other pathways outside of HIFs. It is possible that these other effects are integrated into the Treg response and may be polarising these results, but many of these studies reverse their observed phenotype with HIF-1α knockout, so unless it is the interaction of HIF-1α with some of these other potentially affected players that is responsible for the phenotypes, there is good evidence that HIFs are sufficient in altering Foxp3 expression. Additionally, most studies focus on induction of Foxp3 on naïve T cells, so HIFs might have different effects on mature, already differentiated Tregs, a distinction seldom made in these studies.

Other Th Transcription Factors

Expression of Th transcription factors is often associated with plasticity and loss of Treg identity (*see section 1.2c*). PHD2 silencing caused an increase in *Tbet* expression on Tregs[255], and Lee et al. found that *VHL* knockout skewed Tregs toward a Th1-like phenotype, which is consistent with increased *Tbet* expression although they did not measure *Tbet* expression directly[258]. No changes in *RORγT* were noted in either PHD2 silencing[255] or *HIF-2α* knockout[260], despite evidence of HIF-1α mediating the Treg/Th17 balance[99,261]. IL-17 secretion in global $CD4^+$ T cells was decreased in hypoxia as well[256], which is inconsistent with a HIF-mediated skewing toward Th17 cells, although the opposite trend was also shown supporting it[257].

While acquiring Th transcription factor expression can sometimes be a sign of dysfunctional Tregs and be associated with loss of Foxp3, there is no clear shift toward a universal phenotype noted. The studies that support HIFs being beneficial to Tregs and *Foxp3* stabilisation note no change in Th transcription factors[254,256], so it is unlikely that HIFs are increasing Th transcription factor expression independently of Foxp3 expression and Treg stability, but rather that in cases where HIFs seem to negatively affect Tregs they also increase their plasticity and convert them to more Tconv-like phenotypes. Whether this is driven by HIFs directly or by concomitant loss of Foxp3 (which is not always seen) is unclear. As the opposite conversion of Tconvs into Tregs is also shown, it is unclear exactly how HIFs skew the Tconv:Treg balance, but they do seem to play a central role in its equilibrium.

Treg Surface Markers

Tregs express several co-inhibitory surface markers that help define their phenotype and contribute to their suppressive capabilities (*see section 1.2a*). Our group found that PHD2 silencing led to a decrease of CD25 on Tregs[255], whereas CTLA-4, GITR, LAG3, and folate receptor 4 – all inhibitory markers usually expressed on Tregs – were not affected by deficiency of either HIF-1α or HIF-2α[260], nor by increased HIF-1α[257]. Lee et al. also found these and other Treg markers to be comparable to WT controls, and even noted that CTLA-4, GITR and CD39 were slightly higher in VHL KO[258]. PD-1 expression was increased on hypoxic Tregs both *in vitro* and in hypoxic cancer environments[256], although indirect immune factors rather than hypoxia might play a role.

It seems that any effects HIFs have on Tregs are further upstream of these surface markers so understanding how HIFs control Foxp3 might be a higher priority if surface markers are not reinforcing feedback loops to alter Treg phenotype. It is also somewhat surprising that although such starkly opposing results are reported regarding Treg transcription factor expression, this doesn't seem to translate to obvious changes to the surface proteins under the control of these transcription factors.

Cytokines and Other Soluble Factors

Much of Treg suppression is contact-dependent, but IL-10, TGFß, and IL-35 secretion also play a role in suppressing immune responses (*see section 1.2b*). Hsu et al. found that neither HIF-1α nor HIF-2α deletion affected either TGFβ or IL-10 secretion from Tregs[260]. Neither systemic or Treg-restricted PHD2 silencing[255] nor increases in HIF-1α due to Deltex deletion[257] affect IL-10 or TGFß secretion either. However, Westendorf et al. found that hypoxia increased transcription of IL-10 in Tregs, which they suggest is responsible for their observed increase in suppression[256]. They also found decreased transcription of pro-inflammatory cytokines, but VHL knockout led to increased IFNγ production by Tregs, and HREs were found in the *Ifng* promoter[258]. IFNγ was found to be slightly increased in Deltex1 knockout Tregs which have high HIF1-α expression, as well as IL-17, TNF-α, and IL-4[257], but we found that PHD2 silencing only caused increased TNF-α and none of the other above cytokines[255], perhaps suggesting that HIF1-α and HIF-2α control different cytokine modules, although very few papers differentiate between the two.

Although not a cytokine, extracellular adenosine is produced by Tregs to increase intracellular cAMP (*see section 1.2b*). Several adenosine receptors and the CD73 gene are HIF transcriptional targets[262], and hypoxia slows adenosine uptake by repressing expression of extracellular nucleoside transporters[262]. These links show that hypoxia enhances adenosinergic signalling at several levels, and as this is known to enhance Treg conversion and suppression this is further evidence of hypoxia being beneficial to Tregs, although the hypoxia-adenosinergic pathway hasn't been investigated in the specific context of Tregs.

Treg suppressive function

While expression of Foxp3 and surface markers are useful measurements of Treg abundance and phenotype, they do not necessarily correlate with Treg suppressive function. Indeed, our PHD2 silencing model showed increased $Foxp3^+$ population among $CD4^+$ cells despite a Treg-driven systemic inflammatory phenotype, and PHD2-deficient Tregs were even shown to be inherently pathogenic[255]. In parallel, Treg-restricted VHL knockout led to loss of Treg suppression and widespread lethal inflammation, and when these Tregs were adoptively transferred into a colitis model they were unable to control the disease[258]. Increased HIF-1α expression from Deltex1 knockout in Tregs also failed to control colitis, lung inflammation, and antigen-specific memory responses *in vivo*[257]. Additionally, HIF-1α deficient mice were shown to be resistant to autoimmune disease[99], suggesting that a lack of HIF improves Treg regulatory function *in vivo*. This is supported *in vitro*, where Treg-restricted HIF-1α knockout enhanced suppressive activity[263], further supporting the theory of HIF-1 α restraining Treg suppression.

However, there is also evidence that hypoxic signalling is beneficial to Treg function: hypoxia-treated Tregs were more suppressive *in vitro* than normoxic Tregs[250,256], and HIF-1α-deficient Tregs were less suppressive *in vitro* and *in vivo*[254]. VHL knockout Tregs were also capable of normal – but not enhanced – suppression *in vitro*[258]. It is difficult to compare *in vivo* data that uses different disease models, and differences in mice and HIF modulation strategy could have strong effects. Additionally, as some inflammatory models are driven by type I or Th17 responses and HIF's effect on Treg plasticity might affect their ability to control some flavours of inflammation differently than others. Nonetheless, there is clear evidence that HIFs can affect Treg suppressive function quite drastically, despite contradictory data.

Metabolism

A clear link exists between hypoxic signalling and metabolic and respiratory adaptations which is relevant to T cell biology. TCR signalling and T cell activation leads to downstream activation of mTOR, which in turn can activate HIF even in normoxic conditions[178]. mTOR can also inactivate FOXO1 and 3, which affects Treg suppression and migration[142]. Interestingly,

HIF-1α knockout was shown to enhance Treg suppression *in vitro* via pyruvate import into the mitochondria and decreased glycolysis[263]. Glut1 is a very well-known target of HIF-1α, and increased glycolysis is one of the key adaptations of hypoxic cells that cannot rely on oxidative phosphorylation, so this pathway supports HIF-1α being metabolically unfavourable for Tregs.

HIF Isoforms

Further frustrations stem from the fact that most of these studies only study the HIF-1α isoform, and the few that do take HIF-2 α into account showed completely different effects from one isoform to the other, so many of the studies only looking at HIF-1α might be missing key effects driven by HIF-2α. This is not to mention the HIF-3α isoform that is widely ignored by science at large and certainly in Treg studies. Our group found that Treg loss of suppression and increased infiltration caused by PHD2 knockdown was reversed by concomitant knockdown of HIF-2α, but not HIF-1α[255]; this implies that the high HIF-2α levels were causing the loss of regulation in Tregs. To see whether extra low levels of HIF-2α would have the opposite effect and improve Treg function, the one and only Kento Kawai used a pharmacological HIF-2α inhibitor in an *in vitro* Treg suppressive assay and found that it did boost Treg function, but HIF-2α KO Tregs were incapable of suppressing alloresponses in a transplant model *in vivo* (data available in his thesis), adding our research to the long list of studies with discordant results *in vitro* and *in vivo*, although the differential effects of pharmacological vs. genetic inhibition might also be at play.

The only other researchers that targeted HIF-2α were Hsu et al., who found that knocking it out led to Treg dysfunction in *in vivo* colitis and airway inflammation models[260]. However, they also demonstrated that HIF-1α was increased during HIF-2α knockout, and that it was in fact this increase in HIF-1α levels that was responsible for their phenotype, as knocking out both HIFs reversed it. Similarly, Lee et al.'s Treg-specific VHL knockout model which caused loss of Treg regulation was also reversed with HIF-1α knockout[258]. This contradicts our findings of a HIF-2α-driven model but it's interesting that a single isoform was behind the respective phenotypes and not a combination of both. The different isoforms of HIF are known to have some redundancy and overlap as well as some differences in their target genes. As most of the

other studies focused solely on HIF-1α or used models that did not discriminate between the two isoforms, it is difficult to know what role HIF-2α may have played in these circumstances as it was measured or manipulated in only a few studies, and HIF-1α knockout would not affect it whereas hypoxia or VHL/PHD inhibition alters both. It is possible that the contradicting results on Treg phenotype are driven by differing amounts of HIF-1α and HIF-2α in different experimental approaches, but the exact role of the HIF-1α:HIF-2α balance in Tregs is itself unclear and sorely understudied.

Differences in vitro and in vivo

To complicate matters further, several inconsistencies have been reported in how HIF signalling affects Tregs *in vitro* and *in vivo*, which sometimes contradict each other within the same study. In several studies, Tregs that were shown to be suppressive *in vitro* were unable to control colitis *in vivo*[258,260]. This was seen even in Treg-restricted alterations, which makes it unlikely that this is due to effects from either the rest of the immune system or other more subtle biological complexities that *in vitro* models fail to capture, but rather suggests that perhaps it is not phenotype markers or suppressive function that is being disrupted; perhaps migration or activation are impaired, or an increased susceptibility to exhaustion driven by longer-term stimulation that is not replicated in shorter in vitro experiments. Several studies do however show similar results *in vitro* and *in vivo*[99,250,254,261], so it is unlikely to be a quirk of HIF manipulation itself.

It is difficult to untangle the various approaches employed in the above studies and the conclusions they reach, as many of them use slightly different approaches. Differences in pharmacological vs genetic inhibitions, overlap between which isoforms are targeted, and different disease models as well as timing and duration of interventions can all have drastic effects on observed results. A summary of the differences that set different experiments apart is summarised below (*Table 3*) and highlights some of the technical differences that might explain the opposing results found.

Table 3 – Summary of Treg and HIF experiments by different approaches

APPROACH	STUDY	CONDITIONS	RESULTS	DIFFERENCES
In vitro hypoxic cultures	Ben-Shoshan et al., 2008	Hx pre-culture of human PBMC and mouse splenocytes	Improved suppression	Bulk immune populations
		Jurkat cells	Induced higher Foxp3	16h culture, reversed by HIF1 siRNA
	Clambey et al., 2012	Jurkat cells	Induced higher Foxp3	6-8h hypoxia
		Naïve mouse CD4 T cells	↑ Foxp3 mRNA, reversed by HIF1 KD	
		Naïve mouse CD4 T cells w/ TGFb + IL2	↑ % $Foxp3^+$ cells, TGFb-dependent, reversed by IL-6	3 days hypoxia, 0.75ng/ml TGFb
	Hsiao et al., 2015	DO11.10 T cells	↓ % $Foxp3^+$ cells, reversed by Dltx1	3 days hypoxia
	Dang et al., 2011	Naïve mouse T cells w/ TGFb + IL2	↓ % $Foxp3^+$ cells, direct HIF-mediated protein degradation	6 days hypoxia, 5ng/ml TGFb
	Hsu et al., 2020	Naïve mouse T cells w/ TGFb + IL2	↓ % $Foxp3^+$ cells, unless HIF1 KO, HIF2 KO no effect	0-5ng/ml TGFb, no other studies investigated Hx HIF2 *in vitro*
In vitro suppression assay	Lee et al., 2015	Tregs from $Foxp3^{Cre}$ VHL KO mice	Comparable to WT	Naïve T cell suppression
	Ben-Shoshan et al., 2008	Hx pre-culture of human PBMC and mouse splenocytes	Improved suppression	Bulk immune populations
	Clambey et al., 2012	HIF1 KO Tregs	Decreased suppression	Consistent results
	Hsu et al., 2020	$Foxp3^{Cre}$ HIF1 KO	Decreased suppression	
		$Foxp3^{Cre}$ HIF2 KO	Comparable to WT	Mouse vs. human cell comparison
	Kento Kawai (unpublished)	PT2385 pre-treatment of human Tregs	Improved suppression	
	Yamamoto et al., 2019	PHD2 KD Tregs	Decreased suppression	
HIF1 KO/ inhibition	Shi et al., 2011	$CD4^{Cre}$ KO, naïve T cell culture w/ TGFb	↑ % $Foxp3^+$ cells	5 days Hx, 1 or 10ng/ml TGFb
	Dang et al., 2011	$CD4^{Cre}$ KO, naïve T cell culture w/ Th17 or Treg conditions	↑ % $Foxp3^+$ cells	6 days hypoxia
	Hsu et al., 2020	$Foxp3^{Cre}$ HIF1 KO	No change in % $Foxp3^+$ cells *in vivo* or in *in vitro* iTreg	3d Hx, consistent w/ other short expts

	Clambey et al., 2012	Suppression assay with Tregs from HIF1 KO mice	↓ *in vitro* suppression	Internally consistent
HIF2 KO/ inhibition	Hsu et al., 2020 Kento Kawai (unpublished)	$CD4^{Cre}$ and $Foxp3^{Cre}$ HIF2 KO	Normal immune development, normal iTreg development w/ TGFb, but dysfunctional w/o HIF1 KO	Difference between resting and inflammatory conditions
		PT2385 treatment of mouse Tregs	HIF1 upregulation and IL-17 production	12-48h
		PT2385 pre-treatment of human Tregs	Improved *in vitro* suppression	3 days
HIF1 over-expression	Ben-Shoshan et al., 2008	Forced expression of VHL-resistant HIF1 in Jurkat cells *in vitro*	Dose-dependent increase in Foxp3 mRNA and protein	Inconsistent with Dang et al. but different HIF1 directions
		Hydrodynamic DNA injections into mice	↑ Foxp3 mRNA and protein	
	Hsiao et al., 2015	Deltex KO increases HIF1	KO Tregs as suppressive as WT in *in vitro* suppression	No direct HIF measurement
		Deltex KO increases HIF1, $CD4^{+}CD25^{-}$ polarisation w/ TFGb	No effect on iTreg generation	
	Lee et al., 2015	Hydroxylation resistant HIF1	↑ IFNγ production by Tregs	Did not measure same parameters as most others
PHD KO/ inhibition	Clambey et al., 2012	*In vitro* AKB-6899 on Jurkat cells	↑ Foxp3 mRNA	1h treatment
	Yamamoto et al., 2019	shRNA KD	Autoimmune-like phenotype and increased Treg, reversible by HIF2 KO only	Only phenotype observed at baseline
VHL KO/ inhibition	Lee et al., 2015	$Foxp3^{Cre}$ VHL KO	KO Tregs no proliferation defect *in vivo* but lose Foxp3 after proliferation, also produce more cytokines	↑ IFNγ, IL-10, GM-CSF, IL-4, MIP-1a/b, RANTES, and TNFα

In vivo survival	Hsiao et al., 2015	1w coadministration of Tconv and WT/Dltx KO Treg into $Rag^{-/-}$ mice	Fewer $Foxp3^{+}$ Tregs recovered in mice receiving Dltx KO Tregs	High HIF1 impairs Treg stability/survival *in vivo,* implications for *in vivo* inflammatory models
$CD45^{RB}$ CD4 transfer colitis model	Hsu et al., 2020	Co-transfer WT or HIF2KO Tregs	HIF2KO Tregs <u>do not</u> prevent colitis	Internally consistent
		Co-transfer WT or HIF1KO Tregs	HIF1KO Tregs <u>do</u> prevent colitis	
	Clambey et al., 2012	Co-transfer WT or HIF1KO Tregs	HIF1KO Tregs <u>do not</u> prevent colitis	Consistent with Hsu et al.
	Hsiao et al., 2015	Deltex KO increases HIF1	KO Tregs barely prevent colitis, additional HIF1 KO regains suppression	Effects could be due to HIF2, not assessed
	Lee et al., 2015	Tregs from $Foxp3^{Cre}$ VHL KO mice	VHL KO Tregs do not prevent colitis, unless also KO HIF	KO Tregs lost Foxp3 expression in vivo after 8w
OVA airway allergy model	Hsiao et al., 2015	Deltex KO increases HIF1, OVA allergen induced allergy with OVA re-challenge	KO Tregs did not prevent allergy	Different HIFs targeted
	Hsu et al., 2020	$CD4^{Cre}$ HIF2 KO mice	HIF2 KO Tregs do not prevent allergy	
EAE model	Dang et al., 2011	$CD4^{Cre}$ HIF1 KO mice	HIF1 KO mice resist, ↓Th17, ↑Treg	Only EAE model
In vivo cancer model	Hsu et al., 2020	Syngeneic MC38 colon adenocarcinoma	HIF2KO mice resistant to tumour	Only tumour model
		B16F10 melanoma	HIF2KO mice not resistant, but $Foxp3^{Cre}$ HIF2KO suppressed metastasis to lungs	
Skin transplant	Yamamoto et al., 2019	PHD2 shRNA KD Tregs	Tregs unsuppressive and even pathogenic	Only transplant model

Clambey et al. and Ben-Shoshan et al.'s shorter term experiments with only a few hours of *in vitro* hypoxia induced Foxp3, whereas experiments that showed that HIF was bad for Foxp3 in vivo were carried out for 5-6 days[99,261], so the timing might be responsible for discrepancies. Furthermore, Clambey et al. showed that IL-6 impaired hypoxic induction of Foxp3, so its use in Th17 skewing studies might explain those results[260]. Hsu et al. showed that low doses (0.5ng/ml) of TGFß could improve iTreg differentiation in hypoxia, despite their findings that hypoxia impaired Foxp3 induction in hypoxia otherwise[260]. Therefore, even minute differences in dosage can have opposing effects on Foxp3 in hypoxia and this could explain some of the disparity between experiments. Additionally, the table above highlights that even similar experiments had slightly different experimental approaches, and are therefore not exactly comparable.

There are significant data showing both stabilisation and deregulation of Treg phenotype and function, without one side having clearly more supporting evidence than the other. Furthermore, the effects of increased HIF expression are not necessarily the opposite effects of decreased HIF expression, and homeostasis within a comfortable range is likely needed to maintain balance. In a practical inflammatory context, it would be beneficial for inflammatory hypoxia to drive either decreased suppression from Tregs to allow clearing of the infection or challenge, or an increase in Tregs to drive resolution and limit immunopathology. Timing and complex immunological cues from the microenvironment may be able to determine which of these outcomes is predominant. Based on the current literature, there is clearly a need for more research on HIF function in Tregs.

1.5b – Iron Signalling and Tregs

In contrast to HIF signalling, much less work has been done to understand iron handling in Tregs. The authors who identified iron-related genes as the predictors of operational tolerance in liver recipients[234] also used iron chelation during iTreg generation *in vitro* and found that fewer Tregs were generated and that they had decreased CD25 expression and STAT5 phosphorylation, but not when chelators were added 24h after activation, indicating that low iron only impaired early activation and differentiation of Tregs[264]. They also used diet-induced systemic iron deficiency and found no change in Treg presence or production of IL-10 and

TGFß[265]. In a different model however, low iron diet did increase the proportion of Tregs, which stayed increased even in an SLE model and slowed disease progression due to increased Treg:Th17 ratio[220]. There is further evidence that iron deficiency impairs Th17 induction *in vitro*[266], indicating that iron can impair other T cell subsets and overall polarisation of the T cell compartment. Iron deficiency was also shown to affect CD4 T cells disproportionately to CD8 cells, with lower CD4:CD8 ratios seen in children with iron deficiency anaemia[267], which might have implications for Tregs. In thalassemia patients with iron overload, Tregs were also found to be increased, and correlated with ferritin[268], indicating that iron imbalance either way seems to increase Tregs proportion.

Mechanistically, little is known about how iron might differentiate Tregs from Tconvs. One study showed that iron chelation inhibited mTOR signalling and promoted glucose metabolism which increased Treg proportion and decreased inflammation[269]. In SLE patients, serum iron deficiency and anaemia are fairly common, but their $CD4^+$ T cells have been known to be iron-loaded as seen by increased expression of Tfrc; Tfrc deletion impaired Th1 cells but improved Foxp3 expression and IL-10 secretion in iTregs via altered mTOR signalling and mitochondrial fitness[221], and Tfrc blockade induced Treg genes even under Th17-skewing conditions[218]. Tfrc expression is naturally higher on Tregs, which might help them survive better in low iron conditions but could equally be responsible for their loss of function in aberrant cellular iron loading such as is seen in SLE T cells. Disruption of PI3K-mTOR signalling could reduce Tregs within the CD4 compartment, and Treg-specific disruption induced ROS overload and iron accumulation, leading to apoptosis and decreased suppression *in vitro* and *in vivo* despite normal Foxp3 levels[270,271]; this is further indication that iron overload is detrimental to Tregs and T cells.

Furthermore, not only does iron impact Tregs but Treg activation was shown to affect systemic iron storage and handling: Treg-restricted STAT5 induction led to mobilisation of iron stores from the liver and spleen into adipose tissue in mice on high fat diets[272]. Tregs accumulate in visceral adipose tissue where they rely of fatty acid oxidation and the hormone leptin, which increases after meals and in obese individuals, induces mTOR signalling to impair Tregs[273] and provides a further link for how Tregs might regulate systemic nutrient availability and combine nutrients such as iron with inflammatory patterns.

1.6 – AIMS AND OBJECTIVES

As the previous section highlights, there is much to learn about the subtleties of how hypoxic signalling and iron availability might affect Tregs. Immune research often focuses on conventional T cells, but Tregs are a clearly functionally distinct subset with huge implications on tolerance and the wider immune landscape; better understanding how they function in hypoxic and hypoferremic environments such as sites of inflammation is of great advantage in realising their full potential as powerful immune mediators and has implications in all aspects of immunity and disease, ranging from cancer and infections to autoimmunity and transplants.

GLOBAL AIM: To explore how the HIF pathway and iron availability impact immune responses with a focus on Tregs

SPECIFIC AIMS:

1. To better understand the impact of individual components of the HIF signalling pathway on Tregs and immune responses
2. To understand how HIF signalling impacts the Treg transcriptional programme
3. To investigate how iron deprivation affects Treg phenotype and function
4. To understand how iron limitation affects immune responses to a transplant

2 – METHODS

2.1 – REAGENTS

Table 4 – List of general reagents

REAGENT	CATALOG NO.	MANUFACTURER
2ppm iron diet	TD.99397	Teklad
200ppm iron diet	TD.07801	Teklad
Apotransferrin	T1147	Sigma-Aldrich
Beta-mercaptoethanol	31350010	Gibco
$CD4^+$ T cell isolation kit	130-104-454	Miltenyi
cDNA RT kit	4368814	Thermofisher
Collagenase P	11213857001	Sigma-Aldrich
DNAse I	10104159001	Sigma-Aldrich
EDTA	15575020	Sigma-Aldrich
Foetal bovine serum	26140-087	Sigma-Aldrich
Fc block	101302	BioLegend
Foxp3 staining buffer set	00-5523-00	eBioscience
Holotransferrin	T0665-50MG	Sigma-Aldrich
IL-2	575406	BioLegend
αIL-2	503706	BioLegend
L-glutamine	49419	Sigma-Aldritch
LS columns	130-042-40	Miltenyi
mini-Hepcidin	Custom	Chinese Peptide Company
Pannexin serum	P04-95080	Pan Biotech
Penicillin/streptomycin	P4458	Sigma-Aldritch
PCR probe Arnt1	Mm00507824_m1	TaqMan
PCR probe Arnt2	Custom probe to span exon 5	TaqMan
PCR probe B2M	Mm00437762_m1	TaqMan
PCR probe Hif1a	Mm01283756_m1	TaqMan
PCR probe Epas1	Mm00438712_m1	TaqMan
PCR probe Pgk1	Mm00435617_m1	TaqMan
PCR probe Vegfa	Mm00437306_m1	TaqMan
PharmLyse	555899	BD Bioscience
Perfecta qPCR supermix	101414-204	Quanta Bio
Qubit High Sensitivity kit	Q33230	Invitrogen
RNA extraction mini kit	74104	Qiagen
RPMI 1640	12-0453-82	Gibco
SL220	DSPE-020CN	NOF
T cell activator beads	11452D	Gibco
UltraComp eBeads	01-2222-41	Invitrogen
VPD	562158	BD Bioscience
Zombie NIR	423105	BioLegend

Table 5 – List of antibodies used

TARGET	CLONE	FLUOROCHROME	CATALOG NO.	MANUFACTURER
B220	RA3-6B2	APC e780	47-0452-82	Life Technologies
B220	RA3-6B2	FITC	103206	BioLegend
B220	RA3-6B2	FITC	553088	BD Bioscience
B220	RA3-6B2	PE-Cy7	24-0452-82	eBioscience
CD3	17A2	BV605	100237	BioLegend
CD3	17A2	PE	100206	BioLegend
CD3	145-2C11	PE-Cy7	25-0031-82	eBioscience
CD4	GK1.5	APC	17-0041-83	eBioscience
CD4	GK1.5	APC e780	47-0041-82	eBioscience
CD4	GK1.5	e450	48-0041-82	Life Technologies
CD4	GK1.5	FITC	100405	BioLegend
CD4	RM4-5	FITC	11-0042-82	eBioscience
CD4	GK1.5	PE	12-0041-83	eBioscience
CD8	53-6.7	AF700	100730	BioLegend
CD8	53-6.7	APC	17-0081-83	eBioscience
CD8	53-6.7	BV785	100749	BioLegend
CD8	52-6.7	FITC	11-0081-55	eBioscience
CD11b	M1/70	APC-Cy7	101225	BioLegend
CD11b	M1/70	PE-Cy7	25-0112-82	Life Technologies
CD19	1D3	PE	12-0193-83	eBioscience
CD25	PC61.5	APC	17-0251-82	Invitrogen
CD25	3C7	BV421	564370	BD Horizons
CD25	PC61.5	PE	12-0251-83	eBioscience
CD25	PC61	PE CF594	562695	BD Bioscience
CD25	PC61	PE-Dazzle	102048	BioLegend
CD28	37.5	PE	12-0281-81	eBioscience
CD44	IM7	BV605	103047	BioLegend
CD44	IM7	e450	48-0441-82	eBioscience
CD44	IM7	PE	12-0441-83	eBioscience
CD44	IM7	PE-Cy7	103030	BioLegend
CD45	30-F11	e450	48-0451-82	Invitrogen
CD45	30-F11	PE e610	61-0451-82	Invitrogen

CD45.1	A20	APC	17-0453-82	eBioscience
CD45.1	A20	PE	12-0453-82	Life Technologies
CD45.2	104	e450	48-0454-80	eBioscience
CD26L	MEL-14	PE	553151	BD Bioscience
CD62L	MEL-14	PE-Cy7	25-0621-82	eBioscience
CD69	H1.2F3	BV510	104531	BioLegend
CD69	H.2F3	PE	12-0691-82	eBioscience
CD71	R17217	e450	48-0711-80	eBioscience
CD71	RI7217	PE-Cy7	113811	BioLegend
CD95	SA367H8	PE-Cy7	152618	BioLegend
CTLA-4	UC10-4B9	APC	17-1522-82	eBioscience
CTLA-4	UC10-4F10	PE	A27090	Life Technologies
CXCR3	CXCR3-173	FITC	11-1831-80	eBioscience
Foxp3	FJK-16s	APC	17-5773-80	Invitrogen
Foxp3	FJK-16s	e450	1988692	Invitrogen
GATA3	TWAJ	PE e610	61-9966-42	Invitrogen
GITR	DTA-1	APC e780	47-5874-82	Life Technologies
Gr1	RB6-8C5	APC	17-5931-82	Invitrogen
GzmB	NGZB	PE e610	61-8898-82	Life Technologies
Helios	22F6	e450	48-9883-42	Invitrogen
Icos	C398.4A	PE-Cy7	25-9949-80	eBioscience
IgD	11-26c.2a	APC	405713	BioLegend
Ki67	16A8	FITC	652410	BioLegend
Ki67	SolA15	PerCP e710	46-5698	eBioscience
NKG2D	CX5	PE	12-5882-82	eBioscience
RORγT	AFKJS-6	PE	12-6988-82	eBioscience
PD-1	RMP1-30	FITC	11-9881-81	eBioscience
Tbet	4B10	PE-Cy7	25-5825-82	eBioscience
TCRβ	H57-597	BV510	109233	BioLegend
TCRβ	H57-597	e450	48-5961-82	eBioscience
7-AAD	-	-	00-6993-50	Invitrogen

2.2 – In Vivo Mouse Studies

2.2a – Mice

Mice were housed in individually ventilated cages with food and water ad libitum in the biomedical services unit at the tile-clad John Radcliffe hospital and the Wellcome Trust Centre for Human Genetics. Male and female mice were aged 6-15 weeks unless otherwise stated. All procedures and husbandry were according to the Animal Scientific Procedures Act (1986) under the Oxford establishment license XEC303F12, project licenses P8869535A and P38BE32DE, and PIL no. I07781948.

Table 6 – List of mouse strains used

Mouse Strain	Abbreviation	Use
CBA/Ca	CBA	$H2^k$ full mismatch skin donors
C57BL/6	WT B6	WT controls
C57BL/6 $RAG^{-/-}$	$RAG^{-/-}$	"Empty" recipients without T and B cells for adoptive cell transfer
C57BL/6 $Foxp3^{GFP}$ reporter	$Foxp3^{GFP}$	GFP^+ Tregs, control cells
$RosaERTCre^{+/+}$ $HIF\text{-}1\alpha^{fl/fl}$	HIF-1α KO	HIF-1α KO
$RosaERTCre^{+/+}$ $HIF\text{-}2\alpha^{fl/fl}$	HIF-2α KO	HIF-2α KO
$RosaERTCre^{+/+}$ $HIF\text{-}1\alpha^{fl/fl}$ $HIF\text{-}2\alpha^{fl/fl}$	HIF1/2 DKO	HIF1/2 DKO
$RosaERTCre^{+/+}$ $ARNT1^{fl/fl}$ $ARNT2^{fl/fl}$	ARNT1/2 DKO	ARNT1/2 DKO
$RosaERTCre^{-/-}$	$Cre^{-/-}$ control	Controls for HIF/ARNT KOs with various floxed alleles
WT B6.SJL-Ptprca Pepcb/BoyJ	SJL	Expression of CD45.1
$Tfrc^{Y20H/Y20H}$	Tfrc	Hypomorphic transferrin receptor for cell-intrinsic iron deficiency

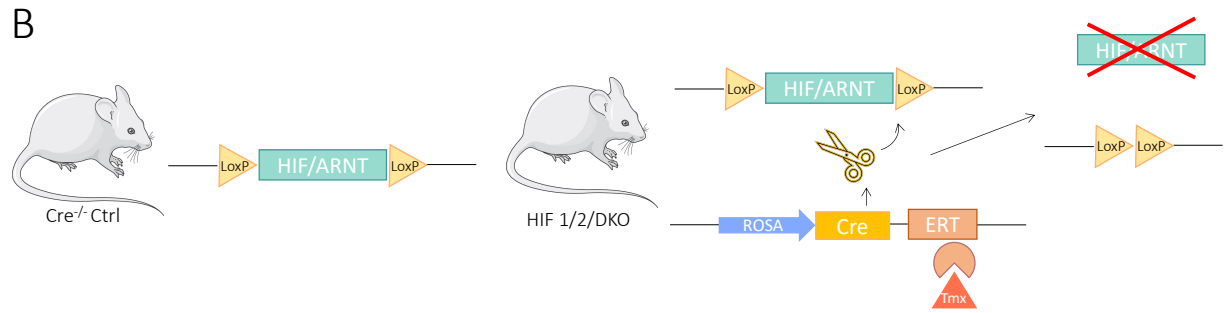

Fig 2.1 – Schematic overview of PHD2 KD and HIF/ARNT KO mice. (A) Mice with a reverse tetracycline transactivator (rtTA) element under the CAGG promoter were used as a control. These mice were bred with PHD2 KD mice that have a tetracycline response element (TRE) that responds to the rtTA protein, activated by doxycycline administration. In mice with both these elements, the doxycycline drug activates the downstream motif of mRNA encoding a short hairpin RNA (shRNA) that interferes with PHD2 mRNA translation to protein, as well as GFP protein for easy identification. Mice generated by Atsushi Yamamoto. Figure adapted from Kento Kawai's thesis. (B) Floxxed mice without the Cre allele were used as controls. HIF-1α KO mice have LoxP sites around exons 13-15[274], HIF-2α around exon 2[275], ARNT1 around exon 6[276], and ARNT2 around exon 5, as generated by Ben Davies (more data available in Maria Prange-Barczyńska's thesis). When crossed with mice expressing the Cre allele downstream of ubiquitous Rosa26 promoter, the Cre enzyme is able to recombine the LoxP sites and delete the exon framed between them. This Cre allele is bound to a mutated estrogen receptor (ERT) which only activates the Cre enzyme when bound to tamoxifen (tamoxifen)[277], allowing it to be drug-inducible.

2.2b – Skin Transplantation

Tail skin was harvested from wildtype CBA mice by making a long incision along the ventral length of the tail and a circular incision at the top of the tail, which allowed the tail skin to be degloved with forceps. The skin was cut into 1cm^2 squares with a scalpel and kept in cold PBS on ice until transplantation. Recipient mice on a B6 background mice were anaesthetised with volatile isoflurane for both induction and maintenance anaesthesia. Surgery was performed with sterile surgical gloves and autoclaved surgical instruments that were heat-sterilised between mice. Anaesthetised recipient mice were placed on a heating pad and a 1cm^2 section of skin was excised from their left flank. The full thickness grafts were placed on and either glued to the graft bed with Histoacryl glue or sutured in place with 6-0 prolene sutures. 1cm^2 squares of Mepitel dressing and Inadine, as well as rolled gauze for compression, were applied to the graft, followed by plasters and autoclave tape around the abdomen for compression and protection. Mice were allowed to recover in warmed recovery chambers and given nestlets and soggy food on the floor of their cages for the following week. Bandages were removed after a week and replaced under anaesthesia if removed prematurely by the mice. Graft rejection was measured on a 5-point system (*Table 7*).

Table 7 – Graft scoring system

GRAFT SCORE	DESCRIPTION
0	No damage/change
1	Dryness, roughness, hair loss, small red blood spots
2	Active lesions (large blood spots), contraction, significant dryness/roughness
3	Significant necrosis, darkening, scabbing, lifting/peeling of edges
4	Graft has fallen off

2.2c – ADOPTIVE CELL TRANSFERS

Recipient mice were previously warmed in a warming chamber for 30min prior to injection and secured in restrainer tubes. Cells were injected intravenously into the tail lateral vein: 100µl of purified $CD4^+CD25^-$ T cells at 10^5/ml (10^4/mouse) in RPMI for the T cell adoptive transfer (*section 6.2d*), 150µl of $CD4^+CD25^+$/ $CD4^+CD25^-$ cells mixed 5:1 at 400,000/ml in PBS for the Treg adoptive transfer (*section5.2c*), and 200µl of bone marrow cells at 10^6/ml ($2x10^5$/mouse) in PBS for the chimera experiments (*sections 5.2d, 6.2e*). Pressure was applied to the tail until bleeding subsided. IV injections were kindly performed by Roo Bhasin and Fadi Issa.

2.2d – MIXED BONE MARROW CHIMERAS

Female SJL (CD45.1) mice aged at least 8 weeks in order to withstand the irradiation were irradiated with 4.5 Gy for 300s, followed by a 3-hour rest, and a subsequent 4.5 Gy dose for 300s. In the meantime, spleens were harvested from male SJL (CD45.1), WT B6 (CD45.2), and Tfrc (CD45.2) mice and cell suspensions were created with a mix from 6 SJL mice and 3 WT/Tfrc mice to create two distinct mixes of 50:50 SJL:WT and SJL:Tfrc (the same mix of SJL was used for the CD45.1 portion of both mixes). Upon repeat of this experiment, 2 distinct biological replicates were created with 4 SJL mice, 4 WT mice, and 4 Tfrc mice to create 4 distinct mixes (2 SJL:Tfrc mixes and 2 :WT:SJL mixes), allowing for a total of 3 biological repeats when combined with the first experiment. Mice were allowed to reconstitute for 12

weeks during the first iteration of this experiment and 8 for the second, as no further changes were observed past 8 weeks the first time. Mice were given 0.16mg/ml of Baytril antibiotics in drinking water for 4 weeks after irradiation. Half the cohort was harvested at baseline and the other half was given fully mismatched CBA skin transplants and harvested at day 10 during peak rejection.

2.2e – Environmental Hypoxia

Mice on a Cre^+ background and tamoxifen-treated Cre^- controls were treated daily for 5 days with tamoxifen at a dose of 2mg/day in 100µl oral gavages administered by staff at the Wellcome Trust Centre for Human Genomics. Tamoxifen was made up by resuspending 400mg of tamoxifen in 1.6ml of 100% ethanol for 30 minutes at 37˚C, and dissolving in 20ml of corn oil with shaking and intermittent vortexing at 37˚C over 6-7 hours, which was generously prepared by Julie Adams. After 5 days treatment Monday-Friday, mice were rested for 4 days and hypoxia was induced on the following Wednesday. Mice from the 4-week single cell experiment were kindly provided with 2mg/ml doxycycline ad libitum in drinking water with 30% sucrose with 1 week of pre-treatment prior to hypoxia by Tammie Bishop. Mice were housed in a sealed normobaric chamber and oxygen tension was gradually reduced to 10% over the course of the first 3 days. Mashed feed mixed with water was provided on their cage floor to counteract weight loss in the first few days of hypoxia treatment. At the end of the harvest, mice were euthanised by exposure to an isoflurane overdose while in the hypoxic chamber to avoid reoxygenation.

2.2f – Blood Sampling

In order to encourage vasodilation, mice were either warmed in a warming chamber for 30min or had their tails held by hand for a few minutes prior to injection and were secured in restrainer tubes. A small incision into the lateral tail vein was made with a sterile scalpel blade and 50-70µl of blood was collected into capillary action collection tubes and supplemented with 50µl heparin. Pressure was applied to the tail until bleeding subsided. In terminal experiments, mice were put under terminal volatile anaesthesia and the inferior vena cava was exposed and drained with a 25-gauge needle prior to Schedule 1 confirmation.

2.2g – Intraperitoneal Drug Administration

Mini-hepcidin PR73 (da-TH-Dpa-bhPro-RCR-bhPhe-Ahx-Ida(Hexadecylamine)-NH2, mHep) was dissolved in 80% ethanol and mixed with 60mg of Purebright SL220/Sunbright DSPE-020CN (SL220), and control mHep-free SL220 carrier was dissolved in ethanol. The ethanol was evaporated at 50˚C in a vacuum chamber to create a gel, which was stored at 4˚C for up to 24h. This was mostly prepared for us by Joe Frost. Gel was dissolved in sterile water by vortexing for 10-15mins and injected at 1mM in 100µl.

αCD28 kindly sent to us by the Vanhove lab was prepared at 2mg/ml in PBS and 100µl was injected into each mouse for a dose of approximately 10mg/kg. αIL-6 sent to us by the Vanhove lab was prepared at 1.125mg/ml in PBS and 200µl was injected into each mouse for a dose of approximately 11.25mg/kg. IL-2 complex (IL-2c) was prepared at 6.66µg/ml with 150µl injected into each mouse for a dose of approximately 0.05mg/kg. IL-2c was prepared with IL-2 and αIL-2 at a ratio of 1:5 which were incubated at 37ºC for 30mins to bond. Mice were scruffed and 100-200µl of substance was injected with an insulin needle through the skin and peritoneum into the lower abdomen, lateral to the midline.

2.3 – Flow Cytometry

2.3a – Cell Suspension Preparation

Spleens and peripheral (inguinal, brachial, and axillary) lymph nodes were harvested from mice sacrificed by Schedule 1 cervical dislocation and kept in PBS on ice. In experiments requiring FACS sorting of Tregs, cervical lymph nodes were also included in order to achieve necessary number of Tregs. Organs were mechanically disrupted through a 70µm cell strainer (BD Bioscience) with a striated plastic plunger recycled off the back of a pipette or LS column and washed through with FACS buffer (PBS supplemented with 4% FBS and 0.2% sodium azide) into 50ml falcon tubes. Splenocytes were pelleted by centrifugation and resuspended in 5ml of 10X diluted PharmLyse buffer in diH_2O and incubated for 5-10mins at room temperature before washing with 5ml PBS. Suspensions from whole blood were resuspended 1ml of the same diluted PharmLyse buffer for 10mins at room temperature before centrifugation, which was repeated once more before staining.

For skin digestion, skin grafts were excised with a scalpel during harvest, and transferred into RPMI supplemented with 10% FBS to make 10% RPMI and kept on ice. Grafts were finely cut into smaller pieces with a scalpel and transferred into a 6-well plate containing 3ml of RPMI + 10% FBS + 1mg/ml collagenase P and incubated at 37˚C for 30 mins. 1ml and then 2ml of the same collagenase P 10% RPMI media were added at 30min intervals with mixing and agitation with a Pasteur pipette, and mixing at 30min intervals continued for a further hour without adding more media. After those two hours of incubation, 1ml of 0.1mg/ml DNAse I in 10% RPMI was added to improve cell viability with more mixing for a final half hour, after which wells were strained and mashed through a 70µm filter with thorough rinsing of the wells. Enzymatic reactions were stopped with 10mM EDTA in PBS and further washed in 10% RPMI before resuspending in 200µl FACS buffer for staining.

2.3b – Staining Protocol

Cell suspensions were transferred to V bottom 96-well plates. Cells were resuspended in 100µl of αCD16/32 Fc block solution in PBS at 1µg/10^6 cells for 15 mins in the dark at room temperature and rinsed with PBS. Cells were pelleted by centrifugation and extracellular antibodies were added at 0.25µl/well in 10µl FACS buffer. Extracellular antibodies were incubated in the dark at 4°C for ~30 min before washing with FACS buffer. For intracellular staining, this was followed by fixation and permeabilization with the Foxp3/Transcription Factor Staining Buffer Set) according to manufacturer instructions, with incubation in the fixation/ permeabilization buffer either for 45mins or overnight. Permeabilised cells were pelleted by centrifugation and intracellular antibodies were added at 0.5µl/well or according to Kento Kawai's previous titrations in 10µl FACS buffer for 45mins. Cells were then washed with 200µl/well permeabilization buffer according to manufacturer instructions and resuspended in 200µl FACS buffer. Cells were processed on the same day or left overnight in the dark at 4°C to be run the next day as it was usually 3am by this point. Compensation was performed with 0.25-1µl of antibody in 100µl of 1drop/ml of UltraComp counting beads, which was incubated for ~20mins at 4°C and washed with FACS buffer.

2.3c – Data Acquisition and Statistical Analysis

Flow cytometry was run on either the BD FACSCanto II or the Attune Nxt Flow Cytometer. Data was analysed with FlowJo software (version 10). Statistical analysis was performed on GraphPad prism with the following annotations for p values:

Table 8 - P value annotations used throughout thesis

Symbol	P Value
ns	$p > 0.05$
*	$p < 0.05$
**	$p < 0.001$
***	$p < 0.005$
****	$p < 0.001$

2.4 – In Vitro Experiments

2.4a – Magnetic Cell Enrichment

$CD4^+$ cells were isolated by negative selection using the Miltenyi $CD4^+$ T cell isolation kit with a few deviations from the manufacturer's protocol: as high purity was not paramount in cells destined for FACS sorting, amount of antibody cocktail and magnetic beads added was decreased down to a quarter of manufacturer-suggested volumes. Furthermore, to conserve LS columns, columns were used up to three times with flushing out of $CD4^-$ magnetically labelled fraction in between separations and repeating the pre-rinsing step before applying the next volume. Cells to be cultured without subsequent FACS sorting were isolated without these deviations, and purity was further ensured by applying the enriched $CD4^+$ population on a second, clean and pre-rinsed LS column. Buffer was made with PBS + 2% FCS + 2mM EDTA.

2.4b – Fluorescence Associated Cell Sorting

After magnetic enrichment, cells were counted and pelleted by centrifugation. Approximately1µl/10^6 cells of CD4/CD25 antibody and 2.5µl/10^6 cells of 7-AAD were added in residual volume and stained for ~30mins in the fridge. Cells were washed in PBS, resuspended in RPMI + 2% FCS, and filtered through a 10µm filter, before sorting on the BD FACSAria II.

2.4c – Low Iron Culture Assays

Pannexin media was prepared with RPMI + 10% Pannexin NTS serum substitute + 100IU/ml Penicillin + 0.1mg/ml streptomycin + 55µM β-mercaptoethanol. Iron was titrated in with decreasing amounts of holotransferrin (transferrin bound to 2 iron molecules) and corresponding increasing amounts of apotransferrin ("empty" transferrin unbound to iron), keeping total transferrin levels constant at 1.2 mg/ml (*Table 9*). 100,000 cells per well were seeded at 1x10^6/ml in 200µl in U-bottom plates with 50,000 αCD3/CD28 coated beads for a cell:bead ratio of 2:1, along with 100IU/ml of IL-2. IL-2 but no beads were added to unstimulated wells. Practically, media with transferrin was prepared at 2X concentration for each condition and 100µl was added to wells, with cells at 2x10^6/ml (2X) in 50µl of transferrin-free Pannexin media, and beads at 1x10^6/ml (2X) in 50µl of transferrin-free Pannexin media, for correct final concentrations.

Table 9 – Iron titration conditions used for *in vitro* studies

Holotransferrin	0.625 mg/ml	0.125 mg/ml	0.025 mg/ml	0.005 mg/ml	0.001 mg/ml
Apotransferrin	0.575	1.075	1.175	1.195	1.199

2.4d – Treg Suppression Assays

After sorting out Tregs and Tconvs with FACS sorting (section 2.4b), Tconvs were resuspended at 2x10^6/ml in complete media (RPMI + 10% FCS+ 100IU/ml Penicillin + 0.1mg/ml streptomycin + 55µM β-mercaptoethanol) and 100,000 cells (50µl) were plated. Tregs were resuspended at 1x10^6/ml and 100µl were added to the 1:1 condition before 2X serial dilution with complete media to add 50,000, 25,000, and 12,500 to the 1:2, 1:4 and 1:8 conditions respectively. αCD3/CD28-coated T cell activator beads were rinsed in RPMI on a

magnet to remove sodium azide and resuspended at $1x10^6$/ml in complete media, and 50µl (50,000 beads) were added for a 1:2 ratio with responder T cells. In unstimulated controls and positive controls, 50µl complete media was added in place of beads and Tregs respectively.

2.4e – VPD LABELLING

VPD was kept in 1mM aliquots at -80˚C and thawed before use, keeping light exposure to a minimum. Cells were washed twice with excess PBS to remove protein and resuspended at 10-30$x10^6$/ml (minimum of 1ml if fewer than $10x10^6$ cells) and 1µL/ml of 1mM VPD was added and incubated for 10-15mins at 37˚C before rinsing with 10X the volume of PBS.

Division index was calculated by gating on individual VPD peaks to gate individual division cycles and calculated according to the following equation. % of suppression was normalised to the Treg-free positive control.

Equation 1 – Division Index

$$\text{Div. Index} = \frac{\text{\# cell divisions}}{\text{\# precursor cells}} = \frac{\frac{(\text{\# cell divisions}_1)}{2^1} + \frac{(\text{\# cell divisions}_2)}{2^2} + \cdots + n\frac{(\text{\# cell divisions}_n)}{2^n}}{\frac{(\text{\# cell divisions}_0)}{2^0} + \frac{(\text{\# cell divisions}_1)}{2^1} + \cdots + n\frac{(\text{\# cell divisions}_n)}{2^n}}$$

n= # of the division peak

2.5 – SINGLE CELL RNA SEQUENCING

Cells were isolated from mouse lymph nodes as described above and resuspended in PBS + 1% BSA. Cells were then incubated with 1µl/10^6 cells of TruStain FcX anti-mouse CD16/32 (BioLegend) for 10mins at 4C. 1µl/10^6 cells of TotalSeq-B hashtag oligo (HTO) antibodies (BioLegend) was added to the 5 biological groups and incubated for 30mins at 4°C in the dark. Cells were then washed 3 times with PBS + 1% BSA and all 5 groups were pooled together for CD4 bead sorting, as described above (*see section 2.4a*). The cell preparation was performed by Kento Kawai before I joined the lab to analyse the data. Cell count and viability was assessed with a Countess II Automated Cell Counter and cells were processed with Chromium Single Cell 3' Reagent Kits with Feature Barcoding Technology for Cell Surface Protein (10X Genomics). Libraries were sequenced on 2 or 3 separate cartridges by the Wellcome Trust Centre for Human Genomics.

Fastq files was pre-processed and reads were aligned to the mm10 reference genome using CellRanger by the Wellcome Trust Centre for Human Genomics using the mkfastq and multi pipelines with default parameters. Data was imported into RStudio (R version 3.6.2) via the Seurat Read10X function (Sajita Lab), and hashtag oligo demultiplexing, data filtering, normalisation, PCA regression, and tSNE/UMAP clustering was performed according to Seurat package workflow (Sajita Lab) using code written by Ran Li. Contaminant $CD8^+$, γ∂ T cell, myeloid cell, and B cell populations identified by cluster gene expression were removed from the analysis to reduce noise. Comparisons between hashed groups and between cell clusters was performed with the FindMarkers function of the Seurat package (Sajita Lab) and differentially expressed genes with adjusted p values > 0.05 were filtered out. Remaining differentially expressed genes (with adjusted p values < 0.05) were ordered by LogFoldChange for GSEA enrichment against the MSigDB Hallmark dataset with the fgsea package in R, where positive fold change at the top of the list showed genes represented in controls and negative fold change at the bottom of the list showed genes represented in the target group. Lisa analysis for transcription factor enrichment[278] was performed on genes positively enriched in the PHD2 KD Tregs and input into the Lisa analysis software online. Top 30 ranked genes output by Lisa analysis were plotted using ggplot2 in R.

2.6 – Bulk RNA Sequencing

$Foxp3^{GFP}$ mice were exposed to environmental hypoxia (*see section 2.2e*) for 6 weeks, and their peripheral and cervical lymph nodes were harvested. Cells from 2 mice were pooled together to reach appropriate numbers and $CD4^+$ cells were enriched by magnetic selection (*see section 2.4a*). Cells were separated into $7AAD^-CD4^+GFP^+CD25^+$ and $7AAD^-CD4^+GFP^+CD25^-$ fractions by FACS sorting (*see section 2.4b*). Samples were frozen as dry cell pellets at -80°C and shipped to Novogene for RNA extraction and RNA library preparation with poly A enrichment using their low input library preparation pipeline.

Output counts were aligned to the mouse genome by Oliver McCallion, for which I will forever be eternally grateful: reads were aligned to the reference mouse genome GRCm38 using STAR (version 2.7.10) on the Advanced Research Computing HPC at the University of Oxford.

SAM files were sorted and indexed using samtools (1.15.1). Pre- and post-alignment quality control was performed (fastqc 0.11.9, multiqc 1.12, picard 2.27, samtools flagstat, samtools idxstat). Aligned reads were quantified with featureCounts (subread 2.0.1) against the GRCm38 annotated gene list. I then processed raw aligned counts in R and differential expression was performed using DESeq2. Significant genes with an adjusted p value < 0.05 were selected and plotted using the EnhancedVolcano and pheatmap packages in R.

2.7 – qPCR Analysis

Cells for RNA extraction were resuspended in 350µl of RLT buffer from the Qiagen Mini Kit and frozen at -80˚C. Cells were later thawed and RNA extraction was performed using the Qiagen Mini Kit according to manufacturer instructions, starting from the step after RLT buffer addition. RNA was eluted in 30-40µl of RNAse-free water and RNA levels were quantified using the Qubit High Sensitivity kit on a Qubit 4 Fluorometer. RNA samples were measured 3 times each to take an average. cDNA was prepared using the High Capacity cDNA Reverse Transcription Kit (ThermoFisher) according to manufacturer instructions, and combined 20µl reactions with 0.25µg of RNA in 20µl water for each sample. Samples were incubated in the thermocycler at 37 ˚C for 2 hours, then at 85˚C for 5 mins, and then kept at 4˚C for up to a week before use. qPCR reactions were prepared using PerfeCta supermix (Quanta Labs) and 2µl of cDNA with 10X diluted RNA probes (*see Table* 4). Samples were loaded onto 96-well or 384-well optical plates, centrifuged vertically to remove bubbles, and run using the Quant Studio 7 Flex System for Comparative Ct (ΔΔCt) using a fast run. Relative expression was calculated against the B2M housekeeping gene from Ct values using the following equation:

Equation 2 – ΔΔCt values for qPCR

$$\Delta Ct = (Ct \text{ of target gene}) - (Ct \text{ of housekeeping gene})$$

$$\Delta\Delta Ct = (\Delta Ct \text{ KO}) - (\Delta Ct \text{ in } Cre^{-} \text{ ctrl}) \text{ for } n \text{ target genes}$$

$$\text{Relative expression} = 2^{-\text{Log}\Delta\Delta Ct}$$

3 – Effects of Hypoxia and HIF Signalling on Tregs and the Immune System

3.1 – INTRODUCTION AND AIMS

Inflammatory settings often involve consumption of nutrients and oxygen, and therefore immune cells are likely to operate in areas of hypoxia. Prior to my arrival, the TRIG lab (namely Kento Kawai, who carried out much of the work discussed in this chapter introduction) collaborated with the Ratcliffe Group – chiefly Chris Pugh and Atsushi Yamamoto – to try to make use of a novel mouse model with PHD2 KD that allowed study of elevated HIF signalling in normoxic conditions. This model was engineered by Atsushi Yamamoto and made use of a shRNA targeting PHD2, which is the most ubiquitously expressed of the PHDs. This was placed under the control of a tetracycline-dependent promoter that allowed this to be inducible and reversible via administration of doxycycline. This model was originally anticipated to be useful for studying haematological parameters and HIF's role in anaemia and wound healing, so our lab's involvement was originally to provide surgical assistance to experiments; unexpectedly, the mice seemed to develop an immune phenotype, and Fadi Issa harvested the lymph nodes during harvest after noticing their enlargement. Conveniently, as an immunology and Treg lab, we were well-placed to study this phenotype further in collaboration with Chris Pugh.

Further study revealed an autoimmune-like phenotype characterised by weight loss, alopecia, greasy fur, and immunological disbalance in the form of enlarged lymph nodes, multilineage immune infiltration into a variety of tissues, and autoreactive antinuclear antibodies (*Fig. 3.1*)[255]. The presumed loss of tolerance inevitably prompted investigation of the Treg compartment in these mice. Interestingly, the $Foxp3^+$ compartment within CD4 T cells was actually increased, although CD25 expression on Tregs appeared to be decreased (*Fig 3.2b).* To study whether PHD2 KD Tregs were becoming plastic and leaning toward other helper T cell phenotypes, transcription factors and cytokines associated with Th1, Th2, and Th17 cells were measured, and Tregs showed increased Tbet and TNFα expression[255]. However, TSDR analysis showed that PHD2 KD Tregs maintained stable Foxp3 expression and true Treg identity, even in $CD25^-$ Tregs[255]. Both Tconvs and Tregs showed increased activation.

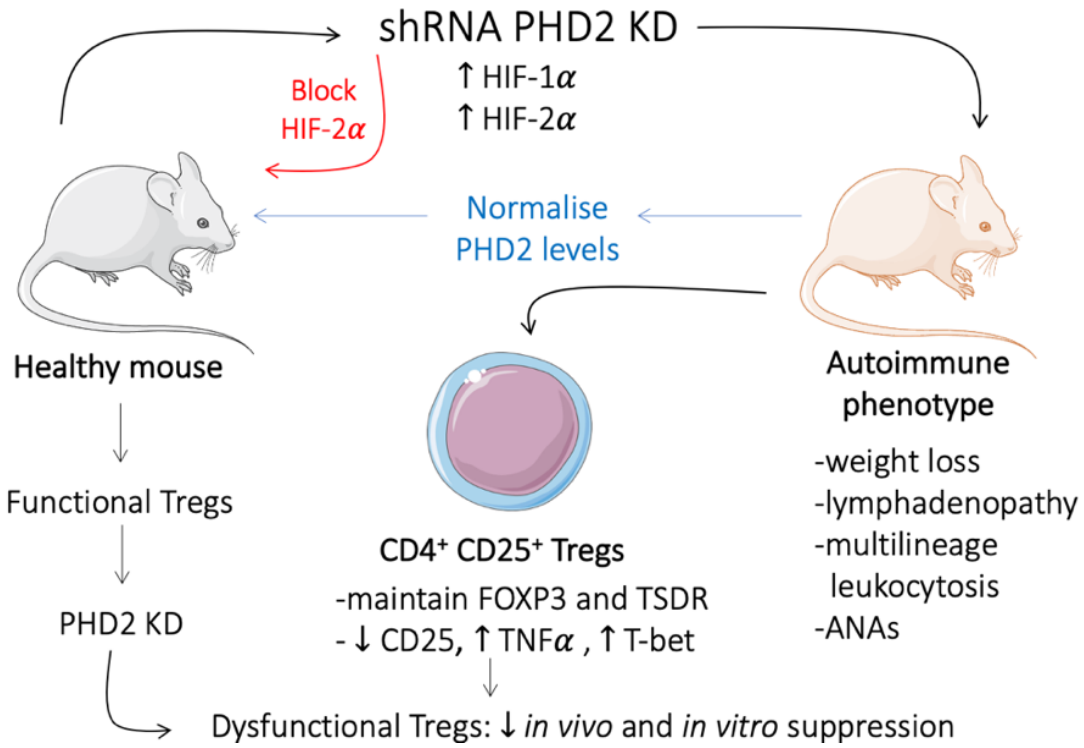

Fig 3.1 – PHD2 KD deregulates the immune system/induces an autoimmune-like phenotype. C57BL/6 mice with a shRNA KD for PHD2 were administered doxycycline (2mg/ml with 30% sucrose in ad libitum drinking water) for 4 weeks. Removing doxycycline for 1 week reversed the phenotype (blue arrow) as did crossing with HIF2 KO mice (red arrow) but not HIF1 KO mice. Isolating Tregs from these mice either after global doxycycline induction or with doxycycline administered to the Tregs in the context of an otherwise normal mouse induced dysfunction. Work by Kento Kawai and Atsushi Yamamoto, figure adapted from Yamamoto et al., 2019[255].

To study function, PHD2 KD Tregs were transferred alongside $CD4^{+}CD25^{-}$ Tconvs into $RAG^{-/-}$ mice with skin transplants; they were found to be incapable of preventing rejection, and even seemed to accelerate rejection[255]. Therefore, control or PHD2 KD Tregs were transferred on their own into transplanted $RAG^{-/-}$ mice, and KD Tregs caused rejection, indicating that the KD had not only rendered them non-suppressive but inherently aggressive[255]. The PHD2 KD was also restricted to Tregs via a $Foxp3^{Cre}$ model, and this replicated the phenotype but to a lesser extent than the systemic KD, suggesting that the Tregs are responsible for the majority but not the entirety of the phenotype. A bone marrow transfer confirmed that restricting the phenotype to the haematopoietic compartment was enough to transfer the phenotype[255], indicating that the remainder of the effects not caused by Tregs were of immune origin.

To investigate whether individual HIF isoforms might be responsible for this, the PHD2 KD mice were crossed with either HIF-1α or HIF-2α KO to study these individually. HIF-2α but not HIF-1α KO reversed the phenotype, indicating that it is driven by high levels of HIF-2α (*Fig. 3.2a*). As HIF-2α seemed to be deregulating Tregs, it was hypothesised that inhibiting it might enhance their function. Pharmacological inhibition of HIF-2α and use of HIF-2α KO Tregs *in vitro* did enhance their suppression, but HIF-2α KO Tregs did not prevent rejection in an *in vivo* transplant suppression model (unpublished data by Kento Kawai, who carried out all the work presented above). These inconsistencies are all too familiar from similar published studies on HIF in Tregs, but as chronic hypoxia was able to recreate a similar phenotype to the PHD2 KD model, this model was used to further probe the role of individual HIF isoforms in Treg and immune biology in the course of my PhD continuing this work.

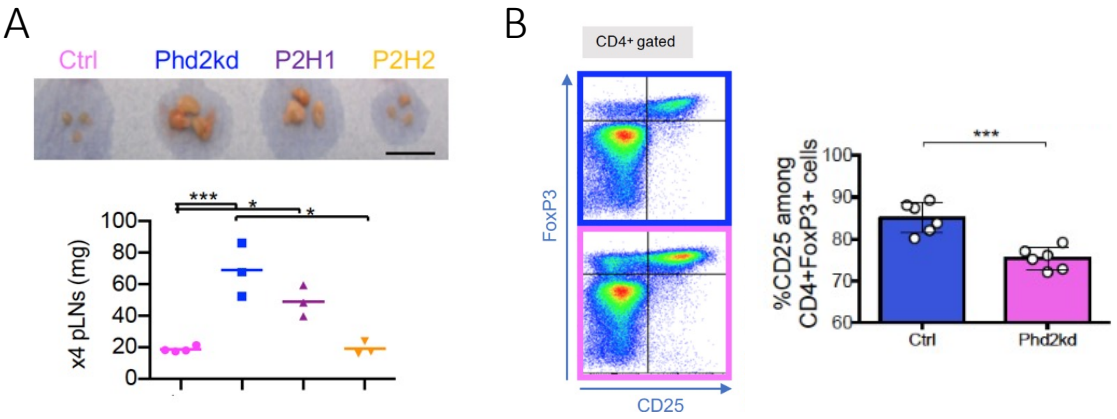

Fig 3.2 – HIF2a but not HIF1a KO reverses the PHD2 KD phenotype. C57BL/6 mice with a shRNA KD for PHD2 either alone (blue) or alongside HIF-1α (purple) or HIF-2α (yellow) KO were administered doxycycline (2mg/ml with 30% sucrose in ad libitum drinking water) for 4 weeks. Points represent individual mice. Work and figure by Kento Kawai from Yamamoto et al., 2019[255], mice generated by Atsushi Yamamoto.

CHAPTER AIM: To better understand the impact of individual components of the HIF signalling pathway on Tregs and immune responses

HYPOTHESIS: Chronic hypoxia will recreate the PHD2 KD phenotype which will be driven by increased HIF-2α levels.

3.2 - RESULTS

3.2a – HYPOXIC HIF-1A KO MICE HAVE AN EXACERBATED IMMUNE PHENOTYPE

As chronic exposure to environmental hypoxia could recreate the inflammatory phenotype observed in PHD2 KD, I (collaboratively with Kento Kawai and Atsushi Yamamoto) confined HIF-1α and HIF-2α KO mice treated with 4 weeks of tamoxifen to the hypoxic chamber, expecting to find that HIF-2α but not HIF-1α KO would reverse the inflammatory hypoxia previously observed. Unexpectedly, HIF-1α KO had very large lymph nodes, much larger than seen in previous hypoxia experiments (*Fig 3.3b*). Lymph node size is usually the first visual clue about the phenotype during harvest, so this enlargement could indicate that HIF-1α KO might be exacerbating this same phenotype.

However, HIF-2α KO reduced the hypoxic lymphadenopathy (*Fig. 3.3c*). We had previously sought to enhance Treg suppression with HIF-2α inhibition *in vitro*, which did enhance suppression with pharmacological and genetic approaches, but this was not replicated *in vivo* (*see Chapter Introduction*). Therefore, normoxic HIF-2α mice were included to investigate whether they would have improved Treg function, but as the same result was not expected from HIF-1α KO mice and not enough were available, normoxic HIF-1α controls were not included. This limits conclusions that can be drawn as hypoxic HIF-1α KO results had to be compared to control rather than HIF-1α KO normoxic mice. Although insignificant, a slight decrease in lymph node size is observable compared to the normoxic controls (*Fig 3.3c*), which could suggest that HIF-2α KO is boosting Treg function and minimising inflammation. However, this was not reflected in cell counts (*Fig 3.4a*). Hypoxic HIF-2α KO in mice seemed to reverse the increased counts in hypoxic lymph nodes (*Fig 3.4a*) but it is unclear why HIF-2α KO had the opposite trend in normoxia. The increased lymph node size of HIF-1α KO mice was not entirely matched by lymph node cellularity (*Fig 3.4a*) suggesting that perhaps there was a level of oedema or non-immune driven swelling accounting for this. Additionally, counts in the spleen were unchanged except for a specific increase in granulocytes in hypoxia and especially HIF-1α KO (*Fig 3.4b*). This contrasts the even multicellular increase across the entire leukocyte compartment seen in PHD2 KD, which is visible in both spleens and lymph nodes but more severe in lymph nodes[255].

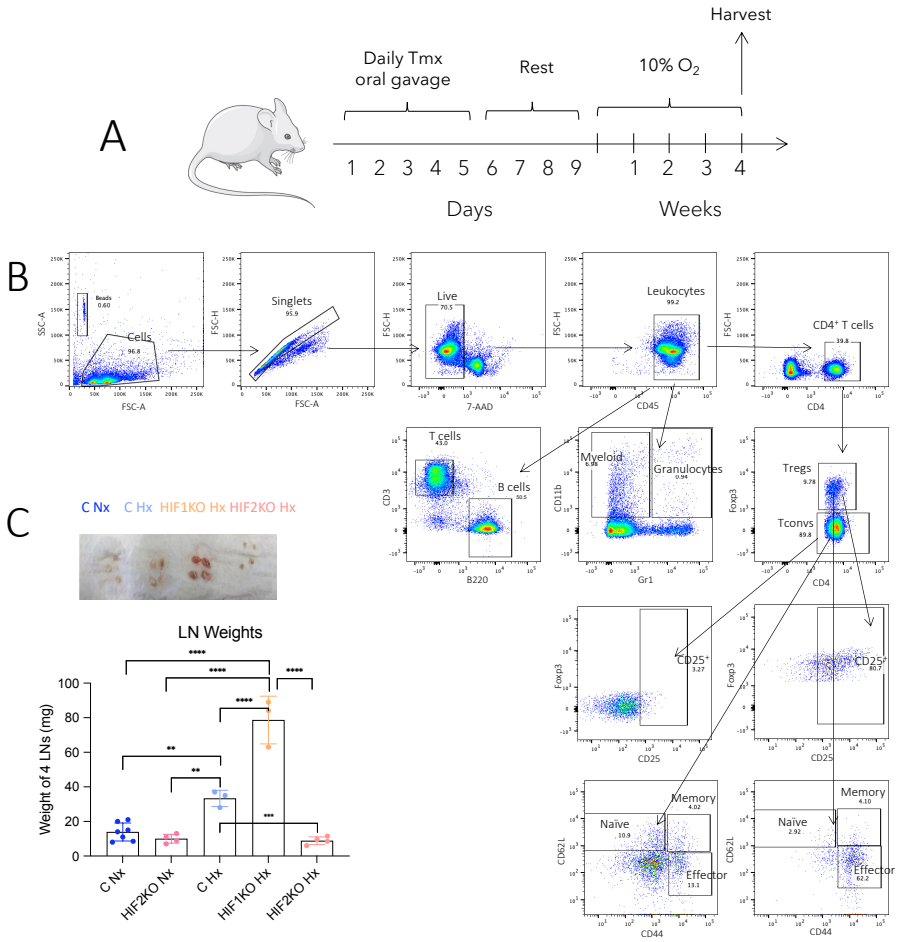

Fig 3.3 – HIF2 KO reverses lymphadenopathy but HIF1 KO lymph nodes are surprisingly enlarged. Control HIF1/2 Cre$^-$ mice (blue), HIF1 KO (orange), or HIF2 KO (pink) mice were treated with 5 daily 2mg/ml doses of oral tamoxifen and after 4 days' rest, hypoxic mice were exposed to 10% chronic hypoxia. Tissues were harvested at 4 weeks. (A) Gating strategy from a representative lymph node sample, summarising 3 separate panels. (B) Lymph nodes were blotted on tissue paper to remove excess liquid and weighed. Points represent individual mice (n = 4). Mean ± SD. C – control, Nx – normoxia, Hx – hypoxia.

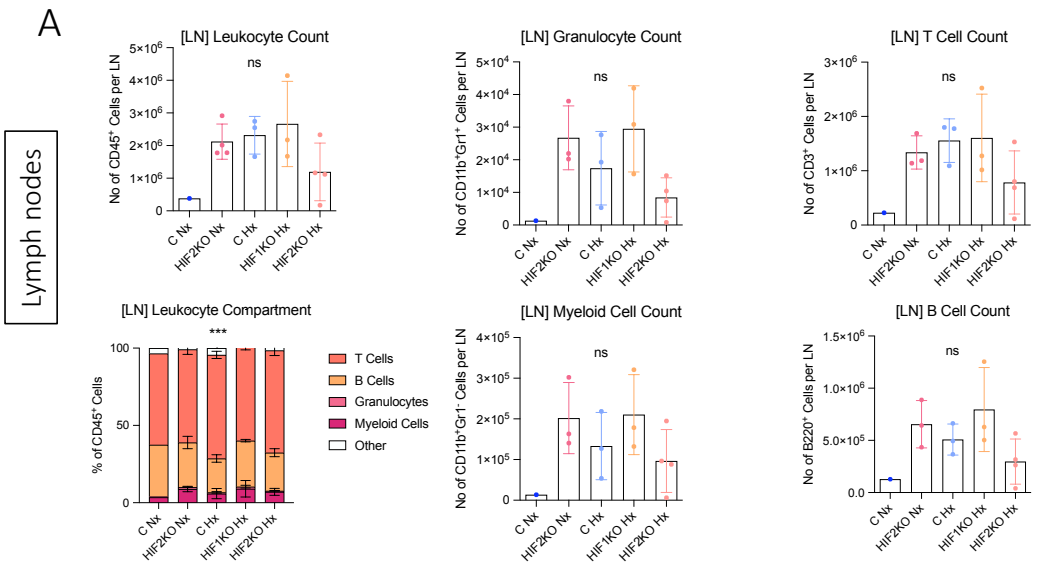

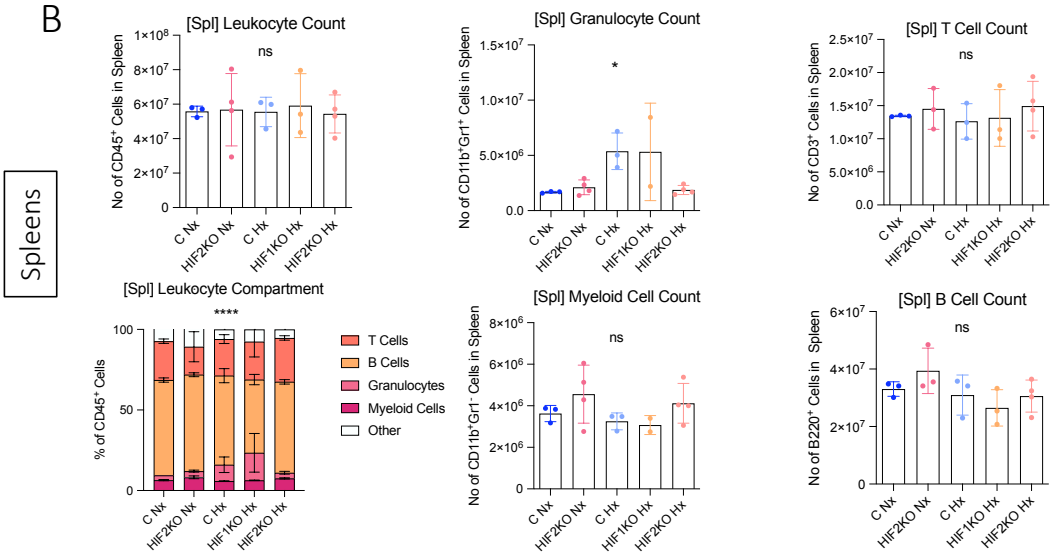

Fig 3.4 – Leukocyte counts from hypoxic HIF1 and 2 KO mice. Control HIF1/2 Cre$^-$ mice (blue), HIF1 KO (orange), or HIF2 KO (pink) mice were treated with 5 daily 2mg/ml doses of oral tamoxifen and after 4 days' rest, hypoxic mice were exposed to 10% chronic hypoxia. Tissues were harvested at 4 weeks for analysis. (A) Lymph node and (B) spleen cell counts and percentage of CD45$^+$ cells. Points represent individual mice (n = 3). Ordinary 1-way ANOVA with Tukey's multiple comparisons test, 2-way ANOVA showing column-row interaction for the stacked column plots. Mean ± SD. Nx – normoxia, Hx – hypoxia.

The Treg compartment was investigated to assess how the different HIF isoforms might drive the Treg phenotype observed in hypoxia, especially as the HIF-2α KO had such striking effects in reversing lymph node sizes in hypoxia. HIF-2α KO reversed the increase in Treg count and CD44 expression on Tregs, which is in line with a HIF-2α-driven phenotype, but the normal expression of CD44 and CD25 on normoxic HIF-2α Tregs does not hint at any enhanced suppressive function (*Fig 3.5*). While Treg counts were not significant, the percentage of Tregs across the CD4 compartment was increased by hypoxia, and HIF-2 α KO reversed the high Treg percentages on both control and HIF-1α KO spleens (*Fig 3.5*). HIF-1α KO did not produce anything exceptional regarding the Treg phenotype, which might indicate that it is not worsening the Treg-driven phenotype seen in PHD KD, but as HIF-1α was not believed to be driving any changes in that phenotype, it is possible that it could be showing an entirely new phenotype in hypoxia, driven by separate pathways that are not Treg-related. However, lack of normoxic HIF-1α KO controls makes it difficult to compare directly to HIF-2α KO results.

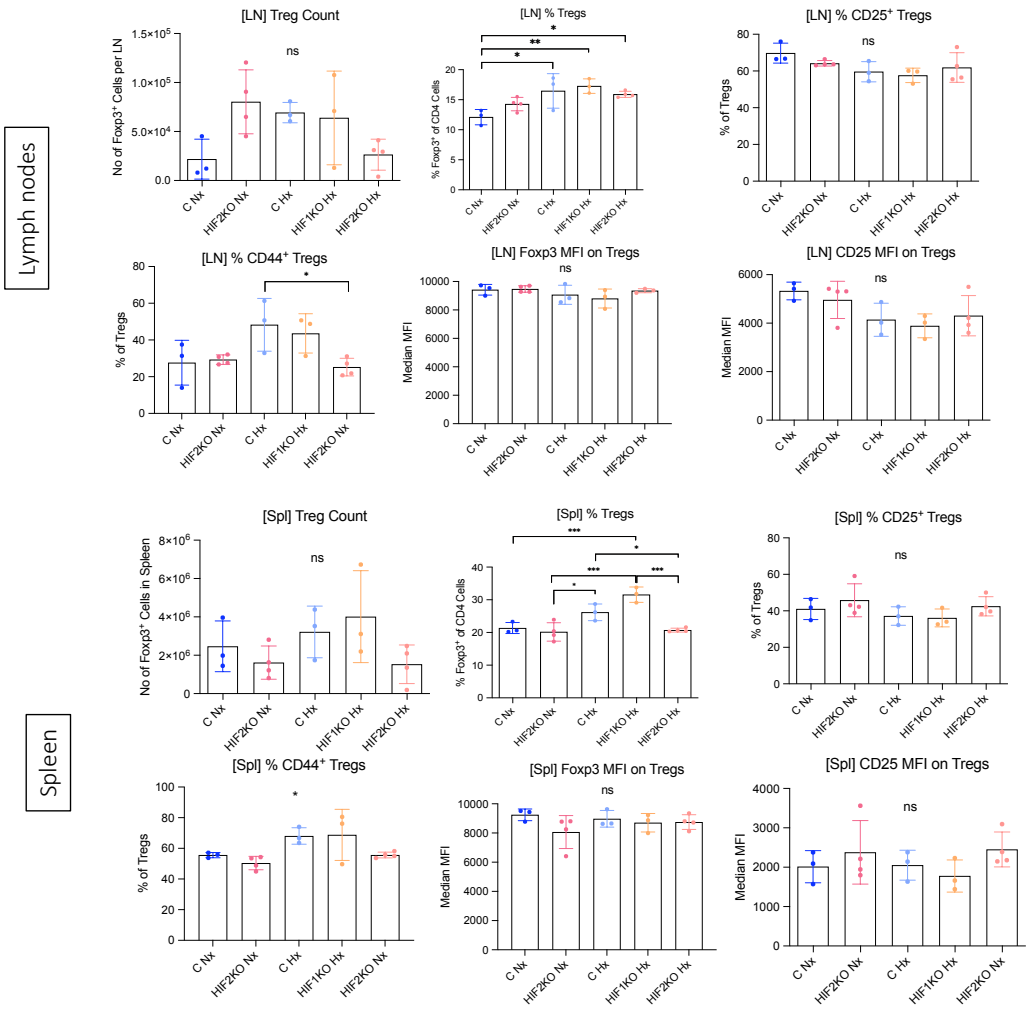

Fig 3.5 – HIF2 KO reverses the hypoxic phenotype in Tregs and HIF1 KO Tregs are not abnormal. Control HIF1/2 Cre$^-$ mice (blue), HIF1 KO (orange), or HIF2 KO (pink) mice were treated with 5 daily 2mg/ml doses of oral tamoxifen and after 4 days, hypoxic mice were exposed to 10% chronic hypoxia. Spleens (Spl) and lymph nodes (LN) were harvested at 4 weeks for flow cytometric analysis. Points represent individual mice (n= 3). Ordinary 1-way ANOVA with Tukey's multiple comparisons test. Mean ± SD. Nx – normoxia, Hx – hypoxia, MFI – median fluorescence intensity.

As a skewing toward Tbet expression in Tregs was previously observed in PHD2 KD[255], T helper transcription factors expression was assessed in this experiment. Tbet levels were not elevated in this experiment, although the high spread in this data and low sample size do make this difficult to interpret. HIF-2α KO did not reverse the observed high levels of Tbet in hypoxia (*Fig 3.6*), so either HIF-2α KO behaved differently in hypoxia than in PHD2 KD or Tbet expression might not be driving the immune phenotype. Expression of the other transcription factors was uninteresting (*Fig 3.6*), consistent with the PHD2 KD model[255].

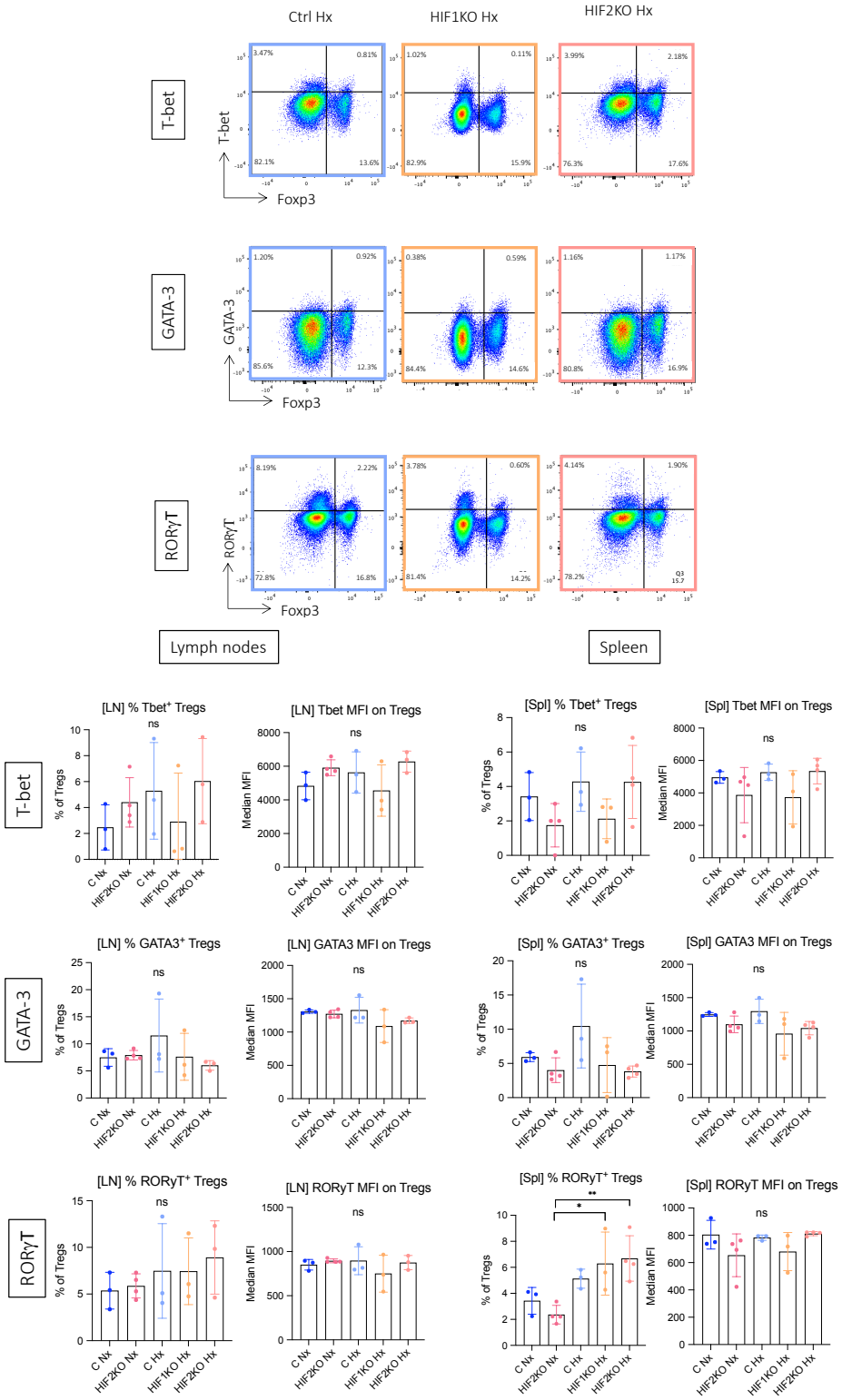

Fig 3.6 – Expression of Th transcription factors on Tregs. Control HIF1/2 Cre$^-$ mice (blue), HIF1 KO (orange), or HIF2 KO (pink) mice were treated with 5 daily 2mg/ml doses of oral tamoxifen and after 4 days' rest, hypoxic mice were exposed to 10% chronic hypoxia. Tissues were harvested at 4 weeks for analysis. Representative flow cytometry plots show transcription factor expression gated on CD4$^+$ cells in lymph nodes. Points represent individual mice (n = 3). Ordinary 1-way ANOVA with Tukey's multiple comparisons test. Mean ± SD. Nx – normoxia, Hx – hypoxia, MFI – median fluorescence intensity.

This experiment aimed to replicate the results observed in PHD2 KD, where reversal of HIF-2α but not HIF-1α levels reversed the observed phenotype. Indeed, HIF-2α KO reversed the lymphoid organ size and cellularity, if not the high expression of Tbet – which was highly variable across samples and might not be reliable here. However, despite a lack of normoxic controls, hypoxic HIF-1α KO mice exhibited an unexpected phenotype which contradicted our findings in PHD2 KD (*Fig 3.3a*). There is a large degree of redundancy between the HIF isoforms and lack of one has been shown to be compensated for by an increased expression of the other[159,160,260]. Therefore, it was hypothesised from these results that perhaps HIF-1α KO led to even higher levels of HIF-2α than hypoxia or PHD2 KD alone, which would explain why it seemed to mostly recreate our hypoxic (HIF-2α driven) phenotype to an aggravated extent. This is in line with Hsu et al. who observed the opposite, in that HIF-2α KO drove an inflammatory systemic and Treg phenotype that was driven by compensatory high levels of HIF-1α[260].

3.2b – Hypoxic HIF DKO Mice Have Even More Exacerbated Immune Phenotype

Because the abnormal results in the HIF-1α KO was hypothesised to result from compensatory high levels of HIF-2α, the chronic hypoxia experiment was repeated with a combined HIF-1/2α double KO (DKO). The hypothesis was that HIF DKO would reverse the immune phenotype observed in chronic hypoxia, and especially in hypoxic HIF-1α KO mice if this was being driven by high HIF-2α levels. The knockout was confirmed with qPCR and showed excellent efficiency in HIF-1α and about a 75% reduction in HIF-2α (*Fig 3.7*). I did not assess knockout efficacy in single KOs as they were frequently used by others in the lab and had been previously characterised[279], and Cre inheritance was confirmed by Tammie Bishop.

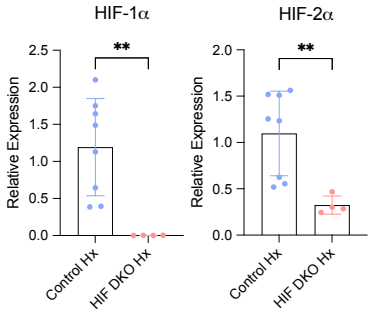

Fig 3.7 – PCR measurement confirming HIF knockout efficacy. Control Cre$^-$ mice (blue) and HIF1/2 DKO (pink) mice were treated with 5 daily 2mg/ml doses of oral tamoxifen and exposed to 10% chronic hypoxia after 4 days' rest. Tissues were harvested at day 7. Lymph nodes were frozen in RLT buffer at -80°C, then thawed for RNA extraction, cDNA preparation, and qPCR. Expression is shown as $2^{-\Delta\Delta Ct}$ values, normalised to the B2M housekeeping gene and the mean of the Cre$^-$ controls for each gene. Points represent individual mice (n = 7). Unpaired t test with Welch's correction. Mean ± SD. Hx – hypoxia.

We had concerns about how the mice would respond in the hypoxic chamber, and whether they would be unable to make the necessary physiological adjustments to survive the full 4 weeks. The mice typically lose weight sharply at the onset of hypoxia but recover after a few days after adapting, and then begin to lose weight again after 4-6 weeks as the immune phenotype becomes apparent. The mice were monitored very closely and did not seem to recover their weight after the initial drop, and had to be culled early at days 8 and 10 (*Fig 3.8a*). This was thought to be due to poor physiological adaptation and consequently, their large lymph node sizes were quite unexpected, and seemed to indicate that their weight loss might reflect an immune phenotype. The PHD2 KD mice had been investigated at 1 week as part of a time course experiment and already started showing lymphadenopathy, T cell activation and increased Tregs (data available in Kento Kawai's thesis). The control hypoxic mice had never been investigated this early and did not show any signs of illness at 1 week.

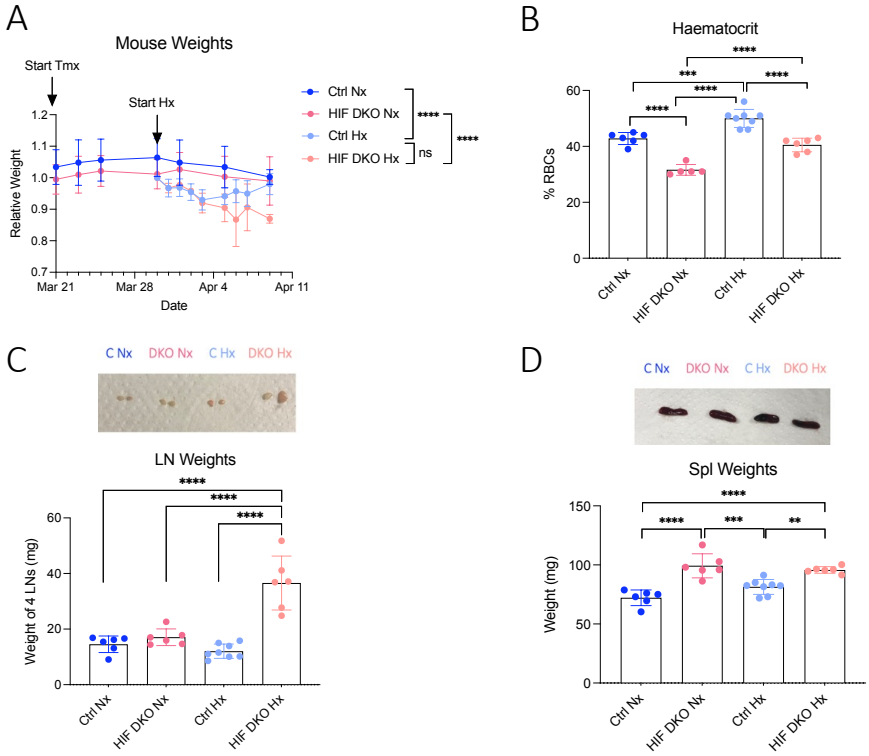

Fig 3.8 – HIF1/2 DKO mice develop a very strong immune phenotype at a rapid pace. Control HIF1/2 Cre$^-$ mice (blue) or HIF1/2 DKO (pink) mice were treated with 5 daily 2mg/ml doses of oral tamoxifen and after 4 days' rest, hypoxic mice were exposed to 10% chronic hypoxia. Tissues were harvested at 8-10 days for analysis. (A) Relative weight normalised to individual mice's starting weight before tamoxifen treatment. (B) Haematocrit was measured from venous blood via capillary tube centrifugation and RBC measurement. (C) Lymph nodes and (D) spleens were blotted on tissue paper to remove excess liquid and weighed. Points represent individual mice (n = 6). Ordinary 1-way ANOVA with Tukey's multiple comparisons test. Mean ± SD. Nx – normoxia, Hx – hypoxia.

Upon flow cytometric analysis, lymph node sizes in the HIF DKO mice reflected the leukocytosis seen in previous models (*Fig 3.9a*), suggesting that this could be the same immune phenotype but exacerbated. However, for the first time, spleen and lymph node results differed, and the spleen leukocytosis was restricted to myeloid cells (*Fig 3.9b*). Previous models usually showed an even increase across all immune types with no changes in percentage, but here a shift in B and T cells was observed in both hypoxic lymph node groups, and an increase in myeloid cells at the cost of B cells in HIF DKO spleens (*Fig 3.9*). It was surprising to note that counts in the hypoxic controls trended toward being lower than normoxic controls, as they are known to be elevated at later timepoints. In order to ascertain whether leukocytes were leaving the lymphoid organs for the blood, peripheral blood was also examined but no increased counts in the blood of hypoxic controls were observed (data not shown), suggesting that the cells are either migrating to peripheral tissues or somehow being deleted at this early timepoint, only to later be enriched in the spleens and lymph nodes with continued exposure to hypoxia.

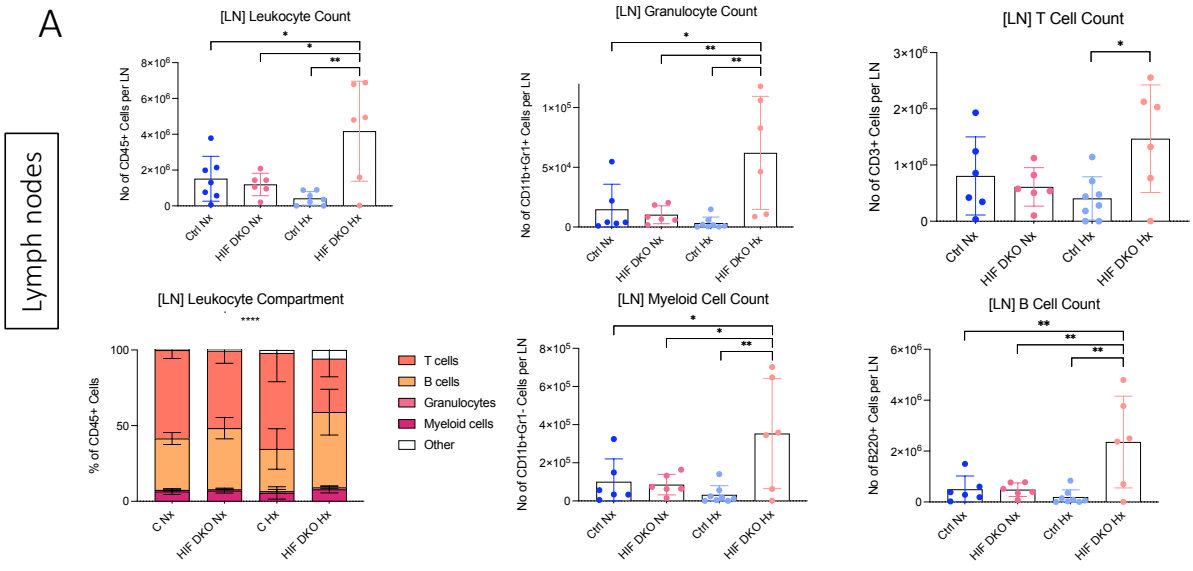

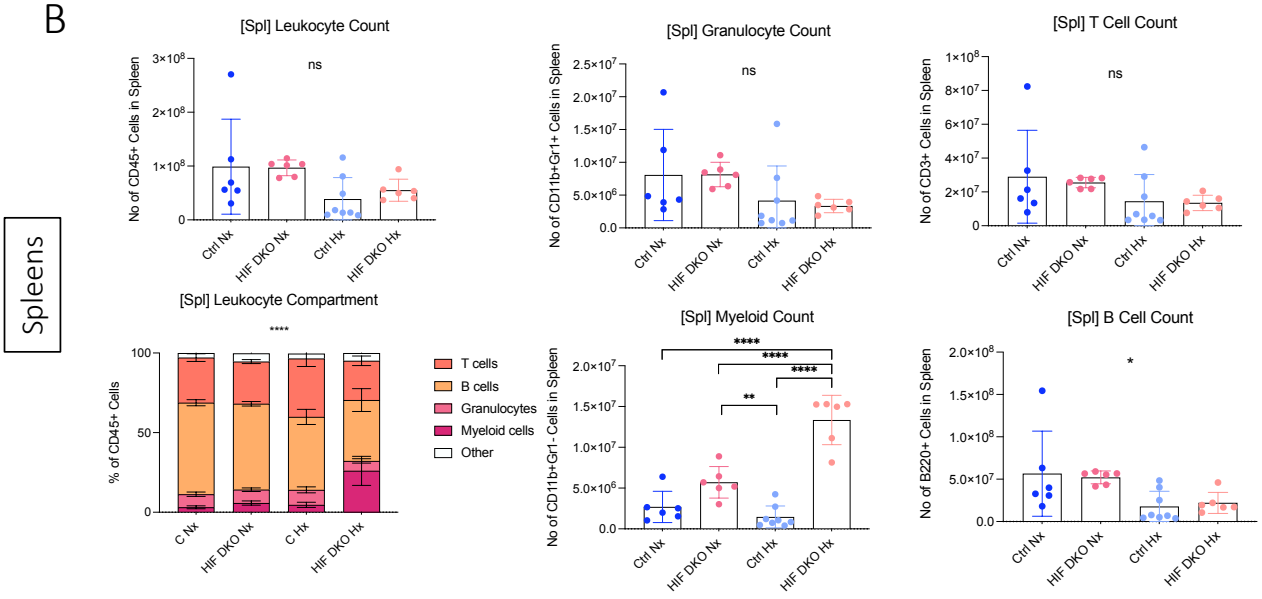

Fig 3.9 – HIF1/2 DKO mice show extreme leukocytosis in lymph nodes but not spleens. Control HIF1/2 Cre$^-$ mice (blue) or HIF1/2 DKO (pink) mice were treated with 5 daily 2mg/ml doses of oral tamoxifen and after 4 days' rest, hypoxic mice were exposed to 10% chronic hypoxia. Tissues were harvested at 8-10 days for analysis. (A) Lymph node and (B) spleen cell counts and population percentage of CD45$^+$ cells (stacked bar plots). Points represent individual mice (n = 6). Ordinary 1-way ANOVA with Tukey's multiple comparisons test, 2-way ANOVA for stacked barplots showing column-row interaction term. Mean ± SD. Nx – normoxia, Hx – hypoxia.

An enrichment of Foxp3$^+$ cells within the CD4 compartment was observed in hypoxic HIF1/2 DKO mice, which is consistent with the general phenotype trends – however, the lack of CD25 loss is not (*Fig 3.10*). Treg counts followed the same trends as the rest of the T cells, despite changes in their percentage, and the increase in CD44 on Tregs is consistent with the phenotype observed in previous models (*Fig 3.10*). Additionally, Foxp3 MFI was increased in hypoxic HIF DKO lymph nodes (*Fig 3.10a*), which has not been observed before. This is in line with the paradox of the general phenotype observed across PHD2 KD and hypoxia, as all measures point to healthy and abundant Tregs, despite a very aggressive phenotype hypothesised to be autoimmune in nature. Additionally, the loss of cellularity in control hypoxic tissues could have been explained by Treg suppression and deletion of these cells, but the number, percentage, and activation of Tregs is decreased here (*Fig 3.10*), so this seems unlikely. However, no data regarding the functionality of the Tregs was acquired in this experiment.

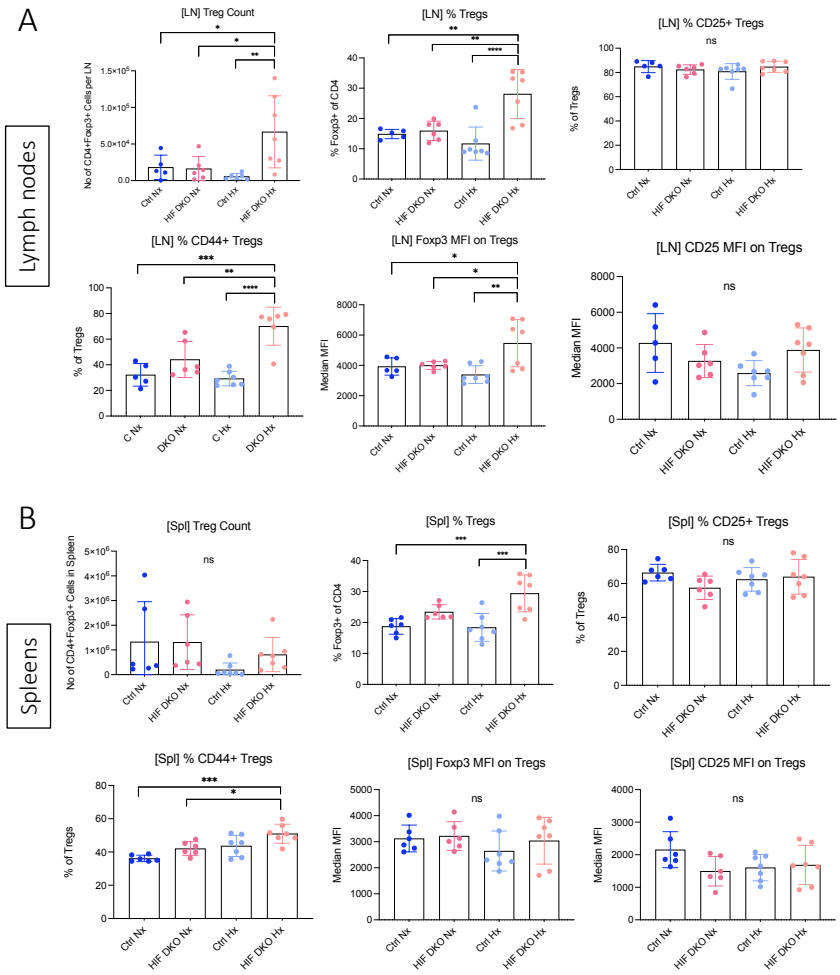

Fig 3.10 – The Treg compartment is altered in HIF1/2 DKO in hypoxia. Control HIF1/2 Cre$^-$ mice (blue) or HIF1/2 DKO (pink) mice were treated with 5 daily 2mg/ml doses of oral tamoxifen and after 4 days' rest, hypoxic mice were exposed to 10% chronic hypoxia. Lymph nodes (A) and spleens (B) were harvested at 8-10 days for flow cytometric analysis. Points represent individual mice (n = 6). Ordinary 1-way ANOVA with Tukey's multiple comparisons test. Mean ± SD. Nx – normoxia, Hx – hypoxia, MFI – median fluorescence intensity.

As PHD2 KD mice exhibited a shift toward a Th1-like phenotype with increased T-bet and TNF-α expression on both Tregs and Tconvs and IFNγ production by Tconvs[255], Treg plasticity was assessed in this model. Surprisingly, very striking increases in GATA3 and RORγT expression were observed in HIF DKO lymph nodes, as well as a decrease in T-bet on both spleens and lymph nodes (*Fig 3.11*). This is further evidence that the HIF DKO hypoxic phenotype is distinctive from previous models, despite similar immune infiltration in lymph nodes. Additionally, quite high expression of T-bet was observed in the control hypoxic mice; this is in line with the phenotype observed in previous models, but had not previously been detected this early. Its early appearance could point toward T-bet in Tregs being either causative or strongly correlated to the hypoxic immune phenotype.

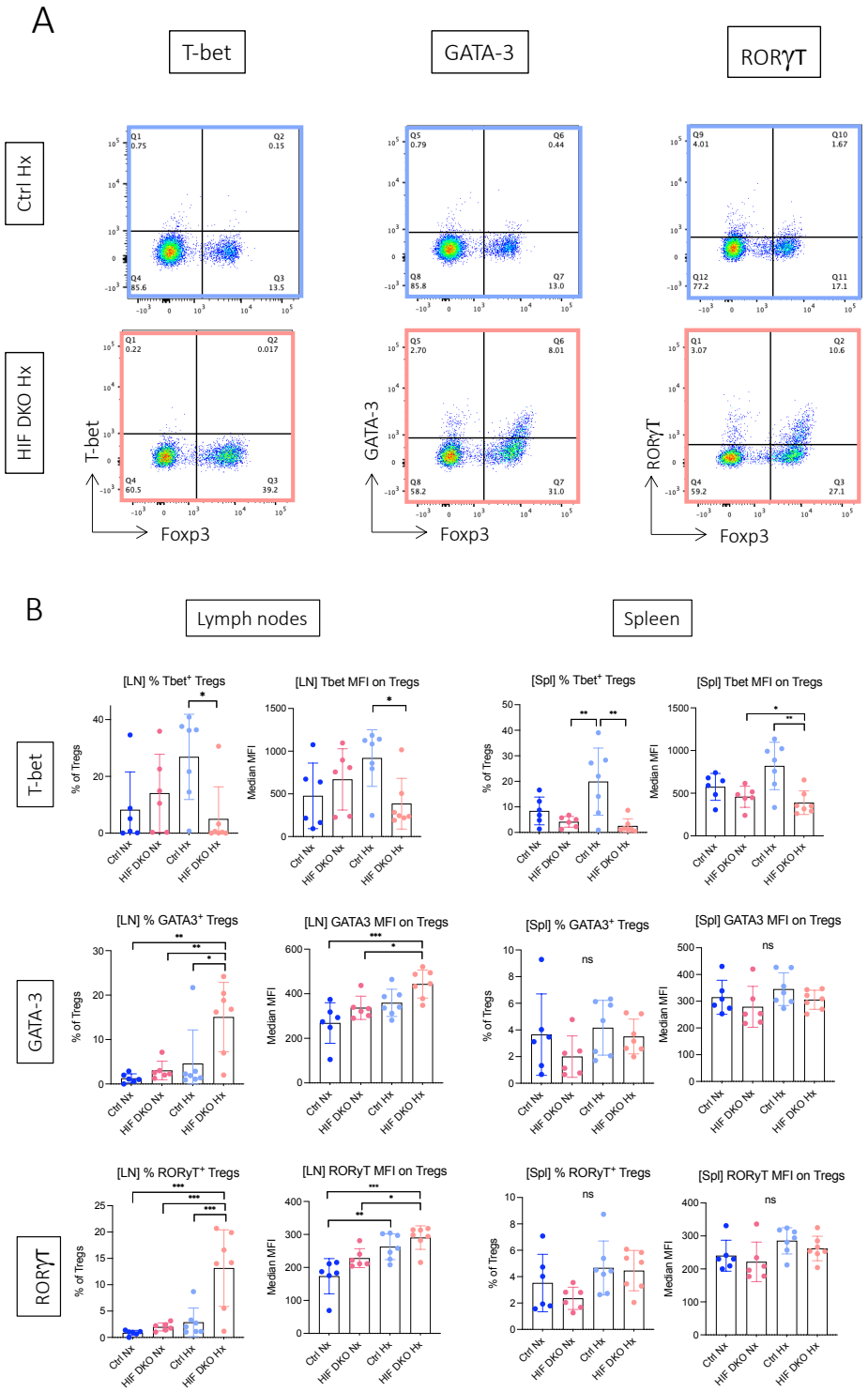

Fig 3.11 – Expression of Th transcription factors on Tregs. Control HIF1/2 Cre$^-$ mice (blue) or HIF1/2 DKO (pink) mice were treated with 5 daily 2mg/ml doses of oral tamoxifen and after 4 days' rest, hypoxic mice were exposed to 10% chronic hypoxia. Tissues were harvested at 8-10 days for flow cytometric analysis. (A) Representative flow cytometry plots show transcription factor expression gated on CD4$^+$ cells in lymph nodes. (B) Points represent individual mice (n = 6). Ordinary 1-way ANOVA with Tukey's multiple comparisons test. Mean ± SD. Nx – normoxia, Hx – hypoxia, MFI – median fluorescence intensity.

3.2c – Hypoxic ARNT DKO Mice do not Replicate the Same Immune Phenotype

By this point, some surprising facets of the hypoxic phenotype had been unearthed at early timepoints, and the immune phenotype expected to be reversed by HIF DKO was exacerbated by it, but also altered on a few points. Upon repeating this experiment, some ARNT1/2 DKO mice were also included. Theoretically, no HIF signalling should be possible in these mice as HIF cannot signal unless it dimerises with ARNT, so they should be equivalent to the HIF DKO model in terms of HIF signalling. Of course, ARNT is a binding partner for other transcription factors, which is entirely likely to have some effect, but I hoped the model would at least shed some light on the extent to which HIF levels might be driving the (now seemingly multiple) phenotypes observed to date. The efficacy of the knockout was relatively high in leukocytes (*Fig 3.12*), whereas previous PCR measurements in other tissues performed by Maria Prange-Barczyńska had not shown very efficient knockout (data available in her thesis).

In order to assess signalling downstream of HIF, the well-known HIF targets Vegfa and Pgk1 were included as proxy measurements of downstream HIF signalling so that whether any incomplete knockout still resulted in a reduction of HIF signalling could be assessed. Regrettably, expression of the target genes was not decreased by HIF and ARNT DKO (*Fig 3.12*). This could be due to their being controlled by factors other than HIF, as various cytokines have been shown to induce Vegfa expression in immune cells[280] and Pgk1 is associated with regulatory cells[281] so its increase might reflect the high Treg proportion. This does cast some doubt on how much HIF signalling might be present in these mice and whether the small amount of ARNT expression still visible might be sufficient to induce transcription. Pgk1 expression did seem diminished in most of the HIF DKO samples but not the ARNT DKO, which might perhaps indicate that the small amount of ARNT that persisted was sufficient to keep inducing HIF transcription, and that its decreased levels in HIF DKO reflects the higher efficacy of the knockout. Both knockouts showed a modest increase in Vefga, so perhaps this is being controlled predominantly by immune factors rather than HIF in this model and might not be as reliable as a marker of HIF transcriptional activity. Not enough mice were available for normoxic controls to be included in this experiment, and as expression of HIFs and target genes are very low in normoxia, control hypoxic mice represent a baseline normal transcriptional response to hypoxia.

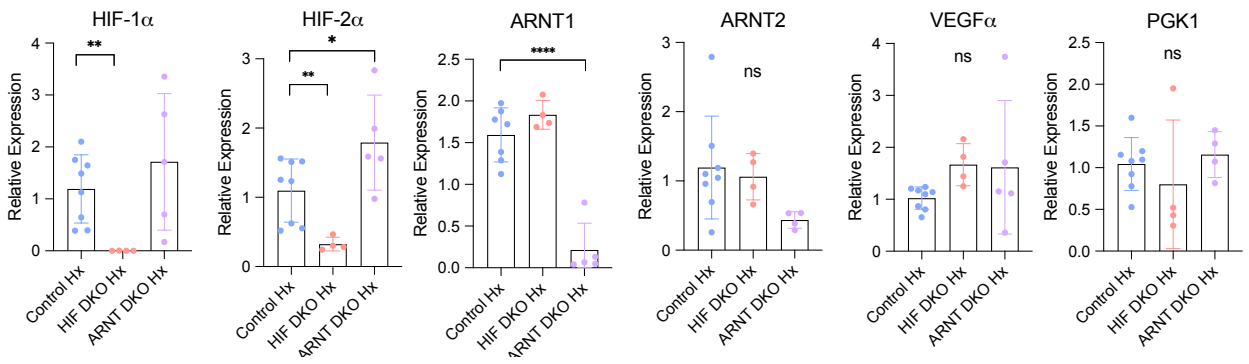

Fig 3.12 – PCR measurement confirming ARNT knockout and measuring VEGFA. Control Cre$^-$ mice (blue), HIF1/2 DKO (pink) and ARNT1/2 DKO (lilac) mice were treated with 5 daily 2mg/ml doses of oral tamoxifen and exposed to 10% chronic hypoxia after 4 days' rest. Tissues were harvested at day 7 for analysis. Lymph nodes were frozen in RLT buffer at -80°C, and then thawed for RNA extraction, cDNA preparation, and qPCR. Expression is shown as $2^{-\Delta\Delta Ct}$ values, normalised to the B2M housekeeping gene of each mouse and the mean of the Cre$^-$ controls for each gene. Points represent individual mice (n = 4). Unpaired t tests. Mean ± SD. Hx – hypoxia.

ARNT DKO was expected to recreate the extreme changes seen in hypoxic HIF DKO in the lymph nodes and haematocrit, but it did not (*Fig 3.13*). As ARNT is required for HIF signalling because it is an obligate dimer, a lack of ARNT should impair any HIF signalling equivalently to a HIF knockout and produce the same results, at least if the phenotype is driven by HIF. The lack of decrease in haematocrit in ARNT DKO is further indication that the KO may not have been sufficient to impair HIF signalling (*Fig 3.13b*), but lack of normoxic controls makes it difficult to understand how much could be due to ARNT's interactions with other genes.

Furthermore, the phenotype was different in the spleen and the lymphadenopathy was actually increased by ARNT DKO (*Fig 3.13*); in PHD2 KD and previous hypoxia experiments, the spleens usually show the same phenotype as the lymph nodes, if somewhat less severe[255], and this was the first time a discordance between tissues was observed. The lymph node weights were reflected by cell counts, with ARNT DKO again not being able to replicate the HIF DKO phenotype (*Fig 3.14a*), but spleens seemed to maintain counts of most cell types apart from myeloid cells (*Fig 3.14b*). As lymph node tissue was used for the qPCR, the efficacy of the knockout was in spleens remains unknown, especially since previous measurements by Maria Prange-Barczyńska showed high discordance between different tissues, so higher efficiency in the spleens would explain a better replication of the HIF DKO phenotype in spleens but not lymph nodes.

However, the haematocrit was only decreased in HIF DKO (*Fig 3.13b*), and as EPO production is under the control of HIF (predominantly HIF-2α[160]) this acts as a further functional measure of downstream HIF signalling, similarly to the expression of *Vegfa* and *Pgk1*. This might indicate that the small residual levels of ARNT that were not knocked out are sufficient for HIF transcription, especially since ARNT is stable at the protein level so small amounts of transcript can be expected to be long-lived. This also matches the trend in *Pgk1* transcription, and so it is quite likely that the discordance between HIF and ARNT DKO phenotypes results from a failure in abrogating ARNT dimerisation with HIF-α rather than induction of a new phenotype controlled by an entirely different signalling pathway altogether.

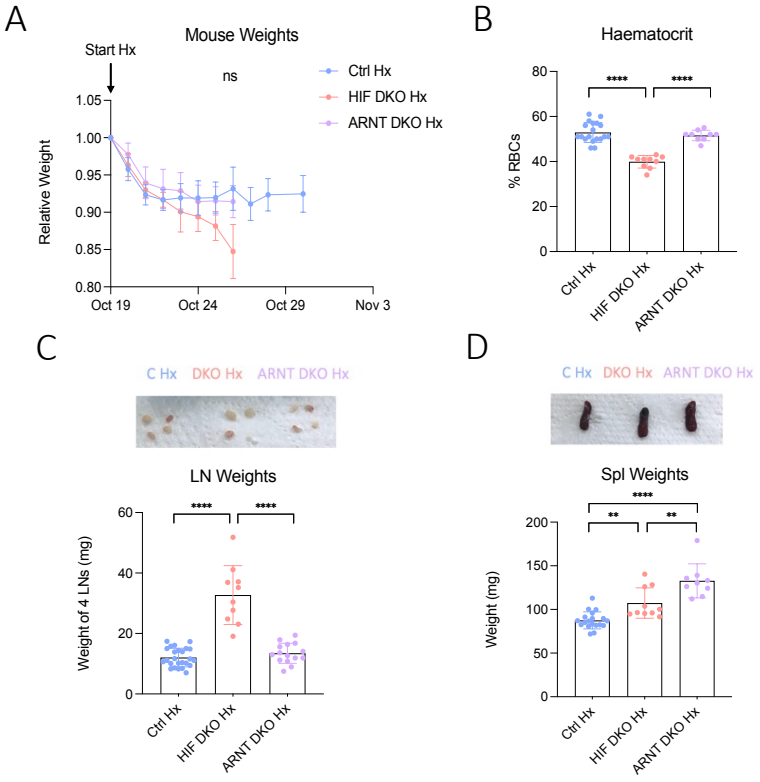

Fig 3.13 – ARNT DKO mice do not replicate the intense phenotype of HIF1/2 DKO mice. Control Cre$^-$ mice (blue), HIF1/2 DKO (pink) and ARNT1/2 DKO (purple) mice were treated with 5 daily 2mg/ml doses of oral tamoxifen and exposed to 10% chronic hypoxia after 4 days' rest. Tissues were harvested at day 7 for analysis. (A) Relative weight normalised to individual mouse's starting weight before initiation of hypoxia. (B) Haematocrit was measured from venous blood via capillary tube centrifugation and RBC measurement. (C) Lymph nodes and (D) spleens were blotted on tissue paper to remove excess liquid and weighed. Data represents 4 individual experiments with various groups. Points represent individual mice (n = 10). Ordinary 1-way ANOVA with Tukey's multiple comparisons test. Mean ± SD. Nx – normoxia, Hx – hypoxia.

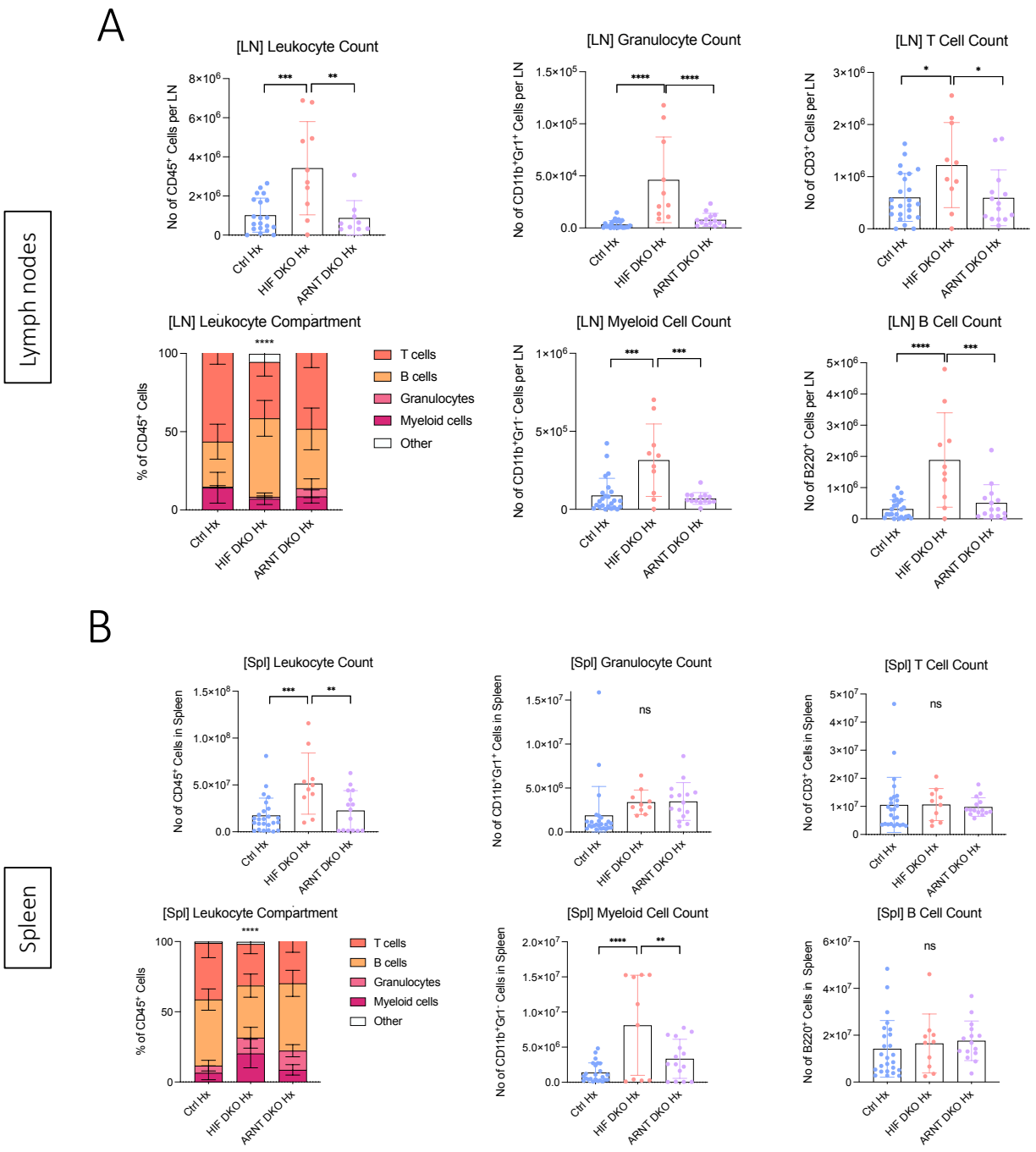

Fig 3.14 – ARNT DKO mice do not replicate the intense phenotype of HIF DKO mice. Control Cre$^-$ mice (blue), HIF1/2 DKO (pink) and ARNT1/2 DKO (purple) mice were treated with 5 daily 2mg/ml doses of oral tamoxifen and exposed to 10% chronic hypoxia after 4 days' rest. Tissues were harvested at day 7 for analysis. (A) Lymph node and (B) spleen cell counts population percentage of CD45$^+$ cells (stacked bar plots). Points represent individual mice (n = 10). Ordinary 1-way ANOVA with Tukey's multiple comparisons test. Mean ± SD. Nx – normoxia, Hx – hypoxia.

When investigating the Treg compartment, ARNT DKO did not cause the same increase in Treg counts and activation in lymph nodes (*Fig 3.15*). In spleens, the increase caused by HIF DKO was not as dramatic, so ARNT DKO was able to recreate it, but neither were very different from the hypoxic controls (*Fig 3.15*). The biggest change was in Treg counts which again were exacerbated in ARNT DKO in the spleen (*Fig 3.15*), potentially indicating that the knockout was more successful than in lymph nodes and that this might be the reason for the discordance between these tissues. A decrease in CD25 expression was not observed on Tregs in HIF DKO but Tregs in ARNT DKO did show a mild decrease (*Fig 3.15*), so it is unclear how closely linked CD25 expression is to HIF signalling and exactly which levels of HIF are present in each of the tissues for both genetic models.

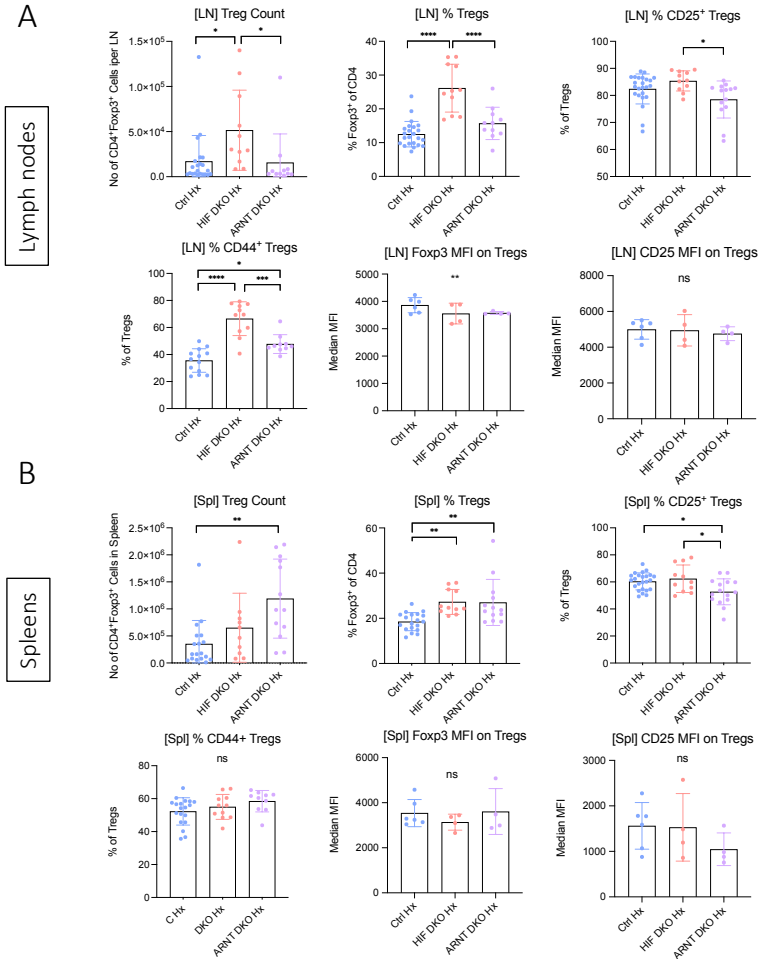

Fig 3.15 – Treg phenotype in hypoxic HIF and ARNT DKO mice. Control Cre$^-$ mice (blue), HIF1/2 DKO (pink) and ARNT1/2 DKO (purple) mice were treated with 5 daily 2mg/ml doses of oral tamoxifen and exposed to 10% chronic hypoxia after 4 days' rest. Tissues were harvested at day 7 for flow cytometric analysis. Data represents 4 individual experiments with various groups, except MFI data which is within a single experiment. Points represent individual mice (n = 10). Ordinary 1-way ANOVA with Tukey's multiple comparisons test. Nx – normoxia, Hx – hypoxia, MFI – median fluorescence intensity.

The GATA3 and RORγT expression in Tregs that was found to be elevated in HIF DKO was also reversed in ARNT DKO lymph nodes, but exacerbated in spleens (*Fig 3.16).* However, the expression of Tbet was more variable, with little difference between the HIF and ARNT DKO in lymph nodes but a mild increase in ARNT DKO spleens (*Fig 3.16).* Overall, the phenotype in ARNT DKO spleens seemed to replicate that of the HIF DKO lymph nodes, showing an increase in Treg numbers and activation, and potentially a loss of Treg phenotype and plasticity toward Th-like cells as indicated by the high expression of Tbet, GATA3, and RORγT, despite their maintenance of Foxp3 expression. This discordance between spleens and lymph nodes might potentially be due to differences in knockout efficiency between tissues, although we normally see a more extreme phenotype in lymph nodes in PHD2 KD and hypoxia in general, with ARNT DKO being the only time such a strong disparity of trends and of magnitude of difference between the two lymphoid organs is observed. However, lack of normoxic controls make these interpretations difficult as it does not allow us to infer whether ARNT DKO might have other extraneous effects affecting these markers outside of its relationship with HIF-α.

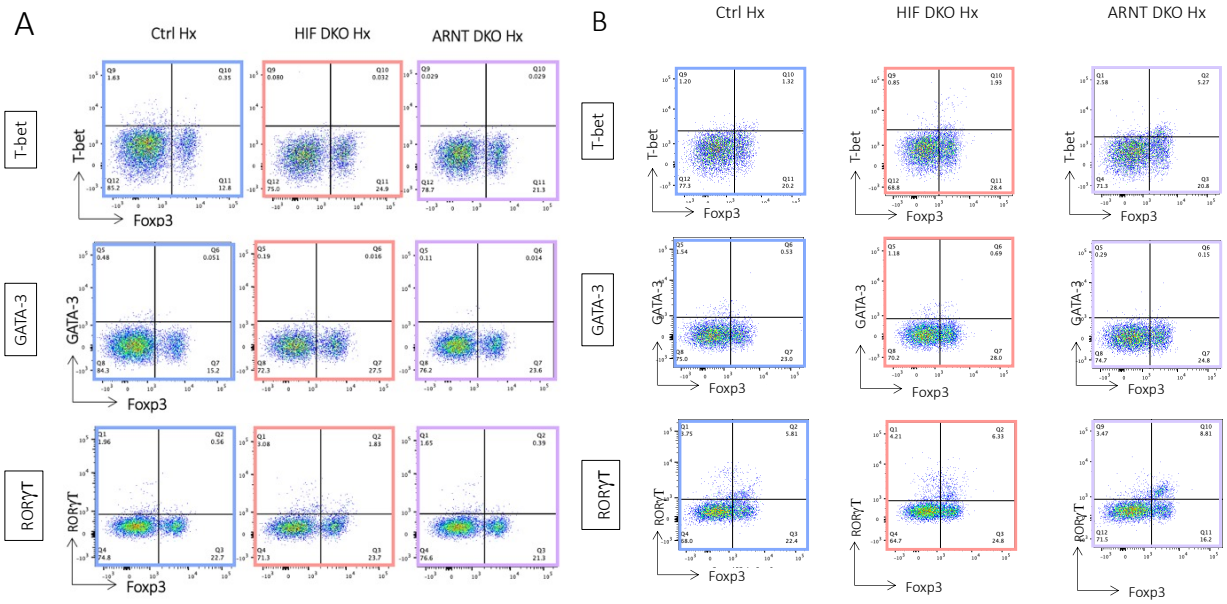

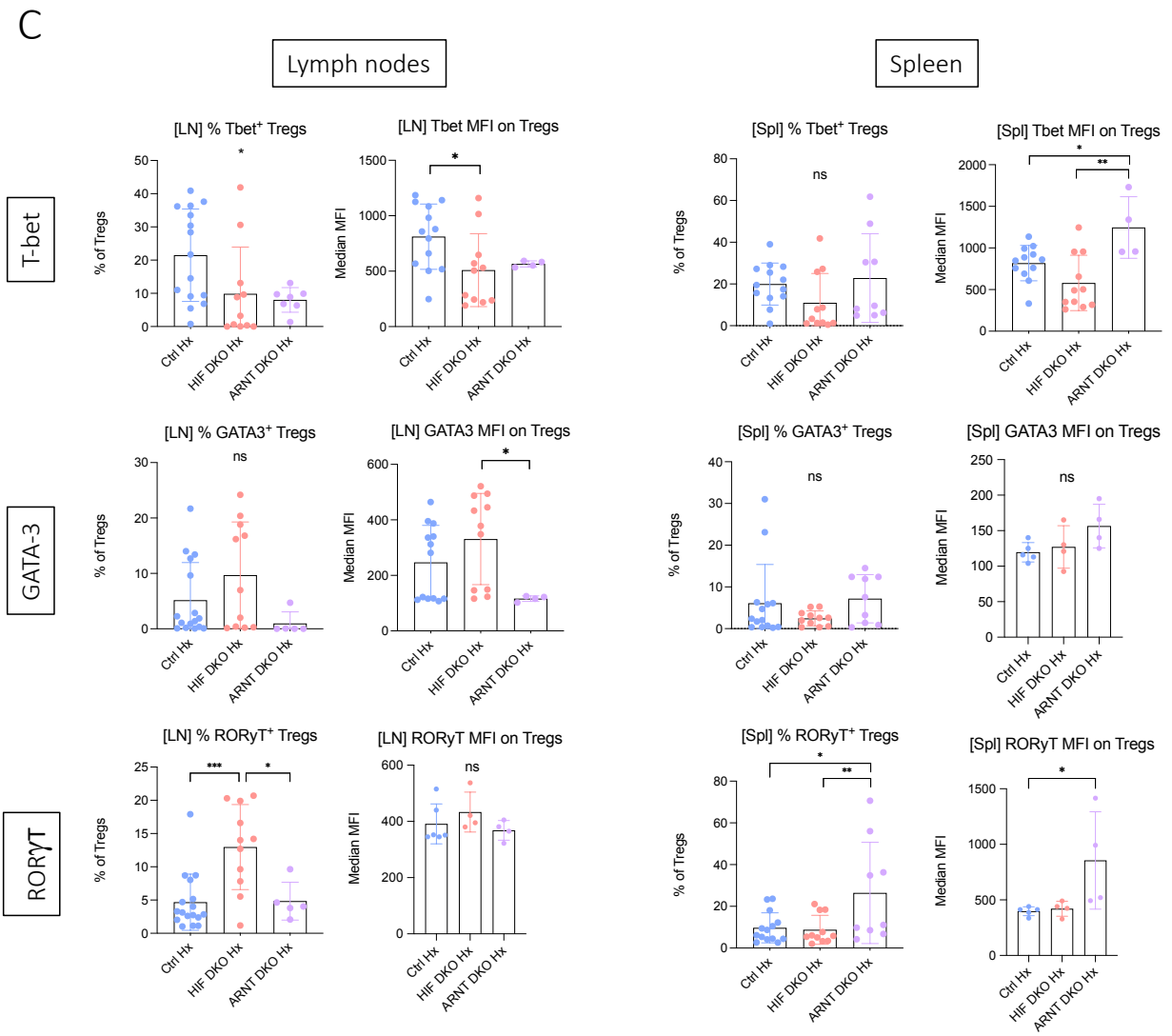

Fig 3.16 – Expression of Th transcription factors on Tregs. Control Cre$^-$ (blue), HIF1/2 DKO (pink), or ARNT1/2 DKO (purple) mice were treated with 5 daily 2mg/ml doses of oral tamoxifen and after 4 days' rest, hypoxic mice were exposed to 10% chronic hypoxia. Tissues were harvested at 7-10 days for flow cytometric analysis. Representative flow cytometry plots show transcription factor expression gated on CD4$^+$ cells in (A) lymph nodes and (B) spleens. (C) Data represents 4 individual experiments with various groups, except MFI data which is within a single experiment. Points represent individual mice (n = 10). Ordinary 1-way ANOVA with Tukey's multiple comparisons test. Mean ± SD. Nx – normoxia, Hx – hypoxia, MFI – median fluorescence intensity.

3.3 – DISCUSSION

The work presented in this chapter aimed to better understand how the individual contribution of the HIF isoforms affect Tregs and the immune system. First, the single HIF KO experiments previously done in PHD2 KD that had showed that HIF-2α but not HIF-1α KO reversed the phenotype (*Fig 3.2*) were repeated but this time with physiological hypoxia, expecting to find the same trends. Although HIF-2α KO did reverse the inflammation as expected, hypoxic HIF-1α KO mice had unexpectedly exacerbated lymphadenopathy (*Fig 3.3*). This was hypothesised to be due to compensatory high levels of HIF-2α in this model, so the experiment was repeated with a HIF1/2 DKO model, but this only aggravated the lymphadenopathy and cellular infiltration (*Fig 3.9*). When this was repeated with ARNT DKO, a model that should be functionally similar to HIF DKO, the same results were not reproduced, and varied between lymph nodes and spleens (*Fig 3.14*). The manipulation of these different HIF isoforms and subunits seem to have led to discrepancies between the results, which may be biological or technical in nature.

When HIF-1α or HIF-2α KO mice were exposed to chronic hypoxia, HIF-2α KO reversed the inflammation caused by hypoxia as had been observed in PHD2 KD, but HIF-1α KO mice had dramatically enlarged lymph nodes (*Fig 3.3*). The cellularity of the lymph nodes did not reflect their enlargement (*Fig 3.4*) indicating that perhaps an element of oedema or swelling was contributing to their size: hypoxia and inflammation are often intertwined in inducing oedema, so it is difficult to separate out the involvement of HIF signalling, but HIF has been shown to induce oedema in some conditions[282,283]. The lymph node enlargement was not previously thought to be driven by artifact non-immune drivers in the PHD2 KD model, but the immune infiltration seen in other tissues in histology and the weight and hair loss observed in that model do indicate that there is more at play than simple fluid relocation. Altogether, this hypoxic HIF-1α KO phenotype seemed to differ from the PHD2 KD phenotype which was shown to be HIF-2α-driven, and it is unclear to what extent the HIF-1α KO mice had other autoimmune features compared to the PHD2 KD mice, as histological or autoantibody analysis was not performed that might inform this, nor was tissue available to confirm flow cytometric results with PCR. Additionally, normoxic HIF-1α KO controls were not available to help fully analyse the unexpected hypoxic HIF-1α KO results.

Furthermore, combined PHD2 KD with HIF-1α KO did not worsen inflammation compared to the PHD2 KD alone and actually decreased it (*Fig 3.2a*), so physiological hypoxia appeared to affect HIF activity differently than genetic PHD2 inhibition. Although both of these are expected to raise HIF levels, several other enzymes are inhibited in environmental hypoxia that are not affected by PHD2 KD, such as the other PHD enzymes and FIH, so it is possible that HIF levels differ between the physiological and genetic approaches. PHD2 has also been shown to preferentially regulate HIF-1α over HIF-2α , whereas PHD3, a HIF target itself[167], has greater influence over HIF-2α[166]; thus, genetic modulation might affect isoforms unevenly compared to environmental hypoxia which affects all PHDs and FIH. Environmental hypoxia would be expected to be more extreme as it targets all of these, but it is unlikely to be severe enough to cause the complete aberration that shRNA KD can achieve, so this is probably the reason why PHD2 KD induces a more severe phenotype than chronic hypoxia. Ethics and animal welfare limit hypoxia treatment to a maximum of 10%, which already approximates levels found at base camp of Everest; more extreme hypoxia could probably be achieved locally in tissues, and likely does occur in tumours, ischemia, or extreme local inflammatory hypoxia, but this is difficult to recreate without other confounding variables that would greatly impact the immune response.

It was hypothesised that perhaps HIF-2α was driven to even higher levels than in control hypoxic mice in order to compensate for the loss of HIF-1α, and because normalising HIF-2α levels reversed the PHD2 KD phenotype, further increasing its levels might aggravate the hypoxic phenotype. This is similar to Hsu et al.'s study, where HIF-2α KO raised HIF-1α levels and reversing this increased HIF-1α with a double KO reversed the phenotype[260]. While these are opposite isoforms to our model, it does provide basis for KO of one HIF isoform driving the rise of the other, causative isoform, and inducing loss of Treg function. However, they used colitis and airway inflammation models whereas we only investigated autoimmune features at baseline, so perhaps the additional inflammatory challenge could be affecting Treg function and HIF isoforms differently. HIF-2α is normally induced in more chronic hypoxia than HIF-1α[160], so extreme inflammation could induce a more acute inflammatory hypoxia that would favour HIF-1α. The effects of HIF levels on Treg function are strongly debated and few studies have investigated HIF-1α and HIF-2α together (*see section 1.5a*), so it is difficult to place ourselves in the scientific context, especially when our own data is inconsistent between models and tissues.

The surprising levels of inflammation in hypoxic HIF DKO mice (*section 3.2b*) made us reconsider the interpretation of a HIF-2α-driven phenotype. The knockout efficiency was not complete for HIF-2α reduction in this DKO (*Fig 3.7*), so it is possible that enough HIF-2α was still present to signal and induce transcriptional changes in Tregs, but this does not explain why this small residual HIF-2α would induce a stronger phenotype than HIF-1α KO alone where HIF-2α wasn't inhibited at all. It was thought that due to HIF-2α levels driving Treg dysfunction, extra low levels might improve their suppression, which Kento Kawai showed with pharmacological inhibition *in vitro* but not with HIF-2α KO Tregs *in vivo* (data available in his thesis). The small lymph node size and high percentage of Tregs in normoxic HIF-2α KO could support our hopes of making "super Tregs" but the unexplained high counts in normoxic HIF-2α KO lymph nodes (*Fig 3.4*) make this less likely and not enough data is available about Treg functionality in this model to draw conclusions about effects on Treg suppressive function.

The HIF DKO result introduces the question of whether HIF-2α was driving the previous phenotype and that a different factor was now responsible for the phenotype in HIF DKO, coincidentally inducing similar changes as HIF-2α, or whether a different driver was responsible for the phenotype all along and was masked by HIF-2α trends, taking centre stage in HIF DKO when uninhibited by the other HIFs. Indeed, the spleen myeloid compartment (*Fig 3.9b*) and abnormal Th transcription factor expression (*Fig 3.11*) do seem to point to different mechanisms than previously observed. HIF-3α is a potential suspect, and it can be induced by HIF-1 and -2α in various tissues[284,285], although whether immune cells express it is unknown. Furthermore, it is not known if HIF-3α can compensate for low HIF-1/2α levels the way that HIF-1α and -2α can for each other[159,160], although HIF-3α overexpression has been shown to induce expression of HIF-1α or HIF-2α target genes despite mostly antagonising their transcriptional activity[285,286]. However, not all of its splice variants are transcriptionally active[287], so even if it were stabilised and binding ARNT in our data, it might not be inducing transcriptional changes.

Another potential explanation for the HIF DKO phenotype is that lack of HIF frees up ARNT to bind its alternative dimerization partner, AHR, and that increased AHR activity is responsible for our observed phenotype. Hsp90 is also a coactivator for AHR[288], which would likewise be freed up by HIF DKO. Low AHR serum agonism is correlated with MS severity in patients, and the novel therapeutic laquinimod for MS is thought to act as an AHR agonist[289,290].

However, AHR KO in $CD4^+$ T cells increased recovery from EAE by affecting the microbiome, despite a slight decrease in Foxp3 and IL-10 expression visible on Tregs[289]. In Tregs, multiple reports show that AHR expression is beneficial to Tregs, improving their induction from naïve cells, suppressive function, and preventing pro-inflammatory cytokine production as well as promoting Th17 to Treg switching[291–295]. Based on these results, perhaps increased AHR is not a good candidate for causing Treg dysfunction, but these results do show high number and activation of Treg that seem mostly functional in terms of phenotype and cytokine production – perhaps AHR is signalling to a higher or different level than in other studies and inducing a previously undescribed dysfunction, or combining with another factor in hypoxia that alters its effects on Tregs.

Due to the weight loss of the HIF DKO mice, I was forced to terminate the experiment early instead of carrying it to 4 weeks as planned. This also meant that the control hypoxic mice were analysed at an earlier timepoint than previously, and which not significant, cell counts trended toward being decreased this early in hypoxia (*Fig 3.9*), despite knowing that the opposite is true after 4-6 weeks of hypoxia. Kento Kawai had done a time-course experiment with PHD2 KD mice at 1-week intervals and found that increased inflammation and cell counts were already detectable, which contrasts findings in hypoxia. It was hypothesised that leukocytes could be leaving the lymphoid organs for the blood, but no increased counts in the blood of hypoxic controls were observed (data not shown). Therefore, leukocytes might be migrating to peripheral tissues – tissues from various organs were fixed to analyse this (*see section 7.4a*) – or somehow being deleted at this early timepoint, only to later be enriched in the spleens and lymph nodes with continued exposure to hypoxia. HIF signalling can promote migration of non-immune cells[296,297] and mostly seems to do the same in leukocytes[178,189]. HIFs are also known to induce matrix metalloproteinase expression[298,299], which might be playing a role in leukocyte escape from lymphoid structures and promoting tissue infiltration.

Based on these results and the serendipity of Tammie Bishop having a hypoxia experiment already set up, immune analysis was repeated on hypoxic ARNT DKO mice, which should exhibit the same lack of HIF signalling as the HIF DKO. However, the ARNT DKO phenotype did not in fact recapitulate the HIF DKO phenotype (*section 3.2c*). All the markers that increased

in HIF DKO were reversed in ARNT DKO, although not in the spleens. If AHR was responsible for the induction of the HIF DKO phenotype, lack of ARNT would indeed reverse this, whereas it would not reverse a HIF-driven phenotype (despite our low confidences that HIF DKO could induce a HIF-2α or perhaps HIF-3α-driven phenotype). However, based on the incomplete recombination of ARNT and the inconclusive target expression in the qPCR (*Fig 3.12*), it seems more likely that the reversal of ARNT phenotype is a result of incomplete knockout, especially when considering the haematocrit as a reflection of EPO which was not decreased in ARNT DKO as it was in HIF DKO (*Fig 3.13*). The incomplete recombination in the lymph nodes supports this, and it is possible that the reason why the phenotype was not reversed in spleens was due to better knockout efficiency, as RNA was not measured in spleens. Maria Prange-Barczyńska had measured knockout efficiency of ARNT DKO in kidney and carotid bodies in her thesis and found quite poor efficiency and high variability of knockout between these tissues, so it is possible that knockout efficacy in spleens would not match lymph nodes and might explain the mismatch in results. Additionally, lymph nodes are known to be an especially hypoxic environment[147] which may exacerbate what little HIF levels remain in the HIF DKO, should these be indeed driving that phenotype.

The work in this chapter aimed to further investigate the hypoxic phenotype and confirm that it was similar to PHD2 KD so that the mechanisms HIF-2α was driving in Tregs could be better understood, but this led to new questions much more complex than a simple confirmation of previous results. Overall, it is impossible for HIF-2α and HIF DKO to be driving the same phenotype and for HIF and ARNT DKO to show opposite trends. The efficacy of ARNT DKO is less convincing and seems the most likely reason why this should differ from HIF DKO, especially knowing that it is reduced by only 20-50% in other tissues (data in Maria Prange-Barczyńska's thesis). The mismatch between previous results and the HIF DKO is then either driven by suspiciously low remaining levels of HIF-2 α or perhaps an increase in AHR or even HIF-3 α, although it is not confirmed whether these are indeed being activated and what signalling they would induce that could explain the phenotype. Investigating AHR levels and expression of markers downstream of it would allow us to gain some insight into whether this or residual HIF levels might be driving the phenotype (*see section 7.4a*). The signalling in these models has very profound effects on Treg function and the entire immune landscape. This is of

great value in immunological diseases ranging from cancer and infections to autoimmunity and transplant rejection, so being able to understand what drives these changes is of great interest to us if downstream mechanisms could be more precisely targeted. While the hypoxia experiments in this chapter led to unclear conclusions, the PHD2 KD phenotype led to consistent immunological changes, and I sought to complement this avenue of research with an approach to uncover the mechanistic changes that so altered Treg function and are thus therapeutically valuable, which is discussed in the following chapter.

4 – Effects of HIF Signalling on Treg Transcription

4.1 – INTRODUCTION AND AIMS

Based on previous findings both from before I joined the project and those presented in the chapter above, I sought to investigate how HIF signalling affects Tregs in more depth in this chapter. It had been previously observed that PHD2 KD could not only cause Tregs to lose suppressive function but could make them inherently pathogenic[255], which suggests a significant transcriptional reprogramming. The literature on HIFs in Tregs is very conflicted (*see section 1.5a*), but not many studies have examined the mechanisms downstream of HIF that could be driving the observed changes in Treg phenotype and function. Dang et al. showed that HIF was capable of directly causing Foxp3 degradation at the protein level via ubiquination[99] but this could not be replicated by others[254], while others showed that HIF targeted Foxp3 at the mRNA level rather than the protein[261]. An HRE was identified in the promoters for both Foxp3 and TGFß, although TGFß neutralisation was shown to prevent HIF-driven Foxp3 induction[254], suggesting that it might be driving Foxp3 induction indirectly rather than via direct targeting of Foxp3 by HIFs. However, all these studies focused on *de novo* induction of Foxp3 from naïve T cells rather than how HIFs might affect mature, established Tregs.

Our group had previously shown that PHD2 KD had no effect on TSDR methylation in Tregs[255], suggesting that the observed changes in function did not result from epigenetic reprogramming toward plasticity and loss of Treg identity. However, other than an increase in Tbet and TNFα and a decrease in CD25 expression on Tregs[255], little else was observed that could explain the loss of Treg function, so single cell RNA sequencing was utilised to explore and reveal potential transcriptional pathways driving the loss of Treg function that was not adequately explained by the existing data.

CHAPTER AIM: To understand how HIF signalling impacts the Treg transcriptional programme

HYPOTHESIS: HIF-2α activates a downstream inflammatory pathway in Tregs

4.2 – Results

4.2a – PHD2 KD Tregs Have a Transcriptionally Distinct Subset

In order to best interrogate transcriptional pathways downstream of HIF signalling that could be modulating Treg function, single cell RNA sequencing was used to evaluate PHD2 KD mice. The entire CD4 compartment was examined so that transcriptional changes that were unique to Tregs could be identified, as opposed to general cell or T cell adaptations, as the phenotype was observed to be predominantly Treg-driven. PHD2 KD mice were treated with doxycycline for 4 weeks to induce the shRNA KD (*Fig 4.1a*), and several controls were used thanks to the hashtag oligomers that allowed for various subject groups to be kept separate in order to refine our question: a doxycycline-treated control and a control that had been treated with doxycycline for 3 weeks and reversed for the fourth were both included in order to discount any transcriptional changes that were caused by doxycycline itself. Two controls known to reverse the systemic phenotype were also included: HIF-2α KO which had reversed inflammation in PHD2 KD and would allow to separate HIF-1 α targets from the genes specifically downstream from the causative HIF-2α signalling, and reversal of doxycycline treatment during the last week which was known to reverse the phenotype and would indicate whether any transcriptional changes were long-lived. Thus, only the PHD2 KD group should have the expected transcriptional changes driving the observed phenotype, and the hashtag oligomer tagging allowed the labelling of samples from those five individual groups so that they would be discernible and comparable during analysis (*Fig 4.1b)*.

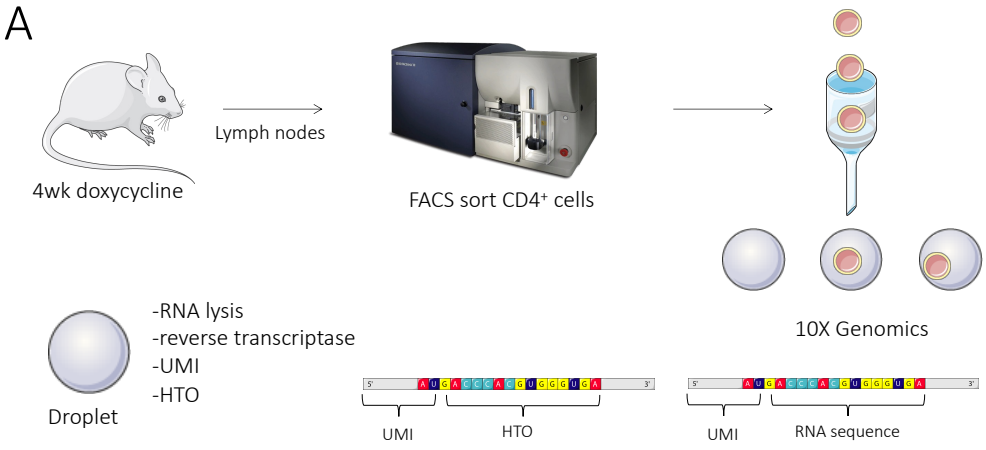

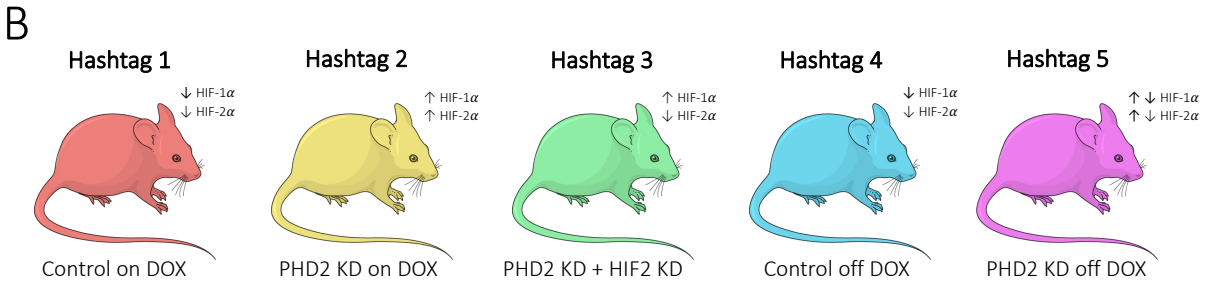

Fig 4.1 – PHD2 KD Tregs are transcriptionally distinct from other Tregs. (A) Mice treated with doxycycline for 4 weeks (some with doxycycline stopped during the last week) had their lymph nodes harvested and $CD4^+$ T cells were isolated and tagged with hashtag oligomers according to their distinct biological groups (B) by Kento Kawai. Samples were processed for 3' Chromium 10X sequencing by the Wellcome Trust Centre for Human Genomics on 3 pooled cartridges. RNA fragments were labelled with unique molecular identifiers (UMIs), and a hashtag oligomer (HTO) sequence corresponding to 5 biological groups.

A total of 32,469 cells were run over 3 separate cartridges and pooled together to be analysed as one, with an average of 9,608 mean reads per cell and 3,219 reads mapping to the transcriptome (*Table 9*). Cell normalisation and clustering was performed according to the standard Seurat package workflow pipeline of the Sajita lab, with data filtering cut-off points of mitochondrial data, number of counts and features per cell, and number of dimensions included for dimensional reduction all being based off of visual plots (*Fig. 4.2*). A resolution of 0.8 was chosen for PCA reduction as this allowed for the best visualisation of biological clusters.

Table 10 – Data summary for 4-week experiment. Calculated mean reads per cell are reads that mapped to the transcriptome and belong to cell barcodes.

Sample	Estimated No of cells	Sequencing Saturation	Mean Reads per Cell	Calculated Mean Reads per cell
Pool 1 RNA	13,297	60.4 %	7,961	3,353
Pool 2 RNA	13,890	62.8 %	8,557	3,588
Pool 3 RNA	5,282	42.8 %	12,308	2,716
Pool 1 HTO	13,927	10.2 %	1,971	
Pool 2 HTO	13,890	10.4 %	2,067	
Pool 3 HTO	5,282	8.2 %	1,848	

A

Classification	Cells Count
Doublet	8141
Hashtag1	5922
Hashtag2	6894
Hashtag3	6790
Hashtag4	8618
Hashtag5	7848
Negative	114

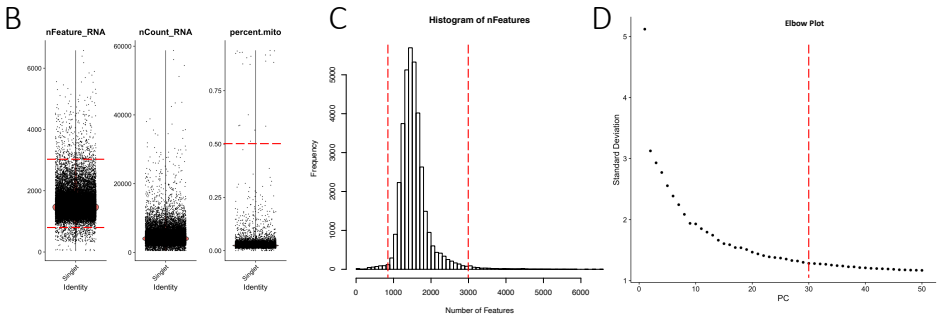

Fig 4.2 – Technical data from single cell RNA sequencing experiments. (A) Cell counts per hashtag. Only singlets were included. (B) Number of genes (nFeature_RNA), number of counts per gene (nCount_RNA), and the percentage of mitochondria genes per cell (percent_mito). (C) Histogram of nFeatures per experiment. (D) Elbow plot of the top 50 dimensions. Dashed lines show cut-off limits that were excluded.

A number of known population-defining markers were analysed across the different clusters in order to identify them, especially the small outlying populations believed to be contaminants (*Fig 4.3*). This allowed for contaminant $CD8^+$, myeloid cell, and B cell populations to be identified and removed from the analysis to reduce noise when comparing between clusters. As well as this, genes that define individual clusters when compared to all other clusters were also investigated to better understand what differentiate the various $CD4^+$ T cells (Appendix A).

The majority of T cells seemed to have little identity separating them from other clusters other than transcriptional signature identified by being negative for Treg markers and a relative decrease in activation compared to other clusters, with few markers upregulated compared to other peripheral clusters. This is in line with expectations that the majority of the $CD4^+$ T cell compartment in mice is made up of naïve cells, which is reflected in the uniform shape of the tSNE plot. A clear antigen-experienced Teff cluster was distinct from these, identifiable by its expression of *Cd44, Il2rb, Icos, Ifng* and low *Sell* and *Ccr7* which are naïve markers (Appendix B). Tregs were identifiable by their expression of *Foxp3*, *Il2ra* (CD25), *Ox40*, *Helios, Ctla4*, and separated into resting Tregs and an active cluster that showed the same expression of activation markers as the cluster identified as effector T cells (Appendix B).

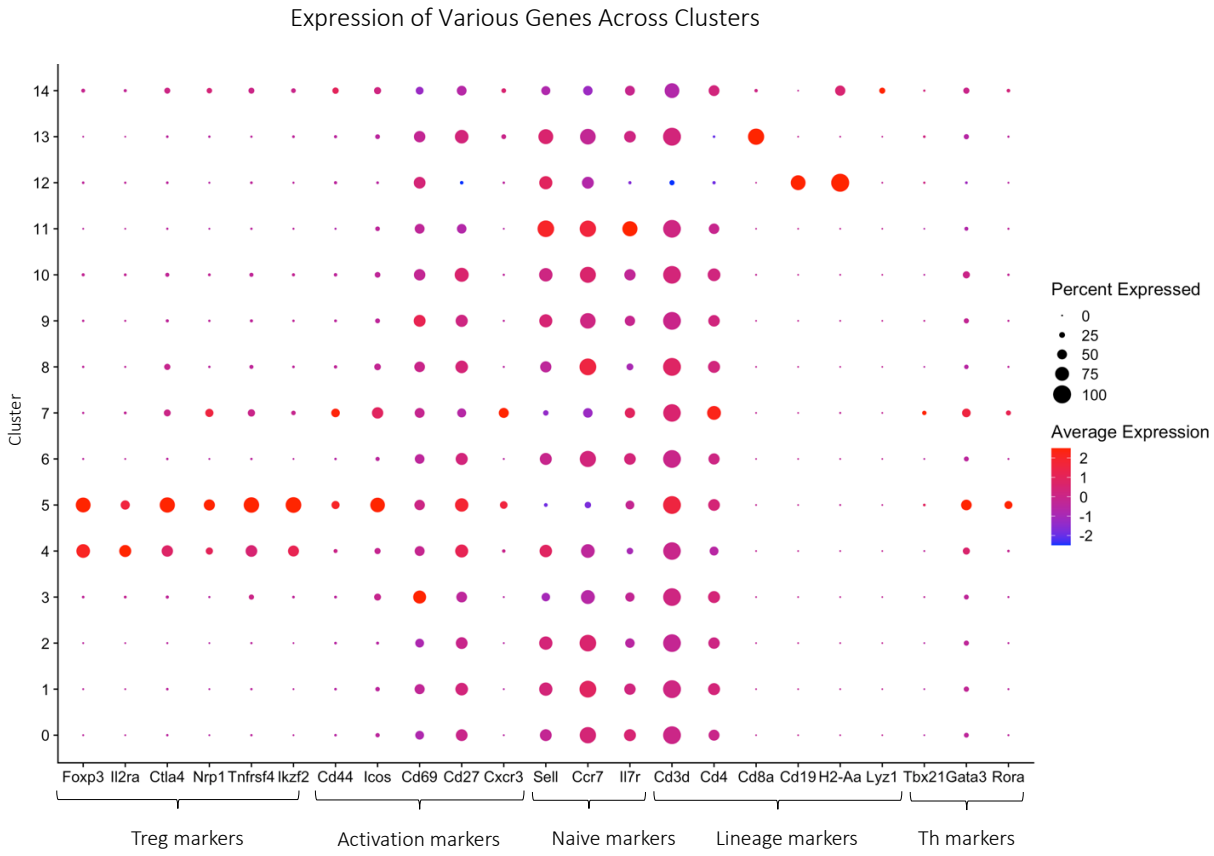

Fig 4.3 – Dot plot showing expression of hand-selected genes to identify and label clusters. Genes known to correspond to different cell signatures were selected and plotted across individual clusters, which allowed for a primary identification of cluster identities. Size of dots represents the percentage of cells in the cluster expressing a given target gene, and colour represents fold change of average expression.

Two clusters were observed with polarity toward type I signalling and IFNγ-responsive genes as well as some NFkB pathway-related transcripts, classic T cell transcriptional programmes which have been found in similar datasets[300–302]. The NFkB pathway has been identified by others as non-lymphoid markers and correlated with activation[301], and might identify cells recently arriving to lymph nodes from peripheral tissues. An interferon response module was also identified in $CD4^+$ T cells in other single cell sequencing sets in humans, which characterised a distinct activation state[300]. Other than the IFNγ-related transcripts which were not accompanied by strong expression of *Tbet*, T cells did not seem to cluster into distinct Th1, Th2, or Th17-like clusters. These do not seem to be identified as separate clusters in other single cell datasets either[300–302], so this polarity of individual Th subsets might be too subtle and thus overshadowed by greater differences in activation status that better separate out clusters.

Differential expression of cells from different hashtag groups was analysed, with differentially expressed genes of adjusted p value < 0.05 plotted (*Fig 4.4*). Only 21 genes were differentially expressed between the two doxycycline control groups, of which only a handful meet the fold change cut-off point for the volcano plot, indicating that the presence or removal of doxycycline during the last week had minimal effects (*Fig 4.4a*). When comparing the PHD2 KD group to control (*Fig 4.4b*), double PHD2/HIF2 KD (*Fig 4.4c*), and PHD2 KD with removal of doxycycline groups (*Fig 4.4d*), many of the genes upregulated in PHD2 KD were Treg genes, such as *Foxp3, Tnfrsf4, Ctla4, Icos, Il2rb*, and *Capg*[303]. Other genes specific to PHD2 KD were *Gdpd3* and *Ywhag* which signal along the PI3K-Akt-mTor axis[304,305], and *Il9r* which can promote Treg suppression in an autocrine fashion but is also commonly associated with autoimmunity[306], both of which might have implications for Treg stability. *Ddx3y* and *Ddit4* were both also upregulated in PHD2 KD cells, and both have links to cancer by regulating cell cycle progression and cell migration[307], which could explain the widespread leukocytosis found in PHD2 KD tissues[255]. Additionally, *Nfkbia*, a regulator of the NFkB pathway, was also enriched in PHD2 KD cells (*Fig 4.4b-d*).

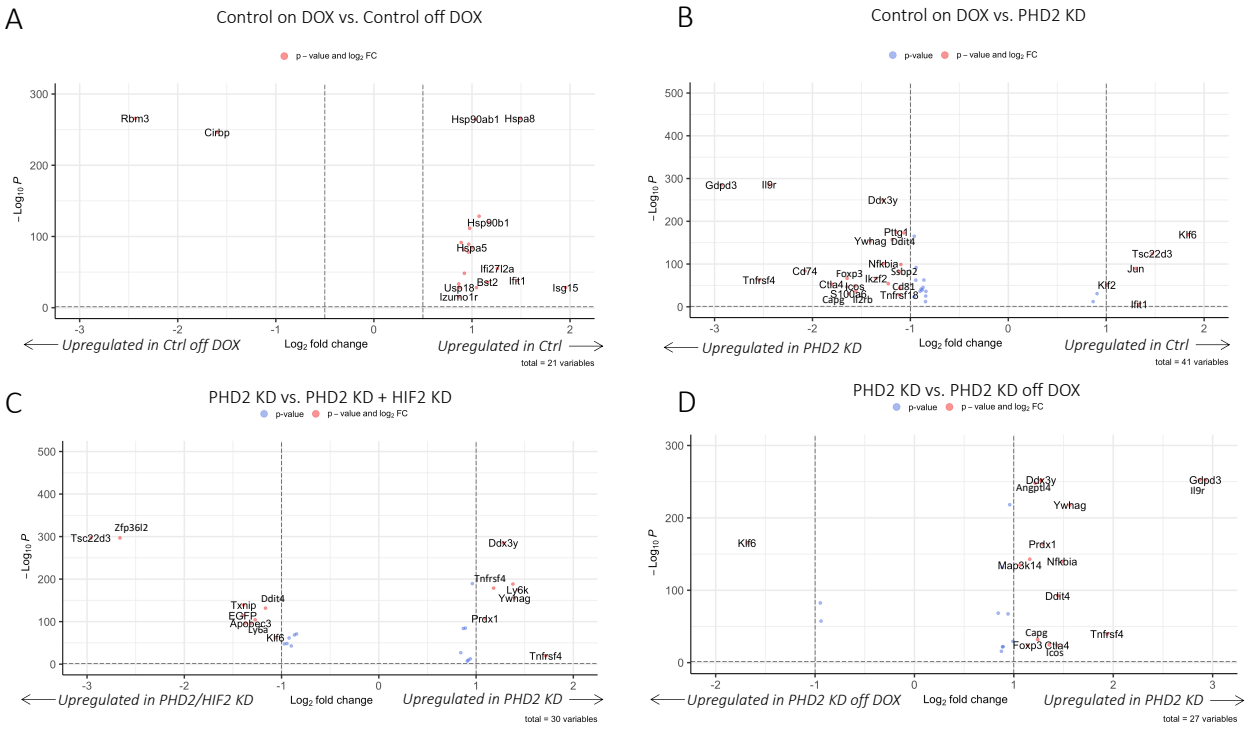

Fig 4.4 – Differential gene expression across biological groups. Differential expression was analysed between hashtag oligomer-labelled groups and genes with adjusted p value < 0.05 were plotted between (A) hashtags 1 vs. 4, (B) hashtags 1 vs. 2, (C) hashtags 2 vs. 3, and (D) hashtags 2 vs 5 (see *Fig 4.1b*). Graphs were generated with Enhanced Volcano in R with standard parameters.

When comparing cells based on biological hashtag-labelled groups rather than unbiased clusters, an island was identifiable in the active Treg cluster that was unique to the PHD2 KD group (*Fig 4.5)*. This was set to the outside edge of the cluster, indicating that these Tregs are transcriptionally unique. Based on this and on previous *in vivo* data showing the importance of Tregs in PHD2 KD, Treg transcription was investigated in more depth: cells expressing a detectable level of Foxp3 expression were selected and unbiased clustering was performed on this selection of cells. This allowed the sample to include any Tregs that might have escaped the unbiased clustering and might be residing elsewhere in the T cell map, as these might be cells of interest that seem to lose Treg identity. Similarly, the active Treg cluster was isolated and unbiased clustering was again performed on cells from that cluster, with a resolution of 1.2 to allow the clustering to overlap with the island cells that arose only from PHD2 KD mice. This provided further reassurance that these cells were transcriptionally distinct from other Tregs, and also allowed for the comparison of these clusters against other Tregs around them.

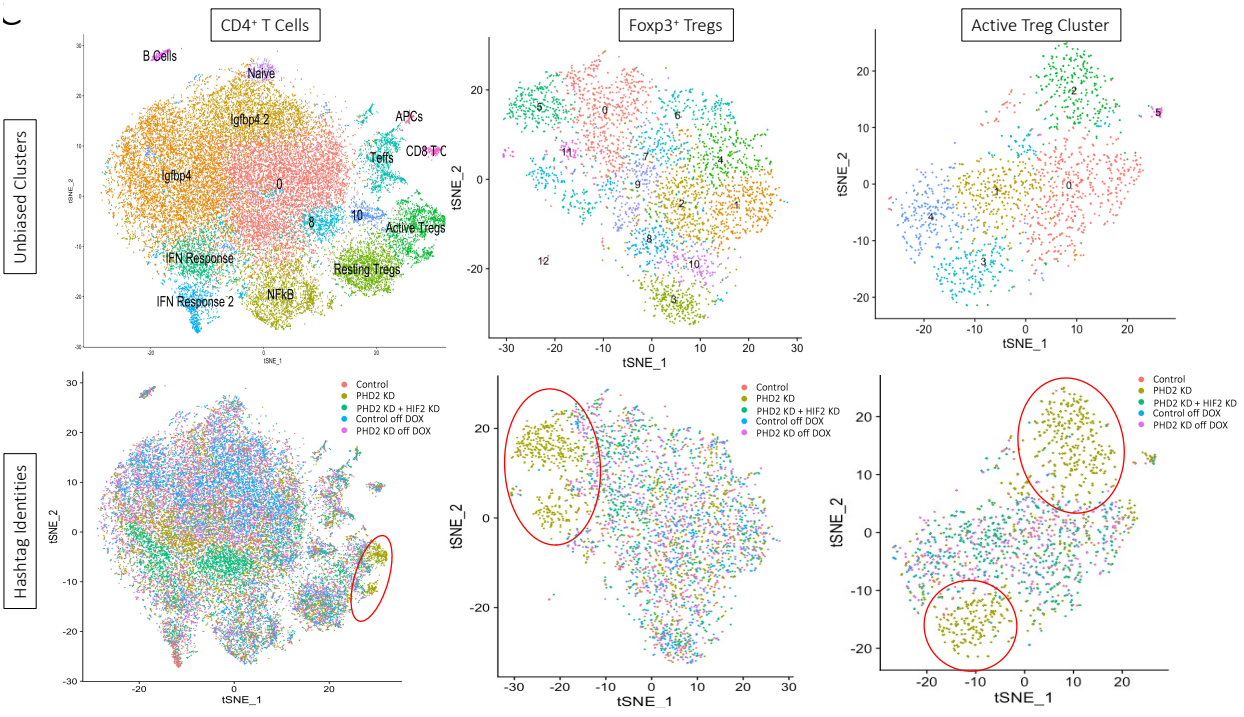

Fig 4.5 – PHD2 KD-specific islands are identifiable across CD4⁺ T cells, Foxp3⁺ cells, and the active Treg cluster. tSNE plots generated with the Seurat package in R. Colours represent unbiased clusters (top) and cell identities as per hashtag oligomer labelling (bottom).

Being able to align the yellow PHD2-specific Treg islands with unbiased subclusters allowed for a direct comparison between the PHD2-specific islands and the rest of the Tregs to identify transcriptional changes specific to the PHD2 KD Tregs that might explain our observed phenotype. When comparing genes from this PHD2 KD-specific cluster to other Foxp3^{+} cells, the majority of the genes that set these cells apart were typical Treg genes, but they were positively differentially expressed in our yellow island Tregs; this indicates that the majority of what differentiates them is that they have even higher expression of functional and phenotypic Treg genes, such as *Tnfrsf4* (OX40), *Icos*, *Ctla4, Ebi3* (IL-35), and *Ccr4* (*Fig 4.7a*) – this increased in expression which should reflect extra functional and committed Tregs was unexpected from Tregs known to be dysfunctional and even pathogenic.

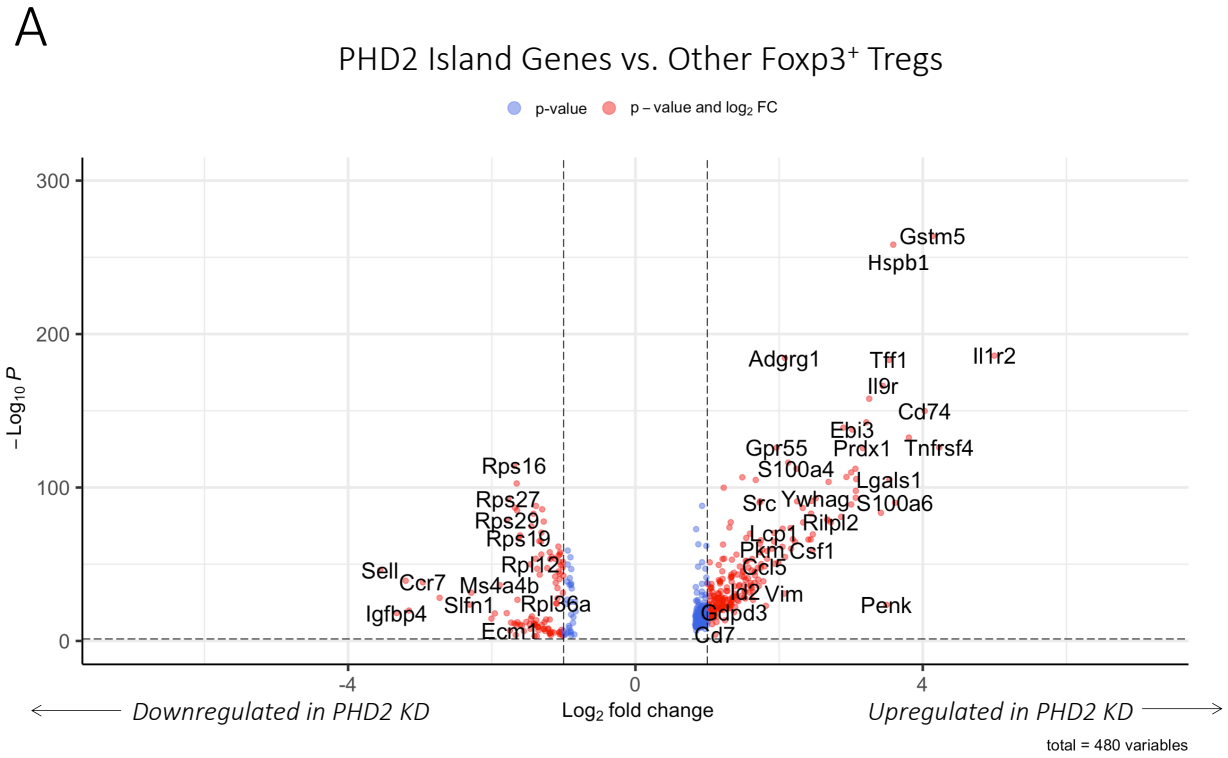

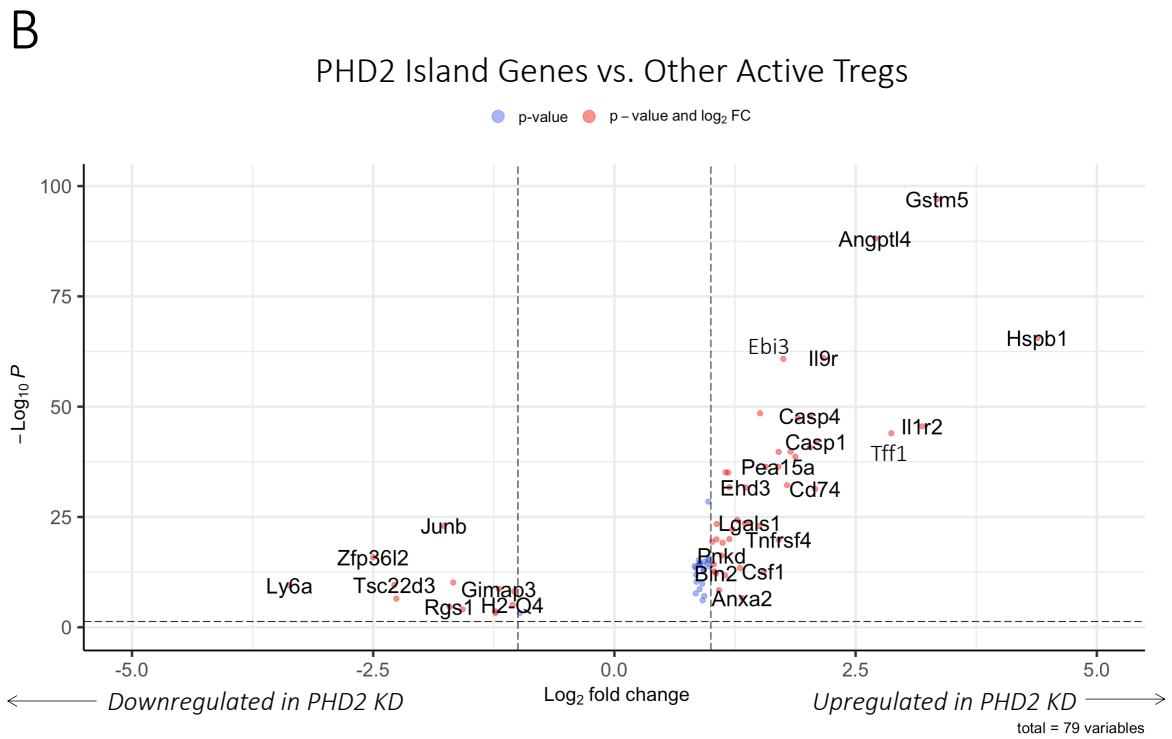

Fig 4.6 – Transcriptional changes that identify PHD2 KD Tregs. Mice treated with doxycycline for 4 weeks had their lymph nodes harvested and CD4$^+$ T cells were isolated and tagged with hashtag oligomers according to their distinct biological groups by Kento Kawai. Samples were processed for 10X sequencing by the Wellcome Trust Centre for Human Genomics. (A) Foxp3$^+$ cells were separated out and reclustered, and differential expression between the clusters overlapping with yellow PHD2-specific islands vs. the rest of the Foxp3$^+$ Tregs were analysed in Seurat. (B) The active Treg cluster originating from unbiased clustering was separated out and reclustered, and differential expression between the clusters overlapping with yellow PHD2-specific islands vs. the rest of the active Tregs were analysed in Seurat.

As well as identifying the genes that differentiate PHD2 KD Tregs, I sought to place these genes in better context, as pathway enrichment analysis can sometimes bring to light patterns that are not clear from a list of genes alone. Pathway enrichment analysis against the hallmark pathway database revealed that the IL-2-STAT5 signalling pathway was lower in PHD2 KD Tregs compared to Foxp3$^+$ cells (*Fig 4.7a*), which is in line with observation of decreased CD25 expression at the protein level[255]. The differential expression against active Tregs was enriched for the apical signalling pathway and a decrease in UV response pathway, but these only had 2 and 4 genes respectively that aligned with the Hallmark dataset (Appendix C). As an additional form of pathway analysis, Lisa analysis was also used, which identifies transcriptional regulators overrepresented in a dataset based on ChIPseq data[278]. This allowed for the investigation of dominant transcription factors active in this data set, which confirmed observations of activation from markers such as *Batf* and *Maf,* various *Stat* signals, and *Jun* and *Nfkb* signalling, along with *Tbet* and *Gata3* (*Fig 4.7b*).

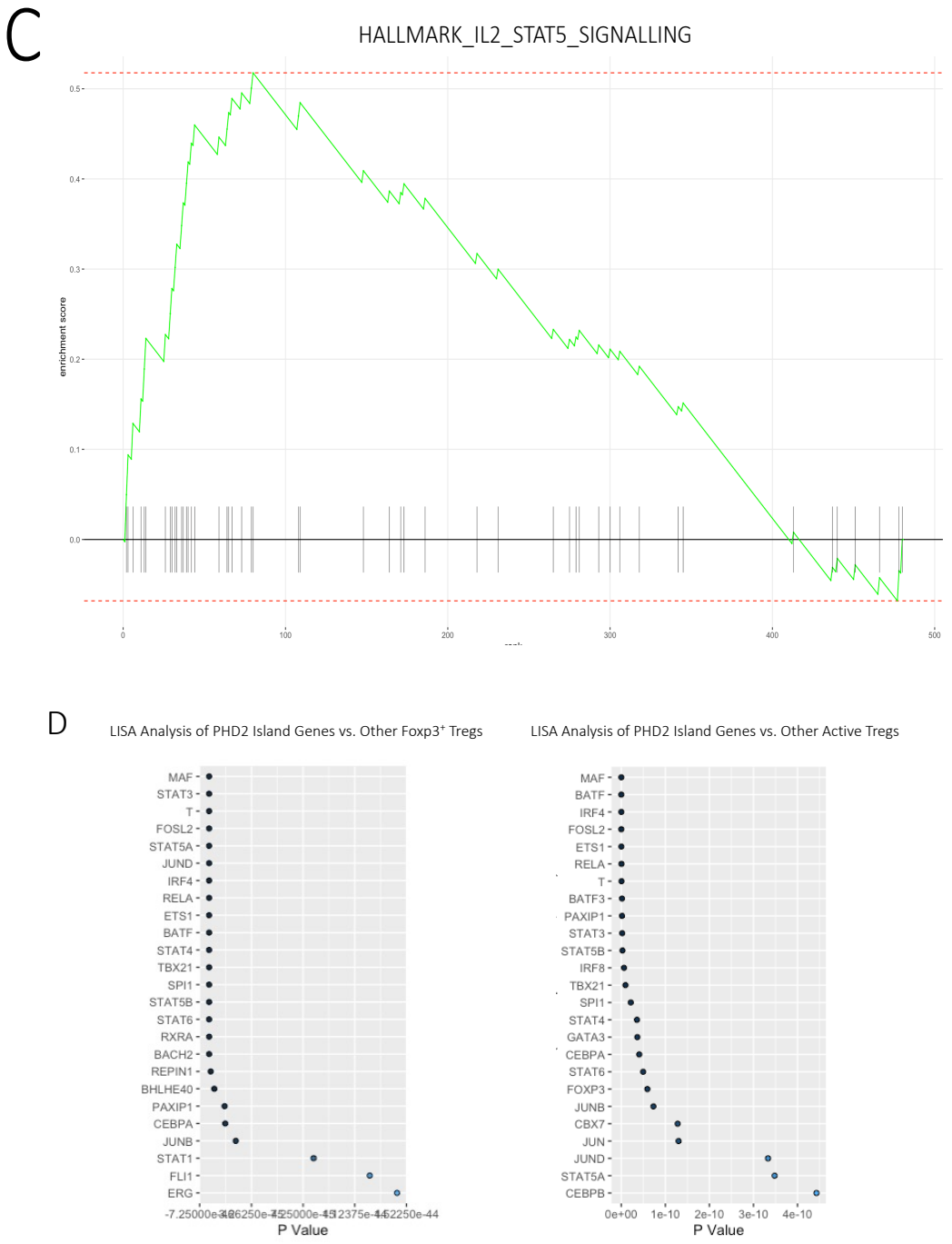

Fig 4.7 – (A) GSEA analysis using PHD2 island genes vs. other Foxp3^{+} cells (*Fig 4.6a*) using the fgsea package in R. Specific genes are listed in Appendix B. (C) Top 25 upregulated transcription regulators output from Lisa analysis of genes upregulated in PHD2 KD-specific islands vs. other Foxp3+ cells (left) and other active Tregs (right).

Highlighted genes were further interrogated to determine whether any of them could explain the pathogenicity of PHD2 KD Tregs. Within non-Treg genes, the topmost differentially expressed was *Hspb1*, which encodes the heat shock protein Hsp27 in humans or Hsp25 in mice (*Fig 4.6*). *Hspb1* responds to cellular stress including temperature and hypoxic stress and helps prevent apoptosis. Despite this, two caspases were upregulated as well, indicating that our Tregs might be attempting to combat stress and apoptosis. Additionally, *Hspb1* has been shown to be downstream of p38 MAPK/NFkB inducing kinase (NIK) activity[308] which was found to be increased in PHD2 KD Tregs (*Fig 4.8*); p38 deficiency could promote Treg differentiation[309] and overexpression of it induced a fatal Scurfy-like syndrome with non-suppressive Tregs and enlarged lymph nodes despite an increase in Treg as a proportion of $CD4^+$ T cells[310], remarkably similar to our observed phenotype. Treg-restricted overexpression of NIK produced ex-Tregs that lost suppressive function and became IL-2 and IFNγ-producing pathogenic cells[311]. RNA expression of enzymes does not reflect the enzyme activity, but increased expression of other p38 substrates such as *LSP1* can be observed (*Fig 4.8*).

Hspb1 and p38 MAPK can also induce non-canonical NFkB signalling[312], which is also hypoxia responsive[187] and classically considered inflammatory. Evidence of non-classical NFkB activation was found in PHD2 KD Tregs with slightly enriched expression of the subunits *p100* and *Relb* (*Fig 4.8*), which was also seen in Tregs from IPEX patients lacking Foxp3[313]. The canonical NFkB pathway is also downstream of Tnf receptors which are often associated with the Treg signature (OX40, 4-1BB, TRAIL, LIGHT), so both might be inducing NFkB concomitantly; however, the canonical subunits *p50* and *p65* were expressed by more cells but at lower levels in PHD2 KD (*Fig 4.8*). Most NFkB gene targets were very lowly expressed in this dataset so it was difficult to query the downstream consequences of this signalling.

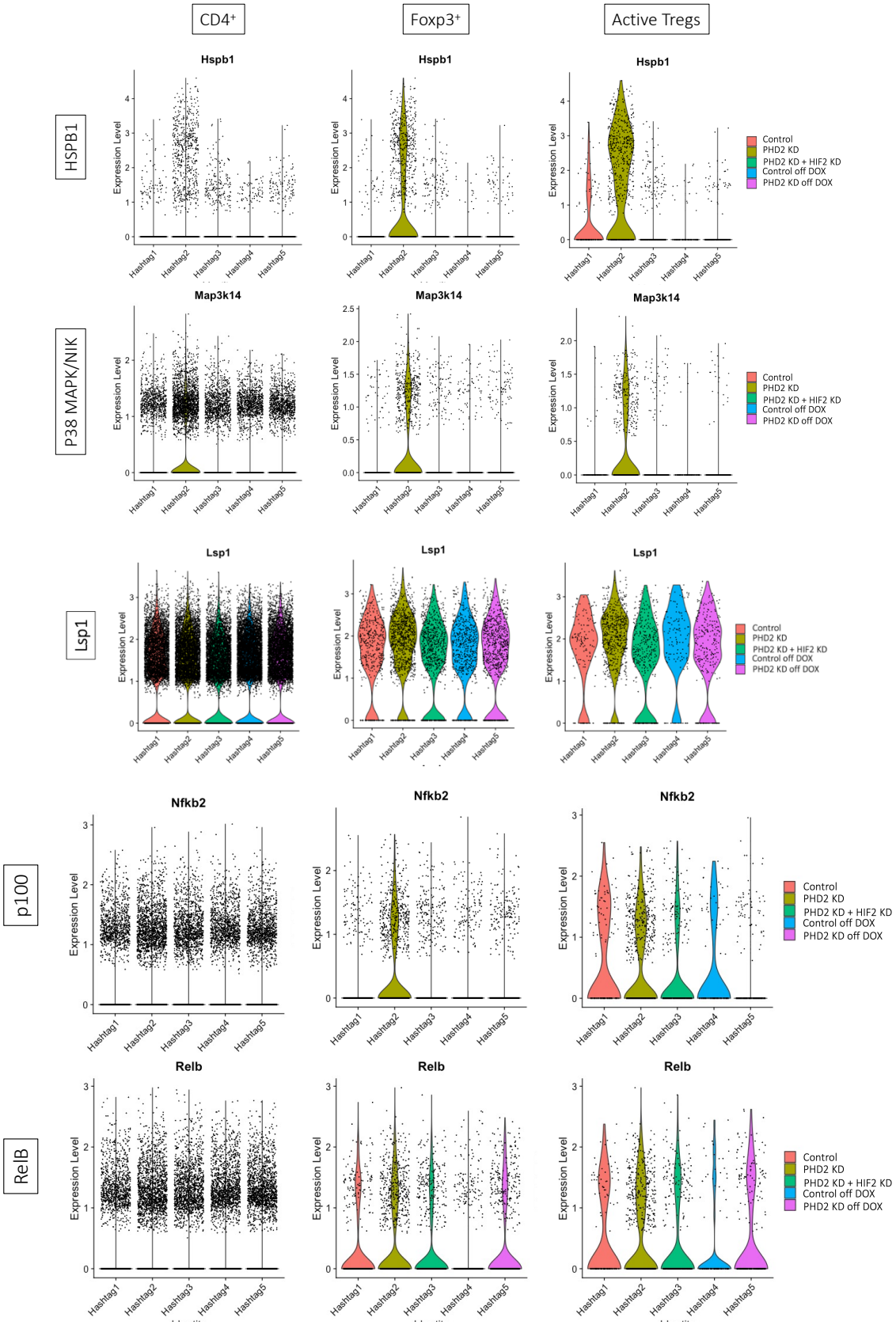
CD4+
Foxp3+
Active Tregs
HSPB1
P38 MAPK/NIK
Lsp1
p100
RelB
Hspb1
Map3k14
Lsp1
Nfkb2
Relb
Expression Level
Hashtag1
Hashtag2
Hashtag3
Hashtag4
Hashtag5
Control
PHD2 KD
PHD2 KD + HIF2 KD
Control off DOX
PHD2 KD off DOX

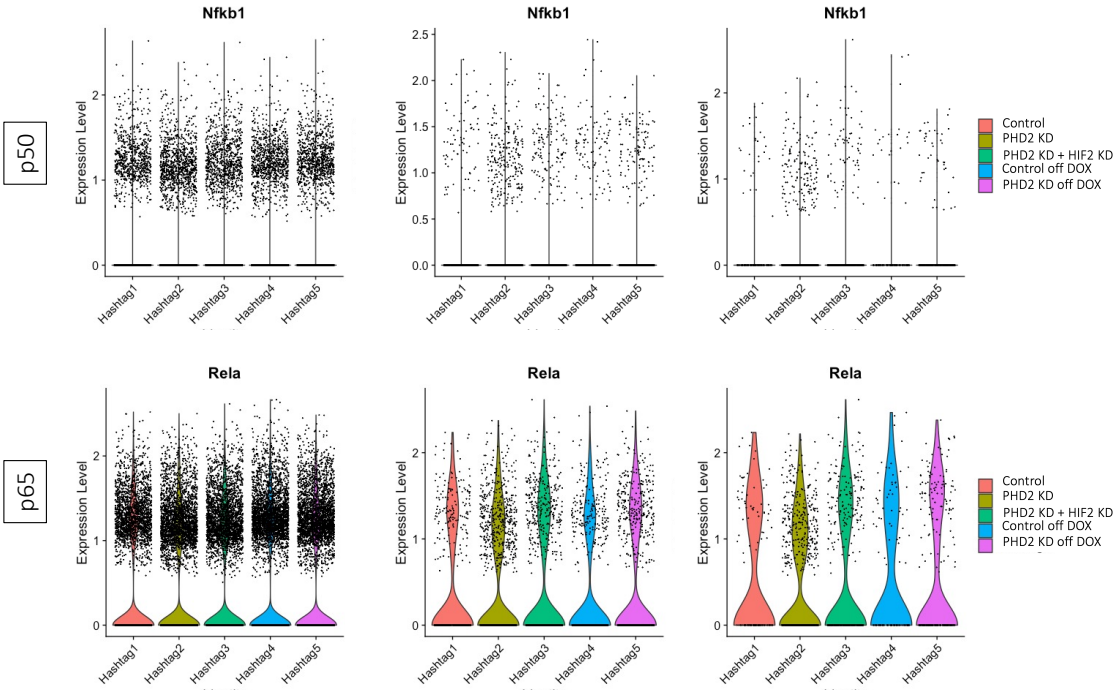

Fig 4.8 – PHD2 KD Tregs are enriched in p38 MAPK and non-canonical NFkB genes. Mice treated with doxycycline for 4 weeks had their lymph nodes harvested and $CD4^+$ T cells were isolated and tagged with hashtag oligomers according to their distinct biological groups by Kento Kawai. Samples were processed for 10X sequencing by the Wellcome Trust Centre for Human Genomics. Violin plots show gene expression of various targets grouped by individual hashtag groups across the entire cell population (left), cells expressing Foxp3 (middle), and cells originating from the unbiased active Treg cluster (right). P100 and RelB are non-canonical NFkB subunits, p50 and p65 are canonical NFkB subunits, and Lsp1 and Hspb1 are downstream of p38 MAPK/NIK.

Another highly differentially expressed gene was *Gstm5* (*Fig 4.6*), a protective detoxifying glutathione transferase enzyme[314]. Interestingly, mutation of another different GST in IBD patients was found to be associated with decreased STAT3 and p38 MAPK signalling[315], potentially linking it to some of the other transcriptional changes observed. The most significantly downregulated genes against $Foxp3^+$ cells (*Sell, Ccr7,* and *Igfbp4*) are all associated with naïve signature, but within other active Tregs, PHD2 KD Tregs show decreased *Ly6a* (*Fig 4.6b)*, associated with activation[316]. *Junb* is also decreased on PHD2 KD Tregs against other active Tregs (*Fig 4.6b)*, which can induce CD25 expression in Treg-inducing conditions[317], so this decreased *Junb* expression could be in part responsible for some of the decreased CD25 expression and downstream IL-2-STAT5 signalling themes that the pathway analysis uncovered. Taken together, this might indicate that although our PHD2-KD Tregs fall within the active Treg cluster, they might have discrete defects in their effector function compared to other effector Tregs in the active cluster.

Altogether, some of the transcriptional changes identified in the yellow islands form a pattern of expression potentially implicating p38 MAPK and NFkB signalling deregulating the function of PHD2 KD Tregs, as this would support the pathogenicity observed in these mice being very similar to that observed by others[310,311]. Additionally, pathway enrichment analysis confirmed a decrease in IL-2 signalling and STAT5 in line with previous observations that CD25 surface expression is lower on PHD2 KD Tregs, which decreased JunB expression might be responsible for.

4.2b – PHD2 KD Tregs Exhibit Loss of IL2ra but no Induction of Pro-Inflammatory Markers

Although the unbiased differential expression analysis shown above identified some potentially interesting pathways, I wanted to combine this with a more targeted approach to examine classic Treg genes, both to confirm the expression observed at the protein level and to identify new markers that had not been previously investigated with flow cytometry. Based on observations regarding CD25 expression at the protein level (see Chapter – Introduction and Aims) and GSEA results implicated decreased IL-2-STAT5 signalling (*section 4.2a*), I wanted to examine CD25 expression in this dataset. CD25 is the alpha chain of the IL-2 receptor with highest affinity for IL-2, and is important to Treg identity and suppressive function[79]. Of the two separate PHD2 KD-specific islands, one of them showed loss of *Il2ra* expression and the other did not (*Fig 4.9a*). In order to understand what separates these two, differential expression between them was investigated and revealed that the $CD25^-$ island had a loss of *Ctla4, Tigit,* and *Klrg1*, potentially indicating that it might be less functional (*Fig 4.9b*). Interestingly, some of the genes that were specific to the PHD2 KD Tregs such as *Hspb1, Gstm5*, and *Il1r2* were more highly expressed in the $CD25^+$ island, so it remains unclear which of the two subsets might be driving the functional changes.

Tcf7 was also upregulated in $CD25^-$ Tregs and is associated with *Lef1* and *Wnt* signalling pathways, both of which are co-upregulated (*Fig 4.9b*). *Tcf7* is normally a marker of naïve T cells[318], which might indicate that the $CD25^-$ PHD2 KD Tregs are less mature or activated than their $CD25^+$ counterpart, and this could result in a lack of effector function. *Tcf7* and *Lef1* are also associated with follicular Treg signature[319], as is *Id3*[320]; *Id3* is also co-expressed in $CD25^-$ Tregs (*Fig 4.9b*) and can also promote Foxp3 stability[321], which might explain why Foxp3 expression and TSDR demethylation are maintained despite loss of function in these Tregs.

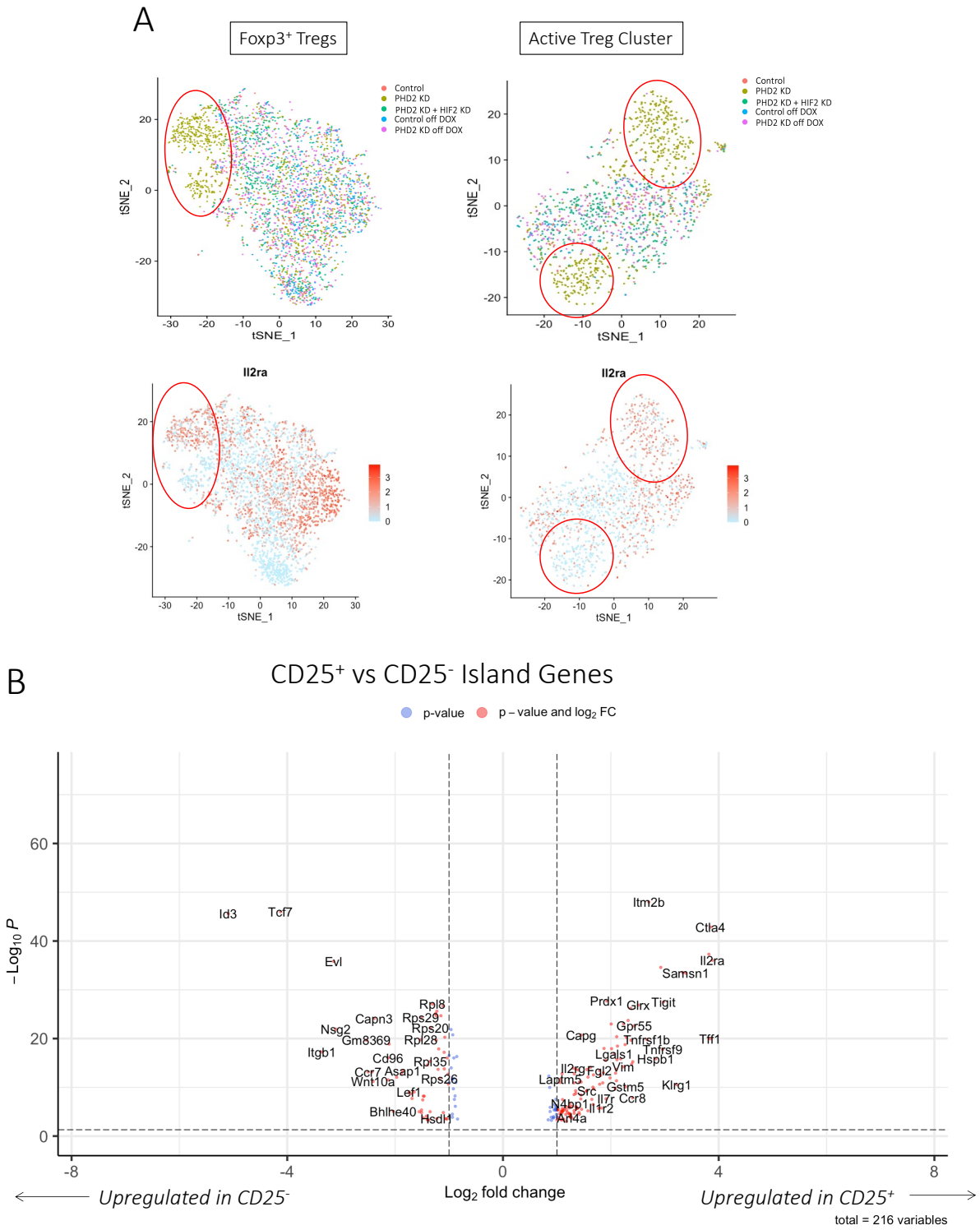

Fig 4.9 – PHD2 KD Tregs separate into two CD25⁺ and CD25⁻ islands with transcriptional differences. Mice treated with doxycycline for 4 weeks had their lymph nodes harvested and CD4⁺ T cells were isolated and tagged with hashtag oligomers according to their distinct biological groups by Kento Kawai. Samples were processed for 10X sequencing by the Wellcome Trust Centre for Human Genomics. (A) tSNE plots generated with the Seurat package in R where colours represent cell identities as per hashtag oligomer labelling (top) and Il2ra expression (bottom). (B) Differential expression between the two unbiased clusters 2 and 3 in active Tregs (see **Fig 4.5**) that overlap with the PHD2 KD-specific clusters to compare CD25⁺ and CD25⁻ PHD2 KD-specific Tregs.

Differential expression was expected to reveal pro-inflammatory genes or transcriptional changes that might otherwise explain the loss of function observed in PHD2 KD Tregs, and as this gain of inflammatory function was quite extreme[255], inflammatory markers were expected to be highly expressed to explain this. However, these were not genes seen in the differential expression analysis shown above, so a more targeted approach was used that allowed us to directly interrogate classic plasticity and inflammatory genes. *Tbet* and *Rorgt* were very lowly expressed across all samples but a slight enrichment in *Tbet*-expressing Tregs was visible (*Fig 4.10)*, which confirms previous flow cytometry results. Surprisingly, *Gata3* was globally enriched in PHD2 KD but lower in Tregs (*Fig 4.10*), which had not been observed previously. Expression of pro-inflammatory cytokines was interrogated and revealed that *Ifng* levels were very low across all cells but slightly more PHD2 KD Tregs were expressing it than other active Tregs, and similarly with *Tnf*, which had been previously observed at the protein level (*Fig 4.10*). None of these changes were drastic enough to explain the pathogenicity observed in PHD2 KD mice but expression in this dataset was consistent with previous observations in flow cytometry.

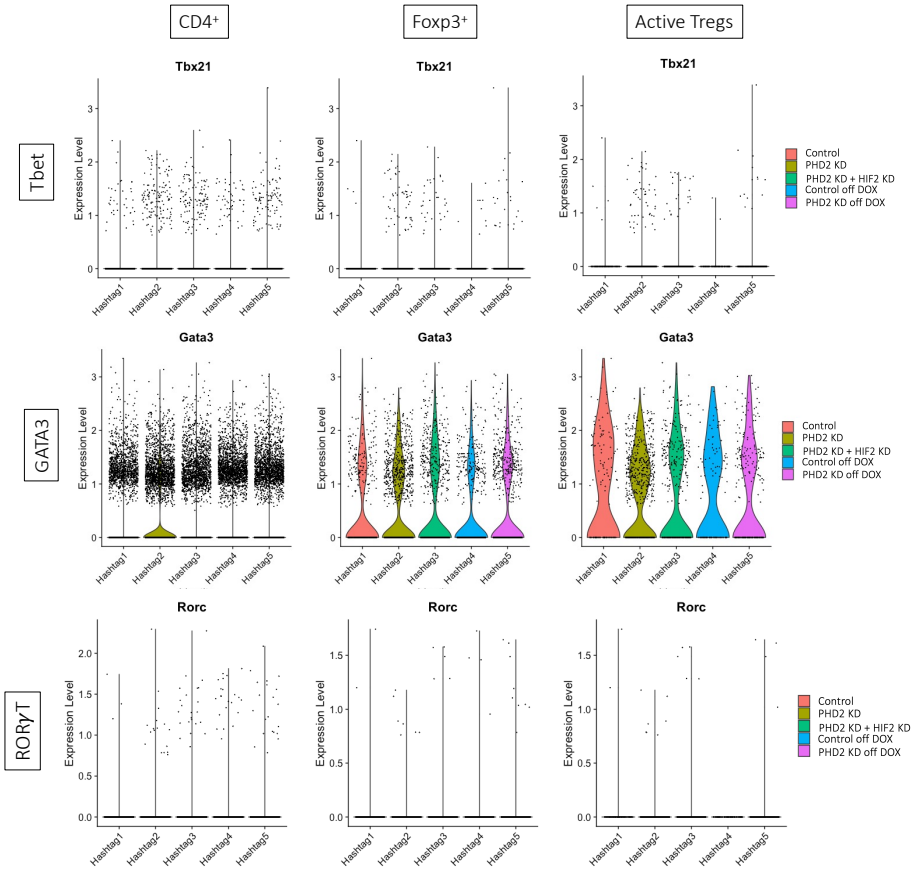

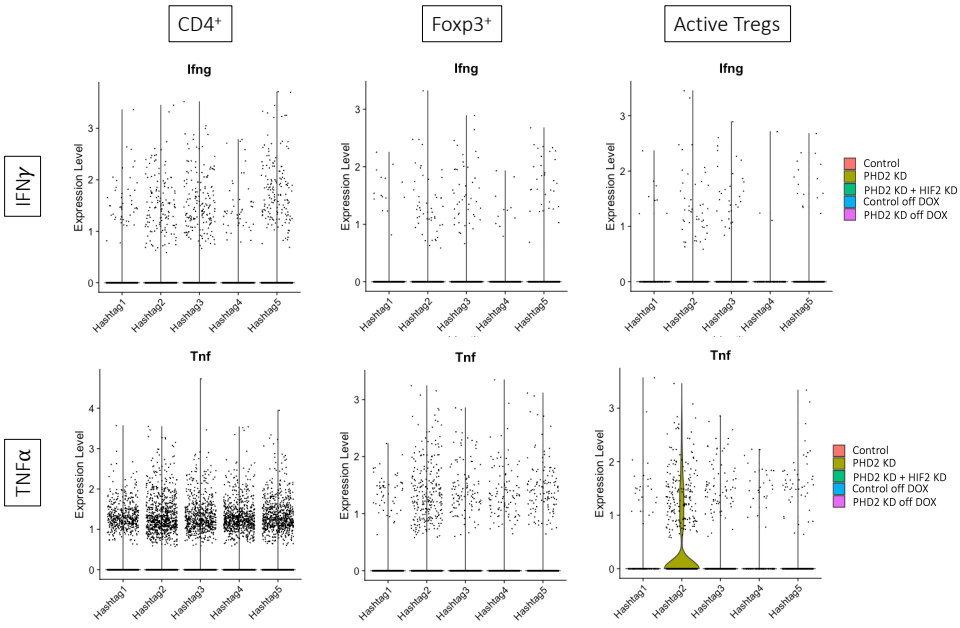

Fig 4.10 – Expression of pro-inflammatory genes in PHD2 KD Tregs. Mice treated with doxycycline for 4 weeks had their lymph nodes harvested and CD4$^+$ T cells were isolated and tagged with hashtag oligomers according to their distinct biological groups by Kento Kawai. Samples were processed for 10X sequencing by the Wellcome Trust Centre for Human Genomics. Violin plots show gene expression of various targets grouped by individual hashtag groups across the entire cell population (left), cells expressing Foxp3 (middle), and cells originating from the unbiased active Treg cluster (right).

In addition to searching for inflammatory genes, classical Treg genes were also examined, especially those relating to stability and suppressive function. As expected from the differential expression and previous flow cytometry work done by Kento Kawai, PHD2 KD Tregs did not seem to decrease their expression of these markers and even seemed to express them more highly than other Tregs (*Fig 4.11*). CTLA-4 is part of Treg suppressive function as it deprives Tconvs of the CD28-mediated signal 2 they require by outcompeting them for costimulatory ligands CD80/86 and even removing them off the surface of APCs through trogocytosis[77]. Production of anti-inflammatory cytokines IL-10, TGFβ, and IL-35 also contributes to suppression and tolerisation of the immune landscape, as well as helping induce new Tregs in the periphery[87,88]. These were expressed quite lowly in this data, but a greater number of PHD2 KD Tregs expressed these genes than other Tregs (*Fig 4.11).* Helios (*Ikzf2*) was originally thought to differentiate nTregs from pTregs[64], and although this has not been supported, Helios is correlated with Treg suppression[65] and regulates stability in a STAT5-dependent manner[66], and *Ikzf2* was found to be enriched against other Foxp3$^+$ Tregs but not active Tregs (*Fig 4.11*).

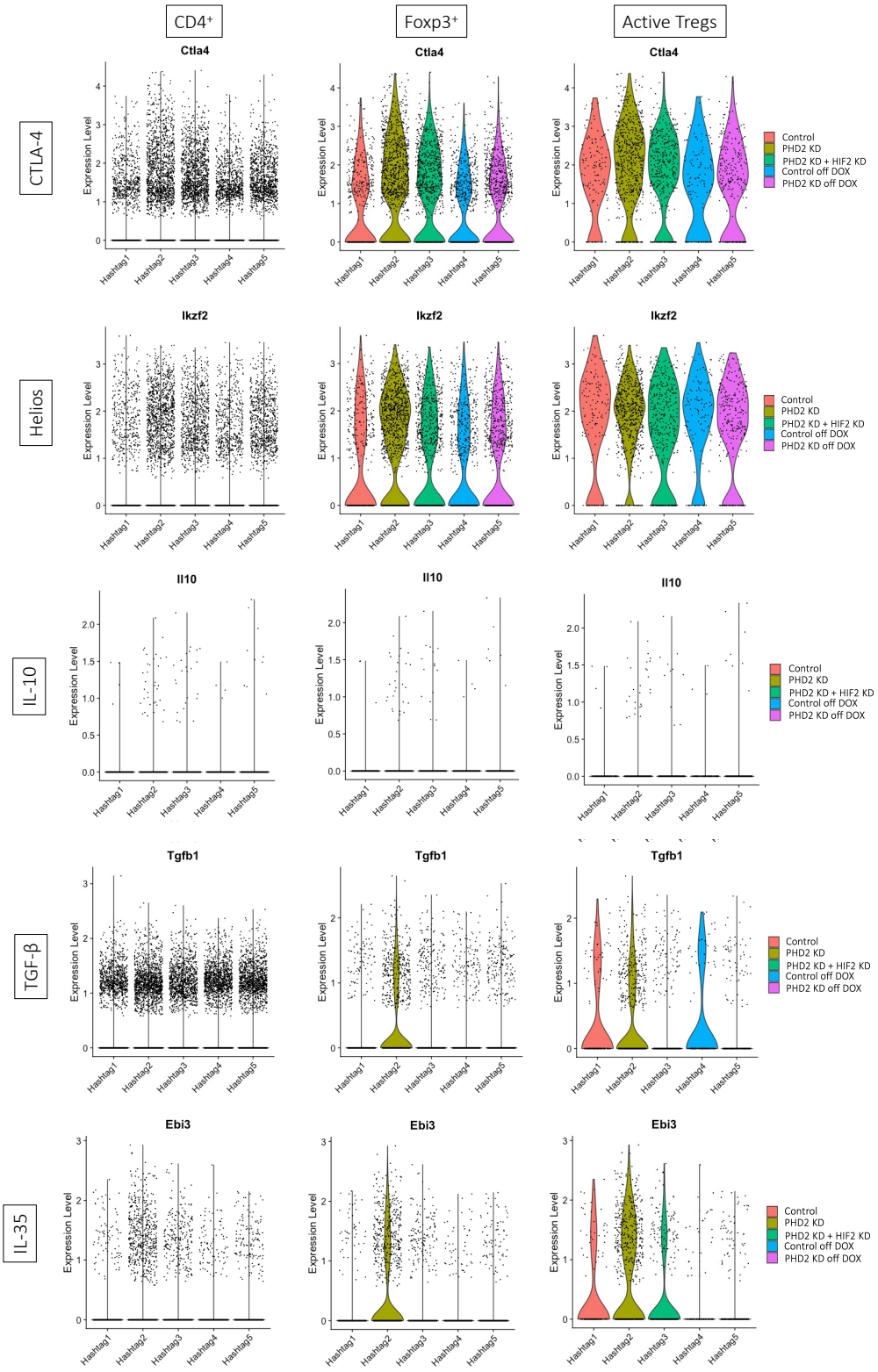

Fig 4.11 – Expression of Treg markers in PHD2 KD Tregs. Mice treated with doxycycline for 4 weeks had their lymph nodes harvested and CD4^{+} T cells were isolated and tagged with hashtag oligomers according to their distinct biological groups by Kento Kawai. Samples were processed for 10X sequencing by the Wellcome Trust Centre for Human Genomics. Violin plots show gene expression of various targets grouped by individual hashtag groups across the entire cell population (left), cells expressing Foxp3 (middle), and cells originating from the active Treg cluster (right).

4.2c – CD25⁻ Tregs are Transcriptionally Different to CD25⁺ Tregs

Based on observations at the protein level (*see Chapter 3 introduction*), results regarding individual CD25⁺ and CD25⁻ PHD2 KD-specific islands (*Fig 4.9b*), and loss of IL-2-STAT5 signalling (*Fig 4.7a*), the phenotype of CD25⁻ Tregs was further investigated. Additionally, Ferreira et al. identified enriched population of human CD25⁻ Tregs in SLE patients which maintained TSDR demethylation, Helios expression, and an activated memory phenotype[322], giving further credence to the notion that CD25⁻ Tregs play a role in autoimmunity. In order to interrogate our CD25⁻ Tregs, CD25⁺ and CD25⁻ Tregs were sorted from hypoxic Foxp3^{GFP} mice for bulk RNA sequencing (*Fig 4.7*). This allowed for greater sequencing depth than the single cell analysis and our hypothesis was that this might reveal other transcriptional changes that could perhaps be driving the phenotype, especially since CD25 has been one of the common running threads throughout. Differential expression based on CD25 expression had samples clustering together on the heatmap and showed that there were clear differences between the two, but samples did not seem to necessarily cluster by hypoxia or normoxia (*Fig 4.12d*).

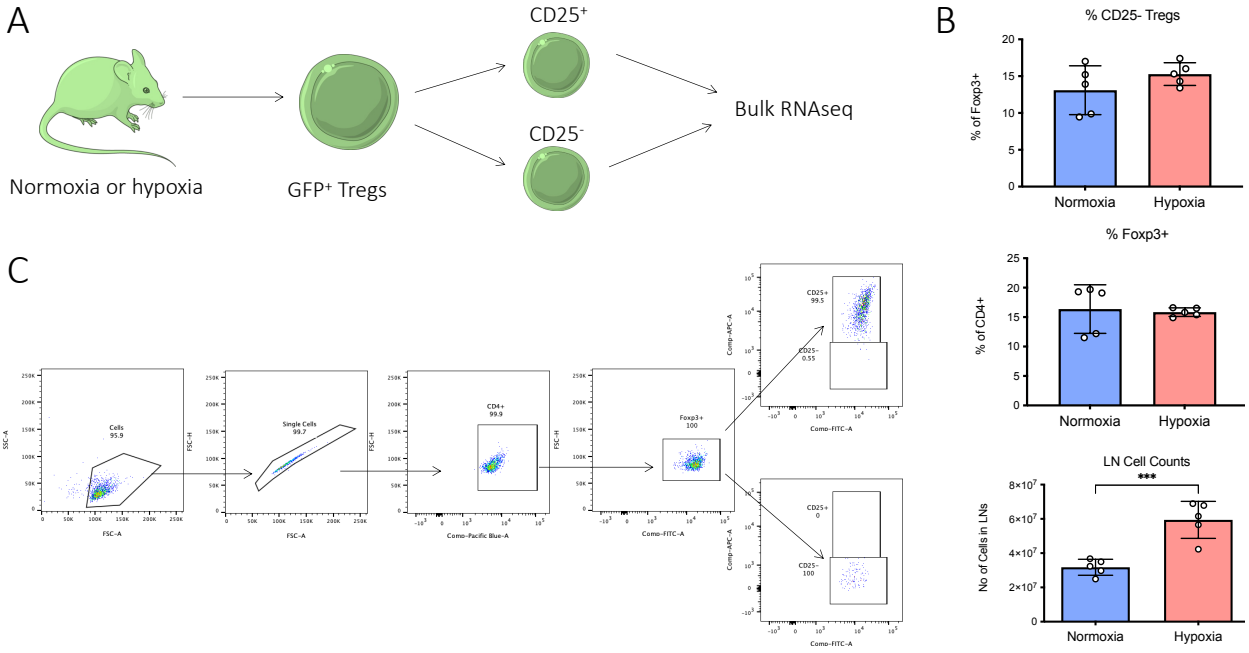

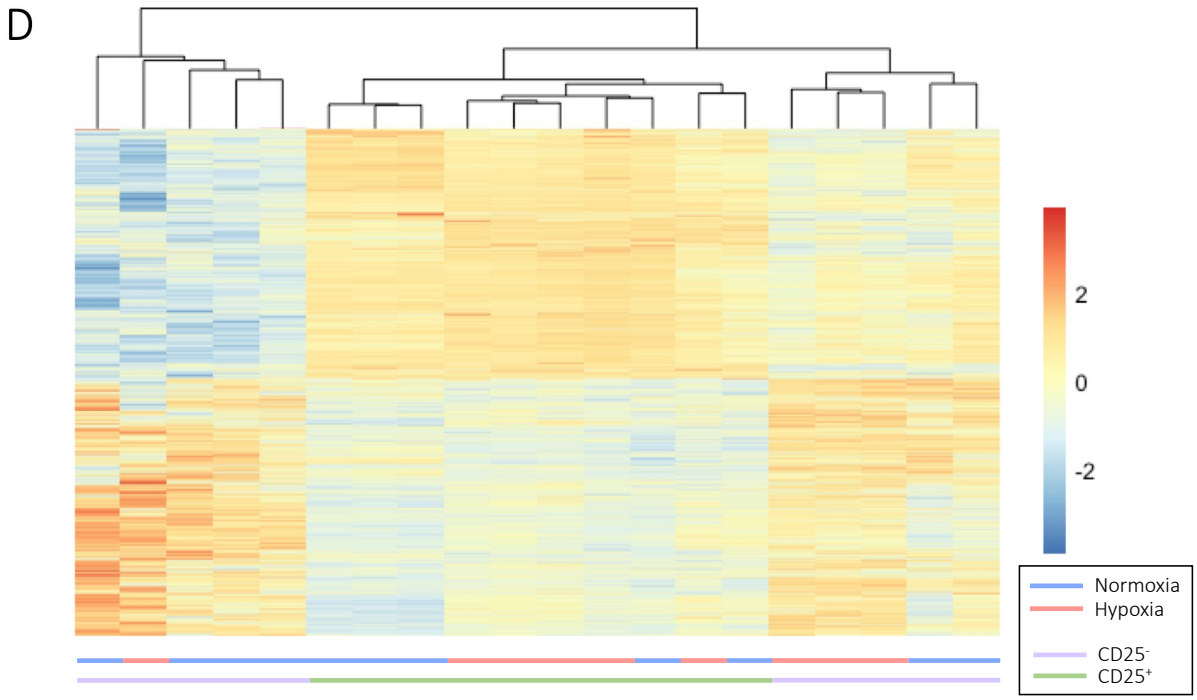

Fig 4.12 – CD25- Tregs are enriched in hypoxia and seem transcriptionally distinct. (A) Lymph nodes from 3-4 Foxp3^{GFP} reporter mice exposed to 10% hypoxia for 4 weeks and normoxic controls were pooled together for magnetic enrichment of CD4^{+} T cells and sorted into Foxp3^{+}CD25^{+} and Foxp3^{+}CD25^{-} populations via FACS sorting and individually sequenced. (B) Phenotypic data from the sort. (C) Gating strategy for FACS sorting of populations. (D) Heatmap of significant genes differentially expressed between CD25^{+} and CD25^{-} samples.

Although CD25^{-} Tregs are enriched in hypoxia and PHD2 KD, they are not unique to this, and the heatmap above did not seem to cluster entirely by oxygen status. This prompted the comparison between CD25^{-} Tregs from hypoxia and normoxia to determine whether they might differ transcriptionally (*Fig 4.a*). Interestingly, very few genes were differentially expressed between hypoxic or normoxic CD25^{-} Tregs, indicating that while hypoxia or PHD2 KD might numerically enrich this population within Tregs, it is not drastically changing them qualitatively. This indicates that whatever transcriptional programme, hypothetically driven by HIF-2α signalling, is responsible for CD25 loss, it is not entirely unique and occurs in control Tregs as well, albeit not many of them. Of the few genes that were specific to hypoxia, it was interesting to see *Nfkbia*, which is degraded for the activation of the canonical NFkB pathway. Additionally, the increase in *Ctla4* is in line with earlier observations that hypoxic and PHD2 KD Tregs have high expression of Tregs markers, including *Ctla4* (*Fig 4.11*). An increase in *Ifngr1* was also interesting and might mean that CD25^{-} Tregs are more sensitive to IFNγ, despite no indications that Tregs are producing IFNγ themselves or transitioning into a Th1-like phenotype.

Based on these minimal differences between normoxic and hypoxic CD25$^-$ Tregs, I decided to look at differential gene expression in CD25$^+$ vs. CD25$^-$ Tregs from all samples, not differentiating on hypoxia (*Fig 4.b*). One of the top genes that was found to be enriched in CD25$^-$ Tregs was *Cd22*, a selectin associated with the Notch1 signalling axis which has been shown to deregulate Tregs in patients suffering from multisystem inflammation following SARS-CoV-2 infection[323]. Authors found that the top pathways enriched in Tregs from these patients were TNF signalling via NFkB and hypoxia, and IL-2-STAT5 and IFNγ response were also on the list[323]. Anti-CD22 treatment restored Treg suppression *in vitro* and *in vivo*[323], indicating that it could be a causative driver. Notch1 has been shown to impair TGFβ-induced Foxp3 expression and especially interestingly, to promote signalling of the HIF co-activator p300[324]. Another upregulated gene, *Asb2*, is an E3 ubiquitin ligase downstream of Notch signalling capable of inducing canonical NFkB signalling[325,326], providing a link between Notch and NFkB pathways. *Pou2af1* is also downstream of Notch signalling[327]. I searched for evidence of this Notch1 signalling axis in the single cell dataset to confirm its presence in PHD2 KD, and while *Cd22* and *Notch1* were lowly expressed, they were clearly enriched but perhaps slightly more lowly expressed than in other groups (*Fig 4.c*).

As well as CD22, CD25$^-$ Tregs expressed higher levels of *Pdcd1* (*Fig 4.b*), which is upregulated with activation and is normally a marker of effector Tregs that can induce IL-10 production[328,329], but very high levels of expression can also induce anergy or exhaustion. *Ebi3* (IL-35) is also enriched in CD25$^-$ Tregs, similar to PHD2 KD Tregs (*Fig 4.11*). Another upregulated gene is the Na/K ATPase *Atp1a3* which is associated with asthma[330]. Expression of the sodium pump is induced after activation in T cells and is downstream of IL-2 signalling[331], so its increased expression despite lack of CD25 is surprising. The IL-2 cascade is mediated via JAK/STAT and Mer/Erk signalling to regulate Na/K/ATPase expression[331], so perhaps CD25$^-$ Tregs have found an alternative signalling pathway to upregulate these in order to compensate for their diminished IL-2 intake. *Tox2* was enriched in CD25$^-$ Tregs and has been shown to repress *Il2ra*[332]. *Socs2*, which can inhibit IL-4 production and is important for iTregs[333], was shown to be downregulated in CD25$^-$ Tregs, who also express *Il4*.

A

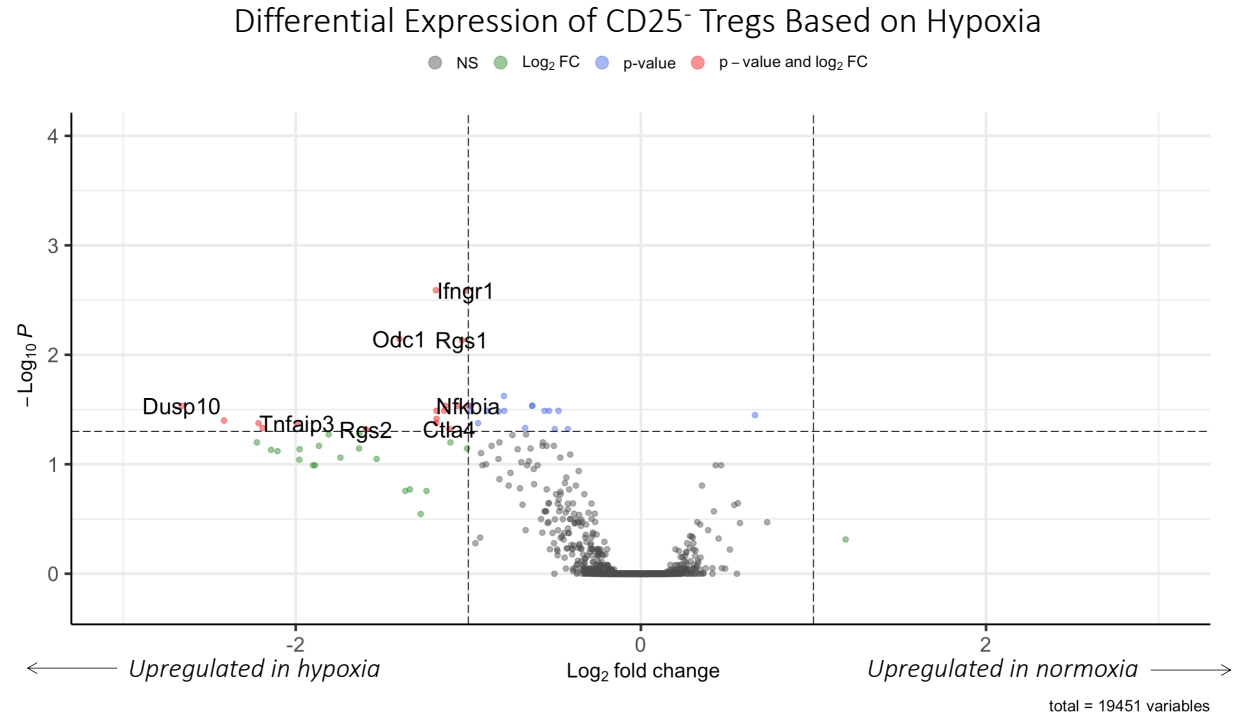
Differential Expression of CD25⁻ Tregs Based on Hypoxia
NS
Log2 FC
p-value
p – value and log2 FC
−Log10 P
Ifngr1
Odc1
Rgs1
Dusp10
Tnfaip3
Rgs2
Nfkbia
Ctla4
Upregulated in hypoxia
Log2 fold change
Upregulated in normoxia
total = 19451 variables

B

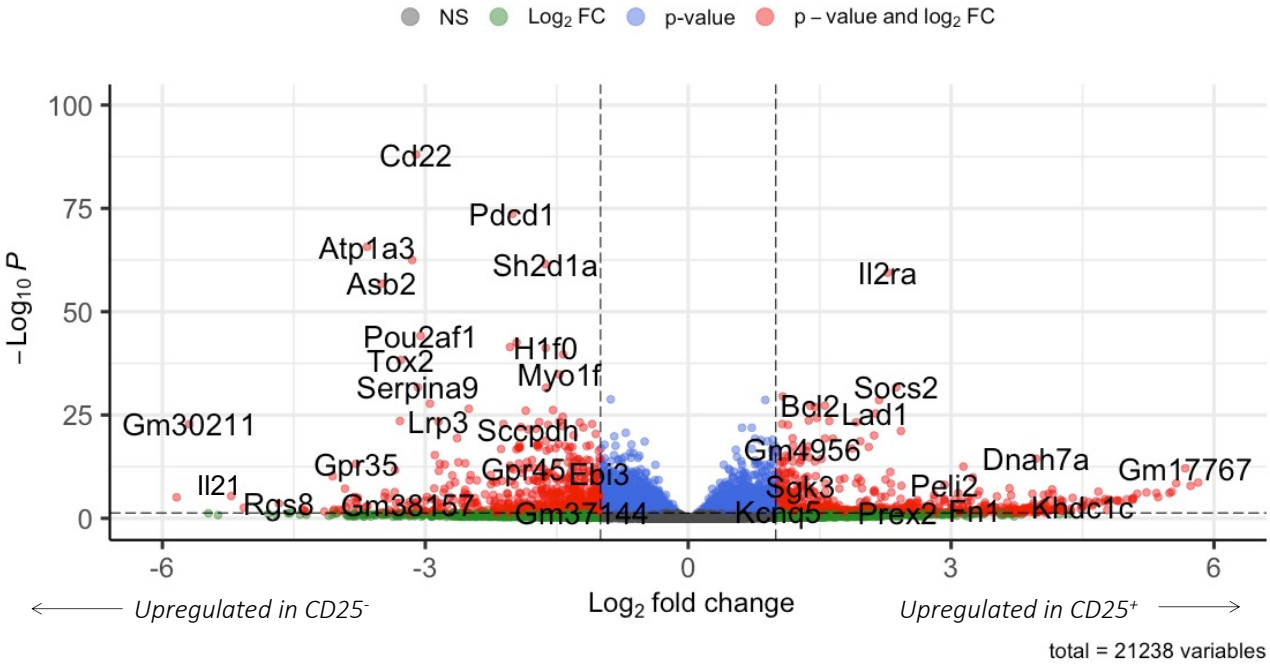
Differential Expression Based on CD25 Expression
NS
Log2 FC
p-value
p – value and log2 FC
−Log10 P
Cd22
Pdcd1
Atp1a3
Asb2
Sh2d1a
Il2ra
Pou2af1
Tox2
H1f0
Myo1f
Serpina9
Socs2
Bcl2
Lad1
Gm30211
Lrp3
Sccpdh
Gm4956
Dnah7a
Gm17767
Gpr35
Gpr45
Ebi3
Sgk3
Peli2
Il21
Rgs8
Gm38157
Gm37144
Kcnq5
Prex2
Fn1
Khdc1c
Upregulated in CD25⁻
Log2 fold change
Upregulated in CD25⁺
total = 21238 variables

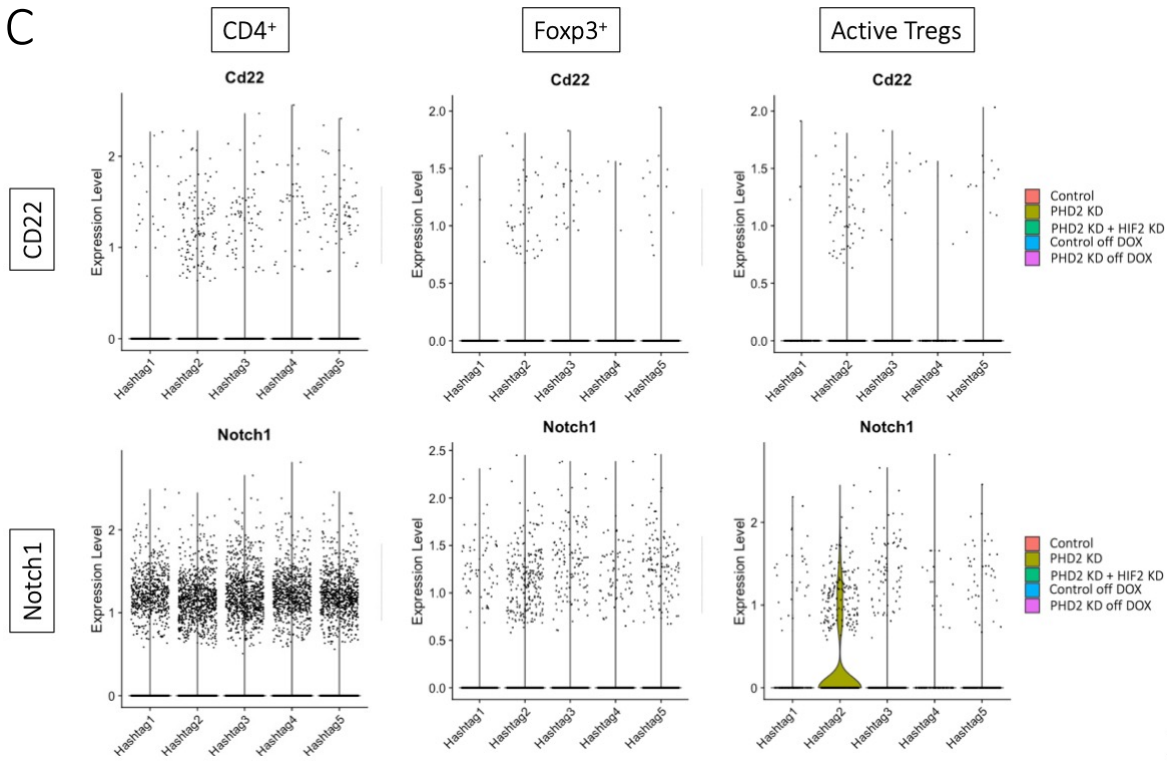

Fig 4.13 – Differential expression of hypoxic CD25$^-$ Tregs. Lymph nodes from 3-4 Foxp3^{GFP} reporter mice exposed to 10% hypoxia for 4 weeks or normoxic controls were pooled together for magnetic enrichment of CD4$^+$ T cells and sorted into Foxp3$^+$CD25$^+$ and Foxp3$^+$CD25$^-$ populations via FACS sorting for bulk RNA sequencing. (A) Differential expression of hypoxic vs. normoxic CD25$^-$ samples generated with DESeq2 and plotted with EnhancedVolcano in R. (B) Differential expression of CD25$^+$ vs. CD25$^-$ samples generated with DESeq2 and plotted with EnhancedVolcano in R. (C) Mice treated with doxycycline for 4 weeks had their lymph nodes harvested and CD4$^+$ T cells were isolated and tagged with hashtag oligomers according to their distinct biological groups by Kento Kawai. Samples were processed for 10X sequencing by the Wellcome Trust Centre for Human Genomics. Violin plots show gene expression of various targets grouped by individual hashtag groups across the entire cell population (left), cells expressing Foxp3 (middle), and cells originating from the unbiased active Treg cluster (right).

Several of the observed transcriptional changes across multiple datasets included genes associated with a follicular Treg signature, such as *Pdcd1, Tcf7, Lef1, Tox2*, and *Il1r2*. CD25$^-$ Tregs also express *Il21* (*Fig 4.b*), which is normally a cytokine produced by follicular helper T cells for providing B cell help to germinal centre B cells[173]. When interrogating genes related to follicular Tregs based on literature[102,173,303,332,334,335], expression patterns of these genes was enriched in CD25$^-$ Tregs along with a decrease in *Stat5* and *Bach2* which normally restrict the follicular signature[173,332] (*Fig 4.1*). Expression of these genes separated out CD25$^+$ vs. CD25$^-$ samples even without using *Il2ra* as an input gene, indicating that CD25 expression is inherently linked to the Tfr signature in these cells. STAT5 signalling was clearly downregulated in CD25$^-$ Tregs and has been shown to impair Tfr generation[173,319], so this change in the signalling axis could be the causative driver or at least a positive feedback loop for the Tfr transcriptional programme, and might play a role in our immune phenotype.

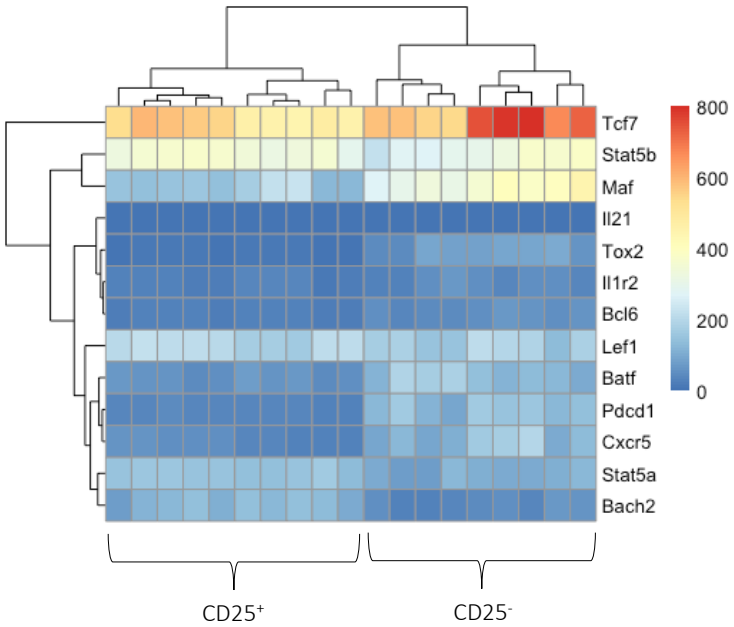

Fig 4.1 – CD25- Tregs have a Tfr signature. Hand-selected genes relating to follicular Treg signature and NFkB pathway genes based on literature. Samples are clustered automatically by the heatmap as shown in the dendrogram (top) and their origin as $CD25^+$ or $CD25^-$ is labelled below. Graph made using the pheatmap package in R with standard parameters.

4.3 – DISCUSSION

This chapter aimed to understand how HIF signalling impacts the Treg transcriptional programme by performing several targeted sequencing experiments. Single cell analysis of PHD2 KD Tregs confirmed findings on flow cytometry that PHD2 KD Tregs express classic Treg markers even more highly than control Tregs. High levels of *Ctla4, Ikzf2*, *Icos, Tnfrsf4, Il10*, and *Tgfb* were found on PHD2 KD Tregs, and low expression of naïve markers *Sell, Ccr7*, and *Igfbp4*, all consistent with highly activated and functional Tregs . When querying genes that would explain the pathogenicity observed in these Tregs *in vivo*, no expression of pro-inflammatory cytokines was observed aside from a slight enrichment in *Tnf* which is consistent with previous observations[255] (*Fig 4.5*). Genes for other cytokines IL-6, IL-1ß, IL-2, IL-17, IL-4, and IL-33 were too lowly expressed across the dataset to interrogate. From these probative inquiries, observations at the protein level were confirmed but no new markers were discovered from this targeted approach based on classical Treg and inflammatory genes. Unbiased differential expression analysis reinforced these ideas by revealing that many of the genes that set PHD2 KD Tregs apart from other Tregs were markers of Treg function, activation, and stability, again pointing to healthy and functional Tregs.

When some of the non-Treg and even non-immune genes that defined PHD2 KD Tregs were investigated, the topmost differentially expressed gene was *Hspb1*, which encodes the heat shock protein Hsp27 in humans or Hsp25 in mice. *Hspb1* responds to cellular stress including temperature and hypoxic stress and helps prevent apoptosis. Despite this, two caspases were upregulated as well, indicating that our Tregs might be attempting to combat stress and apoptosis. *Hspb1* has 2 HREs and is induced in hypoxia[336] but interestingly was shown to have an inverse relationship with HIF-1α in one study using cancer cell lines[337]. *Hsbp1* has been shown to bind to the HIF-2α promoter[338] so it might contribute to a positive feedback loop in some of our HIF-2α-driven results. Interestingly, *Hspb1* induction is dependent on low Erk signalling[337] which is downstream of IL-2-STAT5 signalling and stabilises Foxp3[71,103], so this might explain why *Hspb1* expression is being induced in our Tregs.

Additionally, *Hspb1* has been shown to be downstream of p38 MAPK/NFkB inducing kinase (NIK) activity[308], which was found to be upregulated in PHD2 KD Tregs (*Fig 4.3*). p38 deficiency could promote Treg differentiation[309], indicating that it might be a repressor of the Treg phenotype. Indeed, forced overexpression of NIK in $CD4^+$ T cells induced a fatal Scurfy-like syndrome characterised by weight loss, lymphadenopathy, and multisystem tissue infiltration[310], symptoms nearly identical to our PHD2 KD mice[255]. Similarly to us, Murray et al. observed an increase in the proportion of $Foxp3^+$ cells within the CD4 compartment, and loss of suppressive function *in vitro*[310]. However, they found that Tregs overexpressing NIK had decreased CD44 expression and that CD4 Tconvs expressed higher levels of it and resisted suppression *in vivo*, which was not found in PHD2 KD. They also observed further defects in the Tconv population, which were unable to induce GVHD, whereas our observations of dysfunction seem to be restricted to Tregs. Murray et al. found that OX40 was able to directly induce NFkB signalling independently of NIK, as it is a TNF receptor, and that OX40 also further enhanced NFkB signalling in a second convergent NIK-dependent manner; as Tregs preferentially express high levels of OX40, the restriction of its expression might explain why our phenotype is restricted predominantly to Tregs. This would also explain why $Foxp3^{Cre}$ PHD2 KD recapitulates a slightly milder phenotype, as OX40 does have some extraneous expression, so if it indeed a requirement for NIK induction then its expression outside of Tregs could be the reason for the disparity between the global and $Foxp3^{Cre}$ PHD2 KD, should it be contingent on OX40 induction of NIK. The expression of OX40 and its correlation with or its requirement for p38 MAPK induction and Treg dysfunction in PHD2 KD merits further work (*see– Future* Directions). Other than OX40, TGFß has also been shown to induce p38 MAPK activity and *Hspb1* expression[308], which is also highly expressed on PHD2 KD Tregs. This expression restriction would also explain why our phenotype differs from the genetic approach used by Murray et al. that targeted the entire CD4 compartment.

The same authors published a second study using a $Foxp3^{Cre}$- restricted model in which they showed that Treg restriction did not cause the same systemic autoimmunity but that transgenic NIK overexpressing Tregs were still dysfunctional; they found poor iTreg induction *in vitro* and a large proportion of ex-Tregs *in vivo* despite stability and maintenance of Foxp3 on nTregs *in vitro*[311]. Additionally, NIK overexpressing Tregs produced IFNγ and IL-2, as well as being less

responsive to IL-2 independently of CD25 expression, changes also not seen in our phenotype[311]. The authors observed decreased expression of *CTLA-4, ICOS, LAG3, Il10*, and *Nrp1* on Tregs and intriguingly, they also noted a downregulation of *Hif1a*[311], which could either be in contradiction to our observing a potential increase in NIK activity as a consequence of HIF activity, or perhaps might reflect a HIF-2α-driven regulation of HIF-1α levels, as it can express HIF-1α antisense RNA[160]. NIK overexpression in Tregs led to impaired differentiation of iTregs but stability and maintenance of Foxp3 even when cultured with pro-inflammatory cytokines. Altogether, it is conceivable that HIF-2α or at least PHD inhibition might be inducing p38 MAPK activity (shown to be hypoxia responsive[308]) and downstream NFkB signalling, and that the predominantly Treg-restricted OX40 expression might be the reason why the PHD2 KD phenotype is driven dominantly by Tregs, and despite a few inconsistencies, the two phenotypes are strikingly similar and supported by the transcriptional data.

Further to hints of p38 MAPK activity, NFkB transcription was also observed, which is downstream of this same pathway. *Hspb1*, the top most upregulated gene in PHD2 KD Tregs (*Fig 4.6b*), can also directly induce NFkB expression by degrading the inhibitory IkB subunit[308,312]. Additionally, NFkB has been shown to be hypoxia responsive and downstream of the non-canonical pathway, via the TGFβ-activated kinase TAK1 and Ca^{2+}-calmodulin signalling[187,339]. This effect was shown to be independent of the 3 PHD isoforms and of HIF-1α[187] but the authors did not look into HIF-2α, so it is a very reasonable suspect for the induction of this hypoxic NFkB signalling. Additionally, this hypoxia-induced NFkB signalling repressed PTEN[187], which favours Treg stability and suppression[134,144,145]. In spite of this, NFkB activation in Tregs via the non-canonical pathway (specifically, high expression of *Relb*) leads to uncontrolled Treg proliferation and autoimmune symptoms driven by loss of Treg suppression[340]. Tregs from this model exhibited high *Cd44, Ki67, Ikzf2* (Helios), and *Nrp1* expression, as well as survival and anti-apoptotic pathways, but the transcriptional data did not very much resemble the genes observed here[340]. NFkB was also suspected of potentially being activated by AHR freed up by HIF KO (*see Chapter 3*), so if its activation was driving the phenotype, NFkB activation via an alternate route driven by increased AHR signalling might well be able to recreate it. However, the RelA subunit of the canonical signalling pathway is reported to be the one that interacts with AHR[172], and was expression lower in PHD2 KD (*Fig 4.6*).

Another highly differentially expressed gene was *Gstm5* (glutathione S-transferase mu 5), a detoxifying enzyme that protects cells from drugs and xenobiotic stress most often studied in the context of cancer[314]. Other GSTs have been shown to be important for Treg function through preventing Treg senescence[341] and increasing DC induction of Treg and anti-inflammatory cytokine production[342], but none of these were *Gstm5*, which has not been well studied. Interestingly, mutation of another different GST in IBD patients was found to be associated with decreased STAT3 and p38 MAPK signalling[315], potentially linking it to some of the other transcriptional changes observed. Small heat shock proteins are also shown to increase the intracellular glutathione pool in line with detoxification of ROS[312]. *Il1r2*, a decoy receptor for IL-1, was also increased in PHD2 KD Tregs. *Il1r2* has been identified as a non-lymphoid tissue marker but this is debated[301,343]. It was also identified as a marker of mature, activated Tregs recirculating to the thymus[343], but also induced by tonic signalling and exhaustion in CAR Tregs[344], so its role in Treg function is still unclear but it seems to be involved in Treg regulation of local IL-1β signalling[345]. The most significantly downregulated genes against Foxp3$^+$ cells (*Sell, Ccr7*, and *Igfbp4*) are associated with naïve signature, but within other active Tregs, PHD2 KD Tregs show decreased Ly6a, associated with activation[316], potentially indicating a slight effector defect. JunB is also decreased on PHD2 KD Tregs against other active Tregs, and has been shown to be essential for effector Treg differentiation[346] and suppressive function[347], and for inducing CD25 expression in Treg-inducing conditions[317], so this could be in part responsible for some of the decreased CD25 expression and decreased IL-2 and STAT5 signalling themes uncovered by pathway analysis.

Loss of CD25 was observed at the protein level upon first characterisation of the immune phenotype (*Fig 3.2b*), and was one of the characteristics gleamed from PHD2 KD Tregs in the single cell sequencing (*Fig* . Whether these changes occur in the thymus is unknown, but CD25 is acquired after Foxp3 during thymic Treg development and the maturation of Foxp3$^+$CD25$^-$ Tregs into mature Tregs seems to be dependent on NFkB[348]. Peripherally, Ferreira et al. identified enriched population of CD25$^-$ Tregs in SLE patients which maintained TSDR demethylation, Helios expression, and an activated memory phenotype[322], which is in line with our observations that seemingly functional, activated Tregs with stable Foxp3 expression and demethylation lack only CD25 among their effector markers and yet are incapable of maintaining

tolerance[322]. Others have suggested that CD25 is routinely downregulated on effector and memory Tregs to help them traffic to sites of inflammation[349], although the above data observes this in the lymph nodes and spleens where cells are less likely to be tissue-homing.

When the $CD25^-$ compartment of Tregs was further investigated, hypoxia and normoxia had few transcriptional differences separating them. Interestingly, very few genes were differentially expressed between hypoxic or normoxic $CD25^-$ Tregs, indicating that while hypoxia or PHD2 KD might numerically enrich this population within Tregs, it does not significantly change them transcriptionally. This indicates that whatever transcriptional programme, hypothetically driven by HIF-2α signalling, is responsible for CD25 loss, it is not entirely unique and occurs in control Tregs as well, albeit not many of them. Nevertheless, of the few genes that were specific to hypoxia, it was interesting to see *Nfkbia (Fig 4.9b)*, which is degraded for the activation of the canonical NFkB pathway. Additionally, the increase in *Ctla4* is in line with observations that hypoxic and PHD2 KD Tregs have high expression of Tregs markers, including *Ctla4* (*Fig 4.9b*). An increase in *Ifngr1* was also interesting and might mean that $CD25^-$ Tregs are more sensitive to IFNγ, despite no indications that Tregs are producing IFNγ themselves or transitioning into a Th1-like phenotype. Based on this data, $CD25^+$ vs. $CD25^-$ Tregs from all samples were compared, not differentiating on oxygen status.

Tcf7 was upregulated in $CD25^-$ Tregs and is associated with *Lef1* and *Wnt* signalling pathways, which are both co-upregulated. In a study by Yang et al., Treg-restricted knockout of *Tcf7* and *Lef1* led to systemic autoimmunity and non-suppressive Tregs characterised by loss of function and CD25 expression, both driven by diminished pSTAT5 signalling, which constitutive STAT5 expression could rescue[319]. They also found that $Tcf7^-$ Tregs were mostly $CD44^+$ and their sequencing results were incredibly similar to ours, with high expression of classic Treg genes and *Maf*, and low expression of naïve markers and *Il2ra*[319]. This is puzzling as although the patterns are similar, they are associated with opposite directions of *Tcf* and *Lef1* expression. This could signify that these are not necessarily coupled to CD25 expression and IL-2 signalling which seemed to drive their observed phenotype. Others state that Tcf7 antagonises effector Treg differentiation[335], which would better fit the above findings. Tcf7 and Lef1 are also associated with follicular Treg signature[319], as is Id3[320], which can also promote Foxp3 stability[321] and could explain why PHD2 KD Tregs maintained Foxp3 expression and TSDR demethylation.

One of the top genes that enriched in CD25$^-$ Tregs was *Cd22*, a selectin associated with the Notch1 signalling axis which has been shown to deregulate Tregs in patients suffering from multisystem inflammation following SARS-CoV-2 infection[323]. Authors found that the top pathways enriched in Tregs from these patients were TNF signalling via NFkB and hypoxia, and IL-2-STAT5 and IFNγ response were also on the list[323]. CD22 was able to induce mTORC1 signalling and Treg suppression was restored with rapamycin or anti-CD22 treatment[323]. In transplantation, anti-Notch1 antibody treatment was able to prolong graft outcomes, increase Treg:Tconv balance in tissue infiltrate, and improve Treg suppression by inhibiting mTOR signalling and increasing STAT5 phosphorylation[350,351]. This increase in STAT5 might mean that Notch1 is acting a compensatory pathway to maintain STAT5 signalling in CD25$^-$ Tregs that are deficient in IL-2-STAT5 induction. Notch1 has been shown to impair TGFβ-induced Foxp3 expression via SMAD3 stabilisation and especially interestingly, to promote signalling of the HIF co-activator p300[324]. HIF-1α is able to interact with the Notch intracellular domain to augment its signalling and FIH is able to hydroxylate this same domain to repress Notch signalling[352]; furthermore, Notch intracellular domain has higher binding affinity for FIH-1 than HIF-1α and so is capable of sequestering it to allow HIF-1α signalling[352]. HIF-2α can induce Notch signalling too[353] and Notch1 can also induce HIF-2α signalling which, in some cell lines, was also with a decrease in HIF-1α, potentially indicating a role for Notch in the switch from HIF-1α to HIF-2α[354]. Altogether, there is evidence for a positive feedback loop between Notch and HIF signalling which might deregulate Tregs and aggravate the observed inflammatory phenotype, which could contribute to its severity.

The single cell dataset was investigated for evidence of this CD22-Notch1 signalling axis to confirm its presence in global PHD2 KD, and while *Cd22* and *Notch1* were lowly expressed, they were clearly enriched but perhaps slightly more lowly expressed than in other groups (*Fig 4.c*). The gut-homing selectin *Itgb7* which was found enriched on Notch1-expressing Tregs[323] was upregulated both on PHD2 KD and in the KD mice after removal of doxycycline, indicating that its expression is long lived and persists even after reversal of PHD2 KD, being the only gene so far to do so. Unfortunately, canonical Notch targets *Hes1, Hey1, and Nrarp*[354] were very lowly expressed in our dataset and so their differential expression in PHD2 KD could not be assessed.

Another pattern that slowly emerged was the recurrence of genes associated with follicular Treg (Tfr) signature and B cell-associated genes. PHD2 knockdown-specific Tregs express *Il1r2*, which has been associated with $CXCR5^+PD1^+$ "Tfr-like" cells that also exhibit CD25 loss[343]. *Cd74* was also upregulated in the same dataset, and it is normally found on B cells and APCs, as well as being highly expressed in spontaneous autoimmunity which could be treated with CD74 knockout[355]. $CD25^-$ Tregs from the analysis of sorted $Foxp3^+CD25^+$ and $Foxp3^+CD25^-$ Tregs expressed *Il21* as one of the top differentially expressed genes (*Fig 4.b*), and this is normally associated with B cell help on follicular helper cells and not normally expressed on Tfr[335], although it is also a marker of type I Tregs that suppress but do not express Foxp3[288]. $CD25^-$ Tregs downregulated *Ctla4* which can inhibit differentiation and expansion of Tfr while also contributing to their suppressive function[356], and *Bach2*, which negatively regulates follicular T cells[332]. Meanwhile, they were enriched for Tfr markers *Tox2* and *Pdcd1* (PD-1)[332], and in the single cell analysis, the $CD25^-$ PHD2-specific island was differentiated from the $CD25^+$ island by increased *Tcf7* and *Lef1* which are essential for Tfrs[319,334] and *Id3* which is necessary for their early development[320] (*Fig 4.9b*).

Following up on these leads from Tfr signatures, the literature revealed that CD25 loss is fairly common in Tfrs and that most Tregs in germinal centres are negative for CD25[357,358], and that STAT5 signalling downstream of it restrains the Tfr phenotype[319,335,358]. Furthermore, HIF signalling has been shown to restrain Tregs into a Tfr signature, in that knocking out HIF-1α alone or alongside HIF-2α impaired Ag-specific antibody responses as well as T cell glycolysis and cytokine response[173]. Interestingly, knockout led to a higher Tfr:Tfh ratio, an effect that was strongly HIF-2α-sensitive[173], indicating that low HIF levels favour Tregs and so perhaps, high HIF levels in our model tip the ratio the other way; Tregs are numerically enriched in PHD2 KD and hypoxia so the increased HIF signalling would not decrease the Tfr compartment but might be impairing Tfr function. The only inconsistency is that authors investigated the role of the NFkB pathway in this signalling axis and found that it had no effect on germinal centre localisation[173], despite our observations that the NFkB-p38MAPK signalling axis was seemingly active in PHD2 KD Tregs.

These indications of a HIF-driven Tfr deregulation help answer some previous concerns about the hypoxia/PHD2 KD phenotype. Predominantly, it explains the autoantibody production noted in PHD2 KD mice[255] if Tfrs are providing B cell help instead of suppressing self-reactive B cells. It also fits with the observation that $CD25^-$ Tregs are not qualitatively very different between normoxia and hypoxia and are only enriched, if they correspond with Tfr which are normally present in small frequencies. Additionally, the small subset of PHD2-specific islands within the active Treg compartment that was identified, even if entirely pathogenic, makes up too small a percentage of the Treg compartment to be responsible for systemic pathogenicity, as even a 50:50 ratio of $Foxp3^-$: $Foxp3^+$ Tregs in heterozygous carriers of the IPEX mutation has no autoimmune consequences. Therefore, investigating a small $CD25^-$ subset of an already small population of Tregs within the immune compartment seemed unlikely to yield an explanation for an entire loss of systemic tolerance. However, maybe a small subset within the germinal centres with the ability to polarise B cell responses could impact all of humoral tolerance, and if Tregs within lymph nodes localised to germinal centres and unable to control other T cells in the lymph nodes, it might better explain the systemic phenotype. The small percentage issue still stands, if the rest of the Tregs within the lymph nodes are healthy and functional, and an enrichment of seemingly non-functional Tregs outside the lymph nodes are seen in spleens and blood as well, so perhaps Tfr dysfunction is not enough to explain the entire phenotype, especially in T cell transfer studies that have no B cells. Nevertheless, a number of clues point toward a Tfr phenomenon consistent with a proven link to HIF[173] and the recurring CD25 loss, along with the consequences of diminished IL-2-STAT5 signalling downstream of it. This transcriptional programme, along with activation of the p38 MAPK and NFkB signalling axis, seem to be the HIF-2-driven downstream inflammatory pathways I hypothesised existed in Tregs and which I sought to identify through sequencing experiments investigating how HIF signalling impacts the Treg transcriptional programme.

5 – Effects of Iron on Treg Biology and Function

5.1 – INTRODUCTION AND AIMS

The role of iron in Tregs is poorly understood as very little research has been done on the subject to date (*see section 1.5b*). The most direct study was performed by the Sanchez-Fueyo team who identified iron-related genes as the predictors of operational tolerance in liver recipients[234]: they found that iron chelation *in vitro* impaired iTreg generation and their CD25 expression and STAT5 phosphorylation, but only during early activation and differentiation[264]. *In vivo*, diet-induced systemic iron deficiency increased the proportion of Tregs both at baseline and in an SLE model, slowing disease progression due to increased Treg:Th17 ratio[220], but had no impact on Treg presence or IL-10 and TGFß production in another study[265]. In iron overloaded thalassemia patients, Tregs were also increased, and correlated with ferritin[268], indicating that iron imbalance in either direction might increase Tregs proportion. Mechanistically, iron chelation impairs mTOR signalling which favours Tregs[269], and Tfrc blockade to reduce iron loading in SLE promoted Tregs, Foxp3, and IL-10 via mTOR and mitochondrial pathways[221]. Treg-specific iron accumulation resulted in apoptosis and decreased suppression *in vitro* and *in vivo* despite normal Foxp3 levels[270,271], further indicating that iron overload is detrimental to Tregs and T cells.

We know that Tregs differ from Tconvs in several metabolic parameters which allows us target them without affecting the entire T cell compartment: low-dose IL-2 favours uptake by CD25-expressing Tregs, and decreased dependence on the mTOR signalling axis[135–137] allows improved suppression when mTOR is inhibited. These are both used in transplant recipients[57,102,106,112–114] to help promote Tregs and suppress Tconvs both in *ex vivo* expansions prior to cell infusions and endogenously. Therefore, if iron deprivation might affect Treg biology and metabolism differentially to other T cells, it could have great therapeutic potential. Understanding how Tregs respond in iron-deprived environments which they are likely to face during inflammatory responses is of great value both for our basic understanding of science and therapeutic possibilities that might allow us to modulate Treg behaviour and immune balance.

CHAPTER AIM: To investigate how iron deprivation affects Treg phenotype and function

HYPOTHESIS: Iron deprivation will negatively impact all T cells, but Tregs will respond differently due to their differential metabolic need

5.2 – Results

5.2a – Tregs Are More Resistant Than Tconvs to Iron Deprivation in Vitro

In order to investigate how iron deprivation affects Tregs and Tconvs, $CD4^+$ cells from $Foxp3^{GFP}$ mice were sorted into $CD4^+GFP^+$ Tregs and $CD4^+GFP^-$ Tconvs. Cells were separately labelled with violet proliferation dye (VPD) and stimulated *in vitro* with a titration of iron availability before flow cytometric analysis (*Fig 5.1a*). Iron was manipulated using iron-free serum and a titration of iron-bound transferrin (holotransferrin) to provide known iron concentrations at each titration, which is the most controlled way of providing known iron without measuring intracellular iron levels, the technology for which is not available to us. Tconv proliferation was impaired as iron decreased but Tregs were unable to proliferate under any of these conditions (*Fig 5.1b*). This is not unusual, as mouse Tregs are not especially prone to proliferation *in vitro*[359] and proliferation is not essential to their function. Furthermore, the iron-free pannexin serum is an artificial serum replacement and due to manufacturer secrecy, it is unclear which nutrients may be missing from it that could impair cell proliferation; indeed, certain cell types were unable to proliferate or survive in it even with sufficient iron availability (unpublished data from the Drakesmith lab and ours). This does however caveat the interpretation of our data in that comparing a proliferating cell to a resting one is not quite a fair comparison, especially in terms of metabolic needs and iron requirements for proliferation. Nonetheless, as Tregs are less prone to antigen-stimulated expansion than Tconvs *in vivo*[360], this still offers us a glimpse into Treg behaviour in low iron availability and might still be representative of biological rather than technical differences between these cells.

Tregs better maintained expression of CD71, CD25, and ICOS as compared to Tconvs, which decreased their expression of all of these as iron decreased (*Fig 5.1c*). CD71 is the transferrin receptor, expression of which was hypothesised to increase with iron deficiency in an effort to import more iron[206], but as CD71 upregulation is also an activation response and follows CD25 upregulation[209,232], it may be that iron deficiency decreased the IL-2 and TCR-dependent Myc-Jak signalling pathway required to upregulate CD71[146] and that this effect dominated over IRP-mediated CD71 upregulation. ICOS is an activation marker for Tconvs and Tregs alike, and its expression on unstimulated Tregs is likely a reflection of baseline Treg activation in a naïve

mouse that is not seen in the Tconv compartment. CD25 expression was the only marker that showed decreased expression on Tregs (*Fig 5.1c),* which raises questions about their suppressive function.

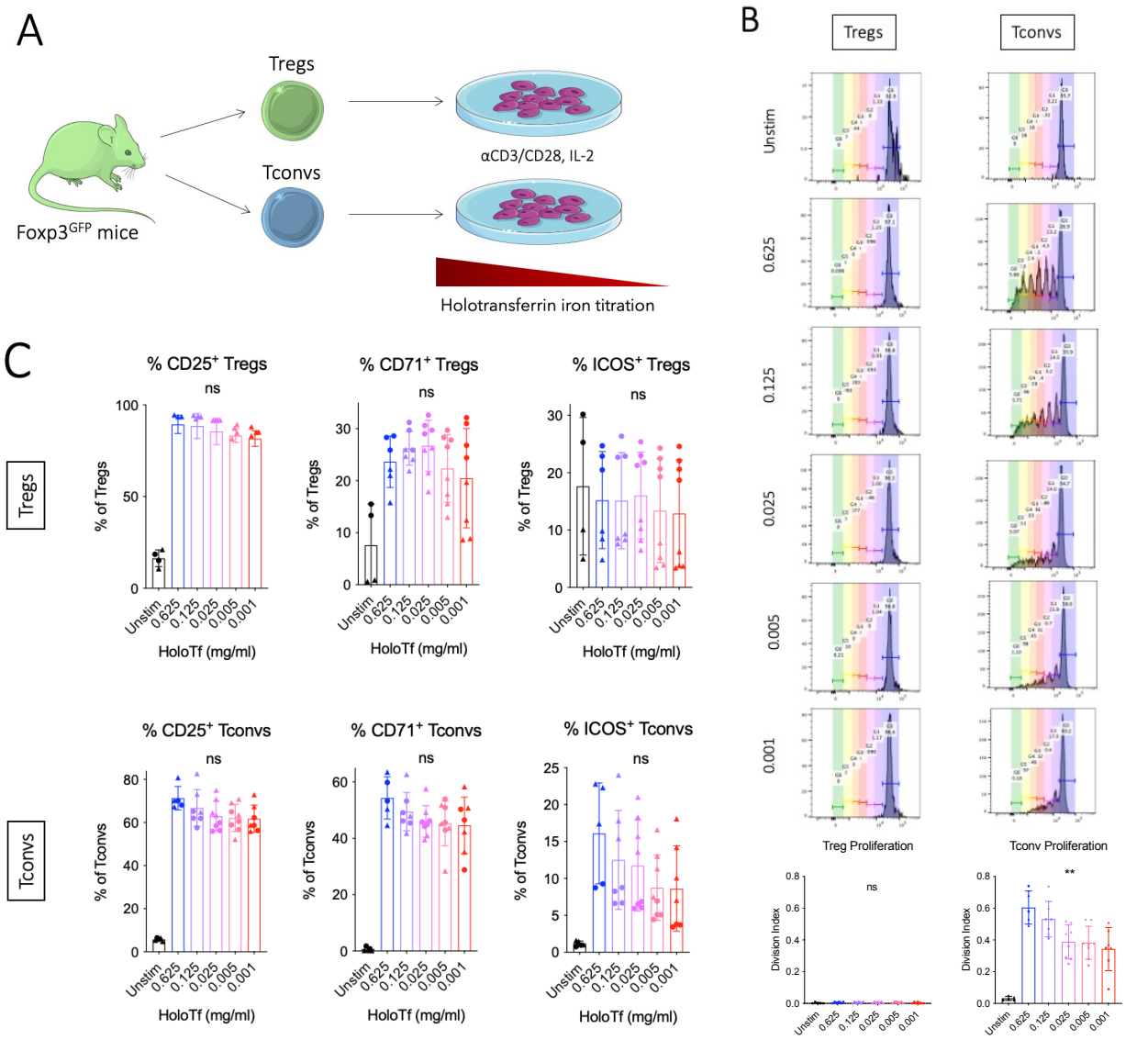

Fig 5.1 – Tregs are less sensitive to decreases in iron availability than Tconvs. (A) Lymph nodes and spleens from 5-6 Foxp3^{GFP} mice were pooled together and CD4$^+$ cells were isolated via magnetic negative selection before FACS sorting into CD4$^+$7-AAD$^-$Foxp3$^-$ Tconvs and CD4$^+$7-AAD$^-$Foxp3$^+$ Tregs. Cells were stained with VPD so that each serial dilution of VPD intensity would mark a proliferation cycle and could be measured via flow cytometry. 100,000 of each cell type was seeded separately with αCD3/CD28-coated beads at a 1 cell:2 beads ratio with 100IU/ml IL-2 for 3.5 days (approximately 85 hours). Media was made using iron-free pannexin serum and a titration of iron-containing holotransferrin from 0.625 – 0.001 mg/ml, with iron-free apotransferrin titrated in to keep total transferrin levels constant at 1.2 mg/ml. Unstimulated control was in 0.625 mg/ml holotransferrin. (B) Representative VPD peaks show proliferation rounds. (C) Expression of CD25, CD71, and ICOS on Tregs and Tconvs. Symbol shape represents two individual experiments. Mean ± SD.

5.2b – Tfrc Tregs Maintain Suppressive Function in in Vitro Suppression Assays

As the same iron deficient media model could not be used to study suppression without also affecting Tconvs and their proliferation, Tregs from the Tfrc$^{Y20H/Y20H}$ mice were used to study cell-intrinsically iron deficient Tregs (*Fig 5.2a*). These Tfrc mutant mice have a hypomorphic transferrin receptor, which leads to inefficient iron import and inherent intracellular iron deficiency. Tregs from Tfrc mice were found to be able to suppress CD4^{+} Tconvs comparably to control Tregs, with only a slight defect visible (*Fig 5.2b)*.

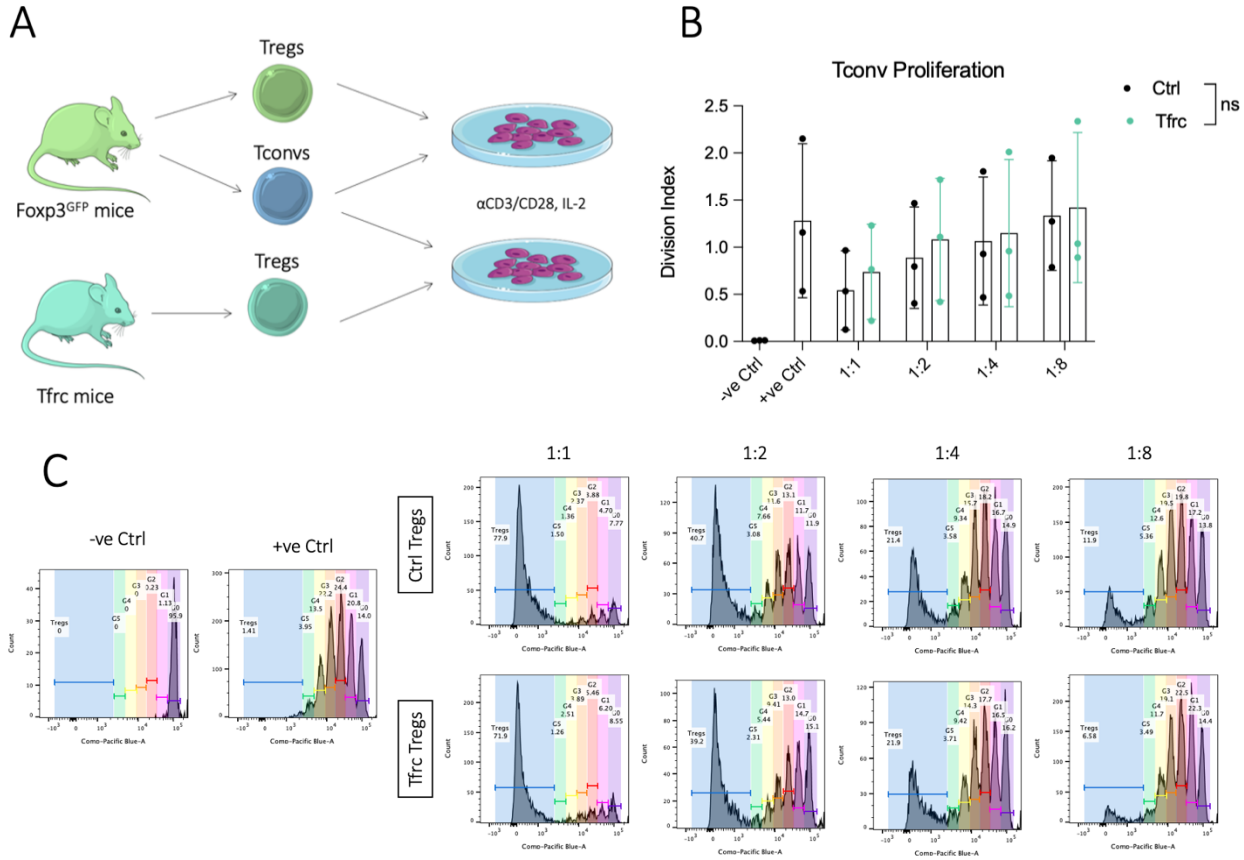

Fig 5.2 –Tfrc Tregs maintain suppressive capabilities *in vitro*. (A) Lymph nodes and spleens from 3 Foxp3^{GFP} (green) or Tfrc$^{Y20H/Y20H}$ (teal) mice were pooled together and CD4^{+} cells were isolated via magnetic negative selection before FACS sorting into CD4^{+}7-AAD^{-}CD25^{-} Tconvs and CD4^{+}7-AAD^{-}CD25^{+} Tregs. Responder Tconvs were stained with VPD so that each serial dilution of VPD intensity would mark a proliferation cycle which could be measured via flow cytometry. 100,000 Tconvs from Foxp3^{GFP} mice were cocultured for 3.5 days (approximately 85 hours) with αCD3/CD28-coated beads at a 1 cell:2 beads ratio alongside either GFP control or Tfrc Tregs at ratios ranging from 1 Treg:1 Tconv to 1 Treg:8 Tconvs. (B) Division index with no beads (negative control), with beads and no Tregs (positive control), and Tregs titrated 1:1 to 1:8. Data represents means from 3 separate experiments with duplicate or triplicate wells for each condition. 2-way ANOVA. Mean ± SD. (C) Representative VPD peaks show proliferation rounds of CD4^{+}CD25^{-} responder Tconvs.

5.2c – Adoptively Transferred Tfrc Tregs Fail to Control Transplant Rejection

In order to assess Treg suppressive function *in vivo*, the Tfrc$^{Y20H/Y20H}$ mice exhibiting inefficient iron import and subsequent cell-intrinsic iron deficiency were again used. RAG$^{-/-}$ mice lacking an adaptive immune system were reconstituted with CD4^{+}CD25^{-} Tconvs from SJL (CD45.1) mice either alone or alongside CD4^{+}CD25^{+} Tregs from either or WT B6 or Tfrc$^{Y20H/Y20H}$ (CD45.2) mice before receiving fully mismatched skin transplants (*Fig 5.3a*). This allowed for the study of WT and Tfrc$^{Y20H/Y20H}$ Tregs side by side, both in terms of phenotype and *in vivo* suppression of responder Tconvs (identifiable by CD45.1 expression). Tregs and Tconvs were detectable in the blood at two weeks and in spleens and lymph nodes at harvest at six weeks, with no differences between groups (*Fig 5.3c*). However, Tfrc$^{Y20H/Y20H}$ Tregs were unable to prolong graft survival (*Fig 5.3d*). Tfrc$^{Y20H/Y20H}$ cells have known defects in proliferation, so their ability to reach the expansion requirements to repopulate an entire empty mouse was questioned, but Tfrc$^{Y20H/Y20H}$ Tregs were comparably detected (*Fig 5.3c*). However, our harvest at 6 weeks is long after rejection so it is possible that the control Tregs were required to proliferate extensively during rejection in a way that Tfrc$^{Y20H/Y20H}$ cells could not match, and that we missed this window with our sampling, but our two-week bleed probably would have showed some differences leading up to rejection if this were the case. Nonetheless, we do not know enough about the potential defects in migration, proliferation, or long-term survival of Tfrc$^{Y20H/Y20H}$ cells to conclude definitively that suppressive function was the only factor driving these results, especially as we know they are effective *in vitro*, but in this model, they failed to prolong survival where the control Tregs could.

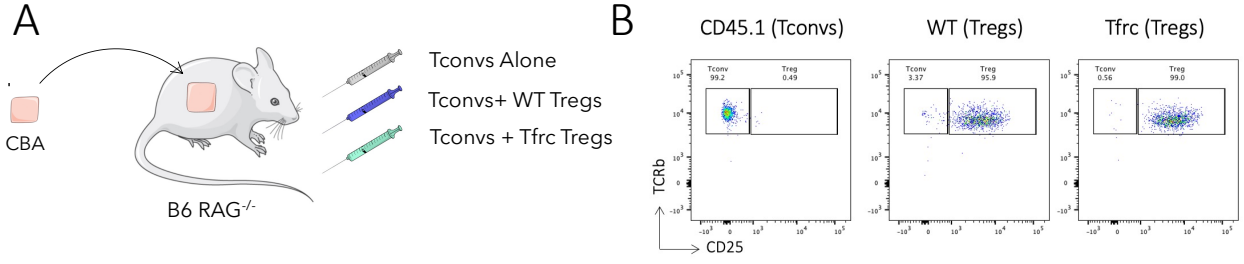

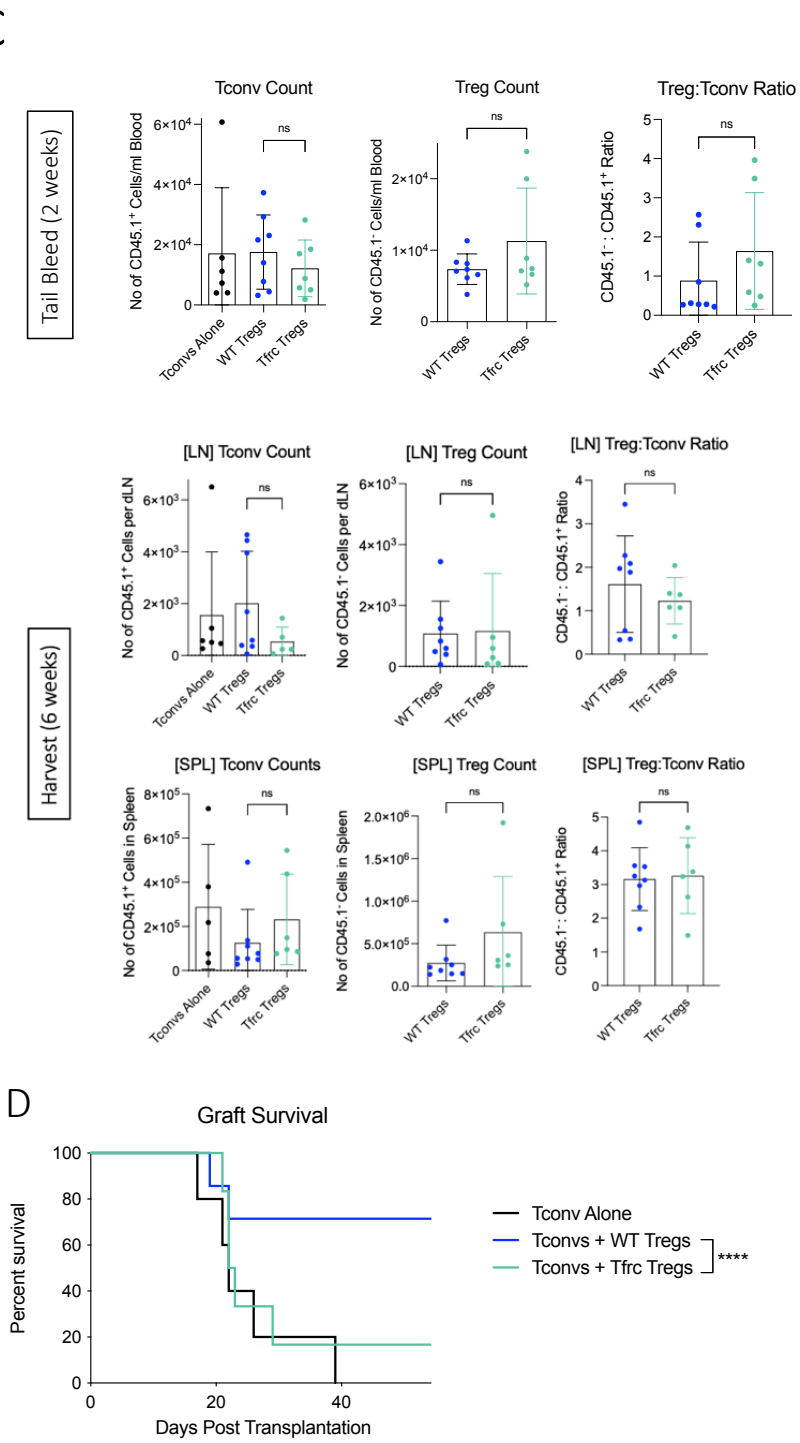

Fig 5.3 – Tfrc Tregs do not prolong skin graft survival in an *in vivo* suppression assay. (A) Splenocytes from CD45.1 SJL (SJL, black), wildtype CD45.2 C57BL/6 (WT, blue) and CD45.2 Tfrc$^{Y20H/Y20H}$ (Tfrc, teal) mice were enriched for CD4 with magnetic negative selection. CD4^{+} cells were FACS sorted into CD4^{+}CD25^{-} SJL Tconvs CD4^{+}CD25^{+} WT/ Tfrc$^{Y20H/Y20H}$ Tregs. C57BL/6 RAG$^{-/-}$ mice received 10,000 SJL Tconvs either alone or alongside 50,000 Tregs via IV injection, and then received a fully mismatched CBA skin graft the following day. (B) Purity of injected cells after FACS sorting. (C) Tail bleeds at day 14 after transplantation and spleen and draining LN harvested six weeks after transplantation were analysed for flow cytometry. Unpaired t test with Welch's correction. Points represent individual mice (n = 6). Mean ± SD. (D) Skin transplant survival with end point of a graft score of 4. Kaplan-Meier analysis.

5.2d – Tfrc Mutant T Cells From Tfrc Chimeras Have Higher Treg:Teff Ratio

In order to examine Tfrc$^{Y20H/Y20H}$ Tregs *in vivo* without the confounding disadvantages posed by a reconstitution model, we opted for a mixed bone marrow chimera model. This allows for the study of Tfrc and control cells side by side in a transplant context without such stringent requirements for proliferation, in which Tfrc cells are disadvantaged. Irradiated SJL recipients (CD45.1) received a 50:50 mix of bone marrow from SJL (CD45.1) mice and either wildtype B6 (CD45.2) mice or Tfrc$^{Y20H/Y20H}$ mice (CD45.2) so that these mice could be reconstituted with either 50% iron deficient cells (SJL:Tfrc mice) or two types of iron sufficient cells (SJL:B6 mice), allowing for the B6 compartment to be compared to the Tfrc$^{Y20H/Y20H}$ compartment across mice, with the same SJL compartment for both (*Fig 5.4a*). Upon challenge with a fully mismatched skin graft, Tfrc$^{Y20H/Y20H}$ Tconv proliferation and activation was not as effective as control Tconvs, whereas Tfrc$^{Y20H/Y20H}$ Tregs were comparatively less impaired: this led to an improved ratio of both total and CD44^{+} Tregs to CD44^{+} Tconvs in the Tfrc$^{Y20H/Y20H}$ cells (*Fig 5.4b-e*). As the balance of the immune response is so delicate, this relative shift in Tregs is quite striking, although it reflects Tconv impairment rather than anything. It is difficult to predict how this would affect functional outcome, and it was thought that the results would be too subtle to result in graft prolongation and therefore, tissue harvest at time of rejection was prioritised.

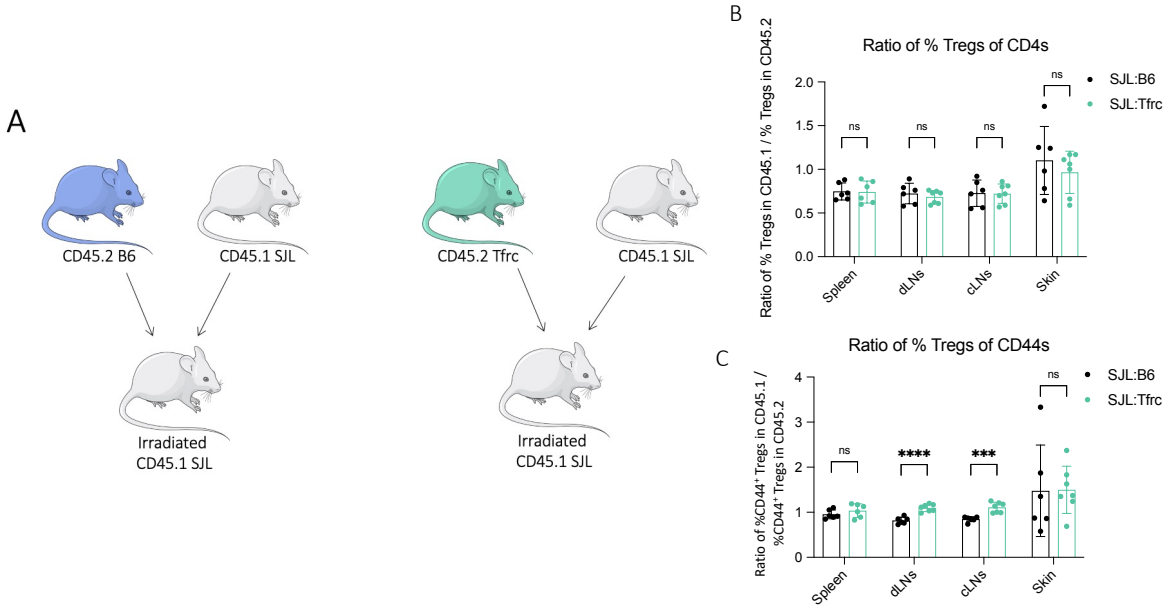

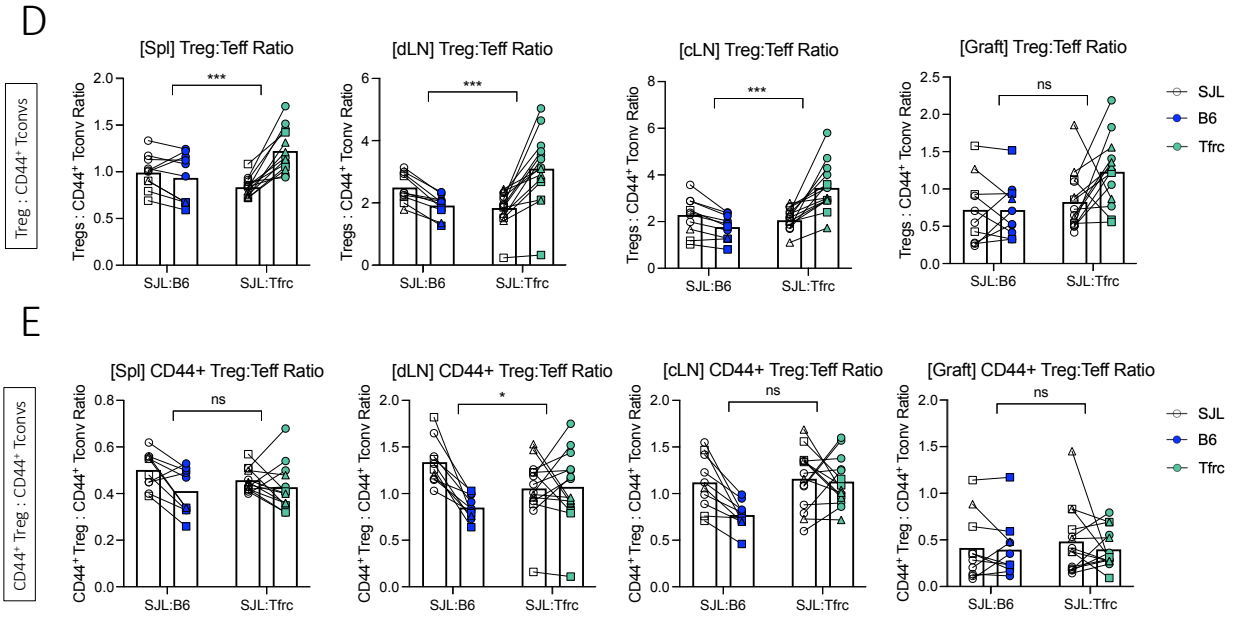

Fig 5.4 – Treg:Teff ratio favours Tregs in Tfrc cells from mixed bone marrow chimeras. (A) SJL (CD45.1) females were irradiated and injected with 106 bone marrow cells mixed 50:50 from SJL males and either WT B6 (blue) or TfrcY20H/Y20H (teal) males, and left to reconstitute for 8-12 weeks before transplant with a fully mismatched CBA skin graft. Spleen, draining and contralateral lymph nodes (Spl, dLN, cLN) were harvested at day 11 after transplantation for flow cytometric analysis. (B) CD45.1 / CD45.2 ratio of % Tregs of $CD4^+$ T cell compartment. 1-way ANOVA with Tukey's multiple comparisons test. (C) CD45.1 / CD45.2 ratio of % Tregs of $CD44^+$ $C44^+$ T cells. 1-way ANOVA with Tukey's multiple comparisons test. Mean ± SD. (D) Ratio between CD4+Foxp3+ Tregs and CD4+Foxp3-CD44+ effector T cells (Teffs). (E) Ratio between CD44+CD4+Foxp3+ Tregs and CD4+Foxp3-CD44+ effector T cells (Teffs). Individual points linked by a line represent individual mice so the slope of the lines represents the CD45.1:CD45.2 trends, and symbol shape represents different biological repeats. Mixed effect analysis with Geisser-Greenhouse correction for comparison between CD45.1 vs CD45.2 x SJL:B6 vs SJL:Tfrc.

5.2e – Tfrc Mutant Tregs in Chimeras Express Higher CD25 and Lower CTLA4

Although functional suppression was not assessed in the Tfrc mixed bone marrow chimera model, CD25 and CTLA-4 expression on Tregs was analysed to give an idea of how these suppressive molecules were affected. After transplantation, CD25 was increased while CTLA-4 was decreased on $Tfrc^{Y20H/Y20H}$ Tregs (*Fig 5.5*). Interestingly however, CTLA-4 was maintained in the draining lymph nodes, which are the site of greatest activation and importance in alloresponses. In both SJL:B6 and SJL: $Tfrc^{Y20H/Y20H}$ chimeras, the SJL proportion showed higher MFI of CTLA-4, which was attributed to the preferential radioresistance of activated memory T cells and assumed to reflect leftover activated memory cells rather than a bias in reconstitution. The different trends in CD25 compared to CTLA-4 suggest that perhaps Tregs alter their choice of suppressive mechanisms when they have low iron availability, and CTLA-4 loss in Tregs has previously been shown to be compensated for with other regulatory mechanisms to maintain suppressive function[356].

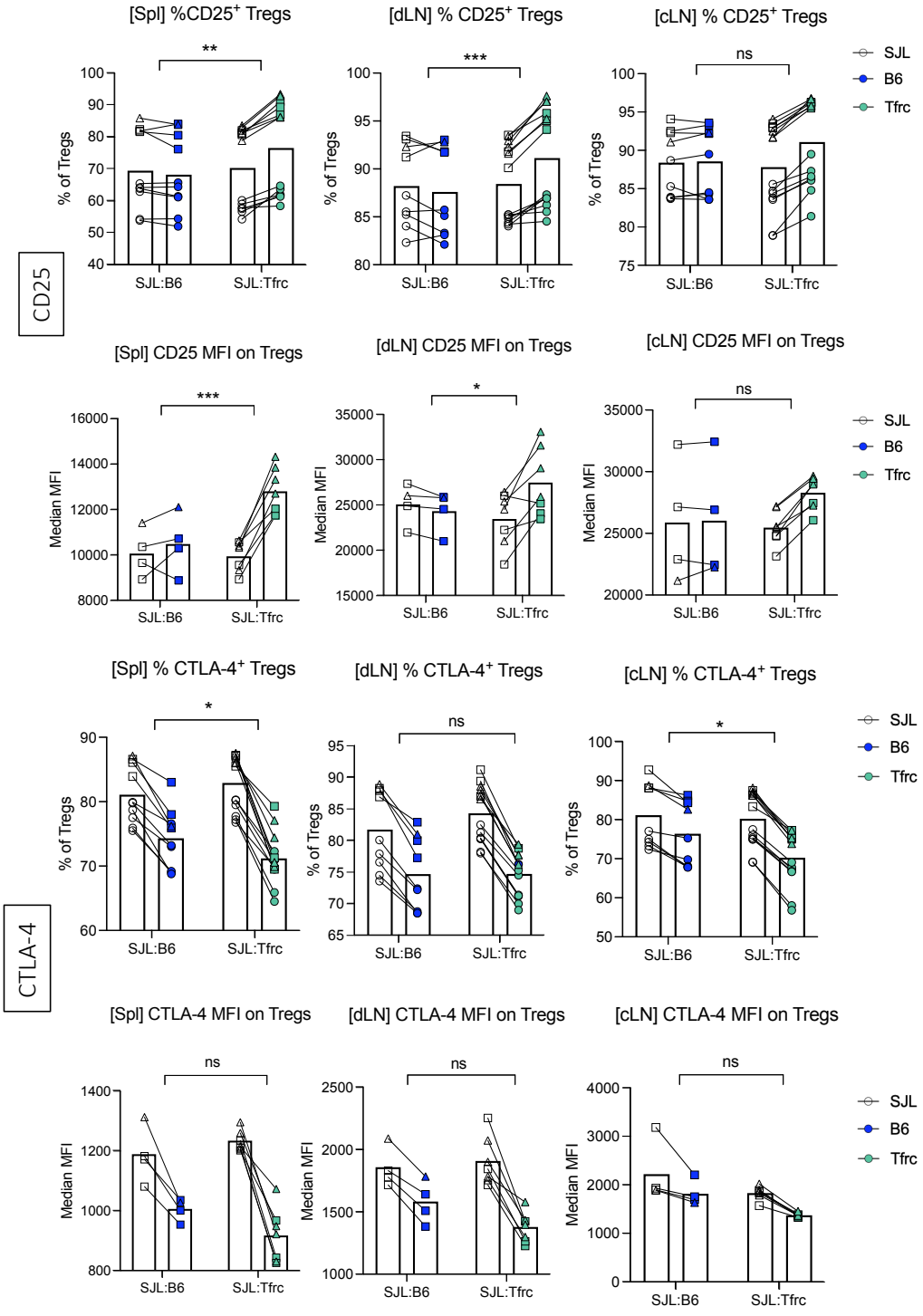

Fig 5.5 – Tfrc Tregs upregulate CD25 and downregulate CTLA-4 in a mixed bone marrow chimera. SJL (CD45.1) females were irradiated and injected with 10^6 bone marrow cells mixed 50:50 from SJL males and either WT B6 (blue) or Tfrc$^{Y20H/Y20H}$ (teal) males and left to reconstitute for 8-12 weeks before transplant with a fully mismatched CBA skin graft. Spleen, draining and contralateral lymph nodes (Spl, dLN, cLN) were harvested at day 11 post transplantation for flow cytometric analysis. Individual points linked by a line represent individual mice so the slope of the lines represents the CD45.1:CD45.2 trends, and symbol shape represents different biological repeats. Mixed effect analysis with Geisser-Greenhouse correction to best compare between CD45.1 vs CD45.2 x SJL:B6 vs SJL: Tfrc$^{Y20H/Y20H}$.

5.2f – Tregs Are Better Activated Than Tconvs in a Malaria Infection Model in Tfrc Mutant Mice

While the chimera model offered the truest head-to-head comparison of healthy vs. iron-deficient Tregs, the complicated nature of the experiment greatly limited the time and resources that could be afforded to it, and the number of markers that could be examined via flow cytometry, so did not allow us to investigate Tregs in excessive depth. Therefore, when Sarah Wideman from the Drakesmith lab ran an infections model experiment on Tfrc mice, I performed flow cytometry on splenocytes from her experiment to interrogate Treg markers in an infectious challenge. Either wildtype C57BL/6 or iron-deficient Tfrc$^{Y20H/Y20H}$ mice with impaired transferrin receptor were inoculated with P. Chapaudi-infected cells in a malaria infection model, and tissues were harvested after 8 days (*Fig 5.6a*)[361]. Sarah's data showed that the Tfrc$^{Y20H/Y20H}$ mice were less capable of mounting an immune response and showed greater weights loss and parasitaemia and decreased immune activation across several parameters[361].

Analysing the Treg compartment showed an increase in the percentage of Tregs and a higher Treg:Teff ratio (*Fig 5.6b*). Further investigation of the Tregs revealed that while Tfrc$^{Y20H/Y20H}$ Tconvs had impaired activation responses, Tfrc$^{Y20H/Y20H}$ Tregs were able to maintain the markers CD44, Helios, ICOS, CD25, and PD-1 readily, even showing an increase in GITR expression, and that although expression of CTLA-4, CD73, and CD39 were decreased, it was to a lesser extent than was observed on Tconvs (*Fig 5.6c*). Overall, these data shows that iron deficient Tregs are more activated than Tconvs in this infection model and may be partly responsible for the impaired immune response to malaria seen in the Tfrc$^{Y20H/Y20H}$ mice.

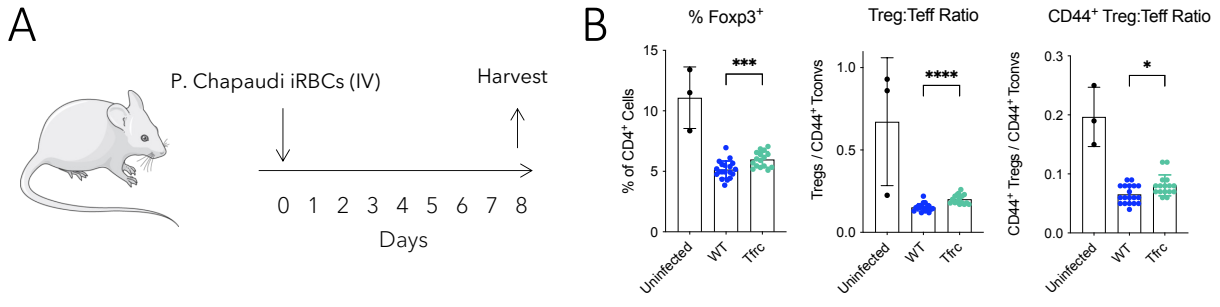

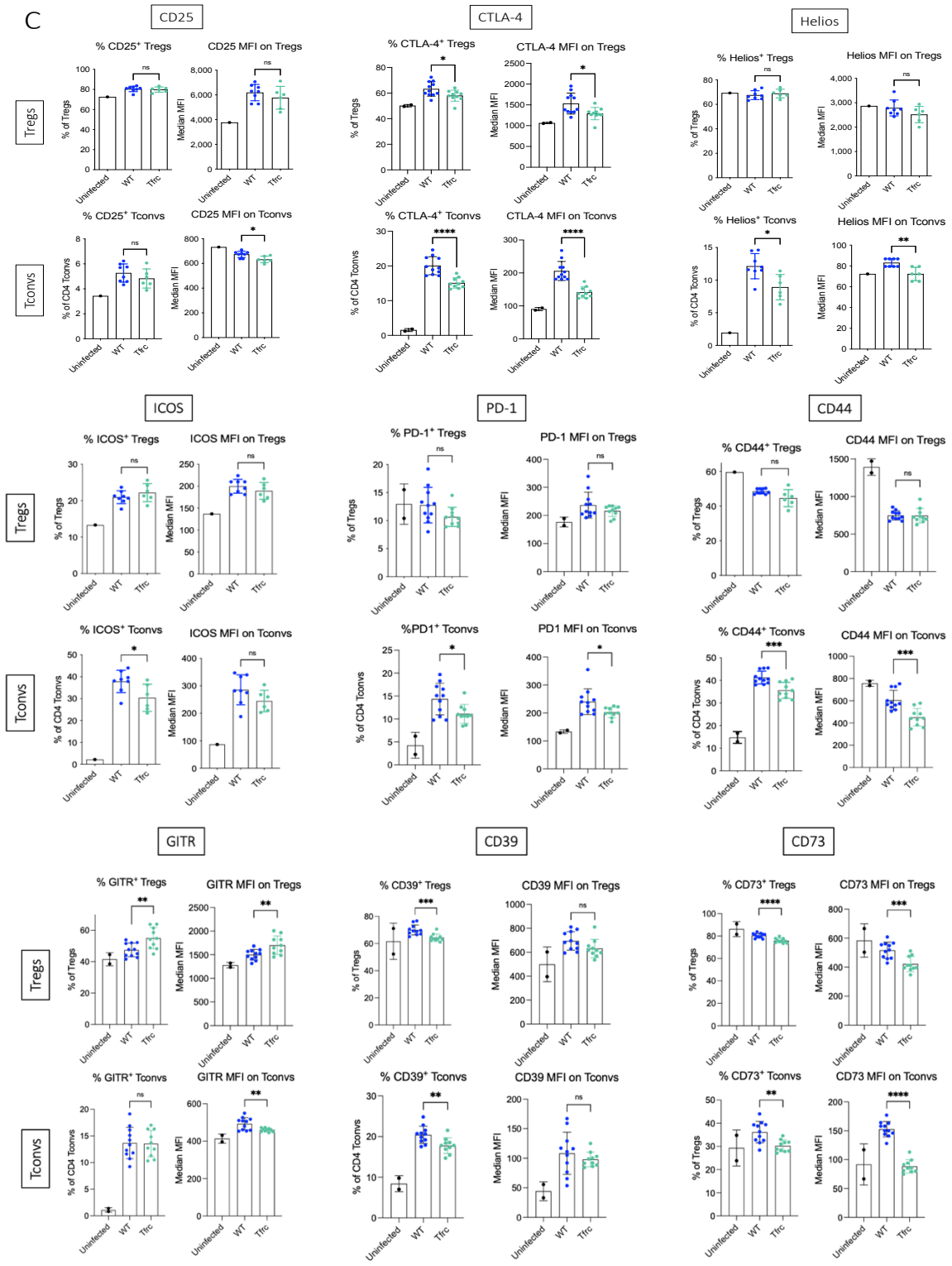

Fig 5.6 – Tfrc Tregs maintain markers of activation better than Tconvs in a malaria infection model. (A) Wildtype C57BL/6 (WT, blue) or $Tfrc^{Y20H/Y20H}$ (Tfrc, teal) mice were inoculated with 10^5 recently mosquito transmitted P. chabaudi infected red blood cells via intravenous injection by Sarah Wideman[361] who harvested tissues at day 8 and kindly provided me with spleen tissue. (B) Flow cytometric analysis of $CD4^+Foxp3^+$ Tregs and $CD4^+Foxp3^-$ Tconvs from two separate experiments. (C) Flow cytometric analysis of $CD4^+Foxp3^+$ Tregs and $CD4^+Foxp3^-$ Tconvs from individual experiments. Each point represents an individual mouse (n = 6). Unpaired t test with Welch's correction. Mean ± SD.

5.3 – DISCUSSION

In this chapter I aimed to investigate how Tregs respond to iron limitation and whether they behave differently to Tconvs in low iron conditions. Tregs maintained markers correlated with their phenotype and activation more readily than Tconvs *in vitro* (*Fig 5.1b)* and in an *in vivo* infection model (*Fig 5.6c*), and that the ratio between Tregs and effector T cells was tipped toward Tregs in several models (*Fig 5.4b, Fig 5.6b*). Cell-intrinsically iron-deficient $Tfrc^{Y20H/Y20H}$ Tregs maintained suppression *in vitro* (*Fig 5.2*) but not *in vivo* (*Fig 5.3*). This is not to say that Tregs thrived in low iron conditions, and both subsets of T cells seemed to be hindered by iron deficiency, but Tregs notably less so. As the balance of inflammatory vs. suppressive signals is much of what governs and steers immune responses, and indeed the volume of costimulatory vs. coinhibitory molecules determines whether T cells become activated or anergised, simply shifting this balance should be enough to alter the immune landscape even without providing a net boost to Tregs.

These studies focused on Tregs and $CD4^+$ Tconvs, in large part due to practicality in isolating these cell types side by side, but $CD4^+$ and $CD8^+$ T cells often differ in their responses so this does not provide us a complete picture of the T cell compartment. However, we do know from other studies that $CD8^+$ T cells are impaired by iron deficiency, as are other cell types including germinal centre B cells, Tfh cells[206,361] and neutrophils[362]. Nevertheless, as Tregs suppress various effectors of the immune response and can tolerise DCs and APCs[68,79,84], if Tregs are the only cell type somehow resistant to iron deprivation (which so far seems to be the case), then their relative abundance or stability is likely to help tolerise the entire immune landscape.

In a mouse influenza model, Joe Frost showed that hypoferremia impaired adaptive responses but increased tissue infiltration by neutrophils and mononuclear cells and increased tissue damage and morbidity[206], which implies an intolerant and immunopathological environment that healthy, functional Tregs should be able to combat, thereby calling the actual suppressive function of iron-deprived Tregs into question. *In vitro*, iron deficient Tregs were comparably capable (*Fig 5.2*) and this type of suppression assay is the most common and best accepted trial for assessing Treg function *in vitro*. However, the controls used were from

Foxp3^{GFP} mice, which can change their transcriptional and epigenetic interactions and decrease *in vitro* suppression compared to WTs[363,364], so true wildtype controls should be used to establish a better comparison. Suppression *in vivo* was more difficult to design a perfect experiment for, as a Foxp3^{Cre}-restricted Tfrc mutation would have been ideal but was not available. All of these experiments comparing iron availability assume that the Tfrc$^{Y20H/Y20H}$ mutation and *in vitro* iron deprivation lead to lower intracellular levels, but direct measurement of intracellular iron was not possible as this requires very specific technology not available to us. The Treg adoptive transfer model showed that Tfrc$^{Y20H/Y20H}$ Tregs did not prolong skin allograft survival whatsoever (*Fig 5.3*), and this might reflect a true impairment in Treg function *in vivo* which is overcome *in vitro* by the strong suppression provided by the beads and the artificial environment of a petri dish.

However, several other factors could be contributing to the failure of the adoptively transferred Tfrc$^{Y20H/Y20H}$ Tregs, namely the huge demand on proliferation required to repopulate an entire mouse with 50,000 Tregs when we know that iron deficiency impairs T cell proliferation (*Fig 5.1*)[209] and that Tfrc$^{Y20H/Y20H}$ cells proliferate poorly[237]. Additionally, the migratory abilities of iron deficient Tregs are unknown, and *in vitro* migration assays and chemokine staining proved to be technically difficult so conclusive data on the matter unfortunately could not be produced. Iron has been shown to promote migration via the IL-2/Jak/STAT3 signalling axis in cancer cells[365], and this pathway is very important in Tregs so it might protect and maintain their migration in iron deficiency, but there is no evidence for this, and iron was implicated in abnormal immune cell homing in Hodgkins' lymphoma[366]. Tregs were shown to proliferate in response to lymphopenia better than to antigen stimulation[360], so the chimera experiment allowed for a better side-by-side comparison of Tfrc$^{Y20H/Y20H}$ and control Tregs without quite so much pressure on challenge-induced clonal expansion. However, the mixed model meant that we were unlikely to see any functional differences that the control Tregs couldn't overcome, as even heterozygous females carrying a single copy of the IPEX mutation (who functionally have half their Tregs completely non-functional, not just somewhat impaired) are healthy[53].

Analysis of surface markers known to be associated with Treg suppression are the best clues we have about their function in experiments where their function could not otherwise be directly

assessed. CD25 expression allows Tregs to mop up available IL-2 and starve surrounding T cells, which can lead to their anergy and apoptosis[68,79,85]. CD25 was upregulated in the Tfrc chimera model (*Fig 5.5*) but slightly downregulated upon *in vitro* activation (*Fig 5.1*), and in the malaria infection model it was unchanged on Tregs but slightly downregulated on Tconvs (*Fig 5.6*). CD25 has been shown to be important for Treg suppression *in vitro*[86,367] but there is comparably much more evidence of its importance *in vivo*. Interestingly, anti-Tfrc antibody had no effect on IL-2R expression *in vivo* but increased its expression *in vitro*[232], which reverses our own findings.

CTLA-4 allows Tregs to moderate signal 2 availability by competing for CD80/86 and removing them from the surface of APCs via trogocytosis[76,77]. CTLA-4 expression was decreased on Tregs *in vivo* (*Fig 5.1, Fig 5.5*), which could be behind their apparent loss of suppression, but CTLA4^{-} Tregs have been shown to maintain function: while Treg-restricted CTLA-4 knockout leads to fatal loss of tolerance in germline knockout[368], CTLA4^{-} Tregs from doxycycline-induced knockout in already mature Tregs (i.e. not suffering any developmental impact) maintained *in vitro* and *in vivo* suppression and prevented autoimmunity, even increasing the relative percentage of Foxp3^{+} cells within the CD4 compartment[356]. This was shown to be due to compensatory increase in IL-10 and IL-10-related genes, and LAG3 and PD-1, and while CD25 was not noted to increase in CTLA4^{-} Tregs, IL-10 expression has been linked to CD25[369] so iron might induce a similar version of this compensatory mechanistic switch in Tregs, causing them to favour CD25 over CTLA-4.

CD39 and 73 are other suppressive mechanisms for Tregs that act together to deprive cells of inflammatory extracellular ATP by catabolising it to ADP/AMP, which CD73 can further convert to anti-inflammatory cAMP[82]. In the malaria infection model, both were decreased on Tregs (*Fig 5.6c*), and their decrease on Tconvs is consistent with decreased activation[370]. Taken together, these data suggest that Tregs might be less suppressive in iron deficiency even despite their conservation or upregulation of activation markers, which supports the data from our *in vivo* Treg suppression assay (*Fig 5.3*).

Activation and phenotype markers including CD44, ICOS, Helios, PD-1, and GITR are associated with Treg stability and phenotype: Helios correlates with but does not seem to drive Treg suppression and stability[65,66], while GITR helps deprive Tconvs of costimulation and is thus suppressive[72].CD44, ICOS, and PD-1 are markers of antigen experience and activation and ICOS has been shown to correlate with Treg proliferation and suppression[359], while PD-1 can induce IL-10 production in Tregs and is increased on effector Tregs[328,329]. These were all maintained on Tregs while being decreased on Tconvs, and GITR was even increased (*Fig 5.1*, *Fig 5.6*), which should correlate with Treg stability and suppression[72]. However, ligation of GITR by GITR-L can inhibit Tregs' suppression function[73], but as no data regarding ligation is available in this experiment, increased GITR expression should be a good sign as far as we know.

It is worth noting that Tregs maintained these markers best when infection or activation did not increase them in the controls, so that the iron deficient Tregs simply maintained already existing levels of these markers seen on naïve Tregs. In contrast, as most Tconvs are naïve in an untreated mouse, the difference in activation between uninfected/unstimulated and the controls was much greater, and the iron-deficient Tconvs were unable to keep up. This may therefore be a slight case of apples and oranges whereby the Tregs may not seem to be as affected by iron deficiency because they are less metabolically active. This difference in metabolic requirements is exactly why we hypothesised that Tregs would respond differentially in the first place, and if a strong upregulation of markers and boost in proliferation is not required for Tregs to maintain suppression, as seems to be the case in control Tregs, then iron deficiency seems a great way to exploit the different metabolic needs between Tregs and Tconvs to tip the balance in their favour. However, it is unclear whether this translates well to humans who are not infection naïve and living in sterile conditions like our mouse models; additionally, if these more mature human Tconvs would require less of a jump in activation, it is unsure whether they might be as hypoferremia-resistant as the Tregs, and perhaps the Treg:Teff ratio would be less changed if more effector and memory Tconvs were present to begin with. A study with human PBMC showed that addition of iron to cultures did not increase percentage of Tregs, but they did not study iron deprivation[371].

Outside of metabolic and activation differences, another plausible reason why Tregs could be more resistant to iron limitation than Tconvs is their expression of the transferrin receptor CD71 which mediates iron import. Our collaborator Andrew Armitage has a comprehensive dataset from many iron deficient patients and healthy controls and noted that CD71 expression was strikingly highest on Tregs (unpublished). Indeed, I have considered whether high expression of CD71 on Tregs might be a suppressive mechanism and act as an iron sink, similarly to how CD25 starves surrounding cells of IL-2. This is however quite difficult to test experimentally, as it is difficult to separate out the iron hoarding abilities of CD71 from its iron import which likely would affect Treg survival and function. A few possible experiments to investigate this theory are proposed in the– Future Directions section. Additionally, iron deficiency-induced downregulation of CD25 on T cells is fairly well documented[146,206,237], and as iron deficiency has been shown to increase IL-2 production[146], Tregs' special relationship to CD25 which seems to allow them to maintain and even upregulate it might give them exclusive access to IL-2 to help them withstand the iron deficiency better than their $CD25^-$ counterparts. CD71 has also been proposed as a marker of regulatory B cells[372], and Shamsideen Yusuf in the Drakesmith lab is currently undertaking work showing that iron-deprived Tregs of all activation states upregulate CD71 whereas it is more selective in Tconvs (unpublished), reinforcing the concept that its expression is governed by mechanisms other than cellular metabolism and activation.

Overall, Tregs seem to exhibit resistance to iron limitations that is not seen in Tconvs and other immune cells[206,237,361,362]. This could be an evolutionary bias that allows iron consumption caused by extreme inflammation to act as a rheostat to disable immune cells and prevent immunopathology, while allowing Tregs to preferentially survive and function in these conditions and bring about resolution of inflammation. This ability of iron deficiency to tip the balance toward Tregs may create a suppressive and tolerogenic immune landscape which could be of use in diseases such as autoimmunity, immunopathology-driven infections, and transplantation.

6 - Effect of Iron Deprivation on Alloresponses and the Immune System

6.1 – INTRODUCTION AND AIMS

Previous work by our collaborators, namely Joe Frost, has shown that iron deprivation severely limits immune responses to infection and vaccines[206] which is supported by many others[210–214], and data from the previous chapter shows that iron limitation seems to favour Tregs. Therefore, it was hypothesised that this ability to promote tolerance could have therapeutic implications in contexts where decreased inflammation would be favourable, such as in a transplantation model. One study by Bohne et al. showed that the genes that most differentiated tolerant liver recipients from recipients experiencing rejection were related to iron homeostasis, showing that high expression of hepcidin and low expression of Tfrc transcripts were the best predictors of operational tolerance[234]. These findings supports our hypothesis that iron limitation might promote tolerance and prolong graft survival. In other studies on iron and transplantation, low iron favoured graft survival[232,233] while increased iron favoured rejection[230,231], but the data on iron in transplantation and autoimmunity is conflicting, with reports showing benefits of both and increase and decrease in iron availability for various organs and little consensus on differentiating between intracellular vs. serum iron availability[228,229,235,236] (*see section 1.4d*). Therefore, in this chapter I sought to investigate how iron limitation would shape alloresponses to better understand the role of iron in tolerance and immune balance, in the hopes of informing potential therapeutic and translational applications of iron availability in a transplant setting.

CHAPTER AIM: To understand how iron limitation affects immune responses to a transplant

HYPOTHESIS: Iron deprivation will impair alloresponses and induce a tolerogenic state, thus extending graft survival

6.2 – Results

6.2a – Hepcidin Extends Graft Survival and Impairs Alloresponses but Tregs are More Resistant

There are many *in vivo* iron limitation models but hepcidin, the master regulator that internalises and degrades ferroportin to impair iron export and lower serum iron, was chosen; hepcidin is upregulated in transplant recipients due to low grade inflammation and mTOR or calcineurin inhibitors used as immunosuppression[228], and correlates with tolerance[234]. All the work presented in this chapter is the result of collaboration with Amy Cross, who worked conjointly with me on most of the *in vivo* work presented here, and Joe Frost, who prepared hepcidin for us nearly every day and carried out much of the flow cytometry. Together, we administrated a synthetic hepcidin mimetic (mHep) with daily intraperitoneal injections, based off an established protocol that lowers iron levels to 5µmol/L and decreases liver hepcidin mRNA levels[206,373]. Mice were given mHep for 14 days following skin transplantation, and one arm also received low (2ppm) iron diet for four weeks prior to skin transplantation to deplete intracellular iron stores as well as serum iron, as established by previous work[206]. Low diet administration was ended alongside with the last mHep injection. (*Fig 6.1a*).

Graft survival was extended from a median of 10.5 days in controls to 12 days in mHep-treated mice and doubled to 20 days in mice with mHep and low iron diet, which is quite difficult for this stringent, fully mismatched model (*Fig 6.1b*). Interestingly, tail bleeds during time of peak rejection revealed that although mHep along did not extend graft survival by very much, it significantly stunted alloresponses: activation, effector, and proliferation responses were stunted on both $CD4^+$ and $CD8^+$ T cells, regardless of diet (*Fig 6.1c*). The mismatch between graft survival and peripheral immune responses is rather puzzling, but alloresponses in blood do not necessarily reflect responses in the graft, so it might be that hepcidin alone impairs responses just enough to allow mobilisation to the site of rejection, leaving the periphery depleted. Strikingly, when investigating the Treg compartment, Tregs seemed to be less severely affected than Tconvs, as evidenced by their proportion to $CD4^+$ Tconvs and $CD44^+$ Teffs (*Fig 6.1d*), corroborating the results from the previous chapter. Expression of CD25 on Tregs was increased by hepcidin, although their activation and proliferation were impaired similarly to other T cells.

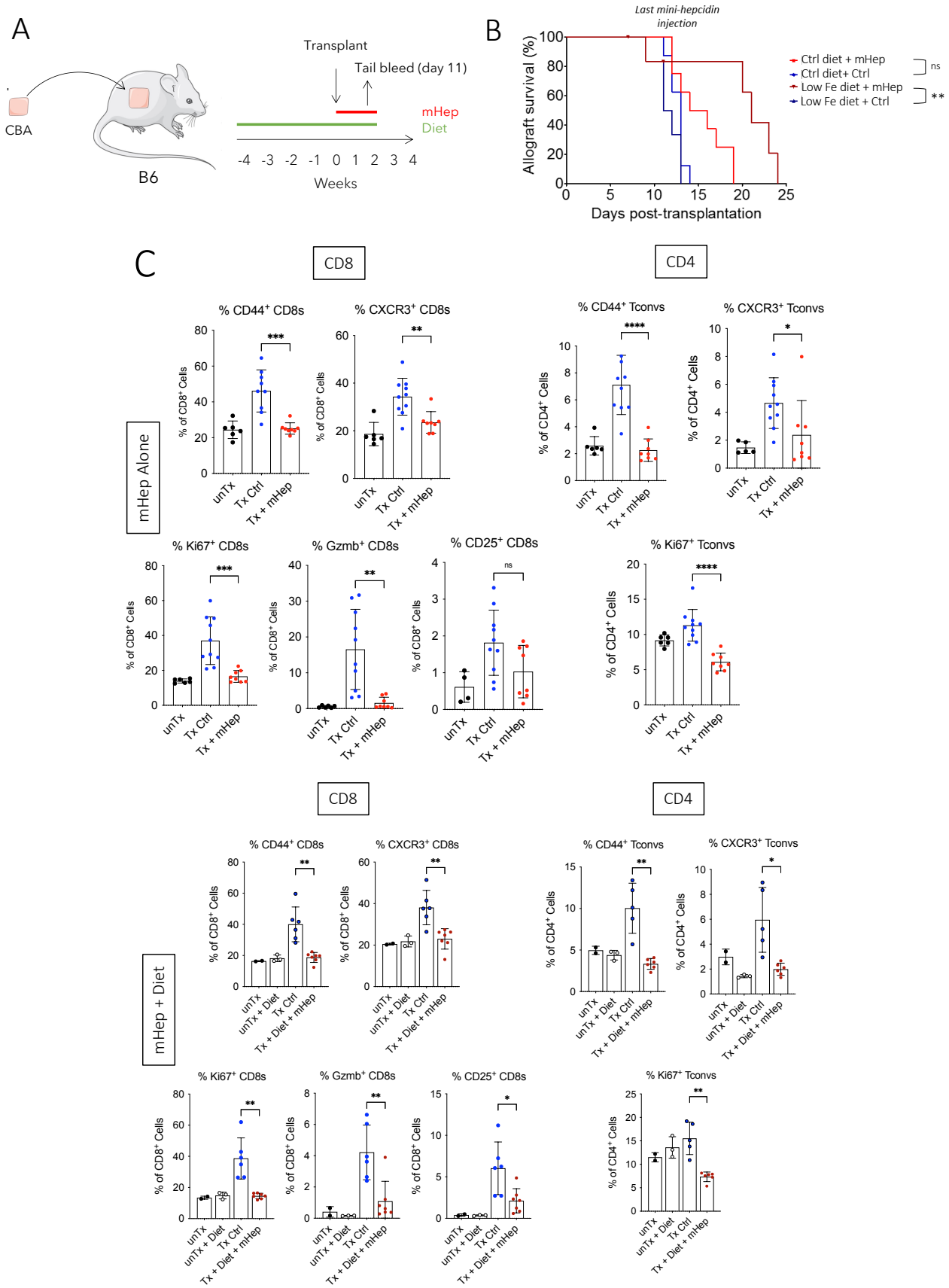
A
CBA
B6
Transplant
Tail bleed (day 11)
mHep
Diet
-4 -3 -2 -1 0 1 2 3 4
Weeks
B
Last mini-hepcidin injection
Allograft survival (%)
Days post-transplantation
Ctrl diet + mHep
Ctrl diet+ Ctrl
Low Fe diet + mHep
Low Fe diet + Ctrl
ns
**
C
CD8
CD4
mHep Alone
mHep + Diet
% CD44+ CD8s
% CXCR3+ CD8s
% CD44+ Tconvs
% CXCR3+ Tconvs
% Ki67+ CD8s
% Gzmb+ CD8s
% CD25+ CD8s
% Ki67+ Tconvs
% of CD8+ Cells
% of CD4+ Cells
unTx
Tx Ctrl
Tx + mHep
unTx + Diet
Tx + Diet + mHep

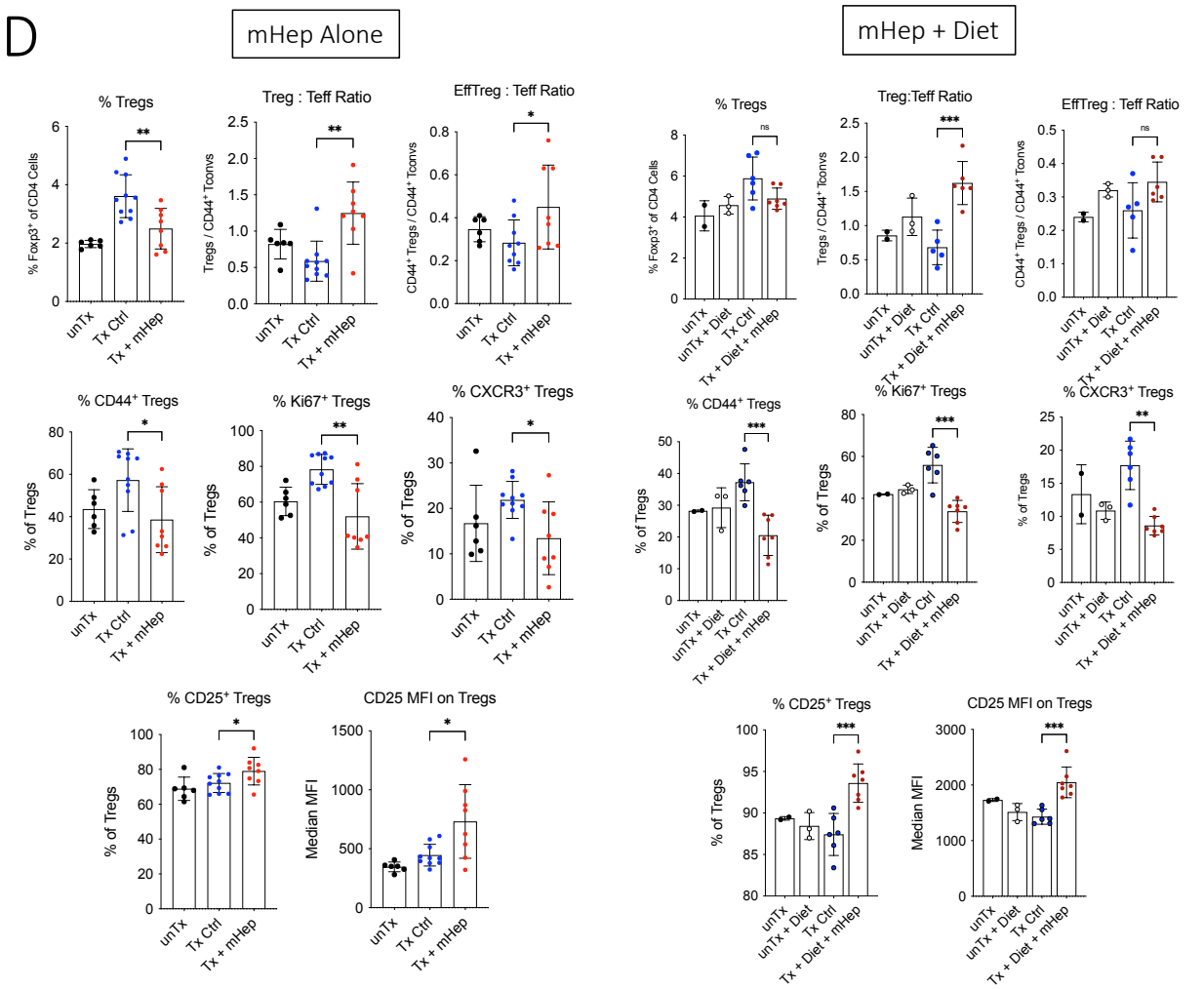

Fig 6.1 – Iron deprivation extends graft survival. (A) B6 mice were given fully mismatched CBA skin grafts and 14 days of daily 1mM mHep or SL220 carrier control via intraperitoneal injections with the help of the incredible Amy Cross, with 4 weeks pre-treatment with 200ppm control diet or 2ppm low iron diet. Last day of hepcidin injections was on day 13 and diet was changed to control for both groups on day 15. (B) Graft survival with cut-off at score of 4. Kaplan-Meier analysis. (C-D) Tail bleeds were performed at day 11 post transplantation for flow cytometric analysis which was performed and acquired by Joe Frost. Each point represents an individual mouse (n = 10). Unpaired t test with Welch's correction. Mean ± SD.

6.2b – Hepcidin Combines with Immunotherapy to Extend Graft Survival

As hepcidin alone seemed to impair alloresponses but not graft survival, it was hypothesised that pairing it with costimulatory blockade immunotherapy could achieve the same graft prolongation without requiring such severe iron deficiency, which would be a more clinically translational approach. mHep was therefore combined with low dose of an IL-2 complex alongside either αIL-6 or αCD28 therapy, as these were used with success in a similar transplant model[374,375]. The IL-2-JES6-1mAb complex has been shown to be highly Treg-specific, increasing their suppressive function *in vitro* and *in vivo* and their expression of CD25, GITR, CTLA-4, and ICOS[131]. It extends the half-life of IL-2 from minutes to hours, and is highly specific for CD25-expressing cells because it binds IL-2 at nearly the exact same binding site as the IL-2Rβγ dimer, thus preventing binding, but this complex is still capable of binding IL-2Rα (CD25), which allows dissociation of IL-2 from the mAb and subsequent IL-2 signalling[376]. Thanks to this inherent Treg specificity and previous work showing promising results using this combination[374,375], hepcidin was thought to be a good candidate to synergise with this combination and improve results.

αIL-6 therapy was not very effective and did not improve mHep's efficacy, but αCD28 extended graft survival from a median of 11.5 days to 15 days and when combined with mHep, to 18 days (*Fig 6.2b-c*). The group receiving αCD28 and mHep had no graft rejection at all during treatment and only started rejecting after their last doses, after which both αCD28-treated groups began to reject rapidly. Peripheral blood analysis at day 17 (during rejection of the αCD28-treatd groups) showed that Tregs were the only T cells that seemed unaffected by the treatment, and the combined treatment increased the percentage of Tregs and their expression of Foxp3, CD25, and CTLA-4 (*Fig 6.2b d-e*). CD28 expression was low on all T cells but showed a slight decrease on Tregs which was boosted by mHep treatment, suggesting that it truly synergised to improve the effects of αCD28 treatment. Peripheral blood responses in the αIL-6-treatement groups were not analysed because these had already mostly rejected at the time of the tail bleed, and so would already be contracting their immune responses.

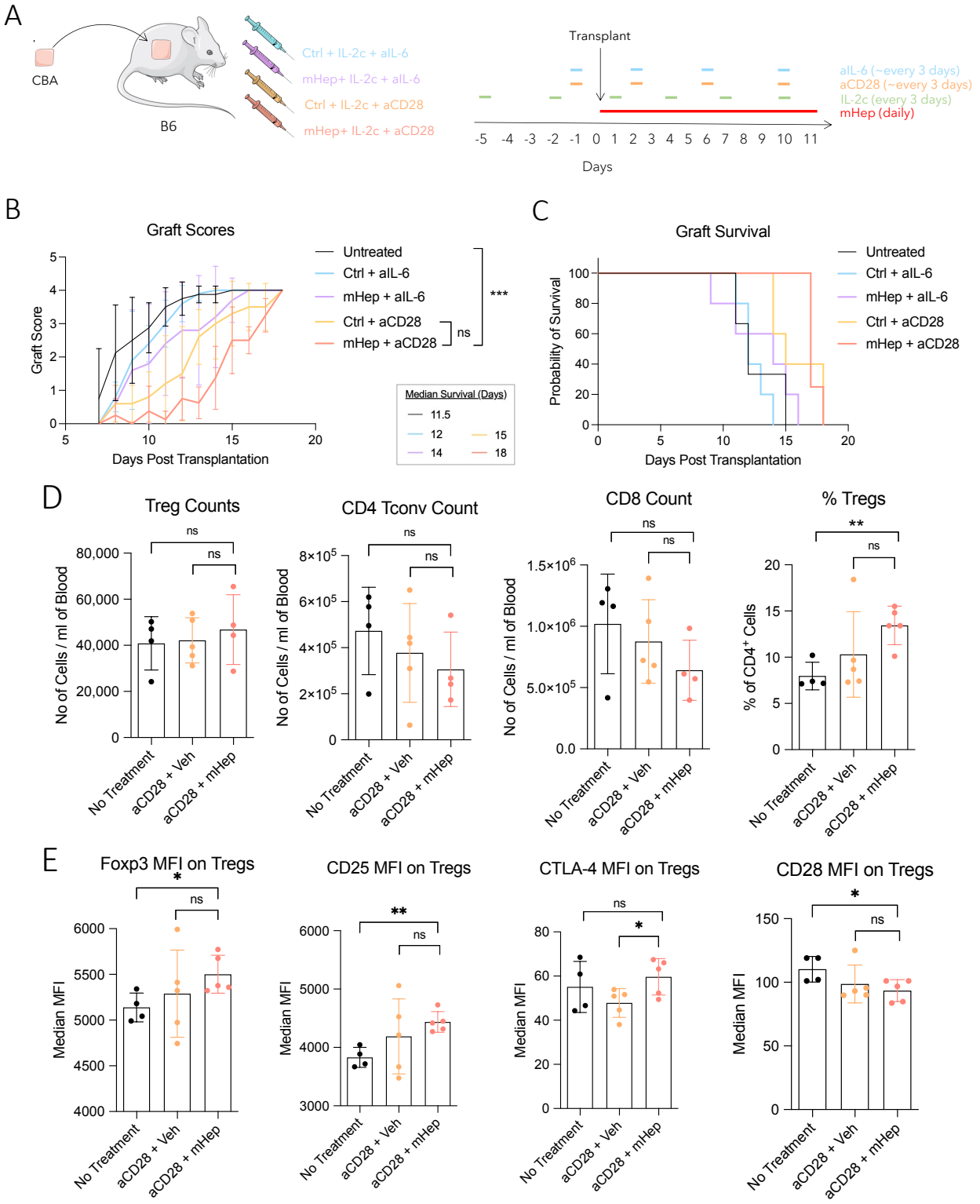

Fig 6.2 – Hepcidin treatment can synergise with costimulatory blockade therapy to extend graft survival. (A) B6 mice with fully mismatched CBA skin grafts were injected intraperitoneally with daily 1mM mHep or SL220 vehicle control and 1µg of IL-2 complex (1:5 IL-2:αIL-2) every 3 days alongside either 200µg of αCD28 or 225µg of αIL-6 approximately every 3 days. (B) Graft survival with cut-off score of 4. (C) Mean graft scores with SD. Kaplan-Meier analysis. (D-E) Tail bleeds at day 17 were taken for flow cytometric analysis. Points represent individual mice (n = 5). Unpaired t tests with Welch's correction. Mean ± SD.

6.2c – Tfrc Mice Reject at a Similar Rate to Wildtype Mice

As anti-Tfrc antibodies have been used to prolong graft survival[232,233], the ability of $Tfrc^{Y20H/Y20H}$ mice with inefficient transferrin receptor to mount alloresponses was assessed, as they mounted poor responses in an infection model (*Fig 5.6*). $Tfrc^{Y20H/Y20H}$ mice rejected at a similar rate to controls (*Fig 6.3b*) but their donor-specific alloresponses were still somewhat impaired in an *in vitro* restimulation challenge (*Fig 6.3c*), although less dramatically than seen *in vivo* with hepcidin treatment. This mismatch betweeen cell responses and graft survival is consistent with previous findings, and reflects iron-impaired cells' ability to mount localised responses at the graft, even when impaired peripherally, as strong stimulation could induce an almost full response. The reason why more pronounced clinical difference was observed in the malaria model might be because it is a systemic infection, whereas alloresponses are more localised to the graft and lymph nodes, which might be easier for iron-impaired cells to keep up with than a systemic challenge. Additionally, malaria is Th1-driven, and Tfrc blockade was shown to selectively impair Th1 responses above other Th subsets[221], which could also explain their expedited disease progression. However, as iron levels were not measured cell-intrinsically or systematically in either model, it is hard to compare between them all and previous data from the Tfrc and mHep models are being relied on to suplement this information[211,237].

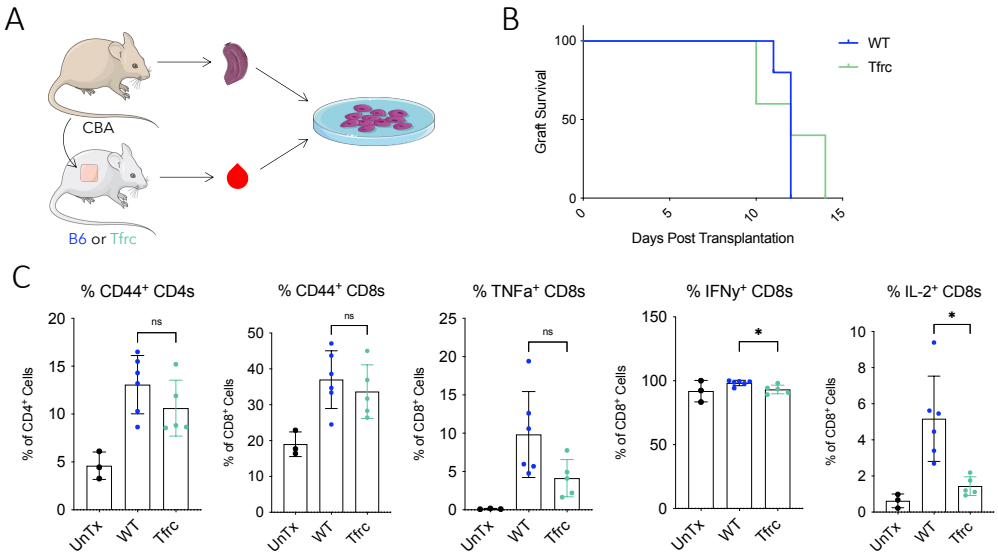

Fig 6.3 – Tfrc mice reject skin graft normally but have slightly impaired alloresponses. (A) Wildtype C57BL/6 (WT, blue) or $Tfrc^{Y20H/Y20H}$ (teal) mice were given a fully mismatched (CBA) skin graft and monitored for rejection. (B) Graft survival with cut-off score of 4. Kaplan-Meier analysis. (C) At day 11, tail bleeds were taken and incubated with donor (CBA) spleens in a mixed lymphocyte reaction before intracellular flow cytometric analysis, which was performed by Joe Frost. Unpaired t test with Welch's correction. Mean ± SD.

6.2d – Adoptively Transferred Tfrc Mutant T Cells Fail to Reject Skin Grafts

As systemic iron deficiency is not an ideal therapeutic strategy, iron deprivation was limited to T cells to determine whether this would be enough to impact graft outcomes. Either wildtype or Tfrc$^{Y20H/Y20H}$ CD4^{+}CD25^{-} Tconvs were adoptively transferred into RAG$^{-/-}$ mice and monitored graft rejection (*Fig 6.4a*). T cells were detectable in peripheral blood both before and after rejection, indicating that they were present and viable throughout (*Fig 6.4b*). Tfrc$^{Y20H/Y20H}$ T cells were completely unable to cause rejection (*Fig 6.4c*), thus indicating that T-cell limited iron deprivation may be sufficient to extend graft survival and improve transplant outcomes. Due to concerns in the previous adoptive transfer experiment about Tfrc$^{Y20H/Y20H}$ cells' ability to reach the proliferation and migration requirements to function in this model, T cell phenotype was assessed around time of rejection and found that Tfrc$^{Y20H/Y20H}$ T cells had comparable levels of activation and migration markers in transplantation.

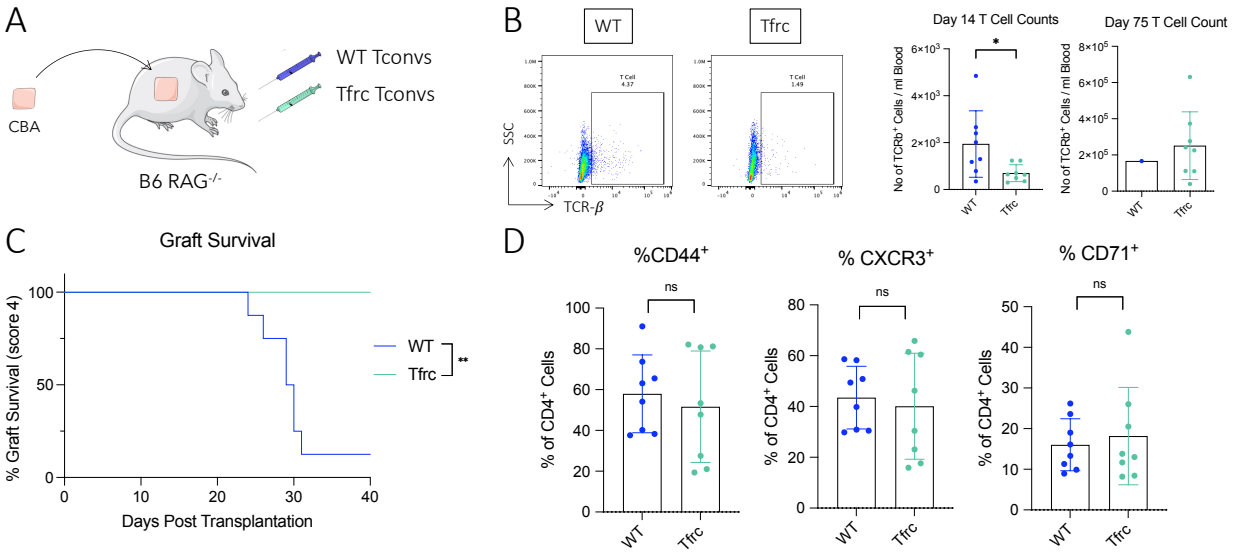

Fig 6.4 – Tfrc mutant Tconvs do not reject allografts. (A) RAG$^{-/-}$ mice were injected with 10,000 CD4^{+}CD25^{-} Tconvs from either WT C57BL/6 (blue) or Tfrc$^{Y20H/Y20H}$ (teal) splenocytes intravenously and given fully mismatched CBA skin grafts the following day. (B) Flow plots gated on CD45^{+} cells from day 14, and CD45^{+}TCRß$^{+}$ cell counts at day 14 (before rejection) and day 75 (after rejection), at which point the untransplanted controls had already been culled. (C) Graft survival with cut-off score of 4. Kaplan-Meier analysis. (D) Expression of markers on TCRß$^{+}$CD4^{+} cells at day 23 (during rejection). Points represent individual mice (n = 8). Unpaired t tests. Mean ± SD.

6.2e –Mixed Tfrc Bone Marrow Chimeras Reconstitute with Slight Impairment

In order to better study Tfrc$^{Y20H/Y20H}$ alloresponses without so much pressure on extensive reconstitution, a chimera model was used for side-by-side comparison of iron deprived and control cells experiencing the same surrounding immune environment. Irradiated SJL recipients (CD45.1) received a 50:50 mix of bone marrow from SJL (CD45.1) mice and either wildtype B6 (CD45.2) mice or Tfrc$^{Y20H/Y20H}$ mice (CD45.2), and spleens and lymph nodes were harvested after reconstitution (*Fig 6.5a*). Tfrc$^{Y20H/Y20H}$ cells were consistently but insignificantly impaired in their reconstitution, which likely reflects their known proliferation defect[237] (*Fig 6.5b*). Thymocytes showed some impairment in their developmental journey through the thymus at all stages of development (*Fig 6.5c*) but not much in their resting levels of naïve, effector, and memory populations (*Fig 6.5d*). Tfrc$^{Y20H/Y20H}$ Tregs' presence within the CD4 compartment was unaffected and CD25 expression trended slightly higher on Tfrc$^{Y20H/Y20H}$ Tregs but with great variability and insignificance (*Fig 6.5e*). Tregs seemed more affected than Tconvs in their maturity and showed a greater percentage of naïve cells, especially in lymph nodes (*Fig 6.5d*).

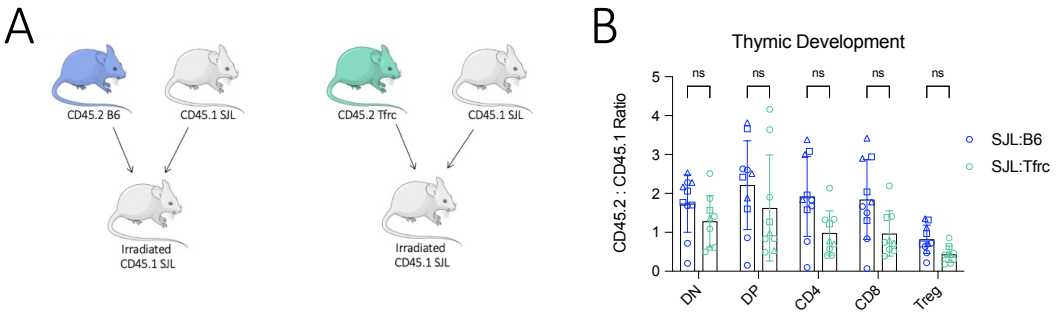

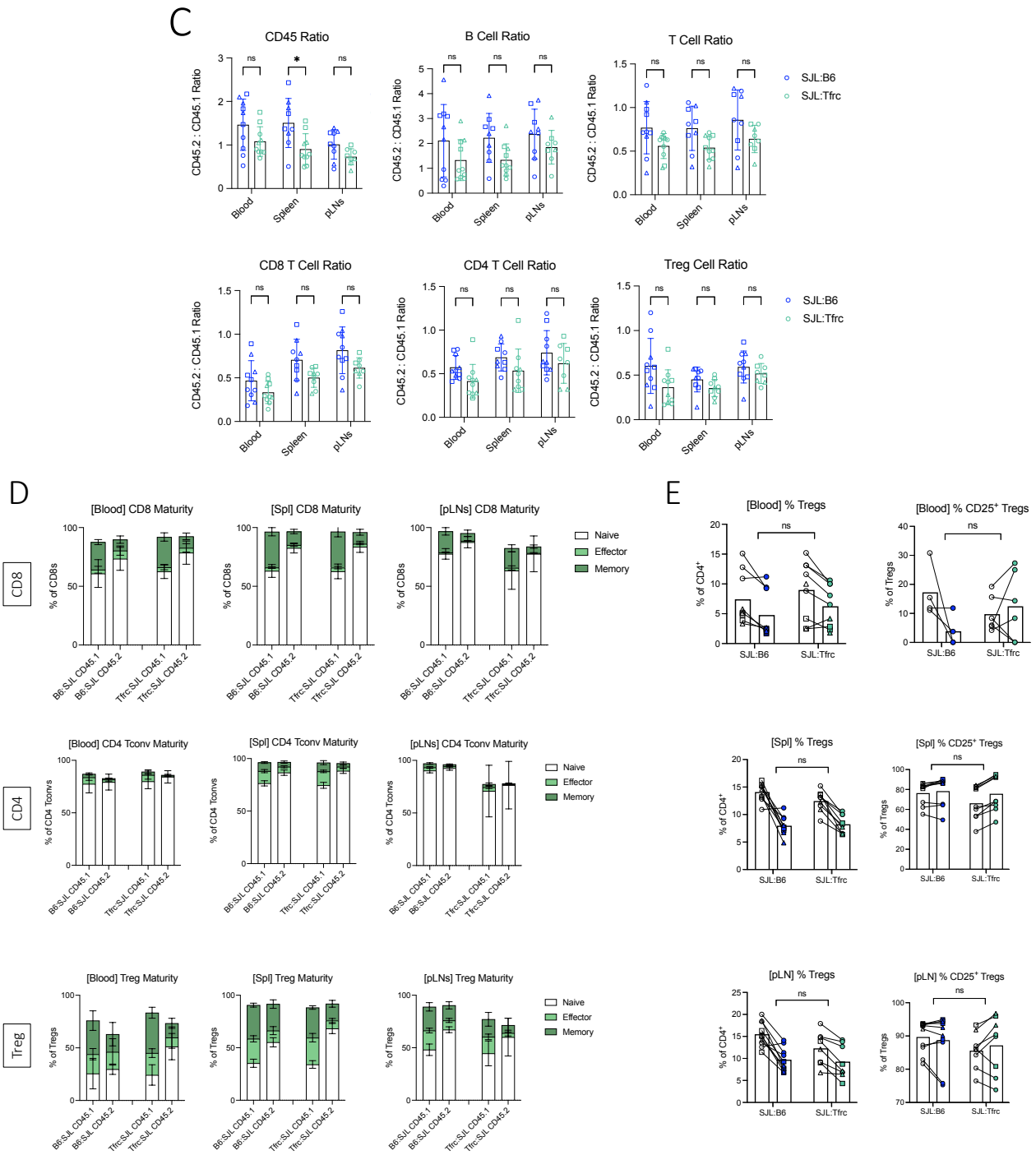

Fig 6.5 – Tfrc cells are capable of adequate reconstitution in a mixed bone marrow chimera model. (A) Tissues were harvested at 8-12 weeks without transplantation for flow cytometric analysis of (B) general reconstitution, (C) thymocyte development of double negative (DN), double positive (DP), and single positive thymocytes, (D) T cell maturity of $CD62L^{+}CD44^{-}$ naïve cells, $CD44^{+}CD62L^{-}$ effector cells, and $CD44^{+}CD62L^{+}$ memory cells, and (E) Tregs. Symbol shape represents separate biological repeats (n = 3). Mean ± SD. Unpaired multiple t tests with Welch's correction (B) and mixed effect analysis with Geisser-Greenhouse correction for comparison between CD45.1 vs CD45.2 x SJL:B6 vs SJL:Tfrc. Points represent individual mice (n = 8).

6.2f – Adaptive Cells from Tfrc Chimeras are Out-Competed After Transplantation

As hypoferremia is known to affect adaptive responses predominantly after an immune challenge, and that mice and patients with the $Tfrc^{Y20H/Y20H}$ mutation are healthy until faced with an immune challenge, chimeras were subjected to a skin transplantation model to compare $Tfrc^{Y20H/Y20H}$ adaptive cells to control cells experiencing the exact same level of antigen presentation and immune landscape at large (*Fig 6.6a*). The total immune compartment and myeloid cells were unaffected, but T cells were impaired in their alloresponses (*Fig 6.6b*). CD4s, CD8s, and Tregs had impaired formation of effector cells with more naïve cells present in the $Tfrc^{Y20H/Y20H}$ compartment, but memory cells were unaffected, likely due to the timing of the peak of the alloresponse before contraction and formation of a memory cohort (*Fig 6.6c*). Similarly, the total B cell compartment was somewhat impaired after transplantation but class-switched activated germinal centre B cell significantly more so, and their presence in $Tfrc^{Y20H/Y20H}$ cells was clearly diminished (*Fig 6.6d-e*). Taken altogether, this indicates that adaptive responses from $Tfrc^{Y20H/Y20H}$ cells are selectively impaired, including Tregs, but we know that Tregs in this model are comparatively more represented than Tconvs, as seen by elevated Treg:Teff ratio in the $Tfrc^{Y20H/Y20H}$ cell compartment (*Fig 5.4*).

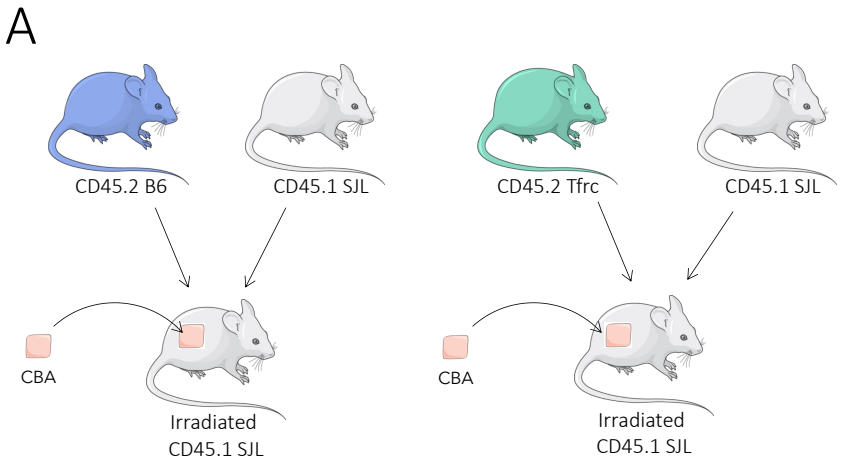

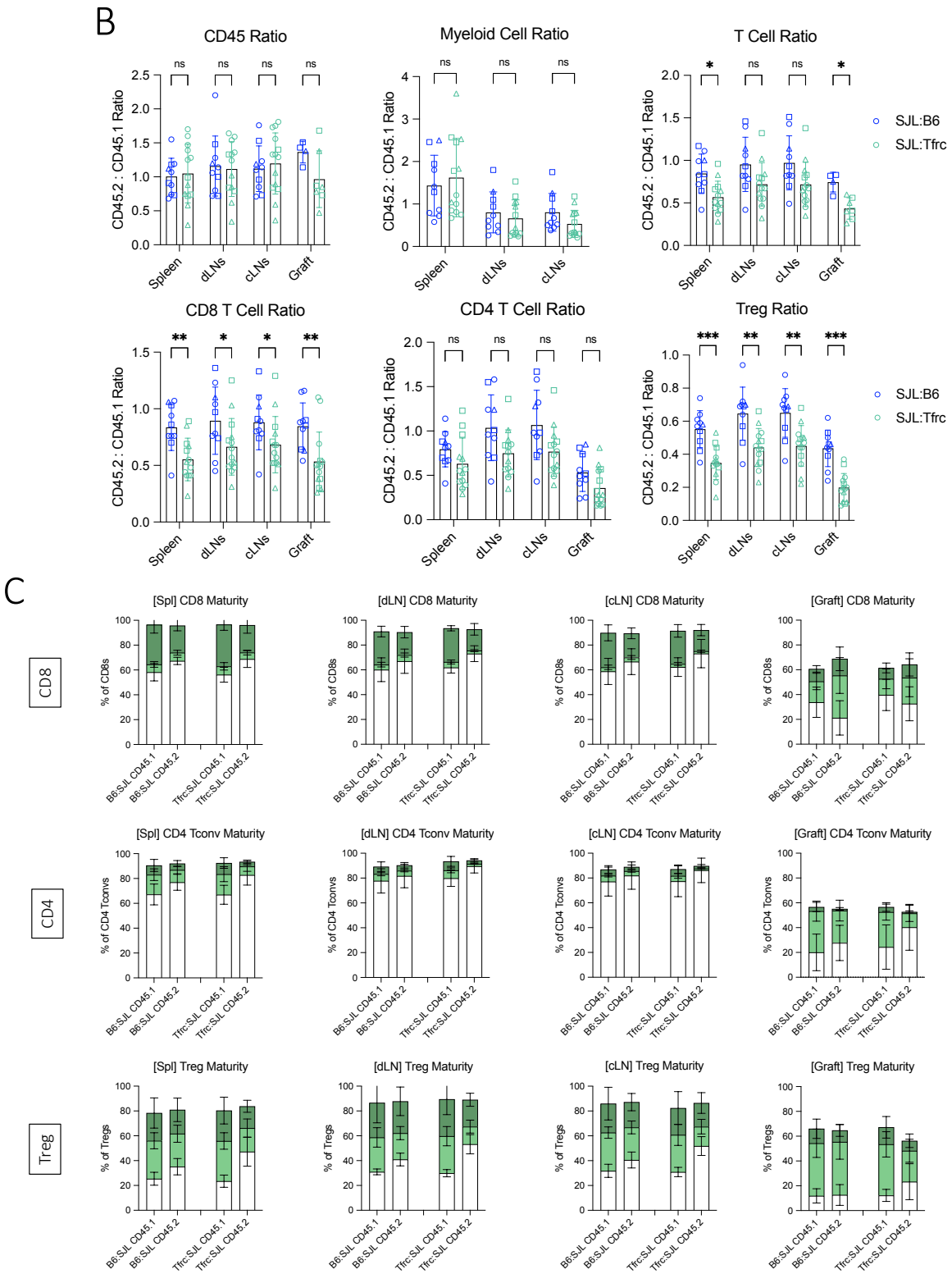
B
CD45 Ratio
Myeloid Cell Ratio
T Cell Ratio
CD8 T Cell Ratio
CD4 T Cell Ratio
Treg Ratio
CD45.2 : CD45.1 Ratio
Spleen
dLNs
cLNs
Graft
SJL:B6
SJL:Tfrc
C
CD8
CD4
Treg
[Spl] CD8 Maturity
[dLN] CD8 Maturity
[cLN] CD8 Maturity
[Graft] CD8 Maturity
[Spl] CD4 Tconv Maturity
[dLN] CD4 Tconv Maturity
[cLN] CD4 Tconv Maturity
[Graft] CD4 Tconv Maturity
[Spl] Treg Maturity
[dLN] Treg Maturity
[cLN] Treg Maturity
[Graft] Treg Maturity
% of CD8s
% of CD4 Tconvs
% of Tregs
B6:SJL CD45.1
B6:SJL CD45.2
Tfrc:SJL CD45.1
Tfrc:SJL CD45.2
Naive
Effector
Memory

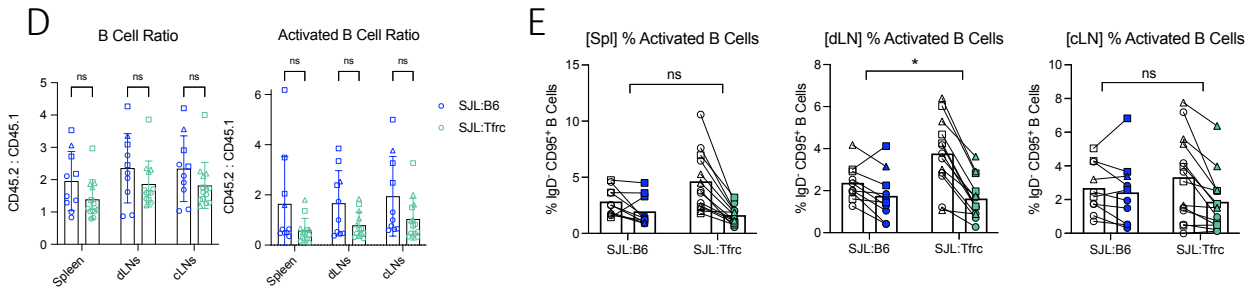

Fig 6.6 – Tfrc mutant T and B cells are out-competed after transplantation in mixed chimeras. (A) SJL (CD45.1) females were irradiated and injected with 10^6 bone marrow cells mixed 50:50 from SJL males and either WT B6 (blue) or $Tfrc^{Y20H/Y20H}$ (teal) males, and left to reconstitute for 8-12 weeks before transplant with a fully mismatched CBA skin graft. Spleen, draining and contralateral lymph nodes (Spl, dLN, cLN) were harvested at day 11 post transplantation for flow cytometric analysis. (B) Ratio of CD45.2 : CD45.1 cells within SJL:B6 or SJL:Tfrc mice. Myeloid cells are defined as $CD11b^+$. Symbol shape represents different biological repeats. Unpaired t tests with Welch's correction. (C) T cell maturity of $CD62L^+CD44^-$ naïve cells, $CD44^+CD62L^-$ effector cells, and $CD44^+CD62L^+$ memory cells. (D) Ratio of CD45.2 : CD45.1 cells within SJL:B6 or SJL:Tfrc mice. Activated B cells are defined as IgD^- $CD95^+$. Symbol shape represents different biological repeats. Unpaired t tests with Welch's correction. Mean ± SD. (E) Individual points linked by a line represent individual mice so the slope of the lines represents the CD45.1:CD45.2 trends, and symbol shape represents different biological repeats. Mixed effect analysis with Geisser-Greenhouse correction for comparison between CD45.1 vs CD45.2 x SJL:B6 vs SJL:Tfrc.

6.3 – Discussion

This chapter aimed to investigate how iron limitation would affect alloresponses and whether it had the potential to extend allograft survival. Iron deficiency has been shown to impair immune responses and especially adaptive responses, which is unfortunate in infection and vaccine responses[206,210–214], but the carefully balanced nature of immunology means that results detrimental on one side (here, infection) become advantageous to the mirrored problems, i.e. in tolerance. Iron deprivation could extend graft survival but only when hepcidin was combined with low iron diet (*Fig 6.1*). It is unclear whether this combination was successful because it was more severe or because intracellular iron deprivation is more effective than serum deprivation; as the serum eventually serves to feed cells, the difference between cellular and serum iron stores might only be meaningful in terms of timing of iron availability, and even then, only by a few hours as IRP-mediated RNA stabilisation is a rapid process. However, even when graft survival wasn't extended, peripheral alloresponses were still significantly impaired (*Fig 6.1*). One study showed that more naïve B cells were detected in peripheral blood during acute rejection[377], which supports our theory that effector cells migrate to the graft during rejection and are therefore nowhere to be found in the periphery. One hypothesis for the disparity between

graft survival and impaired alloresponses in iron deficiency is that iron-impaired cells cannot mount an activation response strong enough to cover both the graft and the periphery, so any activated cells go to the graft. Indeed, the graft was the site with highest proportion of effector and memory cells, with little naïve cell infiltration, but the $Tfrc^{Y20H/Y20H}$ cells in the graft still had the same skew toward fewer effectors and more naïve cells when compared to their control counterparts (*Fig 6.6c*). It seems that even though $Tfrc^{Y20H/Y20H}$ cells had less effector trafficking into the graft, it might have been enough to cause the rejection observed at the macroscopic level, but that this couldn't extend to cover the periphery as well. Ideally, cell-intrinsic iron measurements would help determine whether there are differences between local and peripheral T cell levels, and whether iron is mobilised to rejecting tissues to combat the inflammation-induced anaemia; the technology for this type of assessment was not available to us and previous iron measurements after systemic mHep administration were available to confirm the efficacy of mHep administration in limiting serum iron and liver iron stores[206].

The hypothesis was that stunted alloresponses brought on by hypoferremia would extend graft survival, and more severe iron deficiency could achieve the desired outcome. The role of iron in transplant therapies is unclear: both iron deficiency and iron loading were able to protect against IRI and oxidative stress which are drivers of early rejection[228], and both also accelerated acute rejection in a cardiac allograft model[229]. A transcriptional study revealed that the genes that best predicted operational tolerance were increased hepcidin and decreased *Tfrc* transcription, suggesting that low serum and cellular iron led to better outcomes in liver transplant[234], but the same correlation between inflammation and hepcidin/transferrin was not found in kidney receipients[235,236]. In the above skin transplant experiments, only severe iron deficiency managed to extend graft survival but a difference in peripheral inflammation was not observed, so differences may be very organ specific. The reason for these organ-specific differences might be their differential uses of iron, and as liver is one of the main stores of iron and the site of hepcidin production it may have a higher reliance on iron and be more readily able to up- or down-regulate genes related to iron homeostasis in order to be ready to regulate systemic iron. However, the skin has been proposed to be important in systemic iron homeostasis as well, as it is responsible for about 25% of unregulated iron loss through desquamation[378]. Different organs' roles in regulating systemic iron and their differential susceptibilities to iron-loading might make

it difficult to compare iron in different transplant models, which could be behind some of the discrepancies between various studies and organ models. Additionally, skin transplantation is one of the most stringent experimental transplantation models, whereas livers are by far more tolerogenic, so the immunogenicity of different organs likely also dictates how intense the alloresponse might be and how successful iron deprivation might be in taming it.

We sought to make iron deficiency a more clinically translatable option by restricting it to T cells, as they are the main players in allograft rejection and this would avoid the limitations of systemic hypoferremia in the clinic. Ferritin levels[230] and transferrin receptor expression on T cells[231] were noted to increase before and during rejection, and anti-Tfrc antiobdy prolonged graft survival in cardiac allograft model[232,233], so this approach seems to be useful in a transplantation context. The adoptive Tconv transfer model showed that iron-deficient T cells were incapable of rejecting (*Fig 6.4*), but this approach faces the same caveats of unknown demand on cell proliferation and migration as seen in our Treg adoptive transfer model, although cells still seemed to be reasonably detectable at later timepoints, which would indicate that $Tfrc^{Y20H/Y20H}$ T cells were still present but functionally impaired. Restricting therapies to a specific cell type is not necessarily simple but this could be achieved via genetic modification of a T cell product, such as CRISPR editing to decrease Tfrc expression or increase ferroportin, or perhaps by targetting graft-resident immune cells during organ perfusion[379]. A more easily administered and more scalable approach would be T cell-aimed nanoparticles which are under development but still very limited[380,381], or bi-specific antibody technology linking CD3 to a target which is under investigation in cancer and could potentially be modified to work in cis[382,383]. These approaches are still highly novel but as they develop, they might be good candidates for helping us achieve T cell-restricted iron deficiency.

A more traditional approach is drug combination, and hepcidin was used in synergy with other immunotherapies and found that they worked well in tandem to improve graft survival (*Fig 6.2b).* This might be a good approach to allow the use of therapeutic hypoferremia without causing such severe systemic deficiency, and especially might be useful for acute rejection or autoimmune flare-ups, where transient hypoferremia might be able to halt dangerous acute inflammation. In this combination therapy with αCD28 and mHep that alloresponses were halted during the duration of treatment and rejection only began after the end of the treatment plan, so it

is unclear whether extending the treatment course further could have delayed alloresponses indefinitely or whether this was the maximal extension that this treatment could achieve. Whether transient hypoeferremia would be sufficient to help curb an existing response if it had been administered mid-rejection was not investigated, but this approach could ideally replace increasing immunosuppression dosage as is normally done in patients experiencing rejection. A study using Tfrc-mAb found that administration at days 0 and 1 significantly extended graft survival but administration at days 2 and 3 did not, and further found that 2 or 4-day timecourses did not affect outcomes[232], clearly indicating that timing of intervention impacts alloresponses and might have similar effects in our hepcidin model. Taken with our results on Tregs, perhaps a transient induction of serum hypoferremia, even systemically, might be enough to prevent or even halt rejection and favour Tregs enough to allow a tolerogenic state to be established and hopefully maintained even after returning to normal iron status, which would decrease our reliance on pharmaceutical immune suppression and limit the amount of iron deprivation patients need be subjected to.

Further to finding translational links, a better understand of iron deprivation in the context of alloresponses was sought, as data to date is not very conclusive. In keeping with Joe Frost's findings in infection and vaccine responses[206], iron deprivation severely limited adaptive cell responses in a transplantation model (*Fig 6.6*). Interestingly, total CD45 ratios and myeloid cells were not found to be differentially impacted after transplantation, whereas T and B cell responses were impaired both in their general proliferation and proportional presence as well as in their activation status, as seen in a decrease in activated $IgD^{-}CD95^{+}$ germinal centre B cells and a defect in naïve-to-effector switching in T cells (*Fig 6.6*). This is in line with Joe's findings in influenza, where adaptive responses were inhibited by hepcidin but neutrophils were capable of increased activation and infiltration, causing tissue damage[206] despite his later findings that neutrohpils suffer in immune deprivation in other models[362]. Perhaps because transplant rejection is a heavily T cell and adaptive immunity-driven process, they were relatively more impaired, and it would be very interesting to see whether iron deprivation in an innate-driven model would selectively impair innate cells over T and B cells or whether adaptive immunity really does have a naturally greater sensitivity to iron deprivation regardless of whether its activation is driving a disease response.

It was hypothesised that Tregs might be more resistant to impaired effector T cell responses as we have seen that the Treg:Teff ratio is clearly tipped in favour of Tregs in Tfrc cells (*Fig 5.4*). However, the fact that rejection was completely impaired in the $Tfrc^{Y20H/Y20H}$ Tconv transfer model (*Fig 6.4*) even in the complete absence of Tregs reflects that the lack of Tconv function is more significant than the Treg:Tconv balance, as iron deprivation does not improve Treg function. Indeed, Tregs on their own are impacted by hypoferremia and their relative fitness is only apparent in direct compairson to Tconvs. In fact, at baseline reconstitution, Tfrc mutation did not impair effector T cell generation too severely but Tregs might be more affected than Tconvs (*Fig 6.5*); this could be due to higher Treg effector phenotype in a resting mouse, as they are activated by self-antigen and have to maintain tolerance whereas most Tconvs don't mature in antigen-naïve mice until they experience immune challenge, so this increase demand on Tregs might explain their disadvantage. This is pretty much the reverse of our theory for why Tregs do better in immune challenges, in that they experience less activation demand than Tconvs during an infection because they are already more activated, and are therefore less impaired by iron deficiency, so the same is holding true in naïve mice where Tregs are the ones under higher demand and so their impaired acquisition of effector phenotype in $Tfrc^{Y20H/Y20H}$ cells is apparent even without immune challenge. Overall, Tregs were still impaired in iron deficient conditions, with clear defects in activation and proliferation markers such as CD44, CXCR3, and Ki67 (*Fig. 6.1*), similarly to that observed in Tconvs.

However, hepcidin-mediated serum hypoferremia favoured Tregs in terms of CD25 expression and their relation to Tconvs (*Fig 6.1d*), so perhaps serum vs. cellular iron deprivation have different effects: indeed, as CD71 expression is naturally higher on Tregs than Tconvs (which I suspect might be one of their suppressive mechanisms) perhaps serum hypoferremia allows them to out-compete Tconvs and better survive, whereas the $Tfrc^{Y20H/Y20H}$ mutation which leads to very high CD71 upregulation across all cells[237] might not allow them to take advantage of this as efficiently. Indeed, administered hepcidin was only during transplantation, and it would be interesting to see whether low serum iron in a resting mouse would still tip the Treg:Teff ratio as this would tell us more about whether Tregs are resistant due to their lower metabolic requirements or their aptitude for iron acquisition due to high surface CD71 expression.

In conclusion, hypoferremia was found to readily impair alloresponses but this translated to clinical graft survival outcomes only when supplemented with low iron diet or another immunotherapy. Different organs' unique iron requirements and immunogenicity might affect how hypoferremia influences transplant outcomes in different models, so this work provides valuable information on skin transplantation and the uses of hypoferremia as a potential treatment to prevent its rejection.

7 – DISCUSSION

7.1 – SUMMARY OF RESULTS

This thesis aimed to explore how the HIF pathway and iron availability impact Tregs and immune responses, because Treg balance within the T cell compartment has huge implications on tolerance and the wider immune landscape; better understanding how Tregs function in hypoxic and hypoferremic inflammatory environments will help realise their potential as powerful immune mediators and candidates for cellular therapy in cancer, infections, autoimmunity, and transplants.

My first specific aim was to better understand the impact of individual components of the HIF signalling pathway on Tregs and immune responses (*Chapter 3*). In this chapter, I aimed to study how HIF-1α and HIF-2α affect the hypoxic immune phenotype, expecting HIF-2α KO to reverse it as in our PHD2 KD model[255]. Indeed, this was mostly the case, but hypoxic HIF-1α KO mice showed unexpected lymphadenopathy and inconsistencies with our previous HIF-driven inflammation (*section 3.2a*). Because others have shown that HIF isoforms can compensate for each other in individual knockouts[159,160,260], it was hypothesised that HIF-1α KO induced even higher levels of HIF-2α than hypoxia or PHD2 KD alone, aggravating the phenotype. This was therefore tested with a hypoxic HIF DKO model and revealed that instead, this induced an even more extreme inflammatory phenotype (*section 3.2b*). The incomplete knockout efficacy for HIF-2α might mean HIF-2α was still driving the DKO phenotype, but this does not explain why this small residual HIF-2α would induce a stronger phenotype than HIF-1α KO alone. This was then repeated this with hypoxic ARNT DKO which should recreate the results of HIF DKO but alas, did no such thing: instead, the phenotype was reversed in lymph nodes but not spleens, which I suspect is due to incomplete recombination that might have been more effective in the unmeasured spleens (*section 3.2c*). Altogether, while the results from this chapter were confusing, they show that this signalling pathway has profound effects on Treg function and the entire immune landscape, which could have great therapeutic implications if we could better understand and hopefully manipulate the downstream mechanisms responsible.

Next, I aimed to understand how HIF signalling impacts the Treg transcriptional programme (*Chapter 4*). Single cell sequencing identified a transcriptionally distinct population of PHD2 KD Tregs that was enriched for p38 MAPK-NFkB signalling, which has been shown to deregulate Tregs[310,311], and decreased IL-2-STAT5 signalling (*section 4.2a*). These Tregs exhibited a loss of *Il2ra* expression but no other classical inflammatory markers, and had all the transcriptional markers of highly activated, functional, and suppressive Tregs (*section 4.2b*), which is unexpected for Tregs known to be functionally deregulated and pathogenic[255]. Based on indications that CD25 loss on Tregs was consistently present across multiple experiments, I investigated the transcriptional programme of HIF-induced CD25$^-$ Tregs in more depth through bulk sequencing (*section 4.2c*). Hypoxia did not greatly impact gene expression of CD25$^-$ Tregs, rather enriching them numerically than altering them qualitatively. CD25$^-$ Tregs expressed high levels of *Cd22* which is associated with Notch1 signalling, both of which are implicated in loss of Treg function[323,324]. Some of the genes associated with CD25 loss were also associated with a Tfr phenotype, which was also seen in PHD2 KD. Work in this chapter allowed the identification of potential downstream inflammatory pathways induced by HIF-2α in Tregs, which might be transcriptional programmes that could be manipulated to alter Treg function for therapeutic applications.

In order to investigate how iron deprivation affects Treg biology, I carried out a series of experiments that investigated Treg responses to limited iron and compared these to Tconv responses, hypothesising that iron deprivation would negatively affect all T cells but that Tregs may respond differently due to their unique metabolic needs (*Chapter 5*). Tregs seem more resistant to *in vitro* iron deprivation than conventional T cells, maintaining expression of activation markers across iron concentrations (*section 5.2a*). Tfrc$^{Y20H/Y20H}$ Tregs maintained suppressive function *in vitro* (*section 5.2b*) but not in an *in vivo* adoptive transfer model to control allograft rejection (*section 5.2c*). Due to the strenuous demand of proliferation in this model, which we know to be impaired in Tfrc$^{Y20H/Y20H}$ cells[237], Tfrc$^{Y20H/Y20H}$ Tregs were compared to control Tregs side-by-side in a mixed bone marrow chimera model, and found that Tfrc$^{Y20H/Y20H}$ cells had a higher Treg:Teff ratio, indicating preferential success of Tregs in iron deprivation (*section 5.2d*). Tfrc$^{Y20H/Y20H}$ Tregs in this model also showed higher expression of CD25 and decreased CTLA-4, suggesting a change in surface marker expression as a potential

adaptation (*section 5.2e*). I also investigated Tfrc Tregs in a malaria infection model, and found that Treg:Teff ratio and activation marker expression were raised and preferentially increased on Tregs (*section 5.2f*), confirming results from other models. Overall, Tregs exhibit resistance to iron limitations that is not seen in Tconvs, which might contribute to their suppressive function and could reflect the need for preferential Treg survival in inflammation-induced iron depletion as a potential tolerance mechanism, which could be used therapeutically to create a suppressive and tolerogenic immune landscape.

Finally, in my last chapter, I and the wonderful Amy and Joe investigated how iron limitation affects immune responses in transplant models to see whether iron deprivation would impair alloresponses and induce a tolerogenic state, thus extending graft survival (*Chapter 6*). We showed that iron deprivation can restrain alloresponses and rejection, and that hepcidin alone impaired peripheral immune responses but not graft survival (*section 6.2a*). Tregs were less impaired by hepcidin treatment than Tconvs, and combining hepcidin with IL-2c, αIL-6, or αCD28 to promote Tregs and tolerance proved to be a useful synergistic therapy (*section 6.2b*). Cell-intrinsic iron limitation in $Tfrc^{Y20H/Y20H}$ mice did not extend graft survival at the whole-body level (*section 6.2c*) but did significantly prolong survival when restricted to T cells in an adoptive transfer model (*section 6.2d*). In order to study $Tfrc^{Y20H/Y20H}$ cells in direct comparison to controls without so much proliferative pressure, a mixed bone marrow chimera model was used, which showed that $Tfrc^{Y20H/Y20H}$ cells were slightly impaired in their reconstitution (*section 6.2e*), and that adaptive $Tfrc^{Y20H/Y20H}$ cells were outcompeted in mounting alloresponses compared to controls (*section 6.2f*), confirming previous work[206]. This chapter showed that iron limitation has therapeutic potential in transplantation and might provide a useful alternative to current pharmaceutical immunosuppression if it can be wielded appropriately.

The work presented here seeks to better understand the implications of hypoxic and iron signalling on Tregs. This research enriches and adds to the knowledge on this area of scientific enquiry, and identifying or better understanding the mechanisms that regulate Treg function have potential for therapeutic applications in all diseases arising from immune imbalance.

7.2 – Scientific and Therapeutic Potential

The work presented here aims predominantly to further scientific knowledge of the behaviour of Tregs in hypoxic or iron-deprived environments which they might face during their travels through various physiological niches and during inflammatory responses. Understanding this better allows us to further science's understanding of the basic functioning of immune cells, and taking these subtleties into account during further research can improve the accuracy and use of models *in vitro* and *in vivo*.

The inconsistencies in the literature regarding the effects of HIF signalling in Tregs make it difficult to place this research within that scientific context. Much of the current work uses naïve T cells to study Treg differentiation and induction *in vitro*[99,250,254,256–258,261], which might not translate to our study of mature, differentiated Tregs. Additionally, *in vivo* studies often include challenge models such as colitis or airway hypersensitivity[99,254,257,258], whereas our phenotype arises without additional immunological challenge. We did use splenocytes from hypoxic and Foxp3^{Cre} PHD2 KD mice in a BCG immunisation model and showed that the increased immune activation in these models impaired mycobacterial growth in an *in vitro* assay (manuscript en route). However, this did not include analysis of individual HIF isoforms to know whether HIF-2α was driving these changes. The only other study to specifically investigate HIF-2α in Tregs was by Hsu et al., who found directly opposing results to us by showing a HIF-1α-induced phenotype that arose in HIF-2α KO in Tregs and was reversed in HIF DKO[260]. Very few studies have studied the contributions of both HIF-1 and -2α, and the work in this thesis shows that there is dramatic interplay between the two that warrants further study to better understand how they interact and affect immune cells.

No studies of HIF's effects on Tregs have investigated the signalling pathways downstream of HIF that affect transcriptional changes behind Treg phenotype and function, outside of Foxp3 expression. Our findings of CD25 loss on Tregs are supported by work on Tregs from SLE patients[322] and has been seen in hypoxic Tfrs[173,357,358], which might have implications on Treg function in autoimmunity and perhaps in hypoxic tumours. NFkB has a dual relationship with HIF[167-170], and has been shown to deregulate Tregs[310,311,384], so further work manipulating NFkB expression in Tregs could have implications in infection and cancer.

Very little work has been done to understand iron handling in Tregs, outside of reports that iron chelation during iTreg generation *in vitro* induced fewer Tregs with decreased CD25 expression and STAT5 phosphorylation, but not when chelators were added 24h after activation, indicating that low iron only impaired early activation and differentiation of Tregs[264]. Iron deprivation in mature Tregs did not change CD25 expression *in vitro* and increased it *in vivo*. Both low iron diet and iron overload in thalassemia patients increases the proportion of Tregs[220,268], so further investigation using a wider range of iron levels would provide better insights on immune balance in physiological and pathological conditions. An increased Treg:Teff ratio was observed in several models including Tfrc mutation, and other have shown that Tfrc deletion and blockade both improved induction of Tregs[218,221], so Tfrc might be an interesting Treg-modulatory target and restricting this to T cells might make good immunosuppression.

Iron deficiency in transplant recipients is prevalent but confounded by its association with anaemia pre-transplantation, various medications, surgical blood loss, and change in erythropoesis and EPO production[228]. Its effects on graft survival are mixed, with reports of both iron decrease and iron loading protecting against IRI and oxidative stress[228], and both also accelerating acute rejection in a cardiac allograft model[229]. Ferritin levels[230] and Tfrc expression on T cells[231] increase before and during rejection, and anti-Tfrc antiobdy prolonged graft survival in cardiac allografts[232,233], which is similar to our findings using hepcidin. Bohne et al. found that increased hepcidin and decreased Tfrc transcription were the most differentially expressed genes in tolerant liver recipients[234]. However, hepcidin and ferritin had no correlation with inflammatory markers in kidney recipients[235,236], so different organs' differential iron use and their role in iron homeostasis might determine outcomes, and should be further studied. Our results show a discrepancy between peripheral blood alloresponses and rejection outcomes in skin grafts, so studies using expression of iron-related genes in blood might not reflect its effects in the graft; studies investigating different organs and different iron measures or manipulations are needed, triangulated with a better understanding of how iron affects alloresponses in blood, lymphoid organs, and the graft.

As Tregs are central to maintaining tolerance, they have implications on wider immune outcomes. Specifically, pathways such as p38 MAPK-NFkB, Notch1, or iron and Tfrc could have therapeutic uses in a wide range of immunological diseases and merit further research.

7.3 – LIMITATIONS

As is always the way in both science and life in general, a lack of money and time impedes progress that could otherwise be made with unlimited resources. While the work presented in this thesis aimed to answer questions to the best of my abilities, there are several caveats to the experiments performed and the conclusions able to be reached as the data stands. The limited availability of mice with HIF KOs meant that certain controls were missing, such as normoxic HIF-1α KO mice, and it was difficult to repeat experiments and use consistent genetic models in our hypoxic studies; therefore, I was lucky that Tammie Bishop coincidentally happened to be running experiments with ARNT DKO mice that I was able to use. This limits our analysis of individual phenotypes but might have serendipitously uncovered some subtleties of signalling that would not have been observed otherwise. The inconsistencies in PCR results of HIF target genes (*Fig 3.12*) also make it difficult to interpret what level of HIF signalling is actually present in our different genetic models, and the lack of PCR in the spleens makes it difficult to know how much of the variation between lymph nodes and spleens is due to different knockout efficacies between tissues. There was only enough tissue for PCR confirmation of KO efficacy, and not for confirmation of flow cytometric results such as *Tbet* expression. Additionally, the highly artificial HIF and ARNT DKO models in hypoxia are hardly translatable to humans, although the exploration of their signalling is of scientific interest and manipulation of more targeted downstream pathways could be translationally relevant.

The analysis of transcriptional changes in PHD2 KD and $CD25^-$ Tregs revealed some interesting candidate pathways, but as is always the case in sequencing results, the data is only observational and correlative, and does not inform any actual proof of functional impact. Specifically, the p38 MAPK pathway uncovered (*Fig 4.8*) is a kinase pathway, so mRNA or protein expression levels tell us nothing whatsoever about whether the enzyme is active or not, which has little functional impact without this information. Additionally, genes with the highest fold change and significance tend to be analysed more carefully, but a small change in expression of certain genes can still have a very large impact, so this bias toward dramatic changes might be leading us to ignore more subtle differences in lowly differentially expressed genes that are obscured. As well, the thousands of genes outputted by this type of analysis can be overwhelming and make it difficult to know where to start or what to interpret as biologically

relevant. While refining this with pathway analysis makes it easier to identify patterns, having several dozens of differentially enriched pathways is only somewhat more targeted, or alternatively, using an adjusted p value cut-off to identify a small handful of significant pathways might be artificially restricting biologically interesting findings for the sake of highly manipulated statistical conventions. Additionally, the ability of a tiny subpopulation of Tregs to deregulate the entire immune balance still seems odd to me considering the health of heterozygous IPEX females[53]. Furthermore, all of this work has focused on mice due to the difficulties of recreating genetic and long-term hypoxic manipulation in humans.

Similarly to the hypoxia work, all of the work on iron limitation in Tregs was done in mice. Some of the *in vitro* cultures could have easily been done with human cells, but the artificial iron-free serum was not suitable for certain cell types even when supplemented with iron: Hisashi Hashimoto could not culture established human Tregs in it, nor could Megan Teh differentiate iTregs from naïve $CD4^+$ T cells, and she also found that B cells and some other cell types were not suited to these culture conditions. Iron measurements at the cellular level were nor possible for these studies either, and systemic iron measurements from previous hepcidin studies were not repeated in the transplant experiments due to time restraints during harvest. The $Tfrc^{Y20H/Y20H}$ mutation was also only available to us in mice, and although human patients do exist with this mutation, getting access to those samples was not realistic, nor was using CRISPR to edit the mutation into human cells financially feasible.

The adoptive transfer models using $Tfrc^{Y20H/Y20H}$ cells (*sections 5.2c and 6.2d*) were limited by the strong demand on proliferation that we know $Tfrc^{Y20H/Y20H}$ cells are disadvantaged in[237], and it is difficult to know how iron deficiency impacts long-term survival or migration of these cells and whether those might be confounding variables. I attempted to carry out *in vitro* migration assays on Tregs and Tconvs either from $Tfrc^{Y20H/Y20H}$ mice or using low iron cultures, but these were technically challenging and only yielded very few cells that migrated across transwells, making the counts and analysis difficult to trust. Because of issues in reconstituting $RAG^{-/-}$ mice in adoptive transfer models, chimeras were used to better study cell phenotype of $Tfrc^{Y20H/Y20H}$ cells alongside controls, but these did not give us any functional data regarding Treg suppression, so the suppressive ability of iron-deprived Tregs *in vivo* is still not entirely convincing from this research.

7.4 – Future Directions

While I hope that the work in this thesis is sufficient for the scope of this project, there are several experiments I would undertake to further this research, were I endowed with more time and money to do so.

7.4a – Hypoxia and HIFs

The clear next step in furthering the work on hypoxia is to complement protein and RNA data with their missing counterparts. Having PCR data on spleens from the HIF and ARNT DKO experiments would allow a better understanding of what is governing the differences between tissues, and measuring expression levels and transcriptional activity of AHR and HIF-3α would shed some light on whether their activity is changed across HIF-1/2α single and double KOs and ARNT DKO to determine whether they might be candidates as drivers of immune phenotypes. Similarly, the transcriptional data revealed some potential pathways of interest but without confirmation of expression at the protein level and especially of kinase activity in the case of p38 MAPK, it is not known whether these are functional or causative. Confirmation of expression of the genes highlighted by scRNAseq in Tregs from PHD2 KD, single and double KO, and hypoxic mice is paramount, and both flow cytometry and qPCR would be beneficial for this.

In vitro studies with inhibitors of p38 MAPK and Notch1 or a αCD22 blocking antibody on PHD2 KD cells could be used in Treg suppression assays to see whether inhibition of these reinstates suppressive function, and this could further be tested with combined PHD2/HIF1/2 KOs, or with hypoxic cell cultures, as well as investigating the role of OX40 in inducing this pathway. Additionally, *in vivo* inhibition of similar KD/KO or hypoxic mice might be more physiologically relevant, and a $Foxp3^{Cre}$ genetic inhibition system or bone marrow transplant of these pathways would also have further implications for the subtleties of global, immune-restricted, and Treg-specific contributions, especially if these manipulations have effects on the function of other systems that could cloud our immune phenotype.

CD25 loss is more difficult to study functionally, which is why I had opted for transcriptional analysis of $CD25^-$ Tregs, as even if I were able to separate out enough $CD25^+$ and $CD25^-$ tregs to use for *in vitro* suppression assays or *in vivo* adoptive transfers with skin transplants (a highly unlikely feat due to their rarity and the significant effort and sleep deprivation incurred over 4 days to isolate enough for the transcriptional experiment as it was), there is no assurance that they would maintain this phenotype once transferred: the stimulation *in vitro* might be enough to induce CD25 anew on $CD25^-$ Tregs, or PHD2 KD Tregs might lose CD25 expression spontaneously, making this difficult to study using our cells. A CD25 blocking antibody could be used to show that $CD25^-$ Tregs are less suppressive, but this might be artefact due to CD25 being part of Treg suppressive function, rather than actually informing us on the functionality of Tregs who have spontaneously lost CD25 expression as part of a concerted phenotypic change. A better experiment to design would be one that investigates whether the phenotype and CD25 loss occur during Treg development, or are acquired in the periphery. As mice are adults at the age of tamoxifen or doxycycline administration and are treated for up to 12 weeks, their age means that the thymus is mostly involuted and no longer actively producing many fresh thymocytes. Although congenital PHD2 KD is embryonically lethal, using drug induction at a younger age might allow us to better study T cells in the thymus and periphery as part of a timecourse experiment, which could tell us whether $CD25^-$ Tregs are found in the thymus or whether they only appear over time, and whether activation or maturity play any role in their development.

7.4b – Iron

Based on Tregs' high expression of Tfrc/CD71, I wonder whether its expression might not contribute to their suppressive function and act as an iron sink, similarly to CD25 depriving surrounding cells of IL-2. However, disentangling Tregs' iron hoarding properties from their iron import is technically very challenging, as blocking Tfrc would impair their viability and likely also their suppressive function. One experiment to isolate Tregs' iron-hoarding is to use $Tfrc^{Y20H/Y20H}$ Tregs, with limited iron import but intact iron binding, and compare them to the same $Tfrc^{Y20H/Y20H}$ Tregs pre-treated with αTfrc blocking antibody, which will impair Treg iron hoarding. This requires the blocking antibody not to further impair iron import, so the blocking

affinity must be tailored to match the Tfrc mutation's limitations, which is difficult to achieve, and also requires hope that the antibody is suitable as pre-treatment and will not dissociate and affect target cells. This might also have an impact on Treg viability and fitness, so it is a difficult experiment to plan. This question could also be answered more complexly with the engineering of Tregs that express an additional Tfrc receptor that is capable of binding but not import alongside their native Tfrc receptor, and seeing whether this improves their suppressive function.

Crossing the $Tfrc^{Y20H/Y20H}$ mice with a Foxp3-restricted line would allow for Treg function to be studied more directly, and this would be a better model for Treg suppression of graft rejection *in vivo* than our adoptive transfer model. We have engrafted mice with a global Tfrc mutation (*section 6.2c*) but I have always wanted to try grafting $Tfrc^{Y20H/Y20H}$ or control B6 skin grafts onto CBA recipients, to see whether local iron in the graft had an impact on wound healing and vascularisation and whether it would be capable of tolerising the local immune infiltrate. As a more therapeutically translational model, it was hypothesised that transient hypoferremia might be capable of impairing rejection even after return to normal iron levels or indeed, halting an existing alloresponse, as a study using αTfrc antibody showed that timing of administration had dramatic effects on outcome[232], so further work on kinetics and longevity of iron deprivation-induced tolerance is important. Similarly, the timing and context of an immune response has implications on balance and polarisation of the T cell compartment, and the increased nutrient requirement during activation might change cells' sensitivity to iron, so it would be interesting to see whether hepcidin treatment in a naïve mouse had the same effects on Treg:Tconv ratio, and whether this pre-treatment would have implications on responses to a subsequent challenge, as a way to prime the immune system. Testing an iron overload model in transplantation would also be interesting, as it might either accelerate rejection or perhaps be protective. This could also be done *in vitro* by adding excess levels of holotransferrin to cultures in the same way to study Treg and Tconv responses, and might provide insights into iron-loaded cells in autoimmunity. It would also be interesting to explore whether cells downregulate CD71 expression as a protective measure in iron loading and whether Tregs' high expression of it would be detrimental.

For *in vitro* studies, due to some suspicion that perhaps the reason why Tregs from naïve mice are less impacted by iron deprivation than Tconvs is because a larger proportion of them are already activated and do not need to gain effector function, pre-activation of Tregs and Tconvs before culture with iron-depleted media would help avoid the unfair advantage of Tregs in naïve mice. I have attempted a few migration assays *in vitro* with little success due to very low cell counts migrating across the transwell, but optimisation with number of cells seeded, chemokine concentration, and time allowed for migration might be able to improve this and would yield interesting results that would inform some of our questions about migratory capabilities *in vivo*. To study Treg phenotype stability, I would be interested to study whether iron deprivation changes co-expression of Th transcription factors Tbet, GATA3, and RORγT on established Tregs. The brilliant Megan Teh has already done some work on polarising naïve cells into Th lineages in low iron, but this is different to the gain of expression on mature Tregs, which could be studied with and without polarising cytokines to see whether iron deficiency affects Tregs' willingness to be swayed into a different phenotype. There are several reports that iron deficiency can induce IFNγ production in mice[184-203] and a preference for type I over type II responses[199], so it would be interesting to see whether iron-altered Tregs have any biases in their plasticity. Supernatants from cultured Tregs and Tconvs were frozen for ELISA of both pro- and anti-inflammatory cytokines that would complement analysis of Th transcription factors and Treg stability and function.

7.4c – Bridging the Gap Between Iron and Hypoxia in Immunity and Tregs

Due to the interactions between HIF and iron signalling (*see section 1.4e*), studying their combined effects on Tregs and immunity would be of great interest. It is unlikely that depriving cells of both iron and oxygen would make them particularly lively, but it would be very interesting to investigate to what extent the effects of iron deprivation are mediated via inhibition of PHD enzymes and induction of HIF signalling. I actually had tried to investigate this using *in vitro* T cell activation in low iron conditions with HIF-1α and HIF-2α KO mice, but the cells all died due to technical error and more mice were not available to repeat the experiment. This would be interesting to try again, and especially to compare Tregs to Tconvs as in section 5.2a, as both iron and HIF signalling seemed to have differential impacts on Tregs. Hypoxic cell cultures

could also be used, and if combining this with iron deprivation might be too detrimental, studying iron overload in this model might be useful to study iron-loaded cells in autoimmunity and inflammatory hypoxia. Suppression assays with $Tfrc^{Y20H/Y20H}$ Tregs could also be repeated in hypoxic cultures, to see whether $Tfrc^{Y20H/Y20H}$ cells might be more or less sensitive to its effects, especially in a titration of oxygen concentrations.

In vivo, use of the hypoxic chamber could allow us to study $Tfrc^{Y20H/Y20H}$ mice or mice receiving mHep doses, although IP injection through the gloves of the chamber might not be technically feasible as they greatly reduce dexterity. Based on our results, I would hypothesise that iron-deprived mice would not be able to mount the strong autoimmune and proliferative phenotype induced by hypoxia, and that iron restriction would ameliorate this, although there may be welfare concerns regarding health and weight loss, especially with mHep treatment as this is more severe. PHD2 KD or HIF KO mice could also be placed on low iron diets, or injected with mHep, to again investigate whether iron limitation can reverse immune activation. Restricting this to Tregs would be especially interesting, by either administering low iron diet or mHep injections to $Foxp3^{Cre}$ PHD2 KD mice or breeding $Foxp3^{Cre}$ $Tfrc^{Y20H/Y20H}$ mice that could be placed in the hypoxia chamber. As well as investigating the fundamental development of spontaneous autoimmune-like phenotypes, functionally testing these models with skin transplant rejection or infectious models would provide great insights on the direct impact of combined iron and oxygen consumption during inflammation on immune responses and outcomes.

7.5 – Concluding Remarks

The work presented in this thesis aimed to explore how the HIF pathway and iron availability impact immune responses with a focus on Tregs. Tregs are crucial to maintaining tolerance and immune balance, and impact the entire immunological landscape; better understanding how Tregs function in hypoxic and hypoferremic environments they are likely to face in physiology and inflammation will help us better understand immune responses driving infections, allergy and immunopathology, cancer, autoimmunity, and transplant rejection. Better understanding the pathways and mechanisms that govern Treg function could allow us to manipulate these pathways to modulate their function, which will help realise their potential as powerful immune mediators and candidates for cellular therapy.

7.6 – ACKNOWLEDGEMENTS

I am blessed to have a fantastic academic team who has supported me throughout this work, without whom none of this would have been possible, and I hope you will forgive some amounts of sap as I attempt to thank them all, which is hardly possible with words alone. First and foremost are of course Fadi and Joanna, the best supervisors I could have ever asked for: thank you for your endless support and encouragement, your patience and constant presence, and lightning quick responses on some last minute abstract submissions or late night panics at the lab; I know your time is precious and limited so I am so thankful for all of it which you shared with me, and for being genuinely lovely people. Joanna patiently taught me many of the techniques I used above, including the many mysteries of the Aria, and Fadi personally dedicated quite a few hours of mindless suturing with me and Amy, even coming in to do IV injections at 8pm when cell preparations went awry. As honorary supervisors, the collaborations in this thesis meant I was endlessly lucky to be adopted by Chris Pugh, one of the most remarkable scientists I have ever met and whom I was truly honoured to learn from. My step-supervisor Hal is pretty alright too, and his fantastic puns and good humour only complement his intellectual wisdom and wide perspective.

Next, several magnificent people contributed to my scientific upbringing as sort of guiding elder siblings: first, my eternal love and gratitude to Amy, with whom I spent the most time throughout this work (often entangled grappling an uncooperative mouse), and of all the people to have as my only human contact during Covid, I'm glad it was you. She taught me all I know about animal work and some invaluable lessons on Amy-proofing, and over many cups of tea and hours together in and out of the lab, she has become like a big sister to me. Our partner in crime for much of this work was the rockstar that is Joe Frost, one of the most fearless and accomplished scientists I know and probably one of the smartest people I have ever met. Thank you for imparting some of your rigour and unstoppable energy, and I will always hear your voice whispering "more n" in my conscience as I design experiments. Lastly, the great Kento was another huge teaching force in my early journey: he so very patiently passed on his best knowledge, tips and tricks, and a drawer of scribbled notes he was very proud to pass on as inheritance – I am honoured to have received the HIF baton from your capable hands and hope to have been worthy of it.

I also want to thank the entirety of the TRIG group for being a beautifully cooperative and fun family, and for all their help and ideas. Special thanks to Ollie who saved me hours of toil with his wizard skills aligning the RNA sequencing data for me and all his consultations regarding anything that runs on electricity, as well as his help during surgeries and harvests, and for being a fantastic friend and even temporary husband in Buenos Aires. I also want to thank Guido for all the hours he spent helping me during long hypoxia experiments and harvests, and for always being quick with a helping hand and a joke in the mousehouse. Thank you to the lovely Helen for being a dear friend who patiently taught me how to tie some knots, and for helping on multiple occasions to make mindless mashing and harvests more enjoyable, as did the incomparably sweet Nora, full-of-life Megan, wonderful Merve, and effortlessly cool Sarah. Thank you additionally to Hisashi for his “dumb questions”, sharp insights, 3am conversations about the true meaning of Tregs, and reckless commitment to alcohol, and to Joe Beckett (and the B cells) who would despise being acknowledged and must therefore have his praises shouted from rooftops. Thank you as well to Sush and the Matts for being floating sources of inspiration, wisdom, and advice. Thank you to Monica for actually running this lab, and to Jess for always receiving bad news of various malfunctions with a smile and a solution.

A huge thank you to the adopted Drakesmith and Ratcliffe labs who shared so much of their expertise with me: to Sarah for sharing her spleens and kindness, to the truly delightful and wicked smart Megan for her culturing protocols and emergency bailing of supplies, to Ali for sharing advice and several great times together, and to Shams for the exciting Treg chats. In the Ratcliffe lab, I am very grateful for the short amount of time I spent learning from the brilliant Atsu, who developed the PHD2 KD model and worked on all my early experiments. Thank you to the wonderful Ran for all her help coding, and to Dominik for so selflessly dropping everything and arranging emergency calls to help me analyse data out of the kindness of his heart. I desperately want to thank my fairy godmother Julie Adams, who ordered many supplies, lovingly prepared tamoxifen for my experiments, and generally helped me find my way around the Wellcome, and to Tammie and Maria for all their wonderful work breeding and managing the mice we used, for their help with the hypoxia chamber, and for sharing their experiments with us. I also want to thank Heather and Viv and the entirety of the staff at the FGF who helped with oral gavages, especially to Douglas who had to drive from Bicester at 9pm to rescue me after I’d

locked myself in. I cannot thank enough the staff at the JR BMS, especially Roo and Jonathon who are the very heart and soul (and also blood, sweat, and tears) of the place. I would also like to acknowledge the mice who gave their lives to make this research possible.

Ultimately, I must thank my wonderful family and parents for my existence and for all their support, and my amazing friends, not limited to Quinn, Helena, Kara, JoJo, Nat, Javier, Sian, Anna, Chris, and especially Alkisti, for always being by my side through thick and thin. Finally, thank you to the cast of Bones, Buffy, and the BonesBooth podcast for accompanying me through endless late nights and far too many sunrises; and lastly, thank you, dear reader, for reading these many words: I hope you found them informative, somewhat entertaining, aesthetically pleasing, and hopefully reflective of the nearly 4 years of hard work and late nights that I (with the help of the wonderful scientific team I am blessed with) have poured into this thesis.

BIBLIOGRAPHY

1. Parkin J, Cohen B. An overview of the immune system. *Lancet*. 2001;357(9270):1777-1789. doi:10.1016/S0140-6736(00)04904-7
2. Smyth MJ, Swann J, Kelly JM, et al. NKG2D recognition and perforin effector function mediate effective cytokine immunotherapy of cancer. *J Exp Med*. 2004;200(10):1325-1335. doi:10.1084/jem.20041522
3. Thielens A, Vivier E, Romagné F. NK cell MHC class I specific receptors (KIR): from biology to clinical intervention. *Curr Opin Immunol*. 2012;24(2):239-245. doi:10.1016/j.coi.2012.01.001
4. Burnet M. Cancer—A Biological Approach. *Br Med J*. 1957;1(5023):841-847. doi:10.1136/BMJ.1.5023.841
5. Hanahan D, Weinberg RA. Hallmarks of cancer: The next generation. *Cell*. 2011;144(5):646-674. doi:10.1016/J.CELL.2011.02.013/ATTACHMENT/3F528E16-8B3C-4D8D-8DE5-43E0C98D8475/MMC1.PDF
6. Munn DH, Bronte V. Immune suppressive mechanisms in the tumor microenvironment. *Curr Opin Immunol*. 2016;39:1. doi:10.1016/J.COI.2015.10.009
7. Ledford H, Else H, Warren M. Cancer immunologists scoop medicine Nobel prize. *Nature*. 2018;562(7725):20-21. doi:10.1038/D41586-018-06751-0
8. Rouse BT, Sehrawat S. Immunity and immunopathology to viruses: what decides the outcome? *Nat Rev Immunol*. 2010;10(7):514. doi:10.1038/NRI2802
9. Channappanavar R, Perlman S. Pathogenic human coronavirus infections: causes and consequences of cytokine storm and immunopathology. *Semin Immunopathol 2017 395*. 2017;39(5):529-539. doi:10.1007/S00281-017-0629-X
10. Chen N, Zhou M, Dong X, et al. Epidemiological and clinical characteristics of 99 cases of 2019 novel coronavirus pneumonia in Wuhan, China: a descriptive study. *Lancet*. 2020;395(10223):507-513. doi:10.1016/S0140-6736(20)30211-7
11. Blanco-Melo D, Nilsson-Payant BE, Liu WC, et al. Imbalanced Host Response to SARS-CoV-2 Drives Development of COVID-19. *Cell*. 2020;181(5):1036-1045.e9. doi:10.1016/J.CELL.2020.04.026
12. Dolina JS, Lee J, Moore EL, et al. Developmentally distinct CD4+ Treg lineages shape the CD8+ T cell response to acute Listeria infection. *Proc Natl Acad Sci U S A*. 2022;119(10). doi:10.1073/PNAS.2113329119
13. Laidlaw BJ, Cui W, Amezquita RA, et al. Production of IL-10 by CD4(+) regulatory T cells during the resolution of infection promotes the maturation of memory CD8(+) T cells. *Nat Immunol*. 2015;16(8):871-879. doi:10.1038/NI.3224
14. Sugimoto MA, Sousa LP, Pinho V, Perretti M, Teixeira MM. Resolution of Inflammation: What Controls Its Onset? *Front Immunol*. 2016;7(APR):160. doi:10.3389/FIMMU.2016.00160
15. Lawrence T, Gilroy DW. Chronic inflammation: a failure of resolution? *Int J Exp Pathol*. 2007;88(2):85-94. doi:10.1111/J.1365-2613.2006.00507.X
16. Vong L, Ferraz JGP, Dufton N, et al. Up-Regulation of Annexin-A1 and Lipoxin A4 in Individuals with Ulcerative Colitis May Promote Mucosal Homeostasis. *PLoS One*. 2012;7(6). doi:10.1371/JOURNAL.PONE.0039244
17. Mangino MJ, Brounts L, Harms B, Heise C. Lipoxin biosynthesis in inflammatory bowel

disease. *Prostaglandins Other Lipid Mediat*. 2006;79(1-2):84-92. doi:10.1016/J.PROSTAGLANDINS.2005.10.004
18. Sena A, Grishina I, Thai A, et al. Dysregulation of Anti-Inflammatory Annexin A1 Expression in Progressive Crohns Disease. *PLoS One*. 2013;8(10). doi:10.1371/JOURNAL.PONE.0076969
19. Suzuki K. Chronic Inflammation as an Immunological Abnormality and Effectiveness of Exercise. *Biomolecules*. 2019;9(6). doi:10.3390/BIOM9060223
20. Bezsonov EE, Sobenin IA, Orekhov AN. Immunopathology of Atherosclerosis and Related Diseases: Focus on Molecular Biology. *Int J Mol Sci*. 2021;22(8). doi:10.3390/IJMS22084080
21. Hughes PA, Zola H, Penttila IA, Blackshaw LA, Andrews JM, Krumbiegel D. Immune activation in irritable bowel syndrome: Can neuroimmune interactions explain symptoms. *Am J Gastroenterol*. 2013;108(7):1066-1074. doi:10.1038/AJG.2013.120
22. Ohman L, Isaksson S, Lindmark AC, et al. T-cell activation in patients with irritable bowel syndrome. *Am J Gastroenterol*. 2009;104(5):1205-1212. doi:10.1038/AJG.2009.116
23. Heppner FL, Ransohoff RM, Becher B. Immune attack: the role of inflammation in Alzheimer disease. *Nat Rev Neurosci*. 2015;16(6):358-372. doi:10.1038/NRN3880
24. Helgadottir A, Manolescu A, Thorleifsson G, et al. The gene encoding 5-lipoxygenase activating protein confers risk of myocardial infarction and stroke. *Nat Genet*. 2004;36(3):233-239. doi:10.1038/NG1311
25. Pritchard DI, Falcone FH, Mitchell PD. The evolution of IgE-mediated type I hypersensitivity and its immunological value. *Allergy*. 2021;76(4):1024-1040. doi:10.1111/ALL.14570
26. Strachan DP. Hay fever, hygiene, and household size. *BMJ Br Med J*. 1989;299(6710):1259. doi:10.1136/BMJ.299.6710.1259
27. Murdaca G, Greco M, Borro M, Gangemi S. Hygiene hypothesis and autoimmune diseases: A narrative review of clinical evidences and mechanisms. *Autoimmun Rev*. 2021;20(7):102845. doi:10.1016/J.AUTREV.2021.102845
28. Gale EAM. The Discovery of Type 1 Diabetes. *Diabetes*. 2001;50(2):217-226. doi:10.2337/DIABETES.50.2.217
29. Entezami P, Fox DA, Clapham PJ, Chung KC. Historical Perspective on the Etiology of Rheumatoid Arthritis. *Hand Clin*. 2011;27(1):1. doi:10.1016/J.HCL.2010.09.006
30. Bettelli E, Korn T, Kuchroo VK. Th17: The third member of the effector T cell Trilogy. *Curr Opin Immunol*. 2007;19(6):652. doi:10.1016/J.COI.2007.07.020
31. Zambrano-Zaragoza JF, Romo-Martínez EJ, Durán-Avelar MDJ, García-Magallanes N, Vibanco-Pérez N. Th17 Cells in Autoimmune and Infectious Diseases. *Int J Inflam*. 2014;2014. doi:10.1155/2014/651503
32. Marwaha AK, Leung NJ, McMurchy AN, Levings MK. TH17 cells in autoimmunity and immunodeficiency : Protective orpathogenic? *Front Immunol*. 2012;3(JUN):129. doi:10.3389/FIMMU.2012.00129/BIBTEX
33. Komiyama Y, Nakae S, Matsuki T, et al. IL-17 plays an important role in the development of experimental autoimmune encephalomyelitis. *J Immunol*. 2006;177(1):566-573. doi:10.4049/JIMMUNOL.177.1.566
34. Bush KA, Farmer KM, Walker JS, Kirkham BW. Reduction of joint inflammation and bone erosion in rat adjuvant arthritis by treatment with interleukin-17 receptor IgG1 Fc

fusion protein. *Arthritis Rheum*. 2002;46(3):802-805. doi:10.1002/ART.10173
35. Nakae S, Nambu A, Sudo K, Iwakura Y. Suppression of immune induction of collagen-induced arthritis in IL-17-deficient mice. *J Immunol*. 2003;171(11):6173-6177. doi:10.4049/JIMMUNOL.171.11.6173
36. Kronzer VL, Bridges SL, Davis JM. Why women have more autoimmune diseases than men: An evolutionary perspective. *Evol Appl*. 2021;14(3):629. doi:10.1111/EVA.13167
37. Nemazee D. Mechanisms of central tolerance for B cells. *Nat Rev Immunol 2017 175*. 2017;17(5):281-294. doi:10.1038/nri.2017.19
38. Takaba H, Takayanagi H. The Mechanisms of T Cell Selection in the Thymus. *Trends Immunol*. 2017;38(11):805-816. doi:10.1016/J.IT.2017.07.010
39. Tiegs SL, David $, Russell M, Nemazee D. Receptor Editing in Se•reactive Bone Marrow B Cells. 1993;177.
40. Fu S, Zhang N, Yopp AC, et al. TGF-β induces Foxp3 + T-regulatory cells from CD4 + CD25 - precursors. *Am J Transplant*. 2004;4(10):1614-1627. doi:10.1111/j.1600-6143.2004.00566.x
41. Xing Y, Hogquist KA. T-Cell Tolerance: Central and Peripheral. *Cold Spring Harb Perspect Biol*. 2012;4(6):1-15. doi:10.1101/CSHPERSPECT.A006957
42. Shevach EM, Thornton AM. tTregs, pTregs, and iTregs: similarities and differences. *Immunol Rev*. 2014;259(1):88-102. doi:10.1111/IMR.12160
43. Getahun A. Role of inhibitory signaling in peripheral B cell tolerance*. *Immunol Rev*. 2022;307(1):27-42. doi:10.1111/IMR.13070
44. Di Noia JM, Neuberger MS. Molecular Mechanisms of Antibody Somatic Hypermutation. 2007. doi:10.1146/annurev.biochem.76.061705.090740
45. Detanico T, St Clair JB, Aviszus K, Kirchenbaum G, Guo W, Wysocki LJ. Somatic Mutagenesis in Autoimmunity. doi:10.3109/08916934.2012.757597
46. Morlacchi S, Soldani C, Viola A, Sarukhan A. Self-antigen presentation by mouse B cells results in regulatory T-cell induction rather than anergy or clonal deletion. *Blood*. 2011;118(4):984-991. doi:10.1182/BLOOD-2011-02-336115
47. Nishizuka Y, Sakakura T. Thymus and Reproduction: Sex-Linked Dysgenesia of the Gonad after Neonatal Thymectomy in Mice. *Science (80-)*. 1969;166(3906):753-755. doi:10.1126/SCIENCE.166.3906.753
48. Gershon RK, Kondo K. Cell Interactions in the Induction of Tolerance: The Role of Thymic Lymphocytes. *Immunology*. 1970;18:723.
49. Sakaguchi S, Sakaguchi N, Asano M, Itoh M, Toda M. Immunologic Self-Tolerance Maintained by Activated T Cells Expressing 11-2 Receptor a-Chains (CD25) Breakdown of a Single Mechanism of Self-Tolerance Causes Various Autoimmune Diseases'. 1995.
50. Asano M, Toda M, Sakaguchi N, Sakaguchi S. Autoimmune Disease as a Consequence of Developmental Abnormality of a T Cell Subpopulation.
51. Takahashi T, Kuniyasu Y, Toda M, et al. Immunologic self-tolerance maintained by CD25+CD4+ naturally anergic and suppressive T cells: induction of autoimmune disease by breaking their anergic/suppressive state. *Int Immunol*. 1998;10(12):1969-1980. doi:10.1093/INTIMM/10.12.1969
52. Suri-Payer E, Amar AZ, Thornton AM, Shevach EM. CD4+CD25+ T Cells Inhibit Both the Induction and Effector Function of Autoreactive T Cells and Represent a Unique Lineage of Immunoregulatory Cells. *J Immunol*. 1998;160(3):1212-1218. doi:10.4049/JIMMUNOL.160.3.1212

53. Bacchetta R, Passerini L, Gambineri E, et al. Defective regulatory and effector T cell functions in patients with FOXP3 mutations. *J Clin Invest*. 2006;116(6):1713-1722. doi:10.1172/JCI25112
54. Brunkow ME, Jeffery EW, Hjerrild KA, et al. Disruption of a new forkhead/winged-helix protein, scurfin, results in the fatal lymphoproliferative disorder of the scurfy mouse. *Nat Genet*. 2001;27(1):68-73. doi:10.1038/83784
55. Fontenot JD, Gavin MA, Rudensky AY. Foxp3 programs the development and function of CD4+CD25+ regulatory T cells. *Nat Immunol 2003 44*. 2003;4(4):330-336. doi:10.1038/ni904
56. Hori S, Nomura T, Sakaguchi S. Control of regulatory T cell development by the transcription factor Foxp3. *Science (80-)*. 2003;299(3):1057-1061. doi:10.1126/science.1079490
57. Marson A, Kretschmer K, Frampton GM, et al. Foxp3 occupancy and regulation of key target genes during T-cell stimulation. *Nature*. 2007;445(7130):931-935. doi:10.1038/nature05478
58. Sadlon TJ, Wilkinson BG, Pederson S, et al. Genome-Wide Identification of Human FOXP3 Target Genes in Natural Regulatory T Cells. *J Immunol*. 2010;185(2):1071-1081. doi:10.4049/jimmunol.1000082
59. Kawai K, Uchiyama M, Hester J, Wood K, Issa F. Regulatory T cells for tolerance. *Hum Immunol*. 2018;79(5):294-303. doi:10.1016/j.humimm.2017.12.013
60. Wang J, Ioan-Facsinay A, van der Voort EIH, Huizinga TWJ, Toes REM. Transient expression of FOXP3 in human activated nonregulatory CD4+ T cells. *Eur J Immunol*. 2007;37(1):129-138. doi:10.1002/EJI.200636435
61. Tran DQ, Ramsey H, Shevach EM. Induction of FOXP3 expression in naive human CD4+FOXP3− T cells by T-cell receptor stimulation is transforming growth factor-β–dependent but does not confer a regulatory phenotype. *Blood*. 2007;110(8):2983. doi:10.1182/BLOOD-2007-06-094656
62. Allan SE, Crome SQ, Crellin NK, et al. Activation-induced FOXP3 in human T effector cells does not suppress proliferation or cytokine production. *Int Immunol*. 2007;19(4):345-354. doi:10.1093/INTIMM/DXM014
63. Cozzo C, Iii JL, Caton AJ. Cutting Edge: Self-Peptides Drive the Peripheral Expansion of CD4+CD25+ Regulatory T Cells. *J Immunol*. 2003;171(11):5678-5682. doi:10.4049/JIMMUNOL.171.11.5678
64. Thornton AM, Korty PE, Tran DQ, et al. Expression of Helios, an Ikaros Transcription Factor Family Member, Differentiates Thymic-Derived from Peripherally Induced Foxp3+ T Regulatory Cells. *J Immunol*. 2010;184(7):3433. doi:10.4049/JIMMUNOL.0904028
65. Yu WQ, Ji NF, Gu CJ, Wang YL, Huang M, Zhang MS. Coexpression of Helios in Foxp3+ Regulatory T Cells and Its Role in Human Disease. *Dis Markers*. 2021;2021. doi:10.1155/2021/5574472
66. Chougnet C, Hildeman D. Helios—controller of Treg stability and function. *Transl Cancer Res*. 2016;5(Suppl 2):S338. doi:10.21037/TCR.2016.07.37
67. Kim HJ, Barnitz RA, Kreslavsky T, et al. Stable inhibitory activity of regulatory T cells requires the transcription factor Helios. *Science*. 2015;350(6258):334. doi:10.1126/SCIENCE.AAD0616
68. Anderson AC, Joller N, Kuchroo VK. Lag-3, Tim-3, and TIGIT co-inhibitory receptors

with specialized functions in immune regulation. *Immunity*. 2016;44(5):989. doi:10.1016/J.IMMUNI.2016.05.001
69. Kim D, Kim G, Yu R, et al. Lymphocyte activation gene 3 (Lag3) supports Foxp3 + Treg cell function by restraining c-Myc-dependent aerobic glycolysis. doi:10.1101/2023.02.13.528371
70. Lee SY, Goverman JM. The Influence of Tim-3 Signaling on Central Nervous System Autoimmune Disease is Determined by the Effector Function of the Pathogenic T Cells. *J Immunol*. 2013;190(10):4991. doi:10.4049/JIMMUNOL.1300083
71. Lucca LE, Dominguez-Villar M. Modulation of regulatory T cell function and stability by co-inhibitory receptors. *Nat Rev Immunol*. April 2020:1-14. doi:10.1038/s41577-020-0296-3
72. Kumar P, Bhattacharya P, Prabhakar BS. A Comprehensive Review on the Role of Co-signaling Receptors and Treg Homeostasis in Autoimmunity and Tumor Immunity. *J Autoimmun*. 2018;95:77. doi:10.1016/J.JAUT.2018.08.007
73. Ephrem A, Epstein AL, Stephens GL, Thornton AM, Glass D, Shevach EM. Modulation of Treg cells/T effector function by GITR signaling is context–dependent. *Eur J Immunol*. 2013;43(9):2421-2429. doi:10.1002/EJI.201343451
74. Amoozgar Z, Kloepper J, Ren J, et al. Targeting Treg cells with GITR activation alleviates resistance to immunotherapy in murine glioblastomas. *Nat Commun*. 2021;12(1). doi:10.1038/S41467-021-22885-8
75. Francisco LM, Salinas VH, Brown KE, et al. PD-L1 regulates the development, maintenance, and function of induced regulatory T cells. *J Exp Med*. 2009;206(13):3015. doi:10.1084/JEM.20090847
76. Linsley PS, Greene JAL, Brady W, Bajorath J, Ledbetter JA, Peach R. Human B7-1 (CD80) and B7-2 (CD86) bind with similar avidities but distinct kinetics to CD28 and CTLA-4 receptors. *Immunity*. 1994;1(9):793-801. doi:10.1016/S1074-7613(94)80021-9
77. Tekguc M, Wing JB, Osaki M, Long J, Sakaguchi S. Treg-expressed CTLA-4 depletes CD80/CD86 by trogocytosis, releasing free PD-L1 on antigen-presenting cells. *Proc Natl Acad Sci U S A*. 2021;118(30):e2023739118. doi:10.1073/PNAS.2023739118/SUPPL_FILE/PNAS.2023739118.SM03.MP4
78. Wing K, Onishi Y, Prieto-Martin P, et al. CTLA-4 Control over Foxp3+ Regulatory T Cell Function. *Science (80-)*. 2008;322(5899):271-275. doi:10.1126/science.1160062
79. Vignali DAA, Collison LW, Workman CJ. How regulatory T cells work. *Nat Rev Immunol*. 2008;8(7):523. doi:10.1038/NRI2343
80. Ren X, Ye F, Jiang Z, Chu Y, Xiong S, Wang Y. Involvement of cellular death in TRAIL/DR5-dependent suppression induced by CD4+CD25+ regulatory T cells. *Cell Death Differ 2007 1412*. 2007;14(12):2076-2084. doi:10.1038/sj.cdd.4402220
81. Strauss L, Bergmann C, Whiteside TL. Human circulating CD4+CD25highFoxp3+ regulatory T cells kill autologous CD8+ but not CD4+ responder cells by Fas-mediated apoptosis. *J Immunol*. 2009;182(3):1469-1480. doi:10.4049/JIMMUNOL.182.3.1469
82. Schmidt A, Oberle N, Krammer PH. Molecular mechanisms of treg-mediated T cell suppression. *Front Immunol*. 2012;3:51. doi:10.3389/fimmu.2012.00051
83. Zarek PE, Huang C-T, Lutz ER, et al. A 2A receptor signaling promotes peripheral tolerance by inducing T-cell anergy and the generation of adaptive regulatory T cells. 2008. doi:10.1182/blood-2007
84. Fallarino F, Grohmann U, Hwang KW, et al. Modulation of tryptophan catabolism by

regulatory T cells. *Nat Immunol 2003 412*. 2003;4(12):1206-1212. doi:10.1038/ni1003
85. Pandiyan P, Zheng L, Ishihara S, Reed J, Lenardo MJ. CD4 + CD25 + Foxp3 + regulatory T cells induce cytokine deprivation-mediated apoptosis of effector CD4 + T cells. *Nat Immunol*. 2007;8. doi:10.1038/ni1536
86. Lindqvist CA, Christiansson LH, Simonsson B, Enblad G, Olsson-Strömberg U, Loskog ASI. T regulatory cells control T-cell proliferation partly by the release of soluble CD25 in patients with B-cell malignancies. *Immunology*. 2010;131(3):371. doi:10.1111/J.1365-2567.2010.03308.X
87. Moore KW, De Waal Malefyt R, Coffman RL, O'Garra A. Interleukin-10 and the Interleukin-10 Receptor. *https://doi.org/101146/annurev.immunol191683*. 2003;19:683-765. doi:10.1146/ANNUREV.IMMUNOL.19.1.683
88. Zhang Y, Alexander PB, Wang XF. TGF-β Family Signaling in the Control of Cell Proliferation and Survival. *Cold Spring Harb Perspect Biol*. 2017;9(4). doi:10.1101/CSHPERSPECT.A022145
89. Marie JC, Letterio JJ, Gavin M, Rudensky AY. TGF-1 maintains suppressor function and Foxp3 expression in CD4 CD25 regulatory T cells. *J Exp Med JEM*. 2005;201(7):1061-1067. doi:10.1084/jem.20042276
90. Ghiringhelli F, Ménard C, Terme M, et al. CD4+CD25+ regulatory T cells inhibit natural killer cell functions in a transforming growth factor-beta-dependent manner. *J Exp Med*. 2005;202(8):1075-1085. doi:10.1084/jem.20051511
91. Olson BM, Sullivan JA, Burlingham WJ. Interleukin 35: A Key Mediator of Suppression and the Propagation of Infectious Tolerance. *Front Immunol*. 2013;4:315. doi:10.3389/FIMMU.2013.00315
92. Xu L, Kitani A, Strober W. Molecular mechanisms regulating TGF-β-induced Foxp3 expression. *Mucosal Immunol*. 2010. doi:10.1038/mi.2010.7
93. Freudenberg K, Lindner N, Dohnke S, Garbe AI, Schallenberg S, Kretschmer K. Critical role of TGF-β and IL-2 receptor signaling in Foxp3 induction by an inhibitor of DNA methylation. *Front Immunol*. 2018;9(FEB):1. doi:10.3389/FIMMU.2018.00125/FULL
94. Murphy K, Weaver C. *Janeway ' S 9 Th Edition*.; 2017.
95. Levine AG, Medoza A, Hemmers S, et al. Stability and function of regulatory T cells expressing the transcription factor T-bet. *Nature*. 2017;546(7658):421-425. doi:10.1038/NATURE22360
96. Littringer K, Moresi C, Rakebrandt N, et al. Common features of regulatory T cell specialization during Th1 responses. *Front Immunol*. 2018;9(JUN):1344. doi:10.3389/FIMMU.2018.01344/BIBTEX
97. Halim L, Romano M, Mcgregor R, Lechler RI, Nova-Lamperti E, Correspondence GL. An Atlas of Human Regulatory T Helper-like Cells Reveals Features of Th2-like Tregs that Support a Tumorigenic Environment Accession Numbers GSE99733 Halim et al. *Cell Rep*. 2017;20:757-770. doi:10.1016/j.celrep.2017.06.079
98. Hyung Lim KW, Lee J, Hillsamer P. Regulatory T Cells + Cells and FOXP3 Receptors with Both Polarized Effector T Human Th17 Cells Share Major Trafficking. *J Immunol Ref*. 2008;180:122-129. doi:10.4049/jimmunol.180.1.122
99. Dang E V., Barbi J, Yang HY, et al. Control of TH17/Treg balance by hypoxia-inducible factor 1. *Cell*. 2011;146(5):772-784. doi:10.1016/j.cell.2011.07.033
100. Rudensky AY. Regulatory T Cells and Foxp3. *Immunol Rev*. 2011;241(1):260. doi:10.1111/J.1600-065X.2011.01018.X

101. Floess S, Freyer J, Siewert C, et al. Epigenetic control of the foxp3 locus in regulatory T cells. *PLoS Biol*. 2007;5(2):0169-0178. doi:10.1371/journal.pbio.0050038
102. Charbonnier LM, Cui Y, Stephen-Victor E, et al. Functional reprogramming of regulatory T cells in the absence of Foxp3. *Nat Immunol 2019 209*. 2019;20(9):1208-1219. doi:10.1038/s41590-019-0442-x
103. Liu ZM, Wang KP, Ma J, Guo Zheng S. The role of all-trans retinoic acid in the biology of Foxp3+ regulatory T cells. *Cell Mol Immunol 2015 125*. 2015;12(5):553-557. doi:10.1038/cmi.2014.133
104. Cuadrado E, van den Biggelaar M, de Kivit S, et al. Proteomic Analyses of Human Regulatory T Cells Reveal Adaptations in Signaling Pathways that Protect Cellular Identity. *Immunity*. 2018;48(5):1046-1059.e6. doi:10.1016/j.immuni.2018.04.008
105. Cortez JT, Montauti E, Shifrut E, et al. CRISPR screen in regulatory T cells reveals modulators of Foxp3. *Nature*. April 2020:1-5. doi:10.1038/s41586-020-2246-4
106. Sawitzki B, Harden PN, Reinke P, et al. Regulatory cell therapy in kidney transplantation (The ONE Study): a harmonised design and analysis of seven non-randomised, single-arm, phase 1/2A trials. *Lancet*. 2020;395(10237):1627-1639. doi:10.1016/S0140-6736(20)30167-7
107. Todo S, Yamashita K, Goto R, et al. A pilot study of operational tolerance with a regulatory T-cell-based cell therapy in living donor liver transplantation. *Hepatology*. 2016;64(2):632-643. doi:10.1002/HEP.28459
108. Atif M, Conti F, Gorochov G, Oo YH, Miyara M. Regulatory T cells in solid organ transplantation. *Clin Transl Immunol*. 2020;9(2). doi:10.1002/cti2.1099
109. Jacob J, Nadkarni S, Volpe A, et al. Spatiotemporal in vivo tracking of polyclonal human regulatory T cells (Tregs) reveals a role for innate immune cells in Treg transplant recruitment. *Mol Ther Methods Clin Dev*. 2021;20:324. doi:10.1016/J.OMTM.2020.12.003
110. Goldberg R, Scotta C, Cooper D, et al. Correction of Defective T-Regulatory Cells From Patients With Crohn's Disease by Ex Vivo Ligation of Retinoic Acid Receptor-α. *Gastroenterology*. 2019;156(6):1775-1787. doi:10.1053/J.GASTRO.2019.01.025
111. Bérnard A, Ceredig R, Rolink AG. Regulatory T cells control autoimmunity following syngeneic bone marrow transplantation. *Eur J Immunol*. 2006;36(9):2324-2335. doi:10.1002/EJI.200636434
112. Tran LM, Thomson AW. Detection and Monitoring of Regulatory Immune Cells Following Their Adoptive Transfer in Organ Transplantation. *Front Immunol*. 2020;11:614578. doi:10.3389/FIMMU.2020.614578/BIBTEX
113. Marek-Trzonkowska N, Myśliwiec M, Iwaszkiewicz-Grześ D, et al. Factors affecting long-term efficacy of T regulatory cell-based therapy in type 1 diabetes. *J Transl Med*. 2016;14(1):1-11. doi:10.1186/S12967-016-1090-7/FIGURES/7
114. Dong S, Hiam-Galvez KJ, Mowery CT, et al. The effect of low-dose IL-2 and Treg adoptive cell therapy in patients with type 1 diabetes. *JCI Insight*. 2021;6(18):e147474-e147474. doi:10.1172/JCI.INSIGHT.147474
115. Dall'Era M, Pauli ML, Remedios K, et al. Adoptive Regulatory T Cell Therapy in a Patient with Systemic Lupus Erythematosus. *Arthritis Rheumatol (Hoboken, NJ)*. 2019;71(3):431. doi:10.1002/ART.40737
116. Thonhoff JR, Beers DR, Zhao W, et al. Expanded autologous regulatory T-lymphocyte infusions in ALS: A phase I, first-in-human study. *Neurol Neuroimmunol*

Neuroinflammation. 2018;5(4):465. doi:10.1212/NXI.0000000000000465
117. MacMillan ML, Hippen KL, McKenna DH, et al. First-in-human phase 1 trial of induced regulatory T cells for graft-versus-host disease prophylaxis in HLA-matched siblings. *Blood Adv*. 2021;5(5):1425-1436. doi:10.1182/BLOODADVANCES.2020003219
118. Cord Blood Regulatory T Cells for Prevention of Graft Versus Host Disease. *Blood*. 2017;130:3246. doi:10.1182/BLOOD.V130.SUPPL_1.3246.3246
119. Bader CS, Pavlova A, Lowsky R, et al. Single-center randomized trial of T-reg graft alone vs T-reg graft plus tacrolimus for the prevention of acute GVHD. *Blood Adv*. 2024;8(5):1105-1115. doi:10.1182/BLOODADVANCES.2023011625
120. Brunstein CG, Miller JS, Cao Q, et al. Infusion of ex vivo expanded T regulatory cells in adults transplanted with umbilical cord blood: safety profile and detection kinetics. *Blood*. 2011;117(3):1061-1070. doi:10.1182/BLOOD-2010-07-293795
121. Hoeg RT, Moroz A, Gandhi A, et al. Orca-T Results in High Gvhd-Free and Relapse-Free Survival Following Myeloablative Conditioning for Hematological Malignancies: Results of a Single Center Phase 2 and a Multicenter Phase 1b Study. *Blood*. 2021;138(Supplement 1):98. doi:10.1182/BLOOD-2021-154191
122. Martelli MF, Di Ianni M, Ruggeri L, et al. HLA-haploidentical transplantation with regulatory and conventional T-cell adoptive immunotherapy prevents acute leukemia relapse. *Blood*. 2014;124(4):638-644. doi:10.1182/BLOOD-2014-03-564401
123. Whangbo JS, Nikiforow S, Kim HT, et al. A phase 1 study of donor regulatory T-cell infusion plus low-dose interleukin-2 for steroid-refractory chronic graft-vs-host disease. *Blood Adv*. 2022;6(21):5786-5796. doi:10.1182/BLOODADVANCES.2021006625
124. Sánchez-Fueyo A, Whitehouse G, Grageda N, et al. Applicability, safety, and biological activity of regulatory T cell therapy in liver transplantation. *Am J Transplant*. 2020;20(4):1125-1136. doi:10.1111/AJT.15700
125. Tang Q, Leung J, Peng Y, et al. Selective decrease of donor-reactive Tregs after liver transplantation limits Treg therapy for promoting allograft tolerance in humans. *Sci Transl Med*. 2022;14(669):eabo2628. doi:10.1126/SCITRANSLMED.ABO2628/SUPPL_FILE/SCITRANSLMED.ABO2628_MDAR_REPRODUCIBILITY_CHECKLIST.PDF
126. Roemhild A, Otto NM, Moll G, et al. Regulatory T cells for minimising immune suppression in kidney transplantation: phase I/IIa clinical trial. *BMJ*. 2020;371. doi:10.1136/BMJ.M3734
127. Mathew JM, H-Voss J, LeFever A, et al. A Phase I Clinical Trial with Ex Vivo Expanded Recipient Regulatory T cells in Living Donor Kidney Transplants. *Sci Rep*. 2018;8(1). doi:10.1038/S41598-018-25574-7
128. Gladstone DE, D'Alessio F, Howard C, et al. Randomized, double-blinded, placebo-controlled trial of allogeneic cord blood T-regulatory cells for treatment of COVID-19 ARDS. *Blood Adv*. 2023;7(13):3075. doi:10.1182/BLOODADVANCES.2022009619
129. Terry L V., Oo YH. The Next Frontier of Regulatory T Cells: Promising Immunotherapy for Autoimmune Diseases and Organ Transplantations. *Front Immunol*. 2020;11:565518. doi:10.3389/FIMMU.2020.565518
130. Lim TY, Perpiñán E, Londoño MC, et al. Low dose interleukin-2 selectively expands circulating regulatory T cells but fails to promote liver allograft tolerance in humans. *J Hepatol*. 2023;78(1):153-164. doi:10.1016/J.JHEP.2022.08.035
131. Webster KE, Walters S, Kohler RE, et al. In vivo expansion of T reg cells with IL-2–mAb

complexes: induction of resistance to EAE and long-term acceptance of islet allografts without immunosuppression. *J Exp Med*. 2009;206(4):751. doi:10.1084/JEM.20082824
132. Khoryati L, Pham MN, Sherve M, et al. An IL-2 mutein engineered to promote expansion of regulatory T cells arrests ongoing autoimmunity in mice. *Sci Immunol*. 2020;5(50). doi:10.1126/SCIIMMUNOL.ABA5264
133. VanDyke D, Iglesias M, Tomala J, et al. Engineered human cytokine/antibody fusion proteins expand regulatory T cells and confer autoimmune disease protection. *Cell Rep*. 2022;41(3):111478. doi:10.1016/J.CELREP.2022.111478/ATTACHMENT/B485BEC8-E163-476B-8EA6-5F7069D02FBF/MMC2.XLSX
134. Gomez-Rodriguez J, Wohlfert EA, Handon R, et al. Itk-mediated integration of T cell receptor and cytokine signaling regulates the balance between Th17 and regulatory T cells. *J Exp Med*. 2014;211(3):529-543. doi:10.1084/JEM.20131459
135. Haxhinasto S, Mathis D, Benoist C. The AKT–mTOR axis regulates de novo differentiation of CD4+Foxp3+ cells. *J Exp Med*. 2008;205(3):565. doi:10.1084/JEM.20071477
136. Sauer S, Bruno L, Hertweck A, et al. T cell receptor signaling controls Foxp3 expression via PI3K, Akt, and mTOR. *Proc Natl Acad Sci U S A*. 2008;105(22):7797-7802. doi:10.1073/PNAS.0800928105/SUPPL_FILE/0800928105SI.PDF
137. Merkenschlager M, Von Boehmer H. PI3 kinase signalling blocks Foxp3 expression by sequestering Foxo factors. *J Exp Med*. 2010;207(7):1347. doi:10.1084/JEM.20101156
138. Zeng H, Yang K, Cloer C, Neale G, Vogel P, Chi H. MTORC1 couples immune signals and metabolic programming to establish T reg-cell function. *Nature*. 2013;499(7459):485-490. doi:10.1038/nature12297
139. Valmori D, Tosello V, Souleimanian NE, et al. Rapamycin-Mediated Enrichment of T Cells with Regulatory Activity in Stimulated CD4 + T Cell Cultures Is Not Due to the Selective Expansion of Naturally Occurring Regulatory T Cells but to the Induction of Regulatory Functions in Conventional CD4 + T Cell. *J Immunol*. 2006;177(2):944-949. doi:10.4049/jimmunol.177.2.944
140. Battaglia M, Stabilini A, Roncarolo M-G. Rapamycin selectively expands CD4+CD25+FoxP3+ regulatory T cells. *Blood*. 2005;105(12):4743-4748. doi:10.1182/blood.v99.10.3493
141. Romano M, Tung SL, Smyth LA, Lombardi G. Treg therapy in transplantation: a general overview. *Transpl Int*. 2017;30(8):745-753. doi:10.1111/tri.12909
142. Hashimoto H, McCallion O, Kempkes RWM, Hester J, Issa F. Distinct metabolic pathways mediate regulatory T cell differentiation and function. *Immunol Lett*. 2020;223:53-61. doi:10.1016/J.IMLET.2020.04.011
143. Kurniawan H, Soriano-Baguet L, Brenner D. Regulatory T cell metabolism at the intersection between autoimmune diseases and cancer. *Eur J Immunol*. 2020;50(11):1626. doi:10.1002/EJI.201948470
144. Shrestha S, Yang K, Guy C, Vogel P, Neale G, Chi H. Treg cells require the phosphatase PTEN to restrain TH1 and TFH cell responses. *Nat Immunol 2014 162*. 2015;16(2):178-187. doi:10.1038/ni.3076
145. Lam AJ, Haque M, Ward-Hartstonge KA, et al. PTEN is required for human Treg suppression of costimulation. *bioRxiv*. March 2022:2022.03.06.483188. doi:10.1101/2022.03.06.483188
146. Preston GC, Sinclair L V, Kaskar A, et al. Single cell tuning of Myc expression by antigen

receptor signal strength and interleukin-2 in T lymphocytes. *EMBO J*. 2015;34(15):2008-2024. doi:10.15252/EMBJ.201490252
147. Taylor CT, Colgan SP. Regulation of immunity and inflammation by hypoxia in immunological niches. *Nat Rev Immunol*. 2017;17(12):774-785. doi:10.1038/nri.2017.103
148. Scheele CW. *V. Königl. Schwed. Acad. d. Wissenschaft. Mitgliedes Chemische Abhandlung von Der Luft Und Dem Feuer*. (Swederus M, ed.). Uppsala and Liepzig: Buchhändler; 1777.
149. Jiang BH, Rue E, Wang GL, Roe R, Semenza GL. Dimerization, DNA binding, and transactivation properties of hypoxia- inducible factor 1. *J Biol Chem*. 1996;271(30):17771-17778. doi:10.1074/jbc.271.30.17771
150. Semenza GL, Nejfelt MK, Chi SM, Antonarakis SE. Hypoxia-inducible nuclear factors bind to an enhancer element located 3' to the human erythropoietin gene. *Proc Natl Acad Sci U S A*. 1991;88(13):5680. doi:10.1073/PNAS.88.13.5680
151. Latif F, Tory K, Gnarra J, et al. Identification of the von Hippel-Lindau Disease Tumor Suppressor Gene. *Science (80-)*. 1993;260(5112):1317-1320. doi:10.1126/SCIENCE.8493574
152. Iliopoulos O, Kibel A, Gray S, Kaelin WG. Tumour suppression by the human von Hippel-Lindau gene product. *Nat Med 1995 18*. 1995;1(8):822-826. doi:10.1038/nm0895-822
153. Maxwell PH, Wlesener MS, Chang GW, et al. The tumour suppressor protein VHL targets hypoxia-inducible factors for oxygen-dependent proteolysis. *Nature*. 1999;399(6733):271-275. doi:10.1038/20459
154. Bruick RK, McKnight SL. A Conserved Family of Prolyl-4-Hydroxylases That Modify HIF. *Science (80-)*. 2001;294(5545):1337-1340. doi:10.1126/SCIENCE.1066373
155. Epstein ACR, Gleadle JM, McNeill LA, et al. C. elegans EGL-9 and mammalian homologs define a family of dioxygenases that regulate HIF by prolyl hydroxylation. *Cell*. 2001;107(1):43-54. doi:10.1016/S0092-8674(01)00507-4
156. Schofield CJ, Ratcliffe PJ. Oxygen sensing by HIF hydroxylases. *Nat Rev Mol Cell Biol*. 2004;5(5):343-354. doi:10.1038/nrm1366
157. Eltzschig HK, Bratton DL, Colgan SP. Targeting hypoxia signalling for the treatment of ischaemic and inflammatory diseases. *Nat Rev Drug Discov*. 2014;13(11):852-869. doi:10.1038/nrd4422
158. Schödel J, Grampp S, Maher ER, et al. Hypoxia, hypoxia-inducible transcription factors, and renal cancer. *Eur Urol*. 2016;69(4):646-657. doi:10.1016/j.eururo.2015.08.007
159. Warnecke C, Zaborowska Z, Kurreck J, et al. Differentiating the functional role of hypoxia-inducible factor (HIF)-1α and HIF-2α (EPAS-1) by the use of RNA interference: erythropoietin is a HIF-2α target gene in Hep3B and Kelly cells. *FASEB J*. 2004;18(12):1462-1464. doi:10.1096/FJ.04-1640FJE
160. Koh MY, Powis G. Passing the baton: The HIF switch. *Trends Biochem Sci*. 2012;37(9):364. doi:10.1016/J.TIBS.2012.06.004
161. Willam C, Nicholls LG, Ratcliffe PJ, Pugh CW, Maxwell PH. The prolyl hydroxylase enzymes that act as oxygen sensors regulating destruction of hypoxia-inducible factor α. *Adv Enzyme Regul*. 2004;44(1):75-92. doi:10.1016/J.ADVENZREG.2003.11.017
162. D L, DJ P, JJ G, DA W, ML W, RK B. FIH-1 is an asparaginyl hydroxylase enzyme that regulates the transcriptional activity of hypoxia-inducible factor. *Genes Dev*. 2002;16(12). doi:10.1101/GAD.991402

163. Isaacs JS, Jung YJ, Mimnaugh EG, Martinez A, Cuttitta F, Neckers LM. Hsp90 regulates a von Hippel Lindau-independent hypoxia-inducible factor-1 alpha-degradative pathway. *J Biol Chem*. 2002;277(33):29936-29944. doi:10.1074/jbc.M204733200
164. Peter Ratcliffe P, Bishop T. Signaling hypoxia by hypoxia-inducible factor protein hydroxylases: a historical overview and future perspectives. *Hypoxia*. December 2014:197. doi:10.2147/hp.s47598
165. Takeda K, Ho VC, Takeda H, Duan L-J, Nagy A, Fong G-H. Placental but Not Heart Defects Are Associated with Elevated Hypoxia-Inducible Factor α Levels in Mice Lacking Prolyl Hydroxylase Domain Protein 2. *Mol Cell Biol*. 2006;26(22):8336. doi:10.1128/MCB.00425-06
166. Peyssonnaux C, Nizet V, Johnson RS. Role of the hypoxia inducible factors HIF in iron metabolism. *Cell Cycle*. 2008;7(1):28-32. doi:10.4161/cc.7.1.5145
167. Minamishima YA, Moslehi J, Padera RF, Bronson RT, Liao R, William G. Kaelin J. A Feedback Loop Involving the Phd3 Prolyl Hydroxylase Tunes the Mammalian Hypoxic Response In Vivo. *Mol Cell Biol*. 2009;29(21):5729. doi:10.1128/MCB.00331-09
168. Schroedl C, McClintock DS, Budinger GRS, Chandel NS. Hypoxic but not anoxic stabilization of HIF-1alpha requires mitochondrial reactive oxygen species. *Am J Physiol Lung Cell Mol Physiol*. 2002;283(5). doi:10.1152/AJPLUNG.00014.2002
169. Mandl M, Depping R. Hypoxia-Inducible Aryl Hydrocarbon Receptor Nuclear Translocator (ARNT) (HIF-1β): Is It a Rare Exception? *Mol Med*. 2014;20(1):215. doi:10.2119/MOLMED.2014.00032
170. Hankinson O. Why Does ARNT2 Behave Differently from ARNT? *Toxicol Sci*. 2008;103(1):1. doi:10.1093/TOXSCI/KFN032
171. Maltepe E, Keith B, Arsham AM, Brorson JR, Simon MC. The role of ARNT2 in tumor angiogenesis and the neural response to hypoxia. *Biochem Biophys Res Commun*. 2000;273(1):231-238. doi:10.1006/BBRC.2000.2928
172. Larigot L, Juricek L, Dairou J, Coumoul X. AhR signaling pathways and regulatory functions. *Biochim Open*. 2018;7:1-9. doi:10.1016/J.BIOPEN.2018.05.001
173. Cho SH, Raybuck AL, Blagih J, et al. Hypoxia-inducible factors in CD4+ T cells promote metabolism, switch cytokine secretion, and T cell help in humoral immunity. *Proc Natl Acad Sci U S A*. 2019;116(18):8975-8984. doi:10.1073/pnas.1811702116
174. Watts ER, Walmsley SR. Inflammation and Hypoxia: HIF and PHD Isoform Selectivity. *Trends Mol Med*. 2019;25(1):33-46. doi:10.1016/j.molmed.2018.10.006
175. Koshikawa N, Hayashi JI, Nakagawara A, Takenaga K. Reactive Oxygen Species-generating Mitochondrial DNA Mutation Up-regulates Hypoxia-inducible Factor-1α Gene Transcription via Phosphatidylinositol 3-Kinase-Akt/Protein Kinase C/Histone Deacetylase Pathway. *J Biol Chem*. 2009;284(48):33185. doi:10.1074/JBC.M109.054221
176. Finlay DK, Rosenzweig E, Sinclair L V., et al. PDK1 regulation of mTOR and hypoxia-inducible factor 1 integrate metabolism and migration of CD8+ T cells. *J Exp Med*. 2012;209(13):2441-2453. doi:10.1084/jem.20112607
177. Tao JH, Barbi J, Pan F. Hypoxia-inducible factors in T lymphocyte differentiation and function. A review in the theme: Cellular responses to hypoxia. *Am J Physiol - Cell Physiol*. 2015;309(9):C580-C589. doi:10.1152/ajpcell.00204.2015
178. Palazon A, Goldrath AW, Nizet V, Johnson RS. HIF Transcription Factors, Inflammation, and Immunity. *Immunity*. 2014;41(4):518. doi:10.1016/J.IMMUNI.2014.09.008
179. Kuschel A, Simon P, Tug S. Functional regulation of HIF-1α under normoxia-is there

more than post-translational regulation? *J Cell Physiol*. 2012;227(2):514-524. doi:10.1002/JCP.22798
180. Klotzsche-Von Ameln A, Muschter A, Mamlouk S, et al. Inhibition of HIF prolyl hydroxylase-2 blocks tumor growth in mice through the antiproliferative activity of TGFβ. *Cancer Res*. 2011;71(9):3306-3316. doi:10.1158/0008-5472.CAN-10-3838
181. Noman MZ, Hasmim M, Messai Y, et al. Hypoxia: A key player in antitumor immune response. A review in the theme: Cellular responses to hypoxia. *Am J Physiol - Cell Physiol*. 2015;309(9):C569-C579. doi:10.1152/ajpcell.00207.2015
182. Hatfield SM, Kjaergaard J, Lukashev D, et al. Systemic oxygenation weakens the hypoxia and hypoxia inducible factor 1α-dependent and extracellular adenosine-mediated tumor protection. *J Mol Med 2014 9212*. 2014;92(12):1283-1292. doi:10.1007/S00109-014-1189-3
183. Schmidt A, Oberle N, Krammer PH. Molecular mechanisms oftreg-mediatedt cell suppression. *Front Immunol*. 2012;3(MAR):51. doi:10.3389/FIMMU.2012.00051/BIBTEX
184. Cummins EP, Keogh CE, Crean D, Taylor CT. The role of HIF in immunity and inflammation. *Mol Aspects Med*. 2016;47-48:24-34. doi:10.1016/j.mam.2015.12.004
185. Walmsley SR, Print C, Farahi N, et al. Hypoxia-induced neutrophil survival is mediated by HIF-1α-dependent NF-κB activity. *J Exp Med*. 2005;201(1):105-115. doi:10.1084/jem.20040624
186. Cummins EP, Berra E, Comerford KM, et al. Prolyl hydroxylase-1 negatively regulates IκB kinase-β, giving insight into hypoxia-induced NFκB activity. *Proc Natl Acad Sci U S A*. 2006;103(48):18154-18159. doi:10.1073/pnas.0602235103
187. Culver C, Sundqvist A, Mudie S, Melvin A, Xirodimas D, Rocha S. Mechanism of Hypoxia-Induced NF- B. *Mol Cell Biol*. 2010;30(20):4901-4921. doi:10.1128/mcb.00409-10
188. Devraj G, Beerlage C, Brüne B, Kempf VAJ. Hypoxia and HIF-1 activation in bacterial infections. *Microbes Infect*. 2017;19(3):144-156. doi:10.1016/J.MICINF.2016.11.003
189. McGettrick AF, O'Neill LAJ. The Role of HIF in Immunity and Inflammation. *Cell Metab*. 2020;32(4):524-536. doi:10.1016/J.CMET.2020.08.002
190. Ryu JH, Chae CS, Kwak JS, et al. Hypoxia-Inducible Factor-2α Is an Essential Catabolic Regulator of Inflammatory Rheumatoid Arthritis. *PLOS Biol*. 2014;12(6):e1001881. doi:10.1371/JOURNAL.PBIO.1001881
191. Shi R, Hou W, Wang ZQ, Xu X. Biogenesis of Iron–Sulfur Clusters and Their Role in DNA Metabolism. *Front Cell Dev Biol*. 2021;9(September):1-13. doi:10.3389/fcell.2021.735678
192. Cardenas-Rodriguez M, Chatzi A, Tokatlidis K. Iron–sulfur clusters: from metals through mitochondria biogenesis to disease. *J Biol Inorg Chem*. 2018;23(4):509-520. doi:10.1007/s00775-018-1548-6
193. Ganz T, Nemeth E. Hepcidin and disorders of iron metabolism. *Annu Rev Med*. 2011;62:347-360. doi:10.1146/annurev-med-050109-142444
194. Kowdley K V., Gochanour EM, Sundaram V, Shah RA, Handa P. Hepcidin Signaling in Health and Disease: Ironing Out the Details. *Hepatol Commun*. 2021;5(5):723-735. doi:10.1002/HEP4.1717
195. Šimetić L, Zibar L. Laboratory use of hepcidin in renal transplant recipients. *Biochem Medica*. 2016;26(1):34. doi:10.11613/BM.2016.003

196. Adams PC, Deugnier Y, Moirand R, Brissot P. The Relationship Between Iron Overload, Clinical Symptoms, and Age in 410 Patients With Genetic Hemochromatosis. 1997. doi:10.1002/hep.510250130
197. Nemeth E, Tuttle MS, Powelson J, et al. Hepcidin regulates cellular iron efflux by binding to ferroportin and inducing its internalization. *Science (80-)*. 2004;306(5704):2090-2093. doi:10.1126/science.1104742
198. Babitt JL, Huang FW, Wrighting DM, et al. Bone morphogenetic protein signaling by hemojuvelin regulates hepcidin expression. *Nat Genet 2006 385*. 2006;38(5):531-539. doi:10.1038/ng1777
199. Cronin SJF, Woolf CJ, Weiss G, Penninger JM. The Role of Iron Regulation in Immunometabolism and Immune-Related Disease. *Front Mol Biosci*. 2019;6:116. doi:10.3389/FMOLB.2019.00116/BIBTEX
200. Smith SR, Ghosh MC, Ollivierre-Wilson H, Hang Tong W, Rouault TA. Complete loss of iron regulatory proteins 1 and 2 prevents viability of murine zygotes beyond the blastocyst stage of embryonic development. *Blood Cells Mol Dis*. 2006;36(2):283-287. doi:10.1016/J.BCMD.2005.12.006
201. Kuvibidila S, Warrier RP. Differential effects of iron deficiency and underfeeding on serum levels of interleukin-10, interleukin-12p40, and interferon-gamma in mice. *Cytokine*. 2004;26(2):73-81. doi:10.1016/J.CYTO.2003.12.010
202. Kuvibidila S, Porretta C, Baliga S. Aneuploidy assessed by DNA index influences the effect of iron status on plasma and/or supernatant cytokine levels and progression of cells through the cell cycle in a mouse model. *Cytokine*. 2014;65(2):175-183. doi:10.1016/J.CYTO.2013.11.005
203. Contreras I, Paredes-Cervantes V, García-Miranda LA, Pliego-Rivero FB, Estrada JA. Leukocyte production of IFN-γ and TNF-α in 8- to 12-y-old children with low serum iron levels. *Nutrition*. 2016;32(5):546-552. doi:10.1016/J.NUT.2015.11.005
204. Suega K, Made Bakta I. Influence of Iron on Plasma Interleukin-2 and Gamma Interferon Level in Iron Deficiency Anemia. 2009.
205. Wang Z, Yin W, Zhu L, et al. Iron Drives T Helper Cell Pathogenicity by Promoting RNA-Binding Protein PCBP1-Mediated Proinflammatory Cytokine Production. *Immunity*. 2018;49(1):80-92.e7. doi:10.1016/J.IMMUNI.2018.05.008/ATTACHMENT/D228E976-9674-46E1-89CE-200073DDE86C/MMC4.XLSX
206. Frost JN, Tan TK, Abbas M, et al. Hepcidin-Mediated Hypoferremia Disrupts Immune Responses to Vaccination and Infection Hepcidin-Mediated Hypoferremia Disrupts Immune Responses to Vaccination and Infection. 2021:1-16. doi:10.1016/j.medj.2020.10.004
207. Costa M, Cruz E, Oliveira S, et al. Lymphocyte Gene Expression Signatures from Patients and Mouse Models of Hereditary Hemochromatosis Reveal a Function of HFE as a Negative Regulator of CD8+ T-Lymphocyte Activation and Differentiation In Vivo. *PLoS One*. 2015;10(4):124246. doi:10.1371/JOURNAL.PONE.0124246
208. Cunningham-Rundles S, Giardina PJ, Grady RW, Califano C, Mc Kenzie P, De Sousa M. Effect of Transfusional Iron Overload on Immune Response. *J Infect Dis*. 2000;182(Supplement_1):S115-S121. doi:10.1086/315919
209. Neckers LM, Cossman J. Transferrin receptor induction in mitogen-stimulated human T lymphocytes is required for DNA synthesis and cell division and is regulated by interleukin 2. *Proc Natl Acad Sci U S A*. 1983;80(11):3494.

doi:10.1073/PNAS.80.11.3494
210. Shah AA, Donovan K, Seeley C, et al. Risk of Infection Associated With Administration of Intravenous Iron: A Systematic Review and Meta-analysis. *JAMA Netw Open*. 2021;4(11):e2133935-e2133935. doi:10.1001/JAMANETWORKOPEN.2021.33935
211. Shah A, Frost J, Aaron L, Donovan K, Drakesmith H. Systemic hypoferraemia and severity of hypoxaemic respiratory failure in COVID-19. doi:10.1101/2020.05.11.20092114
212. Oliveira MC, Coutinho LB, Almeida MPO, Briceño MP, Araujo ECB, Silva NM. The Availability of Iron Is Involved in the Murine Experimental Toxoplasma gondii Infection Outcome. *Microorganisms*. 2020;8(4):560. doi:10.3390/microorganisms8040560
213. Stoffel NU, Uyoga MA, Mutuku FM, et al. Iron Deficiency Anemia at Time of Vaccination Predicts Decreased Vaccine Response and Iron Supplementation at Time of Vaccination Increases Humoral Vaccine Response: A Birth Cohort Study and a Randomized Trial Follow-Up Study in Kenyan Infants. *Front Immunol*. 2020;11:1313. doi:10.3389/FIMMU.2020.01313/BIBTEX
214. Drakesmith H, Pasricha SR, Cabantchik I, et al. Vaccine efficacy and iron deficiency: an intertwined pair? *Lancet Haematol*. 2021;8(9):e666. doi:10.1016/S2352-3026(21)00201-5
215. Preston AE, Drakesmith H, Frost JN. Adaptive immunity and vaccination – iron in the spotlight. *Immunother Adv*. 2021;1(1):1-11. doi:10.1093/IMMADV/LTAB007
216. Hametner S, Wimmer I, Haider L, Pfeifenbring S, Brück W, Lassmann H. Iron and neurodegeneration in the multiple sclerosis brain. *Ann Neurol*. 2013;74(6):848-861. doi:10.1002/ANA.23974
217. Grant SM, Wiesinger JA, Beard JL, Cantorna MT. Iron-Deficient Mice Fail to Develop Autoimmune Encephalomyelitis. *J Nutr*. 2003;133(8):2635-2638. doi:10.1093/JN/133.8.2635
218. Li L, Xia Y, Yuan S, et al. Iron deprivation restrains the differentiation and pathogenicity of T helper 17 cell. *J Leukoc Biol*. October 2021. doi:10.1002/JLB.3MA0821-015R
219. Weigel KJ, Lynch SG, Levine SM. Iron chelation and multiple sclerosis. *ASN Neuro*. 2014;6(1):43-63. doi:10.1042/AN20130037
220. Gao X, Song Y, Lu S, et al. Insufficient Iron Improves Pristane-Induced Lupus by Promoting Treg Cell Expansion. *Front Immunol*. 2022;13. doi:10.3389/FIMMU.2022.799331/FULL
221. Voss K, Young AC, Gibson-Corley KN, et al. Dysregulated Transferrin Receptor Disrupts T Cell Iron Homeostasis to Drive Inflammation in Systemic Lupus Erythematosus Running title: Transferrin Receptor and Iron in SLE T Cells. doi:10.1101/2021.11.25.470053
222. Chang R, Chu KA, Lin MC, Chu YH, Hung YM, Wei JCC. Newly diagnosed iron deficiency anemia and subsequent autoimmune disease: a matched cohort study in Taiwan. *https://doi.org/101080/03007995202017485*85. 2020;36(6):985-992. doi:10.1080/03007995.2020.1748585
223. Rolla S, Ingoglia G, Bardina V, et al. Acute-Phase Protein Hemopexin Is a Negative Regulator of Th17 Response and Experimental Autoimmune Encephalomyelitis Development. *J Immunol*. 2013;191(11):5451-5459. doi:10.4049/JIMMUNOL.1203076
224. Fagoonee S, Caorsi C, Giovarelli M, et al. Lack of plasma protein hemopexin dampens mercury-induced autoimmune response in mice. *J Immunol*. 2008;181(3):1937-1947. doi:10.4049/JIMMUNOL.181.3.1937

225. Madda R, Lin SC, Sun WH, Huang SL. Plasma proteomic analysis of systemic lupus erythematosus patients using liquid chromatography/tandem mass spectrometry with label-free quantification. *PeerJ*. 2018;2018(5):4730. doi:10.7717/PEERJ.4730/SUPP-7
226. Guglielmo P, Cunsolo F, Lombardo T, et al. T-Subset Abnormalities in Thalassaemia intermedia: Possible Evidence for a Thymus Functional Deficiency. *Acta Haematol*. 1984;72(6):361-367. doi:10.1159/000206421
227. Tang YM, Chen XZ, Li GR, Zhou RH, Ning H, Yan H. [Effects of iron deficiency anemia on immunity and infectious disease in pregnant women]. *Wei Sheng Yan Jiu*. 2006;35(1):79-81.
228. Vinke JSJ, Francke MI, Eisenga MF, Hesselink DA, de Borst MH. Iron deficiency after kidney transplantation. *Nephrol Dial Transplant*. September 2020. doi:10.1093/ndt/gfaa123
229. Resch T, Ashraf MI, Ritschl PV, et al. Disturbances in iron homeostasis result in accelerated rejection after experimental heart transplantation. *J Hear Lung Transplant*. 2017;36:732-743. doi:10.1016/j.healun.2017.03.004
230. Döring M, Cabanillas Stanchi KM, Feucht J, et al. Ferritin as an early marker of graft rejection after allogeneic hematopoietic stem cell transplantation in pediatric patients. *Ann Hematol*. 2016;95(2):311-323. doi:10.1007/S00277-015-2560-3
231. K Hoshinaga 1, T Mohanakumar, E A Pascoe, S Szentpetery, H M Lee RRL. Expression of transferrin receptors on lymphocytes: its correlation with T-helper/T-suppressor cytotoxic ratio and rejection in heart transplant recipients - PubMed. J Heart Transplant . 1988 May-Jun;7(3):198-204. https://pubmed.ncbi.nlm.nih.gov/2968444/. Accessed April 20, 2022.
232. Bayer AL, Baliga P, Woodward JE. Differential effects of transferrin receptor blockade on the cellular mechanisms involved in graft rejection. *Transpl Immunol*. 1999;7(3):131-139. doi:10.1016/S0966-3274(99)80032-X
233. Woodward JE, Bayer AL, Chavin KD, Boleza KA, Baliga P. Anti-transferrin receptor monoclonal antibody: a novel immunosuppressant. *Transplantation*. 1998;65(1):6-9. doi:10.1097/00007890-199801150-00003
234. Bohne F, Martínez-Llordella M, Lozano JJ, et al. Intra-graft expression of genes involved in iron homeostasis predicts the development of operational tolerance in human liver transplantation. *J Clin Invest*. 2012;122(1):368-382. doi:10.1172/JCI59411
235. Nayyereh Sadat Mortazavi Khorasgani1, Ali Momeni2, Soleiman Kheiri3, Rohollah Masumi2, Saeed Mardani4, Fateme Salehi Choliche1, Maryam Saeedi1, Farzad Rashidi5 SSB. Serum Hepcidin and Ferritin Have Not Correlation With Inflammatory Markers in Kidney Transplant Patients. Acta MedIran, 60(6). https://acta.tums.ac.ir/index.php/acta/article/view/8916/5664. Published 2022. Accessed April 20, 2022.
236. Eisenga MF, Dullaart RPF, Berger SP, et al. Association of hepcidin-25 with survival after kidney transplantation. *Eur J Clin Invest*. 2016;46(12):994-1001. doi:10.1111/ECI.12682
237. Jabara HH, Boyden SE, Chou J, et al. A missense mutation in TFRC, encoding transferrin receptor 1, causes combined immunodeficiency. *Nat Genet*. 2016;48(1):74. doi:10.1038/NG.3465
238. Shah YM, Xie L. Hypoxia-inducible factors link iron homeostasis and erythropoiesis. *Gastroenterology*. 2014;146(3):630-642. doi:10.1053/j.gastro.2013.12.031

239. Schwartz AJ, Das NK, Ramakrishnan SK, et al. Hepatic hepcidin/intestinal HIF-2α axis maintains iron absorption during iron deficiency and overload. *J Clin Invest*. 2019;129(1):336-348. doi:10.1172/JCI122359
240. Peyssonnaux C, Zinkernagel AS, Schuepbach RA, et al. Regulation of iron homeostasis by the hypoxia-inducible transcription factors (HIFs). *J Clin Invest*. 2007;117(7):1926-1932. doi:10.1172/JCI31370
241. Anderson SA, Nizzi CP, Chang YI, et al. The IRP1-HIF-2α axis coordinates iron and oxygen sensing with erythropoiesis and iron absorption. *Cell Metab*. 2013;17(2):282-290. doi:10.1016/j.cmet.2013.01.007
242. Wilkinson N, Pantopoulos K. IRP1 regulates erythropoiesis and systemic iron homeostasis by controlling HIF2α mRNA translation. *Blood*. 2013;122(9):1658-1669. doi:10.1182/BLOOD-2013-03-492454
243. Li H, Liu Y, Shang L, et al. Iron regulatory protein 2 modulates the switch from aerobic glycolysis to oxidative phosphorylation in mouse embryonic fibroblasts. *Proc Natl Acad Sci U S A*. 2019;116(20):9871-9876. doi:10.1073/pnas.1820051116
244. Zhang X, Zhang W, Ma SF, et al. Iron deficiency modifies gene expression variation induced by augmented hypoxia sensing. *Blood Cells Mol Dis*. 2014;52(1):35. doi:10.1016/J.BCMD.2013.07.016
245. Simmen S, Cosin-Roger J, Melhem H, et al. Iron Prevents Hypoxia-Associated Inflammation Through the Regulation of Nuclear Factor-κB in the Intestinal Epithelium. *Cell Mol Gastroenterol Hepatol*. 2019;7(2):339-355. doi:10.1016/J.JCMGH.2018.10.006
246. Triner D, Shah YM. Hypoxia-inducible factors: A central link between inflammation and cancer. *J Clin Invest*. 2016;126(10):3689-3698. doi:10.1172/JCI84430
247. Cavezzi A, Troiani E, Corrao S. COVID-19: hemoglobin, iron, and hypoxia beyond inflammation. A narrative review. *Clin Pract*. 2020;10(2):24-30. doi:10.4081/CP.2020.1271
248. Shang C, Zhou H, Liu W, Shen T, Luo Y, Huang S. Iron chelation inhibits mTORC1 signaling involving activation of AMPK and REDD1/Bnip3 pathways. *Oncogene 2020 3929*. 2020;39(29):5201-5213. doi:10.1038/s41388-020-1366-5
249. Watson A, Lipina C, McArdle HJ, Taylor PM, Hundal HS. Iron depletion suppresses mTORC1-directed signalling in intestinal Caco-2 cells via induction of REDD1. *Cell Signal*. 2016;28(5):412. doi:10.1016/J.CELLSIG.2016.01.014
250. Ben-Shoshan J, Maysel-Auslender S, Mor A, Keren G, George J. Hypoxia controls CD4+CD25+ regulatory T-cell homeostasis via hypoxia-inducible factor-1α. *Eur J Immunol*. 2008;38(9):2412-2418. doi:10.1002/EJI.200838318
251. Lukashev D, Caldwell C, Ohta A, Chen P, Sitkovsky M. Differential Regulation of Two Alternatively Spliced Isoforms of Hypoxia-inducible Factor-1α in Activated T Lymphocytes *. *J Biol Chem*. 2001;276(52):48754-48763. doi:10.1074/JBC.M104782200
252. Lukashev D, Klebanov B, Kojima H, et al. Cutting Edge: Hypoxia-Inducible Factor 1α and Its Activation-Inducible Short Isoform I.1 Negatively Regulate Functions of CD4+ and CD8+ T Lymphocytes. *J Immunol*. 2006;177(8):4962-4965. doi:10.4049/JIMMUNOL.177.8.4962
253. Neumann AK, Yang J, Biju MP, et al. Hypoxia inducible factor 1α regulates T cell receptor signal transduction. *Proc Natl Acad Sci U S A*. 2005;102(47):17071. doi:10.1073/PNAS.0506070102
254. Clambey ET, McNamee EN, Westrich JA, et al. Hypoxia-inducible factor-1 alpha-

dependent induction of FoxP3 drives regulatory T-cell abundance and function during inflammatory hypoxia of the mucosa. *Proc Natl Acad Sci U S A*. 2012;109(41):E2784-E2793. doi:10.1073/pnas.1202366109
255. Yamamoto A, Hester J, Macklin PS, et al. Systemic silencing of Phd2 causes reversible immune regulatory dysfunction. *J Clin Invest*. 2019;129(9):3640-3656. doi:10.1172/JCI124099
256. AM W, K S, A A, et al. Hypoxia Enhances Immunosuppression by Inhibiting CD4+ Effector T Cell Function and Promoting Treg Activity. *Cell Physiol Biochem*. 2017;41(4):1271-1284. doi:10.1159/000464429
257. Hsiao H-W, Hsu T-S, Liu W-H, et al. ARTICLE Deltex1 antagonizes HIF-1a and sustains the stability of regulatory T cells in vivo. *Nat Commun*. 2015. doi:10.1038/ncomms7353
258. Lee JH, Elly C, Park Y, Liu YC. E3Ubiquitin Ligase VHL Regulates Hypoxia-Inducible Factor-1α to Maintain Regulatory T Cell Stability and Suppressive Capacity. *Immunity*. 2015;42(6):1062-1074. doi:10.1016/j.immuni.2015.05.016
259. Shehade H, Acolty V, Moser M, Oldenhove G. Cutting Edge: Hypoxia-Inducible Factor 1 Negatively Regulates Th1 Function. *J Immunol*. 2015;195(4):1372-1376. doi:10.4049/jimmunol.1402552
260. Hsu TS, Lin YL, Wang YA, et al. HIF-2α is indispensable for regulatory T cell function. *Nat Commun*. 2020;11(1):1-16. doi:10.1038/s41467-020-18731-y
261. LZ S, R W, G H, et al. HIF1alpha-dependent glycolytic pathway orchestrates a metabolic checkpoint for the differentiation of TH17 and Treg cells. *J Exp Med*. 2011;208(7):1367-1376. doi:10.1084/JEM.20110278
262. Bowser JL, Lee JW, Yuan X, Eltzschig HK. The hypoxia-adenosine link during inflammation. *J Appl Physiol*. 2017;123(5):1303-1320. doi:10.1152/japplphysiol.00101.2017
263. Miska J, Lee-Chang C, Rashidi A, et al. HIF-1α Is a Metabolic Switch between Glycolytic-Driven Migration and Oxidative Phosphorylation-Driven Immunosuppression of Tregs in Glioblastoma. *Cell Rep*. 2019;27(1):226-237.e4. doi:10.1016/J.CELREP.2019.03.029/ATTACHMENT/013EE91C-32FD-48D6-A57D-B3827D98ABFF/MMC1.PDF
264. Danger, R; Bonaccorsi-Riani, E; Kodela, E; Collins, H; Hider, R; Martínez-Llordella, M; Sánchez-Fueyo A. Iron Deficiency Impairs Regulatory T Cell Induction - ATC Abstracts. American Transplant Congress (Abstract). https://atcmeetingabstracts.com/abstract/iron-deficiency-impairs-regulatory-t-cell-induction/. Published 2015. Accessed May 2, 2022.
265. Bonaccorsi-Riani E, Danger R, Lozano JJ, et al. Iron Deficiency Impairs Intra-Hepatic Lymphocyte Mediated Immune Response. *PLoS One*. 2015;10(8). doi:10.1371/JOURNAL.PONE.0136106
266. Teh MR, Frost JN, Armitage AE, Drakesmith H. Analysis of Iron and Iron-Interacting Protein Dynamics During T-Cell Activation. *Front Immunol*. 2021;12:2943. doi:10.3389/FIMMU.2021.714613/BIBTEX
267. Das I, Saha K, Mukhopadhyay D, et al. Impact of iron deficiency anemia on cell-mediated and humoral immunity in children: A case control study. *J Nat Sci Biol Med*. 2014;5(1):158. doi:10.4103/0976-9668.127317
268. Shokrgozar N, Amirian N, Ranjbaran R, Bazrafshan A, Sharifzadeh S. Evaluation of regulatory T cells frequency and FoxP3/GDF-15 gene expression in β-thalassemia major patients with and without alloantibody; correlation with serum ferritin and folate levels.

Ann Hematol. 2020;99(3):421-429. doi:10.1007/S00277-020-03931-9/FIGURES/2
269. Lai Y, Zhao S, Chen B, et al. Iron controls T helper cell pathogenicity by promoting glucose metabolism in autoimmune myopathy. *Clin Transl Med*. 2022;12(8):e999. doi:10.1002/CTM2.999
270. Oh H, Zhao J, Grinberg-Bleyer Y, et al. PDK1 is required for maintenance of CD4+ FoxP3+ regulatory T cell function. *J Immunol*. 2021;206(8):1776. doi:10.4049/JIMMUNOL.2000051
271. Feng P, Yang Q, Luo L, et al. The kinase PDK1 regulates regulatory T cell survival via controlling redox homeostasis. *Theranostics*. 2021;11(19):9503. doi:10.7150/THNO.63992
272. Zhang Z, Salgado OC, Liu B, et al. An OGT-STAT5 Axis in Regulatory T Cells Controls Energy and Iron Metabolism. *Front Immunol*. 2022;13. doi:10.3389/FIMMU.2022.874863/FULL
273. Zeng H, Chi H. The interplay between regulatory T cells and metabolism in immune regulation. *Oncoimmunology*. 2013;2(11). doi:10.4161/ONCI.26586
274. Tomita S, Ueno M, Sakamoto M, et al. Defective Brain Development in Mice Lacking the Hif-1 α Gene in Neural Cells . *Mol Cell Biol*. 2003;23(19):6739-6749. doi:10.1128/mcb.23.19.6739-6749.2003
275. Gruber M, Hu C, Johnson RS, Brown EJ, Keith B, Simon MC. Gruber et al. - 2006 - Acute postnatal ablation of Hif-2 ␣ results in anemia.pdf. *Am J Physiol - Endocrinol Metab*. 2006;10(2).
276. Tomita S, Sinal CJ, Sun Hee Yim, Gonzalez FJ. Conditional disruption of the aryl hydrocarbon receptor nuclear translocator (Arnt) gene leads to loss of target gene induction by the aryl hydrocarbon receptor and hypoxia-inducible factor 1α. *Mol Endocrinol*. 2000;14(10):1674-1681. doi:10.1210/mend.14.10.0533
277. Vooijs M, Jonkers J, Berns A. A highly efficient ligand-regulated Cre recombinase mouse line shows that LoxP recombination is position dependent. *EMBO Rep*. 2001;2(4):292-297. doi:10.1093/embo-reports/kve064
278. Qin Q, Fan J, Zheng R, et al. Lisa: inferring transcriptional regulators through integrative modeling of public chromatin accessibility and ChIP-seq data. *Genome Biol*. 2020;21(1):1-14. doi:10.1186/S13059-020-1934-6/FIGURES/6
279. Hodson EJ, Nicholls LG, Turner PJ, et al. Regulation of ventilatory sensitivity and carotid body proliferation in hypoxia by the PHD2/HIF-2 pathway. *J Physiol*. 2016;594(5):1179-1195. doi:10.1113/JP271050
280. Geindreau M, Ghiringhelli F, Bruchard M. Vascular Endothelial Growth Factor, a Key Modulator of the Anti-Tumor Immune Response. *Int J Mol Sci*. 2021;22(9). doi:10.3390/IJMS22094871
281. Yang Y, Cui H, Li D, et al. Prognosis and Immunological Characteristics of PGK1 in Lung Adenocarcinoma: A Systematic Analysis. *Cancers (Basel)*. 2022;14(21). doi:10.3390/CANCERS14215228
282. Jiang X, Tian W, Kim D, et al. Hypoxia and Hypoxia-Inducible Factors in Lymphedema. *Front Pharmacol*. 2022;13:851057. doi:10.3389/FPHAR.2022.851057/BIBTEX
283. Sharma K, Mishra A, Singh HN, et al. High-altitude pulmonary edema is aggravated by risk loci and associated transcription factors in HIF-prolyl hydroxylases. *Hum Mol Genet*. 2021;30(18):1734-1749. doi:10.1093/HMG/DDAB139
284. Hatanaka M, Shimba S, Sakaue M, et al. Hypoxia-inducible factor-3alpha functions as an

accelerator of 3T3-L1 adipose differentiation. *Biol Pharm Bull*. 2009;32(7):1166-1172. doi:10.1248/BPB.32.1166
285. Yang SL, Wu C, Xiong ZF, Fang X. Progress on hypoxia-inducible factor-3: Its structure, gene regulation and biological function (Review). *Mol Med Rep*. 2015;12(2):2411-2416. doi:10.3892/MMR.2015.3689/HTML
286. Duan C. Hypoxia-inducible factor 3 biology: Complexities and emerging themes. *Am J Physiol - Cell Physiol*. 2016;310(4):C260-C269. doi:10.1152/AJPCELL.00315.2015/ASSET/IMAGES/LARGE/ZH00021678650003.JPEG
287. Jaśkiewicz M, Moszyńska A, Serocki M, et al. Hypoxia-inducible factor (HIF)-3a2 serves as an endothelial cell fate executor during chronic hypoxia. *EXCLI J*. 2022;21:454. doi:10.17179/EXCLI2021-4622
288. ID M, MC T, A Y, et al. Metabolic control of type 1 regulatory T cell differentiation by AHR and HIF1-α. *Nat Med*. 2015;21(6):638-646. doi:10.1038/NM.3868
289. Merchak AR, Cahill HJ, Brown LC, et al. The activity of the aryl hydrocarbon receptor in T cells tunes the gut microenvironment to sustain autoimmunity and neuroinflammation. *PLOS Biol*. 2023;21(2):e3002000. doi:10.1371/JOURNAL.PBIO.3002000
290. Tsaktanis T, Beyer T, Nirschl L, et al. Aryl Hydrocarbon Receptor Plasma Agonist Activity Correlates WithDisease Activity in Progressive MS. *Neurol Neuroimmunol Neuroinflammation*. 2021;8(2). doi:10.1212/NXI.0000000000000933
291. Campesato LF, Budhu S, Tchaicha J, et al. Blockade of the AHR restricts a Treg-macrophage suppressive axis induced by L-Kynurenine. *Nat Commun 2020 111*. 2020;11(1):1-11. doi:10.1038/s41467-020-17750-z
292. Ye J, Qiu J, Bostick JW, et al. Aryl Hydrocarbon Receptor Preferentially Marks and Promotes Gut Regulatory T Cells. *Cell Rep*. 2017;21(8):2277. doi:10.1016/J.CELREP.2017.10.114
293. Cui X, Ye Z, Wang D, et al. Aryl hydrocarbon receptor activation ameliorates experimental colitis by modulating the tolerogenic dendritic and regulatory T cell formation. *Cell Biosci*. 2022;12(1):1-13. doi:10.1186/S13578-022-00780-Z/FIGURES/9
294. Liu X, Hu H, Fan H, et al. The role of STAT3 and AhR in the differentiation of CD4 + T cells into Th17 and Treg cells. *Med (United States)*. 2017;96(17). doi:10.1097/MD.0000000000006615
295. Cheng J, Wang S, Lv S-Q, Song Y, Guo N-H. Resveratrol inhibits AhR/Notch axis and reverses Th17/Treg imbalance in purpura by activating Foxp3. *Toxicol Res (Camb)*. 2023;12(3):381-391. doi:10.1093/TOXRES/TFAD021
296. Li L, Madu CO, Lu A, Lu Y. HIF-1α Promotes A Hypoxia-Independent Cell Migration. *Open Biol J*. 2010;3(1):8. doi:10.2174/1874196701003010008
297. Fei M, Guan J, Xue T, et al. Hypoxia promotes the migration and invasion of human hepatocarcinoma cells through the HIF-1α–IL-8–Akt axis. *Cell Mol Biol Lett*. 2018;23(1). doi:10.1186/S11658-018-0100-6
298. Burke B, Giannoudis A, Corke KP, et al. Hypoxia-induced gene expression in human macrophages: Implications for ischemic tissues and hypoxia-regulated gene therapy. *Am J Pathol*. 2003;163(4):1233-1243. doi:10.1016/S0002-9440(10)63483-9
299. Klotzsche-Von Ameln A, Muschter A, Heimesaat MM, Breier G, Wielockx B. HIF prolyl hydroxylase-2 inhibition diminishes tumor growth through matrix metalloproteinase-induced TGFβ activation HIF prolyl hydroxylase-2 inhibition diminishes tumor growth

through matrix metalloproteinase-induced TGFb activation. 2012. doi:10.4161/cbt.13.4.18830
300. Szabo PA, Levitin HM, Miron M, et al. Single-cell transcriptomics of human T cells reveals tissue and activation signatures in health and disease. *Nat Commun*. 2019;10(1). doi:10.1038/S41467-019-12464-3
301. Ricardo Miragaia AJ, Gomes T, Chomka A, Haniffa M, Powrie F, Teichmann Correspondence SA. Single-Cell Transcriptomics of Regulatory T Cells Reveals Trajectories of Tissue Adaptation. *Immunity*. 2019;50:493-504.e7. doi:10.1016/j.immuni.2019.01.001
302. Benjamin J. Meckiff1 6, , Ciro Ramírez-Suástegui1 6, , Vicente Fajardo1 6, et al. Single-cell transcriptomic analysis of SARS-CoV-2 reactive CD4+ T cells. 2020.
303. Zemmour D, Zilionis R, Kiner E, Klein AM, Mathis D, Benoist C. Single-cell gene expression reveals a landscape of regulatory T cell phenotypes shaped by the TCR article. *Nat Immunol*. 2018;19(3):291-301. doi:10.1038/s41590-018-0051-0
304. Naka K, Ochiai R, Matsubara E, et al. The lysophospholipase D enzyme Gdpd3 is required to maintain chronic myelogenous leukaemia stem cells. *Nat Commun*. 2020;11(1). doi:10.1038/S41467-020-18491-9
305. Yin X, Rang X, Hong X, Zhou Y, Xu C, Fu J. Immune cells transcriptome-based drug repositioning for multiple sclerosis. *Front Immunol*. 2022;13:1020721. doi:10.3389/FIMMU.2022.1020721/FULL
306. Hoelzinger DB, Dominguez AL, Cohen PA, Gendler SJ. Inhibition of adaptive immunity by IL9 can be disrupted to achieve rapid t-cell sensitization and rejection of progressive tumor challenges. *Cancer Res*. 2014;74(23):6845-6855. doi:10.1158/0008-5472.CAN-14-0836/651449/AM/INHIBITION-OF-ADAPTIVE-IMMUNITY-BY-IL-9-CAN-BE
307. Lacroix M, Beauchemin H, Khandanpour C, Möröy T. The RNA helicase DDX3 and its role in c-MYC driven germinal center-derived B-cell lymphoma. *Front Oncol*. 2023;13:1148936. doi:10.3389/FONC.2023.1148936/BIBTEX
308. Liu T, Guevara OE, Warburton RR, Hill NS, Gaestel M, Kayyali US. Modulation of HSP27 alters hypoxia-induced endothelial permeability and related signaling pathways. *J Cell Physiol*. 2009;220(3):600-610. doi:10.1002/jcp.21773
309. Hayakawa M, Hayakawa H, Ritprajak T, Sutavani P, Jiménez-Andrade. Loss of Functionally Redundant p38 Isoforms in T Cells Enhances Regulatory T Cell Induction*. *J Biol Chem*. 2017;292(5):1762-1772. doi:10.1074/jbc.M116.764548
310. Murray SE, Polesso F, Rowe AM, et al. NF-κB-inducing kinase plays an essential T cell-intrinsic role in graft-versus-host disease and lethal autoimmunity in mice. *J Clin Invest*. 2011;121(12):4775-4786. doi:10.1172/JCI44943
311. Polesso F, Sarker M, Anderson A, Parker DC, Murray SE. Constitutive expression of NF-κB inducing kinase in regulatory T cells impairs suppressive function and promotes instability and pro-inflammatory cytokine production. *Sci Rep*. 2017;7(1):1-16. doi:10.1038/s41598-017-14965-x
312. Yi M-J, Park S-H, Cho H-N, et al. Heat-Shock Protein 25 (Hspb1) Regulates Manganese Superoxide Dismutase through Activation of Nfkb (NF-κB). *Radiat Res*. 2002;158(5):641-649. doi:10.1667/0033-7587(2002)158[0641:hsphrm]2.0.co;2
313. Zemmour D, Charbonnier LM, Leon J, et al. Single-cell analysis of FOXP3 deficiencies in humans and mice unmasks intrinsic and extrinsic CD4+ T cell perturbations. *Nat Immunol*. 2021;22(5):607-619. doi:10.1038/s41590-021-00910-8

314. Hao X, Zhang J, Chen G, Cao W, Chen H, Chen S. Aberrant expression of GSTM5 in lung adenocarcinoma is associated with DNA hypermethylation and poor prognosis. *BMC Cancer*. 2022;22(1):1-13. doi:10.1186/S12885-022-09711-0/FIGURES/8
315. Kim JH, Ahn JB, Kim DH, et al. Glutathione S-transferase theta 1 protects against colitis through goblet cell differentiation via interleukin-22. *FASEB J*. 2020;34(2):3289-3304. doi:10.1096/FJ.201902421R
316. Thornton AM, Lu J, Korty PE, et al. Helios + and Helios − Treg subpopulations are phenotypically and functionally distinct and express dissimilar TCR repertoires. *Eur J Immunol*. 2019;49(3). doi:10.1002/eji.201847935
317. Katagiri T, Yamazaki S, Fukui Y, et al. JunB plays a crucial role in development of regulatory T cells by promoting IL-2 signaling. *Mucosal Immunol 2019 125*. 2019;12(5):1104-1117. doi:10.1038/s41385-019-0182-0
318. Barra MM, Richards DM, Hansson J, et al. Transcription Factor 7 Limits Regulatory T Cell Generation in the Thymus. *J Immunol*. 2015;195(7):3058-3070. doi:10.4049/jimmunol.1500821
319. Yang B-H, Wang K, Lu L-F, Xue H-H, Fu Correspondence W. TCF1 and LEF1 Control Treg Competitive Survival and Tfr Development to Prevent Autoimmune Diseases. *Cell Rep*. 2019;27:3629-3645. doi:10.1016/j.celrep.2019.05.061
320. Miyazaki M, Miyazaki K, Chen S, et al. Id2 and Id3 maintain the regulatory T cell pool to suppress inflammatory disease. *Nat Immunol*. 2014;15(8):767-776. doi:10.1038/NI.2928
321. Rauch KS, Hils M, Lupar E, et al. Id3 Maintains Foxp3 Expression in Regulatory T Cells by Controlling a Transcriptional Network of E47, Spi-B, and SOCS3. *Cell Rep*. 2016;17(11):2827-2836. doi:10.1016/j.celrep.2016.11.045
322. Ferreira RC, Simons HZ, Thompson WS, et al. Cells with Treg-specific FOXP3 demethylation but low CD25 are prevalent in autoimmunity. *J Autoimmun*. 2017;84:75. doi:10.1016/J.JAUT.2017.07.009
323. Benamar M, Chen Q, Chou J, et al. The Notch1/CD22 signaling axis disrupts Treg function in SARS-CoV-2–associated multisystem inflammatory syndrome in children. *J Clin Invest*. 2023;133(1). doi:10.1172/JCI163235
324. Samon JB, Champhekar A, Minter LM, et al. Notch1 and TGFβ1 cooperatively regulate Foxp3 expression and the maintenance of peripheral regulatory T cells. *Blood*. 2008;112(5):1813-1821. doi:10.1182/BLOOD-2008-03-144980
325. Wu W, Nie L, Zhang L, Li Y. The notch pathway promotes NF-κB activation through Asb2 in T cell acute lymphoblastic leukemia cells. *Cell Mol Biol Lett*. 2018;23(1). doi:10.1186/S11658-018-0102-4
326. Nie L, Zhao Y, Wu W, Yang YZ, Wang HC, Sun XH. Notch-induced Asb2 expression promotes protein ubiquitination by forming non-canonical E3 ligase complexes. *Cell Res*. 2011;21(5):754-769. doi:10.1038/CR.2010.165
327. Ryan RJH, Petrovic J, Rausch DM, et al. A B Cell Regulome Links Notch to Downstream Oncogenic Pathways in Small B Cell Lymphomas. *Cell Rep*. 2017;21(3):784-797. doi:10.1016/J.CELREP.2017.09.066
328. Gianchecchi E, Fierabracci A. Inhibitory Receptors and Pathways of Lymphocytes: The Role of PD-1 in Treg Development and Their Involvement in Autoimmunity Onset and Cancer Progression. *Front Immunol*. 2018;9:2374. doi:10.3389/fimmu.2018.02374
329. Aksoylar HI, Boussiotis VA. PD-1+ Treg cells: a foe in cancer immunotherapy? *Nat Immunol 2020 2111*. 2020;21(11):1311-1312. doi:10.1038/s41590-020-0801-7

330. Tang W, Dong M, Teng F, et al. TMT-based quantitative proteomics reveals suppression of SLC3A2 and ATP1A3 expression contributes to the inhibitory role of acupuncture on airway inflammation in an OVA-induced mouse asthma model. *Biomed Pharmacother*. 2021;134:111001. doi:10.1016/J.BIOPHA.2020.111001
331. Karitskaya I, Aksenov N, Vassilieva I, Zenin V, Marakhova I. Long-term regulation of Na,K-ATPase pump during T-cell proliferation. *Pflugers Arch Eur J Physiol*. 2010;460(4):777-789. doi:10.1007/S00424-010-0843-Z/TABLES/2
332. Xu W, Zhao X, Wang X, et al. The Transcription Factor Tox2 Drives T Follicular Helper Cell Development via Regulating Chromatin Accessibility. *Immunity*. 2019;51(5):826-839.e5. doi:10.1016/J.IMMUNI.2019.10.006
333. Knosp CA, Schiering C, Spence S, et al. Regulation of Foxp3+ Inducible Regulatory T Cell Stability by SOCS2. *J Immunol Author Choice*. 2013;190(7):3235. doi:10.4049/JIMMUNOL.1201396
334. Escobar G, Mangani D, Anderson AC. T cell factor 1 (Tcf1): a master regulator of the T cell response in disease. *Sci Immunol*. 2020;5(53). doi:10.1126/SCIIMMUNOL.ABB9726
335. Vaeth M, Wang Y-H, Eckstein M, et al. Tissue resident and follicular Treg cell differentiation is regulated by CRAC channels. *Nat Commun 2019 101*. 2019;10(1):1-16. doi:10.1038/s41467-019-08959-8
336. Koukoulas K, Giakountis A, Karagiota A, et al. ERK signaling controls productive HIF-1 binding to chromatin and cancer cell adaptation to hypoxia through HIF-1α interaction with NPM1. *Mol Oncol*. 2021;15(12):3468-3489. doi:10.1002/1878-0261.13080
337. Musiani D, Konda JD, Pavan S, et al. Heat-shock protein 27 (HSP27, HSPB1) is up-regulated by MET kinase inhibitors and confers resistance to MET-targeted therapy. *FASEB J*. 2014;28(9):4055. doi:10.1096/FJ.13-247924
338. Kristan A, Debeljak N, Kunej T. Integration and Visualization of Regulatory Elements and Variations of the EPAS1 Gene in Human. *Genes (Basel)*. 2021;12(11). doi:10.3390/GENES12111793
339. Koong A, Chen E, Giaccia A. Hypoxia Causes the Activation of Nuclear Factor κB through the Phosphorylation of IκBα on Tyrosine Residues. *Cancer Res*. 1994.
340. Grinberg-Bleyer Y, Caron R, Seeley JJ, et al. The alternative NF-κB pathway in regulatory T cell homeostasis and suppressive function. *J Immunol*. 2018;200(7):2362. doi:10.4049/JIMMUNOL.1800042
341. Guo Z, Wang G, Wu B, et al. DCAF1 regulates Treg senescence via the ROS axis during immunological aging. *J Clin Invest*. 2020;130(11):5893-5908. doi:10.1172/JCI136466
342. Bai X, Jin X, Yang Y, et al. Parasitology Glutathione-S-transferase of Trichinella spiralis regulates maturation and function of dendritic cells. 2019. doi:10.1017/S003118201900115X
343. Nikolouli E, Elfaki Y, Herppich S, et al. Recirculating IL-1R2+ Tregs fine-tune intrathymic Treg development under inflammatory conditions. *Cell Mol Immunol*. January 2020:1-12. doi:10.1038/s41423-019-0352-8
344. Lamarche C, Novakovsky GE, Qi CN, et al. Repeated stimulation or tonic-signaling chimeric antigen receptors drive regulatory T cell exhaustion. *bioRxiv*. June 2020:2020.06.27.175158. doi:10.1101/2020.06.27.175158
345. Zhou C, Tuong ZK, Lukowski SW, Chandra J, Frazer IH. Antigen Nonspecific Induction of Distinct Regulatory T Cell States in Oncogene-Driven Hyperproliferative Skin. *ImmunoHorizons*. 2021;5(2):102-116. doi:10.4049/immunohorizons.2100006

346. Koizumi S ichi, Sasaki D, Hsieh TH, et al. JunB regulates homeostasis and suppressive functions of effector regulatory T cells. *Nat Commun 2018 91*. 2018;9(1):1-14. doi:10.1038/s41467-018-07735-4
347. Wu J, Ma S, Hotz-Wagenblatt A, et al. Regulatory T cells sense effector T-cell activation through synchronized JunB expression. *FEBS Lett*. 2019;593(10):1020-1029. doi:10.1002/1873-3468.13393
348. Schuster M, Plaza-Sirvent C, Visekruna A, Huehn J, Schmitz I. Generation of Foxp3+CD25− regulatory T-cell precursors requires c-rel and IκBNS. *Front Immunol*. 2019;10(JULY):460324. doi:10.3389/FIMMU.2019.01583/BIBTEX
349. Dejaco C, Duftner C, Grubeck-Loebenstein B, Schirmer M. Imbalance of regulatory T cells in human autoimmune diseases. *Immunology*. 2006;117(3):289. doi:10.1111/J.1365-2567.2005.02317.X
350. Magee CN, Murakami N, Borges TJ, et al. Notch-1 Inhibition Promotes Immune Regulation in Transplantation Via Regulatory T Cell-Dependent Mechanisms. *Circulation*. 2019;140(10):846-863. doi:10.1161/CIRCULATIONAHA.119.040563
351. Maillard I, Yan M, Siebel CW, et al. Transplantation Mechanisms in a Mouse Model of Heart Mediated by Cellular and Humoral Ligands Prevents Allograft Rejection Transient Blockade of Delta-like Notch. *J Immunol Ref*. 2015;194:2899-2908. doi:10.4049/jimmunol.1402034
352. Zheng X, Linke S, Dias JM, et al. Interaction with factor inhibiting HIF-1 defines an additional mode of cross-coupling between the Notch and hypoxia signaling pathways. *Proc Natl Acad Sci U S A*. 2008;105(9):3368. doi:10.1073/PNAS.0711591105
353. Yan Y, Liu F, Han L, et al. HIF-2α promotes conversion to a stem cell phenotype and induces chemoresistance in breast cancer cells by activating Wnt and Notch pathways. *J Exp Clin Cancer Res*. 2018;37(1):1-14. doi:10.1186/S13046-018-0925-X/FIGURES/5
354. Mutvei AP, Landor SKJ, Fox R, et al. Notch signaling promotes a HIF2α-driven hypoxic response in multiple tumor cell types. *Oncogene*. 2018;37(46):6083. doi:10.1038/S41388-018-0400-3
355. Zhou Y, Chen H, Liu L, et al. CD74 Deficiency Mitigates Systemic Lupus Erythematosus–like Autoimmunity and Pathological Findings in Mice. *J Immunol*. 2017;198(7):2568-2577. doi:10.4049/jimmunol.1600028
356. Paterson AM, Lovitch SB, Sage PT, et al. Deletion of CTLA-4 on regulatory T cells during adulthood leads to resistance to autoimmunity. *J Exp Med*. 2015;212(10):1603. doi:10.1084/JEM.20141030
357. Wing JB, Tekgüç M, Sakaguchi S. Control of Germinal Center Responses by T-Follicular Regulatory Cells. *Front Immunol*. 2018;9:406217. doi:10.3389/FIMMU.2018.01910/BIBTEX
358. Wing JB, Kitagawa Y, Locci M, et al. A distinct subpopulation of CD25- T-follicular regulatory cells localizes in the germinal centers. *Proc Natl Acad Sci U S A*. 2017;114(31):E6400-E6409. doi:10.1073/PNAS.1705551114
359. Chen Y, Shen S, Gorentla BK, Gao J, Zhong X-P. Murine regulatory T cells contain hyper-proliferative and death-prone subsets with differential ICOS expression. *J Immunol*. 2012;188(4):1698. doi:10.4049/JIMMUNOL.1102448
360. Gavin MA, Clarke SR, Negrou E, Gallegos A, Rudensky A. Homeostasis and anergy of CD4+CD25+ suppressor T cells in vivo. *Nat Immunol 2001 31*. 2001;3(1):33-41. doi:10.1038/ni743

361. Wideman SK, Frost JN, Richter FC, et al. Cellular iron governs the host response to malaria. *bioRxiv*. February 2023:2023.02.05.527208. doi:10.1101/2023.02.05.527208
362. Frost JN, Wideman SK, Preston AE, et al. Plasma iron controls neutrophil production and function. *Sci Adv*. 2022;8(40):5384. doi:10.1126/SCIADV.ABQ5384/SUPPL_FILE/SCIADV.ABQ5384_SM.PDF
363. Darce J, Rudra D, Li L, et al. An N-Terminal Mutation of the Foxp3 Transcription Factor Alleviates Arthritis but Exacerbates Diabetes. *Immunity*. 2012;36(5):731-741. doi:10.1016/J.IMMUNI.2012.04.007
364. Bettini ML, Pan F, Bettini M, et al. Loss of epigenetic modification driven by the Foxp3 transcription factor leads to regulatory T cell insufficiency. *Immunity*. 2012;36(5):717-730. doi:10.1016/J.IMMUNI.2012.03.020
365. Cheng M, Liu P, Xu LX. Iron promotes breast cancer cell migration via IL-6/JAK2/STAT3 signaling pathways in a paracrine or autocrine IL-6-rich inflammatory environment. *J Inorg Biochem*. 2020;210. doi:10.1016/J.JINORGBIO.2020.111159
366. de Sousa M, Path M, Smithyman A, Tan C. Suggested Models of Ecotaxopathy in Lymphoreticular Malignancy A Role for Iron-Binding Proteins in the Control of Lymphoid Cell Migration.
367. Kulhankova K, Rouse T, Nasr ME, Field EH. Dendritic Cells Control CD4+CD25+ Treg Cell Suppressor Function In Vitro through Juxtacrine Delivery of IL-2. *PLoS One*. 2012;7(9):e43609. doi:10.1371/JOURNAL.PONE.0043609
368. Wing K, Onishi Y, Prieto-Martin P, et al. CTLA-4 control over Foxp3+ regulatory T cell function. *Science (80-)*. 2008;322(5899):271-275. doi:10.1126/SCIENCE.1160062
369. Caudy AA, Reddy ST, Chatila T, Atkinson JP, Verbsky JW. CD25 deficiency causes an immune dysregulation, polyendocrinopathy, enteropathy, X-linked-like syndrome, and defective IL-10 expression from CD4 lymphocytes. *J Allergy Clin Immunol*. 2007;119(2):482-487. doi:10.1016/j.jaci.2006.10.007
370. Raczkowski F, Rissiek A, Ricklefs I, et al. CD39 is upregulated during activation of mouse and human T cells and attenuates the immune response to Listeria monocytogenes. *PLoS One*. 2018;13(5):e0197151. doi:10.1371/JOURNAL.PONE.0197151
371. La Manna G, Ghinatti G, Tazzari PL, et al. Neutrophil Gelatinase-Associated Lipocalin Increases HLA-G+/FoxP3+ T-Regulatory Cell Population in an In Vitro Model of PBMC. *PLoS One*. 2014;9(2). doi:10.1371/JOURNAL.PONE.0089497
372. Van De Veen W, Stanic B, Yaman G, et al. IgG4 production is confined to human IL-10–producing regulatory B cells that suppress antigen-specific immune responses. *J Allergy Clin Immunol*. 2013;131(4):1204-1212. doi:10.1016/J.JACI.2013.01.014
373. Preza GC, Ruchala P, Pinon R, et al. Minihepcidins are rationally designed small peptides that mimic hepcidin activity in mice and may be useful for the treatment of iron overload. *J Clin Invest*. 2011;121(12):4880-4888. doi:10.1172/JCI57693
374. Pilat N, Wiletel M, Weijler AM, et al. Treg-mediated prolonged survival of skin allografts without immunosuppression. *Proc Natl Acad Sci U S A*. 2019;116(27):13508-13516. doi:10.1073/pnas.1903165116
375. Besançon A, Goncalves T, Valette F, et al. A selective CD28 antagonist and rapamycin synergise to protect against spontaneous autoimmune diabetes in NOD mice. *Diabetologia*. 2018;61(8):1811-1816. doi:10.1007/S00125-018-4638-7
376. Tomala J, Weberova P, Tomalova B, et al. IL-2/JES6-1 mAb complexes dramatically increase sensitivity to LPS through IFN-γ production by CD25+Foxp3- T cells. *Elife*.

2021;10. doi:10.7554/ELIFE.62432
377. Heidt S, Vergunst M, Anholts JDH, et al. Presence of intragraft B cells during acute renal allograft rejection is accompanied by changes in peripheral blood B cell subsets. *Clin Exp Immunol*. 2019;196(3):403-414. doi:10.1111/CEI.13269
378. Wright JA, Richards T, Srai SKS. The role of iron in the skin and cutaneous wound healing. *Front Pharmacol*. 2014;5. doi:10.3389/FPHAR.2014.00156
379. Bogensperger C, Hofmann J, Messner F, et al. Ex Vivo Mesenchymal Stem Cell Therapy to Regenerate Machine Perfused Organs. *Int J Mol Sci*. 2021;22(10). doi:10.3390/IJMS22105233
380. Schmid D, Park CG, Hartl CA, et al. T cell-targeting nanoparticles focus delivery of immunotherapy to improve antitumor immunity. *Nat Commun 2017 81*. 2017;8(1):1-12. doi:10.1038/s41467-017-01830-8
381. Cevaal PM, Ali A, Czuba-Wojnilowicz E, et al. In Vivo T Cell-Targeting Nanoparticle Drug Delivery Systems: Considerations for Rational Design. *ACS Nano*. 2021;15(3):3736-3753. doi:10.1021/ACSNANO.0C09514
382. Zhou S, Liu M, Ren F, Meng X, Yu J. The landscape of bispecific T cell engager in cancer treatment. *Biomark Res 2021 91*. 2021;9(1):1-23. doi:10.1186/S40364-021-00294-9
383. Zhang T, Lin Y, Gao Q. Bispecific antibodies targeting immunomodulatory checkpoints for cancer therapy. *Cancer Biol Med*. 2023;20(3):181. doi:10.20892/J.ISSN.2095-3941.2023.0002
384. Lu L-F, Gondek DC, Scott ZA, Noelle RJ. NFκB-Inducing Kinase Deficiency Results in the Development of a Subset of Regulatory T Cells, which Shows a Hyperproliferative Activity upon Glucocorticoid-Induced TNF Receptor Family-Related Gene Stimulation. *J Immunol*. 2005;175(3):1651-1657. doi:10.4049/jimmunol.175.3.1651

Appendix A – Cluster Markers

Cluster 0 Markers

	p_val	avg_logFC	pct.1	pct.2	p_val_adj
Cd74	2.23281947995866e-179	-1.58112168657797	0.046	0.162	5.05153079145848e-175
Tnfrsf4	6.67696902110864e-256	-0.831955359099941	0.037	0.182	1.51059747133562e-251
S100a6	9.50111413786157e-141	-0.810865837553179	0.019	0.103	2.1495320625498e-136
Capg	1.20366285445207e-244	-0.787694391012686	0.152	0.317	2.72316684191237e-240
Il2rb	0	-0.737998572245734	0.058	0.237	0
Foxp3	3.69113062549556e-228	-0.699620405699831	0.017	0.139	8.35081392712115e-224
Ctla4	9.74130604040892e-224	-0.60899998897924	0.042	0.178	2.20387307858211e-219
Ikzf2	8.09856290307713e-234	-0.572493165692251	0.012	0.133	1.83221887119217e-229
Rgs1	6.1265124821919e-89	-0.541519453197896	0.18	0.275	1.38606218397109e-84
Izumo1r	2.14055972381141e-109	-0.524201904283044	0.251	0.363	4.84280231915093e-105
Ifi27l2a	1.18956359946978e-165	-0.509370837954429	0.66	0.743	2.69126868744044e-161
Il2ra	1.65566169866519e-186	-0.459675275813654	0.007	0.103	3.74576902706012e-182
Lgals1	6.85446904188337e-60	-0.451036574822122	0.302	0.377	1.55075507603569e-55
Nr4a1	2.98385874740666e-60	-0.447912635070477	0.09	0.158	6.75068203013284e-56
Icos	4.15477326896974e-84	-0.446128823087827	0.157	0.248	9.39975904371714e-80
Cd82	4.87562272893313e-129	-0.44464114390409	0.387	0.504	1.10306088619383e-124
Id3	7.94317972832709e-114	-0.425526902665454	0.208	0.326	1.79706498173672e-109
Isg15	7.49490469006571e-76	-0.415524711791634	0.115	0.198	1.69564723708047e-71
Vim	1.23147350596269e-90	-0.402243333605922	0.667	0.72	2.786085659898998e-86
Tnfrsf18	4.00628739165521e-123	-0.395837547014657	0.267	0.39	9.06382459488074e-119
Nfkbia	2.56938444001482e-80	-0.394701951377084	0.659	0.713	5.81297535708953e-76
Samhd1	6.1704948859496e-141	-0.374205976072395	0.471	0.585	1.39601276299724e-136
Srgn	7.0617417980744e-66	-0.373890086335471	0.753	0.774	1.59764846439635e-61
Dusp1	4.55041291698122e-56	-0.364020496581674	0.579	0.636	1.02948541833783e-51
Zfp36l1	6.10930900146815e-150	-0.363597647322347	0.661	0.749	1.38217006849216e-145
S100a10	4.25763595430922e-68	-0.356101812124498	0.724	0.761	9.63247558302918e-64
Itgb1	4.36651562745289e-92	-0.353003458827073	0.051	0.127	9.87880495554941e-88
Egr1	2.98317273945136e-38	-0.335330585011742	0.137	0.195	6.74913000573475e-34
Cd81	6.22397454302339e-80	-0.334795529139109	0.108	0.192	1.40811200061361e-75
Cd5	2.77159154446879e-141	-0.325112262916395	0.585	0.69	6.27044871020619e-137
Nrp1	1.05087811545572e-169	-0.322761583547338	0.011	0.102	2.37750664840702e-165
Ndfip1	4.12104493465557e-163	-0.31620239594272	0.718	0.793	9.32345206016475e-159
Socs1	3.02888653736435e-93	-0.313203016967837	0.208	0.314	6.8525529021331e-89
Cish	3.44019887216734e-136	-0.311609640710393	0.029	0.117	7.7831059283914e-132
Prr13	8.04421202099725e-88	-0.309344145439465	0.32	0.418	1.81992252763042e-83
Il9r	7.67661897675936e-128	-0.307196214386568	0.033	0.12	1.73675827730204e-123
Ahnak	1.06182804753537e-129	-0.299387990086574	0.024	0.107	2.40227977474402e-125
Ly6c1	1.42106670010592e-126	0.295710153483566	0.414	0.283	3.21502130231962e-122
Wls	1.91257788703705e-95	-0.28890652791181	0.101	0.193	4.32701621163262e-91
Nfkbid	9.44205450683633e-61	-0.286166815187227	0.088	0.155	2.13617041162665e-56
Igtp	1.77790293911037e-65	-0.286069723960767	0.275	0.364	4.02232760944331e-61
Cd6	1.00329098306762e-119	-0.276311879409004	0.503	0.621	2.26984552009219e-115
Pglyrp1	1.22981563345535e-73	-0.269968015944093	0.102	0.18	2.78233488912938e-69
Cd69	3.31414955856824e-67	-0.268645982436092	0.431	0.524	7.49793196130479e-63
Cst7	1.40899018029281e-61	-0.264678735503412	0.082	0.147	3.18769938389445e-57
Pim1	2.17812328305281e-55	-0.263925248647091	0.216	0.293	4.92778611557867e-51
Stat1	8.2040256703517e-53	-0.262497851194463	0.602	0.658	1.85607876766037e-48
Ptprc	3.62972298316233e-175	-0.262073643517709	0.795	0.862	8.21188527710646e-171
Cd2	4.4699116692199e-139	-0.26119798958155	0.815	0.865	1.01127281604431e-134
Ephx1	1.93021454828815e-76	-0.258975980808192	0.203	0.298	4.36691739404711e-72
Pou2f2	4.22981627729442e-111	-0.257973436048273	0.075	0.171	9.5695363457509e-107
Itm2a	6.83791186321 12e-64	-0.257823454797191	0.162	0.247	1.5470091799329e-59
Itm2c	7.77170625986816e-44	-0.256703637711271	0.462	0.521	1.75827082423257e-39
Hspa5	3.54549660314978e-99	-0.250818228647852	0.596	0.687	8.02133151496607e-95

Cluster 1 (lgfbp4) Markers

	p_val	avg_logFC	pct.1	pct.2	p_val_adj
Cd74	3.10694772363693e-168	-1.5726420674494	0.046	0.16	7.0291585299562e-164
Tnfrsf4	4.9176285240034e-238	-0.848571581208425	0.037	0.179	1.11256427727053e-233
S100a6	4.02153448182693e-136	-0.824885054175381	0.018	0.102	9.09831961168525e-132
Capg	4.25472967176722e-224	-0.794742928165229	0.155	0.313	9.62590040940616e-220
Il2rb	9.69216895652171e-307	-0.752149173126045	0.056	0.234	2.19275630472347e-302
Foxp3	2.08897612166463e-218	-0.701557328446824	0.016	0.137	4.72609957765406e-214
Rgs1	1.43912107819292e-103	-0.586004267018641	0.171	0.276	3.25586752730365e-99
Ikzf2	1.43580928987723e-223	-0.580685333437736	0.011	0.132	3.24837493741824e-219
Ctla4	1.04476830437148e-169	-0.577942194921976	0.053	0.172	2.36368381181003e-165
Izumo1r	3.35580425111529e-105	-0.551699305417474	0.252	0.361	7.59217153772322e-101
Igfbp4	3.35556683351872e-257	0.463177554230777	0.739	0.554	7.59163440415276e-253
Srgn	4.04202128506007e-150	-0.455183751800505	0.711	0.787	9.1446689553199e-146
Lgals1	5.60880475063018e-73	-0.446927539514017	0.29	0.38	1.26893598678257e-68
Il2ra	4.95438724630951e-173	-0.446676392209466	0.007	0.102	1.12088057060506e-168
Nfkbia	7.75925555663587e-106	-0.440233942608075	0.647	0.716	1.7554539771333e-101
Icos	1.617619009636 35e-61	-0.426795211612387	0.167	0.243	3.65970124740127e-57
Cd82	1.39186266401142e-98	-0.419289024292282	0.403	0.497	3.14895009105943e-94
Ifi27l2a	1.681586552468 36e-77	-0.380774675935106	0.684	0.734	3.80442141630441e-73
Tnfrsf18	8.99280546695249e-81	-0.366179127256253	0.29	0.381	2.03453230884333e-76
Ly6a	1.34044035721415e-62	-0.364546179067456	0.484	0.554	3.03261226416129e-58
S100a10	4.92652017410771e-64	-0.347139851764916	0.729	0.758	1.11457592419013e-59
Prr13	6.44736123415925e-111	-0.345131694580638	0.308	0.42	1.45865100561619e-106
Isg15	5.0495567262038e-26	-0.344475407898767	0.143	0.188	1.14241171373635e-21
Cst7	1.34057218485758e-101	-0.329473865137992	0.065	0.152	3.03291051102178e-97
Itgb1	5.78376361027398e-58	-0.327819112436536	0.062	0.122	1.30851867918839e-53
Nrp1	1.37240601606141e-157	-0.319847931922571	0.011	0.101	3.10493137073734e-153
Pglyrp1	6.70263375361623e-105	-0.3188185045260 2	0.088	0.183	1.51640386041814e-100
Ly6e	1.04648493649263e-262	-0.313080516342603	0.942	0.973	2.36756752032093e-258
Cd81	6.35564629652283e-56	-0.31214150801222	0.118	0.187	1.43790141812533e-51
Lef1	0	0.304399687826943	0.939	0.788	0
Cish	1.91570025513e-107	-0.297498188846454	0.034	0.113	4.33408025720612e-103
Satb1	8.77950587980208e-195	0.287574594610577	0.584	0.412	1.98627541024642e-190
Ahnak	9.04083623637984e-108	-0.285804724630897	0.028	0.104	2.04539879011857e-103
Pou2f2	4.16992632483071e-116	-0.280956923954999	0.071	0.171	9.43404131729699e-112
Itm2c	4.76102349436233e-51	-0.272825069084644	0.458	0.521	1.07713395536453e-46
Wls	2.12103357647517e-67	-0.268051969211845	0.11	0.188	4.79862636341742e-63
S100a11	1.18432590961064e-33	-0.256265802241393	0.421	0.469	2.67941893790311e-29
Samhd1	9.65490306151784e-48	-0.255061935652726	0.514	0.569	2.1843252686378e-43
Relb	5.78455498190778e-87	-0.25310730483491	0.123	0.217	1.30869771910682e-82

Cluster 2 (Igfbp4) Markers

	p_val	avg_logFC	pct.1	pct.2	p_val_adj
Cd74	3.63333808613135e-107	-1.55048437652454	0.022	0.147	8.22006408606356e-103
Tnfrsf4	4.1618410374289e-106	-0.773810001281139	0.032	0.159	9.41574916307913e-102
Izumo1r	3.49510659100226e-122	-0.714587412257457	0.182	0.354	7.90732915148351e-118
Il2rb	4.16568187329892e-123	-0.665572886418913	0.056	0.208	9.42443867015149e-119
Rgs1	6.37544881909855e-96	-0.648830190921332	0.121	0.267	1.44238154083286e-91
Foxp3	7.48941071577142e-95	-0.636688014312543	0.012	0.12	1.69440428033613e-90
Ctla4	6.5639030858664e-121	-0.610296406552252	0.021	0.158	1.48501743414641e-116
Capg	1.1127179598615e-42	-0.594999233297635	0.203	0.284	2.51741311239066e-38
Icos	1.2455153132547e-129	-0.589829310235265	0.077	0.244	2.81785384470744e-125
Crip1	0	0.588841048750183	0.894	0.697	0
Nfkbia	6.96314350511887e-140	-0.587549938828952	0.577	0.715	1.57534158659809e-135
Smc4	3.77302184122413e-185	-0.567157314504426	0.322	0.546	8.53608461358548e-181
Stat1	2.71959223430129e-143	-0.532666676675727	0.494	0.663	6.15280547088324e-139
Igfbp4	1.20569384389148e-280	0.527030490344344	0.827	0.569	2.72776175242008e-276
Ikzf2	1.23736088731105e-98	-0.518941429279993	0.007	0.115	2.79940527145251e-94
Dusp1	1.19790898450453e-79	-0.478051667178685	0.515	0.635	2.71014928654306e-75
Rasgrp2	4.56110854866839e-260	0.454180111733507	0.664	0.405	1.03190519805074e-255
Tagln2	3.94963504536301e-256	0.447040677545937	0.872	0.719	8.93565432662927e-252
Ly6a	4.84460171217156e-53	-0.429388266534215	0.458	0.547	1.09604269136169e-48
Ccnd3	4.44077882425509e-179	0.392400725547357	0.741	0.576	1.00468180119947e-174
Dtx1	1.20824808567655e-195	0.38930899665036	0.324	0.142	2.73354046903464e-191
Zfp36l1	1.05290672221413e-102	-0.387581124084215	0.622	0.74	2.38209616833725e-98
Srgn	5.94293896624222e-50	-0.382142856380475	0.721	0.775	1.34453051172264e-45
Ifi27l2a	6.47312954554889e-47	-0.380074762265346	0.663	0.729	1.46448082838498e-42
Emp3	1.86021434778174e-275	0.378831503543887	0.936	0.776	4.20854894042141e-271
Ly6e	5.0846382879833e-194	-0.367155279589706	0.943	0.969	1.15034856627334e-189
Cd81	4.48459359223726e-62	-0.366276788126135	0.079	0.182	1.01459445430776e-57
Gdpd3	3.44473278838035e-45	-0.362732175847773	0.032	0.101	7.7933634604317e-41
Tnfaip3	1.86202448294887e-82	-0.34870836586075	0.179	0.325	4.21264419022351e-78
Ifi47	1.25525337475091e-95	-0.34453798977974	0.586	0.715	2.83988523503646e-91
Id3	6.14585082423058e-40	-0.344319664229841	0.212	0.306	1.39043729047393e-35
Pdlim4	5.23944945774072e-117	0.324071112863447	0.271	0.136	1.18537304531926e-112
Apobec3	3.02621958174703e-77	-0.32323361132415	0.186	0.325	6.84651918174449e-73
Isg15	9.18509383102293e-13	-0.317565524813735	0.139	0.182	2.07803562833063e-08
Gimap7	2.630206965904e-69	-0.315870737005132	0.231	0.366	5.9505802396612e-65
Nr4a1	4.98757746564426e-09	-0.311272131068332	0.111	0.144	0.000112838952582736
Ctss	2.82686631707681e-87	-0.308598561688249	0.478	0.614	6.39550235575457e-83
Actg1	0	0.305112664381178	1	0.999	0
Flna	5.75448378463217e-116	0.305003723474511	0.578	0.407	1.30189441143518e-111
Slfn2	3.2437383777038e-117	-0.304153185793832	0.695	0.814	7.33863370571708e-113
Ass1	1.8738747357243e-148	0.300996494508502	0.801	0.637	4.23945420210266e-144
Il9r	1.36323969598037e-63	-0.297429765096777	0.023	0.108	3.08419348818599e-59
Egr1	3.11255248016009e-21	-0.297287739648529	0.127	0.187	7.04183873111419e-17
Itm2c	4.86920180011225e-43	-0.289246684612048	0.422	0.517	1.1016082152574e-38
Batf	2.67718187737416e-55	-0.288915272351433	0.129	0.237	6.05685627937131e-51
Tent5c	2.09900843415056e-77	-0.288839938068616	0.123	0.257	4.74879668142223e-73
Itgb1	1.39558370989078e-28	-0.286505892937892	0.057	0.114	3.1573685852569e-24
Cd28	1.47963642137515e-72	-0.285735517542794	0.393	0.532	3.34752943971914e-68
Igtp	3.90864299984121e-39	-0.283012123277161	0.255	0.352	8.84291392284075e-35
Tnfrsf18	1.07674225308901e-22	-0.282065258142506	0.303	0.366	2.43602167338859e-18
Cd82	3.80971297810227e-15	-0.278330369393339	0.441	0.479	8.61909464165856e-11
Fam169b	5.02943502700094e-70	-0.277461289236756	0.171	0.304	1.13785943548693e-65
Ifi203	4.05509860286786e-63	-0.276874178329527	0.346	0.476	9.17425507912826e-59
Cst7	2.0259290250886e-39	-0.274898525567099	0.066	0.139	4.58346182636045e-35
Zyx	2.57787809491635e-86	0.272529458559853	0.532	0.389	5.83219140193875e-82
Il7r	6.52698812105191e-35	-0.266471609190463	0.474	0.542	1.47666579250678e-30
Traf1	7.95842581652368e-54	-0.262695943964165	0.204	0.32	1.80051425673032e-49
Slfn1	8.2963229996736e-53	-0.262241744329096	0.475	0.578	1.87696011544616e-48
Lpxn	8.9565522860717e-74	-0.261504188823705	0.101	0.225	2.02633038920086e-69
Tcf7	3.4559822416992e-64	-0.258866879872739	0.621	0.706	7.81881422362028e-60
Peli1	1.23706306152371e-71	-0.257575111069586	0.563	0.682	2.79873174039123e-67
Id2	2.54571379945487e-27	-0.256461259214896	0.161	0.234	5.75942289988671e-23
Tox	2.4740745374612e-57	-0.256342077023858	0.104	0.21	5.59734623355222e-53
Adgre5	6.36986537957241e-71	0.25459929677765	0.532	0.404	1.44111834347446e-66
Ephx1	1.78369975518678e-45	-0.254042811934119	0.182	0.285	4.03544232613457e-41
Gbp2	4.30241286174327e-40	-0.25323434395093	0.137	0.227	9.73377885840798e-36
Nfkbid	2.9055326473591e-27	-0.253036942667959	0.083	0.145	6.57347706138523e-23

Cluster 3 (NFkB) Markers

	p_val	avg_logFC	pct.1	pct.2	p_val_adj
Nr4a1	0	1.34379590608029	0.389	0.12	0
Egr1	2.38341149280108e-237	1.11134601471107	0.398	0.163	5.39223016131316e-233
Nfkbid	0	1.02390939756662	0.425	0.115	0
Id3	9.83780757138283e-287	0.869092504290866	0.578	0.273	2.22570558494965e-282
Nfkbia	2.42604211715190e-264	0.829136559546502	0.855	0.687	5.48867768584445e-260
Cd82	4.88397948410477e-221	0.813957322070525	0.691	0.457	1.10495151848386e-216
Relb	0	0.766255729712407	0.547	0.166	0
Cd74	2.91882779358126e-36	-0.759928638935361	0.219	0.125	6.60355600019824e-32
Vim	1.68933977577841e-215	-0.744251770270599	0.464	0.726	3.82196230872106e-211
Cd69	1.0383068707926e-171	0.711294218978978	0.691	0.485	2.34906546448117e-167
Ptpn6	0	0.694231627521766	0.823	0.544	0
Marcksl1	1.00132283363627e-280	0.66914991561428	0.218	0.047	2.2653927788187e-276
Nfkb2	0	0.66015450055812	0.473	0.14	0
Egr2	0	0.650145894366933	0.204	0.019	0
Nab2	0	0.638594719083285	0.393	0.094	0
Tagap	2.93490217850511e-130	0.621095193558605	0.373	0.191	6.63992268864996e-126
Crip1	4.85673004626189e-189	-0.62010325725388	0.507	0.736	1.09878660566629e-184
Itm2a	5.88983108892482e-53	0.614675997526195	0.335	0.216	1.33251538555835e-48
Eif5a	0	0.589846342019494	0.982	0.925	0
Set	5.51055609902954e-196	0.577844672465588	0.67	0.442	1.24670821184444e-191
Phgdh	1.04927604087667e-130	0.556275201118644	0.493	0.301	2.37388211487937e-126
Ncl	7.7220061695359e-148	0.552425265641591	0.807	0.672	1.7470266757958e-143
Cd5	1.19244307999876e-217	0.537711984500252	0.848	0.648	2.69778322418919e-213
Srgn	1.23913593859663e-64	0.535713999082616	0.82	0.764	2.80342114748101e-60
Txnip	4.50421407627106e-185	-0.530626788437374	0.513	0.759	1.01903339261556e-180
Tnfrsf9	6.44369568442762e-168	0.519829609273098	0.212	0.064	1.4578217116449e-163
Ighm	2.35881404068142e-152	-0.510157159932625	0.488	0.702	5.33658088563764e-148
Rgs1	6.21430205895871e-36	-0.505738861312189	0.154	0.258	1.40592369781882e-31
Ptma	0	0.502295906410187	0.999	0.996	0
Selplg	1.04480948605263e-256	-0.502215907461829	0.673	0.871	2.36377698124548e-252
Pa2g4	2.46969797817071e-139	0.500055166981943	0.708	0.533	5.58744470581341e-135
Hspa5	1.95796615014416e-191	0.497925227620919	0.827	0.65	4.42970261808614e-187
S1pr1	3.04278525703048e-154	-0.492685280726866	0.322	0.584	6.88399736550575e-150
Icam1	2.48860187685114e-119	0.488945776978449	0.234	0.093	5.63021288618803e-115
Srm	2.33749582003553e-155	0.485336234090737	0.428	0.216	5.28835054324837e-151
Selenop	1.15188740767592e-124	-0.47730753097303	0.309	0.548	2.60603007112601e-120
Eif4a1	3.30377526332133e-235	0.465519740657024	0.946	0.86	7.47446115573818e-231
S100a10	2.51426873544124e-103	-0.460603179551188	0.62	0.762	5.68828158706227e-99
Ly6c1	1.69939442349922e-47	-0.45630105478888	0.202	0.326	3.84470994372463e-43
Capg	9.15214167210271e-27	-0.454180456444558	0.194	0.281	2.07058053189652e-22
Hsp90ab1	0	0.452889072582281	0.999	0.992	0
Tsc22d3	8.73132968705845e-103	-0.439459513779822	0.372	0.582	1.9753760284001e-98
C1qbp	1.71552239648894e-141	0.432981416335814	0.683	0.485	3.88119786981657e-137
Apex1	3.84088974294765e-179	0.423324155619272	0.422	0.193	8.68962895444476e-175
Samhd1	5.19822833322125e-87	-0.417541067835509	0.386	0.569	1.17604717810798e-82
Sell	1.35738455130993e-115	-0.415179154861587	0.414	0.625	3.07094680888359e-111
Il2rg	7.21558130143329e-279	0.413065640868814	0.988	0.961	1.63245311363627e-274
Ppan	2.89518133973158e-134	0.412310347900458	0.407	0.21	6.55005826300872e-130
Ran	1.419214846374e-146	0.408108273614508	0.861	0.753	3.21083166843653e-142
Rrad	7.61056933717046e-144	0.405327637944906	0.324	0.14	1.72181520684145e-139
Sept7	1.59286527081887e-119	0.399546506837314	0.799	0.658	3.60369838870062e-115
Mif	5.3783357711592e-64	0.399065293571694	0.829	0.755	1.21679468486706e-59
Shmt2	8.97786196153238e-125	0.396174594550445	0.327	0.153	2.03115149017708e-120
Myc	1.6518704556952e-32	0.394105804089675	0.341	0.25	3.73719171896483e-28
Tspo	4.01555133050876e-183	-0.392038352603449	0.717	0.88	9.08478333014302e-179
Thy1	4.29822679312668e-128	-0.391800992596599	0.742	0.861	9.7243082967698e-124
Lgals1	1.70196088258652e-26	-0.39155539090492	0.276	0.365	3.85051630076375e-22
Socs3	3.02298258316997e-60	-0.390676179768675	0.08	0.212	6.83919579616374e-56
Hspd1	8.26399066221262e-89	0.389493031813455	0.623	0.462	1.86964524741898e-84
Rilpl2	1.42988308692186e-110	0.379419879859995	0.27	0.119	3.23496749585202e-106
Nolc1	8.25563015717405e-105	0.374909150530796	0.443	0.26	1.86775376675906e-100
Zfp36l1	2.70946989690002e-108	0.374273006899728	0.846	0.717	6.1299046947466e-104
Gadd45b	2.51041440815982e-117	0.374098169843645	0.219	0.083	5.67956155702077e-113
Jun	3.03408227091381e-73	-0.368609062598358	0.661	0.777	6.86430772971541e-69

Cluster 4 (Resting Treg) Markers

	p_val	avg_logFC	pct.1	pct.2	p_val_adj
Foxp3	0	1.56714616126525	0.734	0.064	0
Il2ra	0	1.50953223295895	0.633	0.04	0
Rgs1	0	1.50084426369002	0.757	0.215	0
Il2rb	0	1.29754029184143	0.76	0.151	0
Izumo1r	0	1.24946389449529	0.833	0.3	0
Igfbp4	5.28523285316633e-288	-1.17828114515404	0.229	0.625	1.19573108070035e-283
Capg	0	1.09629121733781	0.795	0.238	0
Ikzf2	0	1.05253518503429	0.567	0.07	0
Ecm1	0	0.911665708101515	0.501	0.15	0
Cish	0	0.860634995799382	0.42	0.072	0
Samhd1	0	0.85066826338658	0.872	0.534	0
Ctla4	0	0.84265237880129	0.593	0.111	0
Lrrc32	0	0.82379158200234	0.302	0.007	0
Tnfrsf4	0	0.796588872041664	0.608	0.113	0
Dapl1	2.61575678713754e-140	-0.762318063163614	0.027	0.264	5.91788815521996e-136
Socs1	2.64495365024384e-243	0.754839109754725	0.544	0.269	5.98394313831167e-239
Bcl2	2.11740717334728e-284	0.739781868929611	0.61	0.307	4.79042198898089e-280
Tnfrsf18	0	0.721193365443596	0.708	0.334	0
Socs2	0	0.712844800693108	0.276	0.012	0
Pim1	1.83705271937724e-255	0.695560959456471	0.543	0.254	4.15614807231907e-251
Lef1	0	-0.695173068756955	0.57	0.842	0
Coro2a	0	0.66880357768985	0.318	0.025	0
Lta	1.62825491162879e-159	0.666912357275863	0.318	0.13	3.68376391206897e-155
Cd40lg	7.55646690800384e-189	-0.656612600331942	0.126	0.449	1.70957507326679e-184
Smc4	8.81146679085676e-285	0.634949683173309	0.799	0.501	1.99350624676343e-280
Nrp1	0	0.623371902266411	0.334	0.061	0
Tcf7	2.21294125874126e-203	-0.620798599490733	0.41	0.716	5.00655830377623e-199
Tagln2	6.89827721326309e-205	-0.617870133690437	0.48	0.754	1.56066623672864e-200
Ift80	0	0.6108340239841	0.397	0.106	0
Qpr83	0	0.579918977007967	0.237	0.023	0
Pou2f2	3.51817534868718e-285	0.566660901690587	0.396	0.129	7.95951990886987e-281
Resf1	2.72859265148063e-185	0.558109216429588	0.507	0.265	6.17316801470977e-181
H2afz	2.59705110002222e-166	0.555655965537604	0.848	0.765	5.87556840869027e-162
Ifngr1	2.34161067960744e-166	0.554569519713127	0.584	0.359	5.29766000154387e-162
Cd74	2.38696660197333e-126	-0.543117849475135	0.301	0.121	5.40027324030446e-122
Ikzf4	0	0.541805077207028	0.266	0.033	0
Id3	8.42872659148968e-189	0.524374263152374	0.547	0.278	1.90691510405862e-184
Inpp4b	1.0799384518981e-174	0.523343257296158	0.723	0.522	2.44325275357426e-170
Il7r	3.53122946823645e-119	-0.508512705623607	0.292	0.552	7.98905354893815e-115
Ctsw	6.73638942212758e-137	0.506812116136456	0.44	0.238	1.52404074286214e-132
Igf2r	2.032486126527 2e-213	0.506123986314126	0.316	0.107	4.5982966126551 3e-209
Emb	1.27217271364756e-151	-0.500005487812185	0.325	0.615	2.87816354735624e-147
Ly6e	0	0.492848926139085	0.995	0.964	0
Rhoh	1.50996031340608e-175	0.481319314370708	0.739	0.535	3.4161342130499e-171
Chchd10	1.23775246677107e-151	0.479988739273427	0.397	0.188	2.80029118082287e-147
Rgcc	3.02638215689005e-100	-0.479802757993686	0.134	0.355	6.84688699174804e-96
Rflnb	2.44108789128571e-118	-0.475970587820031	0.09	0.326	5.52271724524478e-114
Hopx	0	0.473268483057844	0.274	0.06	0
Nfkbia	3.15633589742962e-159	0.457484970631722	0.838	0.69	7.14089433434478e-155
Mettl9	6.35487296836081e-128	-0.456213860648326	0.127	0.381	1.43772646036195e-123
Ctss	2.50360836964873e-169	0.456181723702391	0.768	0.586	5.66416357549329e-165
Gramd3	4.73022283395465e-115	-0.454338000507738	0.215	0.468	1.0701656139539e-110
Cd81	5.63056895115267e-224	0.451214071684739	0.411	0.153	1.27385991950878e-219
Socs3	1.94877537961072e-67	0.444537368735868	0.33	0.193	4.4089094188313e-63
Wls	1.39884835746997e-151	0.441403014069931	0.359	0.156	3.16475452394006e-147
Bmyc	4.75850384819687e-115	0.438655293562054	0.407	0.224	1.07656391061606e-110
Traf1	3.321564351908 72e-132	0.437688035658611	0.504	0.293	7.51470718975829e-128
Id2	1.6499618680991e-65	-0.432992569326373	0.081	0.236	3.73287373038739e-61
Gmfg	2.72352276529486e-153	-0.428093226918928	0.556	0.798	6.16169790420308e-149
Ifi27l2a	6.02811480987771e-169	0.423611215013123	0.882	0.711	1.36380069458673e-164
Qpr183	3.90838648793497e-95	-0.420979298893967	0.072	0.272	8.84233359030408e-91
Ms4a6b	2.79837308056176e-168	0.414961174302958	0.925	0.839	6.33103925746293e-164
Trim59	3.28610871773508e-128	0.408495006794141	0.307	0.133	7.43449236300385e-124
Tdrp	8.55567801484273e-100	-0.406786918322122	0.047	0.241	1.93563659407802e-95
Pdlim4	3.97531284752769e-89	-0.406075546293148	0.006	0.162	8.99374778624665e-85
Prkca	2.12184486231856e-107	0.402168744631 89	0.452	0.266	4.80046181650952e-103
Gbp3	1.3638468281296e-231	0.395772115237804	0.191	0.04	3.0855670639604e-227
Capn3	0	0.395558025990178	0.194	0.028	0

Cluster 5 (Active Treg) Markers

	p_val	avg_logFC	pct.1	pct.2	p_val_adj
Tnfrsf4	0	2.25987233346799	0.843	0.111	0
Igfbp4	0	-1.99416061110076	0.026	0.626	0
Ctla4	0	1.94030611658412	0.831	0.11	0
Hspb1	0	1.84279273980493	0.406	0.012	0
Capg	0	1.82781714308424	0.931	0.243	0
Ikzf2	0	1.80850442682555	0.857	0.066	0
S100a6	0	1.80643150815459	0.572	0.058	0
Icos	0	1.7623287752161	0.79	0.197	0
Foxp3	0	1.74491478150645	0.807	0.074	0
Tnfrsf9	0	1.55589092971987	0.551	0.052	0
Il2rb	0	1.5376055037885	0.87	0.158	0
Tigit	0	1.4940620196792	0.545	0.016	0
Cd81	0	1.46340723618536	0.736	0.143	0
Lgals1	0	1.40267087045324	0.748	0.339	0
S100a10	0	1.39929580280137	0.961	0.741	0
Tnfrsf18	0	1.38424081430568	0.844	0.335	0
Itm2c	0	1.31900644310135	0.912	0.486	0
Itgae	0	1.30114744154711	0.424	0.012	0
Srgn	0	1.29137095302333	0.959	0.759	0
Pglyrp1	0	1.28754386364564	0.718	0.133	0
Cst7	0	1.28267080416571	0.65	0.106	0
Penk	0	1.2588228710882	0.123	0.006	0
Dusp1	0	1.22437280667957	0.896	0.608	0
Izumo1r	0	1.22380343946217	0.73	0.315	0
Il1r2	0	1.20280577935028	0.27	0.006	0
Glrx	0	1.19066049060923	0.577	0.155	0
Nfkbia	0	1.14474245521531	0.905	0.689	0
Ccr7	0	-1.13639137110815	0.287	0.858	0
Il9r	0	1.12899127443435	0.548	0.076	0
Lef1	0	-1.11291314696449	0.388	0.845	0
Rgs1	0	1.10294167073128	0.659	0.231	0
Cd83	0	1.08930960154175	0.432	0.028	0
Wls	0	1.08671074864042	0.632	0.147	0
Nrp1	0	1.08596249553561	0.578	0.055	0
S100a11	0	1.05970688435871	0.818	0.44	0
Cd82	0	1.01547162895095	0.862	0.456	0
Rilpl2	0	1.00807058246975	0.508	0.112	0
Ly6c1	5.05853425330705e-148	-1.00534962878162	0.018	0.331	1.14444278946819e-143
Vim	1.32767787317315e-174	1.00370009327447	0.846	0.7	3.00373842026694e-170
Cd74	0	1.0016948402356 6	0.792	0.101	0
Ccr8	0	0.995539453610061	0.344	0.019	0
Sell	5.50944282212625e-300	-0.994220526805139	0.126	0.632	1.24645634407784e-295
Ifi27l2a	0	0.986330968194444	0.93	0.712	0
Tnfrsf1b	0	0.980444772194118	0.487	0.067	0
Prr13	0	0.973532376643973	0.802	0.373	0
Ahnak	0	0.962649750585657	0.501	0.066	0
Batf	0	0.960048281523	0.571	0.208	0
Il2ra	0	0.95169982560377	0.461	0.06	0
Samsn1	0	0.950902963649377	0.475	0.099	0
Pim1	0	0.941142901429721	0.638	0.255	0
Ndfip1	0	0.924215710285595	0.959	0.765	0
Zfp36l1	1.13372035563803e-245	0.922360088304865	0.888	0.719	2.56492893259547e-241
Maf	0	0.921058967501893	0.44	0.033	0
Cish	0	0.897382100888179	0.421	0.079	0
Actn1	1.11811968106598e-234	-0.883824282039579	0.11	0.544	2.52963396644367e-230
Cxcr3	0	0.882762076814494	0.362	0.039	0
Bhlhe40	0	0.881957804938108	0.34	0.034	0
Rgs16	0	0.877925690122973	0.27	0.02	0
Sdf4	0	0.874686059881078	0.87	0.637	0
Serinc3	0	0.861777901679816	0.624	0.259	0
Ebi3	0	0.854353478654689	0.375	0.014	0
Cd2	0	0.832716623077519	0.971	0.846	0
Ighm	3.69977279868598e-252	0.832362436147311	0.864	0.678	8.37036597974716e-248
Ccr4	0	0.824170506835779	0.334	0.017	0
Gadd45b	0	0.820964482270468	0.397	0.078	0
Ddit4	4.38686897102113e-185	0.817987858996301	0.599	0.321	9.9248523600382e-181
Tcf7	2.22516358347932e-239	-0.808900981306117	0.271	0.716	5.0342100912636e-235
Psen2	0	0.805754866064442	0.629	0.248	0

Cluster 6 (IFN Response Markers

	p_val	avg_logFC	pct.1	pct.2	p_val_adj
Cd74	6.45901738607218e-19	-1.33811431837852	0.057	0.136	1.46128809342497e-14
Igtp	0	1.09035452410742	0.813	0.321	0
Stat1	0	1.07279348133619	0.971	0.63	0
Tgtp2	0	0.867147811799953	0.681	0.225	0
Ifi47	0	0.816381429683357	0.953	0.69	0
Gbp2	3.75752064742455e-244	0.784753315663671	0.542	0.203	8.50101471273329e-240
Ly6a	1.03515186423239e-216	0.735758165274252	0.848	0.524	2.34192757763936e-212
Tnfrsf4	5.581740495742e-33	-0.706393616641655	0.038	0.149	1.26281296975667e-28
Irf1	6.11719956280475e-159	0.684391319225744	0.72	0.443	1.38395522908895e-154
Capg	5.15613748350644e-36	-0.672590655076801	0.142	0.28	1.1665245442685e-31
Gbp4	5.99455865268031e-190	0.666290616789756	0.523	0.22	1.35620894958239e-185
Tgtp1	0	0.650057191199321	0.414	0.091	0
Il2rb	5.16364105003462e-41	-0.603201131222346	0.057	0.197	1.16822215115983e-36
Izumo1r	3.26259146377493e-34	-0.590178308295025	0.198	0.34	7.3812869276444e-30
Iigp1	5.66910570427595e-288	0.56693465467697	0.303	0.058	1.28257847453539e-283
Irgm1	2.66258011063204e-187	0.566425302984856	0.446	0.163	6.02382124229392e-183
Foxp3	3.68762232496198e-27	-0.560317781143897	0.022	0.111	8.34287674799399e-23
Ly6c1	3.20478932483097e-82	0.545967291680349	0.526	0.308	7.25051536849758e-78
Ctla4	6.7789055187919e-29	-0.509879542178916	0.044	0.147	1.53365958457148e-24
Gbp7	9.24105881110067e-114	0.499598980236542	0.455	0.216	2.09069714542342e-109
Ikzf2	3.74433038232008e-32	-0.485864757225984	0.01	0.106	8.47117305696094e-28
Rtp4	8.00776223008635e-142	0.452691465942166	0.396	0.149	1.81167612693473e-137
Rgs1	1.19308601059156e-12	-0.446919014054226	0.18	0.253	2.69923779036235e-08
Vim	1.28305597031272e-26	-0.428696124406565	0.636	0.71	2.9027858272355e-22
Zbp1	3.08061458923107e-97	0.424422937256604	0.503	0.27	6.96958244667638e-93
Id3	4.94335797649874e-28	-0.42158689195645	0.169	0.301	1.11838530860307e-23
Cd5	1.69495118587109e-48	-0.419516969034936	0.519	0.669	3.83465756291476e-44
Tap1	9.689601764383e-93	0.409733896801496	0.722	0.498	2.19217550317401e-88
Lgals1	4.15028084449816e-12	-0.407423822620929	0.289	0.361	9.38959538259265e-08
Dusp1	1.75840251671391e-17	-0.387844012592146	0.548	0.624	3.97820985381356e-13
Irf9	1.50847333085943e-77	0.386332505415207	0.431	0.231	3.41277006373638e-73
Gbp8	1.53301065541091e-81	0.378880906062732	0.344	0.16	3.46828330680165e-77
Icos	1.62212832116656e-14	-0.37798800530927	0.148	0.228	3.66990311380505e-10
Tnfrsf18	3.5099528511566e-25	-0.374336441541262	0.241	0.364	7.9409173304567e-21
S100a10	2.74520345812278e-25	-0.370252548008743	0.684	0.754	6.21074830365697e-21
Irgm2	3.63608782025328e-174	0.354970107191347	0.205	0.042	8.22628508454102e-170
Nr4a1	3.21072832951412e-10	-0.353196768435691	0.084	0.143	7.26395177269274e-06
Bst2	3.2912459640012e-74	0.350977121782508	0.596	0.4	7.4461148689563e-70
Psmb9	5.02685048004974e-62	0.31859469556779	0.825	0.686	1.13727465260645e-57
Parp9	1.19033652537336e-60	0.315617363275561	0.335	0.172	2.69301735500469e-56
Psmb10	1.01037786796141e-55	0.311904735882252	0.742	0.588	2.2858788884759e-51
Itgb1	2.35487234013655e-15	-0.306216988292154	0.045	0.11	5.32766318232494e-11
Reep5	1.94251407137687e-31	-0.30265074667224	0.416	0.552	4.39474383508303e-27
Ndfip1	3.139426703183e-36	-0.30213522437654	0.687	0.777	7.10263897328122e-32
Irf7	9.02656030885995e-59	0.297999489244083	0.442	0.256	2.04216900427647e-54
Prr13	2.92550824949541e-19	-0.294789039965983	0.293	0.397	6.61866986365842e-15
Slfn1	2.20730470924435e-55	0.291446076980769	0.735	0.559	4.99380617419443e-51
Cd6	9.39738001588811e-25	-0.283943814471032	0.48	0.595	2.12606325479453e-20
Ephx1	4.74621406237172e-23	-0.281615550077957	0.162	0.278	1.07378346947098e-18
Parp14	5.98214556355057e-41	0.279595395349406	0.284	0.157	1.35340061229768e-36
Cd81	2.14913808400306e-12	-0.277671996305264	0.105	0.173	4.86221000124853e-08
Gbp9	5.99579000812218e-42	0.270644082777861	0.281	0.152	1.35648753143756e-37
Crip1	2.22672768723453e-14	-0.26569480138753	0.672	0.721	5.03774871959941e-10
Id2	3.04576472515389e-13	-0.26231907262237	0.148	0.229	6.89073811418815e-09
Pglyrp1	1.78605349199935e-16	-0.259229319141539	0.084	0.164	4.04076742029933e-12
Psme2	3.10469543234841e-60	0.255112094687304	0.917	0.843	7.02406294614505e-56

Cluster 7 (Teff) Markers

	p_val	avg_logFC	pct.1	pct.2	p_val_adj
Ccl5	8.9472644975487e-234	2.62725744022079	0.156	0.019	2.02422911992542e-229
S100a6	0	2.13625616885316	0.654	0.058	0
Igfbp4	0	-1.83625664093022	0.059	0.621	0
Itgb1	0	1.66740199066635	0.684	0.083	0
Nkg7	0	1.61910416640306	0.32	0.022	0
Cxcr3	0	1.24773805561709	0.508	0.035	0
Lgals1	1.42939422163825e-259	1.23401842143494	0.691	0.344	3.23386148703438e-255
Anxa2	0	1.13890551205791	0.436	0.045	0
Gzmk	0	1.13843468949128	0.125	0.001	0
Id2	1.03125865141596e-286	1.13625363597325	0.571	0.211	2.33311957296346e-282
S100a11	0	1.10783352888743	0.816	0.443	0
Ahnak	0	1.09004155757111	0.513	0.068	0
Lef1	0	-1.08769879999294	0.363	0.843	0
Prr13	0	1.02724852135895	0.827	0.375	0
Il2rb	0	1.00541939910658	0.7	0.17	0
Cxcr6	0	0.999891708768534	0.281	0.01	0
Capg	0	0.969839887398497	0.685	0.258	0
Ly6c1	7.22213759158803e-118	-0.95837418415332	0.031	0.328	1.63393640872088e-113
S100a10	0	0.89060207928691	0.939	0.744	0
Cd82	5.55110335746146e-276	0.886478238614717	0.81	0.46	1.25588162359208e-271
Vim	5.15908327692339e-101	0.828727121682448	0.797	0.703	1.16719100057115e-96
Ifng	0	0.823750965584204	0.228	0.007	0
Icos	4.91977132844245e-291	0.822626227307459	0.59	0.21	1.11304906534682e-286
Lag3	0	0.821767673021512	0.192	0.021	0
Pdcd1	0	0.820194853269805	0.268	0.04	0
Cd7	1.6149049439619e-80	0.817510499056996	0.269	0.113	3.6535609452194e-76
Gpm6b	0	0.810146024993117	0.248	0.013	0
Tnfsf8	3.95945887113495e-184	0.809392326637946	0.38	0.126	8.95787975005572e-180
Ly6a	3.34838310594646e-91	0.783949827990617	0.672	0.531	7.57538193889326e-87
Nrp1	0	0.769873891667221	0.394	0.066	0
Bhlhe40	0	0.759611199079791	0.313	0.037	0
Ifi27l2a	9.14302105498945e-115	0.748858814380884	0.842	0.717	2.06851708348081e-110
Rgs1	1.02876490315391e-124	0.711646781576039	0.506	0.24	2.3274777168954e-120
Cst7	2.27146569479101e-274	0.705163227365369	0.435	0.118	5.13896398789518e-270
Cd44	0	0.700110310387551	0.422	0.082	0
Ccr7	1.10397311027166e-215	-0.696184666407875	0.479	0.847	2.49762876467861e-211
Slamf6	7.77800837719231e-156	0.687919958479377	0.513	0.242	1.75969661525599e-151
Smpdl3a	1.17035646780136e-194	0.68213271442778	0.736	0.43	2.64781447275381e-190
Satb1	4.90047365294585e-139	-0.669238458497359	0.114	0.468	1.10868315924247e-134
Il9r	0	0.66586062061546	0.397	0.086	0
Tnf	3.9546680141437e-147	0.661820350370543	0.291	0.088	8.9470409151987e-143
Actn1	2.24091967340051e-141	-0.659500383431066	0.176	0.538	5.06985666910132e-137
S100a4	0	0.657276473970718	0.253	0.015	0
Cd74	3.48460843646369e-09	-0.654255616633464	0.188	0.13	7.88357812665545e-05
Tbc1d4	8.62496172560031e-278	0.645332911883883	0.274	0.049	1.95131134079981e-273
Atp1b1	3.35174075421453e-124	-0.643997016762526	0.034	0.348	7.58297828233495e-120
Tnfsf11	0	0.642864208483442	0.277	0.029	0
Casp1	0	0.634562583706464	0.351	0.059	0
Tmem176b	1.16810323681271e-142	0.631622076576003	0.131	0.022	2.64271676296508e-138
Ctsb	3.02706856252388e-142	0.630000871341508	0.702	0.455	6.84843991585404e-138
Srgn	5.82873931170123e-216	0.629049524329567	0.935	0.762	1.31869398187929e-211
Ucp2	6.2984437452812e-257	0.620926954942104	0.977	0.943	1.42495991293242e-252
Npc2	1.36620611360113e-230	-0.617263175961831	0.773	0.928	3.09090471141119e-226
Sell	2.30718387218597e-147	-0.601593701061658	0.226	0.625	5.21977279243354e-143
Crip1	2.45917526346757e-45	0.599802026378523	0.773	0.717	5.56363811606903e-41
Ndfip1	1.27206616868787e-216	0.594200765146545	0.928	0.767	2.87792250003945e-212
Tigit	2.84578556340641e-171	0.589396265697987	0.184	0.034	6.43830525865066e-167
Itga4	2.87835783078337e-46	0.58684523054933	0.367	0.237	6.5119967563643e-42
S100a13	3.26488579709957e-150	0.582801315059988	0.716	0.46	7.38647762735806e-146
Rps19	0	-0.5795760636849	0.997	1	0
Cd200	2.98741519040888e-179	0.579111015987585	0.269	0.067	6.75872812678106e-175
Ptpn11	8.83251026403119e-160	0.568959263444658	0.306	0.094	1.99826712213442e-155
Wnt10a	0	0.558016448882296	0.156	0.012	0
Ctla2a	0	0.555467819777231	0.173	0.015	0
Izumo1r	4.33221664806164e-53	0.552982835679359	0.5	0.328	9.80120694457464e-49
Gng2	1.99158383890148e-203	0.552980583252789	0.407	0.13	4.5057592771307e-199
Tmem176a	1.95505514851218e-148	0.55265356392635	0.105	0.014	4.42311676799395e-144
Dusp1	2.95511951762862e-58	0.552384424434584	0.734	0.616	6.685662396683e-54

Cluster 8 Markers

	p_val	avg_logFC	pct.1	pct.2	p_val_adj
Crip1	1.21031620207614e-155	-0.896275438669805	0.454	0.729	2.73821937557705e-151
Cd74	1.54359523210226e-13	-0.827709021978311	0.208	0.129	3.49222985310815e-09
Igfbp4	1.09653811296739e-78	-0.76759340790912	0.387	0.607	2.48080782677743e-74
Smc4	8.93507502759428e-202	0.762637815000064	0.819	0.509	2.02147137424293e-197
Ly6c1	9.21483164456281e-60	-0.681857592412408	0.115	0.324	2.08476351126589e-55
Ly6a	1.47161014894718e-67	-0.675152441290565	0.326	0.545	3.3293708009781e-63
Ass1	5.67949147908974e-129	-0.66391459198106	0.358	0.667	1.28492815222926e-124
Tagln2	1.14092553703334e-107	-0.595421670418335	0.519	0.745	2.58122993498423e-103
Rgs10	2.80453540286713e-170	0.570746651567854	0.903	0.701	6.3449808954666e-166
Srgn	4.86943767747858e-68	-0.569997700159183	0.623	0.774	1.10166158015275e-63
Lgals1	1.71759888422651e-29	-0.536879961983274	0.228	0.363	3.88589571567406e-25
Capg	2.11674747531872e-11	-0.506624240036119	0.214	0.277	4.78892948816107e-07
Emp3	7.06864935653254e-103	-0.502641133358538	0.594	0.802	1.59921123042192e-98
Pim1	1.2121781805085e-50	-0.495961206986507	0.094	0.28	2.74243191558244e-46
Vim	5.49278804927641e-38	-0.479567113618781	0.603	0.711	1.2426883682683e-33
Il7r	6.2430769630983e-62	-0.478621262321753	0.312	0.543	1.41243373213136e-57
Foxp3	3.00650995358619e-16	-0.462655860595183	0.04	0.11	6.80192811899341e-12
Itm2a	9.2996476194811e-68	0.462066109395144	0.414	0.218	2.1039522766321e-63
Rgcc	1.01147331979726e-61	0.461941889920933	0.53	0.333	2.28835723870931e-57
Ift80	5.51660648087842e-124	0.450821358392893	0.337	0.117	1.24807705023393e-119
Flna	6.28881573337238e-46	-0.405775741756606	0.247	0.433	1.42278167151817e-41
Itgb7	6.74588159683021e-70	-0.39612582479953	0.682	0.811	1.52618825246687e-65
Tcf7	1.65857296883268e-85	0.394652963772369	0.876	0.689	3.75235548468706e-81
Tubb4b	3.07061600255009e-50	-0.386470975184836	0.38	0.565	6.94696164416932e-46
Nsg2	1.79089017298336e-59	0.378273111650395	0.711	0.533	4.05170992735756e-55
Ramp1	5.10600537366893e-63	0.374553491320682	0.574	0.367	1.15518265573886e-58
Ccr7	1.87626197300728e-68	0.357468024319466	0.922	0.829	4.24485508773166e-64
Pdlim4	6.45139637911598e-39	-0.348772967488267	0.025	0.156	1.4595639168112e-34
Cd28	7.20987864877573e-66	0.345948070340387	0.718	0.508	1.63116294549902e-61
S100a11	3.28579146954821e-21	-0.344315029078891	0.362	0.461	7.43377462070587e-17
Evl	4.18157342760784e-67	0.340527436380893	0.805	0.634	9.46039172261998e-63
Cd82	5.83100156891111e-14	-0.339242185145214	0.405	0.477	1.31920579495045e-09
Izumo1r	2.47221037446022e-56	0.333310149491339	0.537	0.327	5.59312875117879e-52
Ephx1	7.35935007504784e-62	0.331550196176704	0.471	0.266	1.66497936097882e-57
Ier2	3.27334066102944e-37	-0.331295861016556	0.601	0.716	7.40560591151301e-33
Esyt1	4.17643178695968e-38	-0.329580494572232	0.218	0.383	9.44875927481758e-34
C1qbp	1.2774388110064e-41	-0.329075972043465	0.328	0.506	2.8900775660208e-37
Rasgrp2	1.48433783827861e-28	-0.324384352366896	0.3	0.44	3.35816592532152e-24
Pold4	1.17294574786177e-56	0.321466319566273	0.502	0.305	2.65367245996247e-52
Dusp1	5.42606727780345e-31	0.321030819278568	0.731	0.617	1.2275934609302 5e-26
Ikzf2	3.9104996329618e-08	-0.317827559570682	0.059	0.104	0.000884711436961278
Sesn3	1.15157967479853e-52	0.315019201720625	0.435	0.253	2.60533385626419e-48
Il6st	5.01285170001071e-53	0.313997453108704	0.343	0.177	1.13410756861042e-48
Bst2	1.12039197854683e-22	-0.312119465362005	0.286	0.413	2.53477481226434e-18
Srm	2.20419327100248e-35	-0.307858940523271	0.09	0.238	4.986766856316e-31
Klf2	5.52464215875523e-29	-0.305565846160289	0.208	0.356	1.24989504199678e-24
Prdx1	5.26251821643346e-40	-0.300869716074537	0.647	0.768	1.19059212128591e-35
Socs3	1.14448243081741e-22	-0.300769473800143	0.098	0.206	2.58927705148131e-18
H2-Oa	8.0495987299934e-118	0.300316296190947	0.22	0.059	1.82114121667371e-113
Cct6a	8.95621820287754e-34	-0.299979560223924	0.279	0.439	2.02625480621901e-29
Psme2	3.87111477567535e-45	-0.295989641493344	0.772	0.849	8.75801006848791e-41
Ldha	2.75361655357349e-62	-0.29398034613672	0.865	0.932	6.22978209080467e-58
Fam169b	4.31307458394865e-40	0.288027264178826	0.441	0.283	9.75789993872543e-36
Ccnd2	6.21633768830329e-29	-0.287262644497937	0.458	0.593	1.40638423860174e-24
Neurl3	3.76951626416924e-72	0.286068247436 61	0.22	0.079	8.52815359605649e-68
Zfp36l1	4.65938010603 15e-62	0.285865438854921	0.877	0.721	1.05413815518857e-57
Hspa8	2.63862061019521e-82	-0.282710628086177	0.991	0.996	5.96961526850564e-78
Fyb	9.04836702342897e-47	0.28165644658529	0.822	0.7	2.04710255538057e-42
Nme2	4.108294960907e-36	-0.281463755632349	0.438	0.592	9.294606519555 99e-32
Eif4a1	2.78378229645343e-46	-0.281041310964753	0.789	0.869	6.298029067496 24e-42
Adgre5	3.60203939471287e-22	-0.280935691265928	0.302	0.423	8.1492539265984e-18
Foxn3	2.94731829134695e-34	0.279862920116612	0.438	0.295	6.66801290234335e-30
Sdhaf1	5.16012042911088e-37	0.279402284988933	0.397	0.247	1.16742564588205e-32
Mat2a	6.23520328015119e-27	-0.279139817459459	0.322	0.46	1.4106523901014e-22
Chchd10	3.32908328233821e-40	0.278893981434098	0.346	0.196	7.53171801796197e-36
Smc6	3.13281818386274e-32	0.278782498606132	0.596	0.455	7.08768785917107e-28
Gstp3	8.28499510580687e-37	0.277858750123081	0.505	0.351	1.87439729273775e-32
Tmie	5.56772292359201e-48	0.277528430628499	0.228	0.102	1.25964163423346e-43
Myc	1.7106250141325e-16	-0.277406814052659	0.165	0.26	3.87011803197336e-12

Cluster 9 (IFN Response) Markers

	p_val	avg_logFC	pct.1	pct.2	p_val_adj
Isg15	0	2.18493410340272	0.835	0.157	0
Ifit1	0	1.98296418238263	0.771	0.056	0
Ifit3	0	1.63704991622164	0.521	0.018	0
Irf7	0	1.38833564892007	0.861	0.245	0
Usp18	0	1.30859471620218	0.607	0.095	0
Bst2	1.67995464512943e-276	1.24262033560496	0.785	0.396	3.80072938914081e-272
Rtp4	0	1.24008755904108	0.764	0.14	0
Cd74	2.28853495233311e-10	-1.23332191085279	0.068	0.134	5.17758147615844e-06
Ifi27l2a	0	1.20039136474275	0.968	0.714	0
Isg20	0	1.1309408990842	0.518	0.109	0
Zbp1	2.68090672957138e-299	1.07374246410145	0.704	0.266	6.06528338498229e-295
Slfn5	0	1.05363534858515	0.562	0.141	0
Ifi208	2.77926345270187e-260	0.965996950959436	0.773	0.355	6.28780563539271e-256
Slfn1	1.42143808398713e-271	0.960100417556946	0.902	0.556	3.21586152121248e-267
Xaf1	0	0.909256817081649	0.601	0.142	0
Phf11b	4.16714614320646e-204	0.864725576486615	0.593	0.235	9.42775143439029e-200
Ly6a	3.88111164618671e-135	0.860901900431067	0.784	0.529	8.7806269883328e-131
Lgals3bp	0	0.854046846689444	0.582	0.159	0
Ifi209	3.30860443037537e-197	0.852179716860018	0.729	0.364	7.48538666328123e-193
Daxx	9.88078923786587e-189	0.840423258336832	0.64	0.287	2.23542975717477e-184
Ifit3b	0	0.827284502414374	0.269	0.005	0
Stat1	2.65491062200546e-189	0.812217086264237	0.914	0.636	6.00646979122516e-185
Ifi213	9.91387689295618e-227	0.763983857720851	0.534	0.171	2.24291550826241e-222
Ifi203	2.42443861453514e-172	0.760628900558747	0.775	0.451	5.4850499215243e-168
Cmpk2	0	0.75766927029912	0.311	0.022	0
Igtp	7.26108441536222e-165	0.741102014025676	0.682	0.331	1.64274773813155e-160
Ifi47	1.5213257236238e-155	0.726618709704892	0.898	0.694	3.44184731712648e-151
Phf11c	0	0.720799346711342	0.416	0.074	0
Oasl2	0	0.706922628892999	0.334	0.028	0
Parp9	1.03516610044392e-191	0.702685515916605	0.501	0.169	2.34195978564432e-187
Trim30a	3.57949055172826e-193	0.702342580554938	0.467	0.149	8.09823942423001e-189
Qbp7	7.83382077708405e-121	0.679744138197766	0.497	0.217	1.77232361260749e-116
Rnf213	1.50137081879753e-165	0.674186881048551	0.428	0.139	3.39670134044753e-161
Ifi214	4.41237246804112e-213	0.669749010797292	0.401	0.103	9.98255147169623e-209
Ifi35	3.02097703493249e-137	0.669287870000634	0.628	0.326	6.83465844383126e-133
Epsti1	5.96060152098005e-109	0.645272395092034	0.64	0.372	1.34852648810653e-104
Pml	2.08783520088768e-227	0.636117268319109	0.436	0.114	4.72351835848829e-223
Lgals9	5.46527317462575e-124	0.629964451507689	0.833	0.642	1.23646340302733e-119
Slfn8	2.79632858812073e-174	0.620996407287834	0.457	0.149	6.32641379776434e-170
Ifi206	8.24909880823993e-220	0.602805503711981	0.385	0.093	1.8662761143762e-215
Mndal	2.90398046822543e-101	0.592170333803261	0.611	0.349	6.56996541131322e-97
Rsad2	0	0.589719173988189	0.188	0.002	0
Ifit1bl1	8.75157856871058e-151	0.588591820153275	0.357	0.106	1.97995713538508e-146
Dhx58	0	0.575796236501772	0.283	0.033	0
Parp14	3.78736541268062e-139	0.574746822716703	0.433	0.154	8.56853550964863e-135
Tgtp2	5.49391325695086e-110	0.564889385412663	0.515	0.236	1.24294293525256e-105
Ifih1	3.71005710690051e-205	0.561646092484611	0.274	0.052	8.39363319865172e-201
H2-T22	4.61619727505519e-128	0.553047192446199	0.946	0.828	1.04436847150849e-123
Ifi44	0	0.551250243471497	0.197	0.011	0
Sp100	2.69943149946219e-132	0.550936168979808	0.937	0.775	6.10719382438325e-128
Ddx58	5.47223407249103e-108	0.54488627034261 7	0.483	0.217	1.23803823656037e-103
Gbp2	2.88316266353474e-55	0.54049437876195	0.394	0.211	6.522867209981e-51
Irgm1	4.98046775000399e-121	0.537930883336948	0.434	0.167	1.1267810237609e-116
Tnfrsf4	3.14156578221121e-09	-0.532787901785609	0.085	0.147	7.10747842567463e-05
Gbp9	6.59114355227293e-99	0.524621924385155	0.379	0.15	1.49118031726623e-94
Rnf114	1.27255005323301e-92	0.503679143882012	0.729	0.496	2.87901724043437e-88
Oasl1	0	0.499662520992597	0.223	0.016	0
Dtx3l	1.09238918130373e-102	0.499113060043311	0.401	0.161	2.47142128378156e-98
Ms4a4b	1.81083983376925e-121	0.480038753209303	0.989	0.945	4.09684403991955e-117
Eif2ak2	1.47325171725575e-175	0.477755801258532	0.25	0.049	3.3330846851194e-171
Samhd1	1.42553572691398e-46	0.470364780799301	0.711	0.551	3.22513202857019e-42
Gbp4	1.41487399796845e-71	0.46022181813376	0.445	0.226	3.20101093300383e-67
Slfn2	1.61297272724791e-101	0.45726063152548	0.936	0.796	3.64918949812566e-97
Ifit2	1.11504838483974e-105	0.450600964096641	0.276	0.084	2.52268546586142e-101
Irf9	5.76481195033932e-81	0.447754506660514	0.474	0.232	1.30423105564477e-76
Trafd1	8.70816202616731e-73	0.443594457006259	0.271	0.103	1.97013457680009e-68
Ly6c1	9.56917303642669e-14	0.435946651202291	0.406	0.314	2.16492970776117e-09
Iigp1	2.62769543331448e-76	0.435679295320652	0.209	0.064	5.94489814833068e-72
Trim12c	4.77733656725174e-71	0.431892448226807	0.368	0.167	1.08082462497503e-66

Cluster 10 Markers

	p_val	avg_logFC	pct.1	pct.2	p_val_adj
Smc4	3.51298860503228e-29	0.384244619783428	0.723	0.515	7.94778542002503e-25
Trbv12-2	1.72323453071011e-09	0.311162468456982	0.149	0.087	3.89864580227855e-05
Trbv13-2	3.96626622694991e-17	0.298294051379093	0.407	0.263	8.97328071185148e-13

Cluster 11 (Naive) Markers

	p_val	avg_logFC	pct.1	pct.2	p_val_adj
Cd74	1.66413104620888e-10	-1.47585225227903	0.024	0.134	3.76493007894298e-06
Selenop	6.36352234495201e-87	0.876224012846482	0.885	0.527	1.43968329532194e-82
Cd52	1.53400618511228e-128	-0.802141272088281	0.963	0.996	3.47053559319802e-124
Crlf3	2.75137055088189e-74	0.738244870791149	0.861	0.596	6.22470073431518e-70
Capg	4.29082291630084e-15	-0.727059460015019	0.102	0.277	9.70755776583902e-11
Il7r	2.17133911472754e-59	0.717111140307642	0.822	0.531	4.91243761315959e-55
Izumo1r	3.40060863984422e-16	-0.712068569747092	0.144	0.337	7.69353698678356e-12
Rgs1	5.33804691450367e-15	-0.708040242324942	0.079	0.252	1.20767973393731e-10
Cd82	4.6119828982352e-25	-0.672982392730068	0.213	0.477	1.04341501089673e-20
Lcp1	6.70935357726658e-59	-0.668995932020699	0.596	0.876	1.51792415332079e-54
Id3	1.65118947761754e-16	-0.66805591884072	0.113	0.298	3.73565107416193e-12
Ptpn6	5.27489808395707e-35	-0.666049529067777	0.262	0.568	1.19339294251445e-30
Tnfrsf4	8.65977513823193e-10	-0.659508862544585	0.037	0.146	1.95918752727359e-05
Il2rb	3.3231053042118e-15	-0.642242686103768	0.034	0.193	7.51819344024879e-11
Foxp3	6.3823549306112e-10	-0.596394122888799	0.01	0.109	1.44394397950148e-05
Tcp11l2	8.06048830266979e-42	0.592016281558775	0.609	0.339	1.82360487359601e-37
Adgre5	1.84300383713679e-39	0.587663073508662	0.672	0.416	4.16961188113828e-35
Lgals1	2.5324889150521e-11	-0.571836356402014	0.199	0.36	5.72950292141388e-07
Pfn1	1.16422400218909e-126	-0.568622971512619	1	1	2.63394038255261e-122
Ifngr1	3.06349282638362e-49	0.554066791269837	0.688	0.371	6.93084617041031e-45
Sell	3.34308426646605e-52	0.53342886922965	0.913	0.606	7.5633938444528e-48
Klhl6	2.06794859997358e-41	0.527182096154569	0.627	0.354	4.67852691258023e-37
Actb	2.36369212967542e-126	-0.526998056826976	1	1	5.34761707417767e-122
Klf3	2.52193597572317e-44	0.526278968734151	0.378	0.139	5.7056279514761e-40
Cd55	4.39487030422467e-44	0.504713491672528	0.367	0.133	9.9429545762779e-40
Atp6v1d	2.0627045614656e-33	0.503506161655671	0.682	0.451	4.66666279985978e-29
Ctla4	8.26739215551225e-10	-0.494914581167388	0.034	0.144	1.87041480126309e-05
Ptprcap	2.72299542890571e-45	-0.487247711343664	0.766	0.933	6.16050485835629e-41
Tcf7	8.85631261333569e-36	0.473348129260149	0.9	0.694	2.00365216564107e-31
Vasp	1.13234541888636e-26	-0.466752685798095	0.407	0.665	2.56181827568851e-22
Stat1	2.26971052841221e-12	-0.465774095280349	0.496	0.645	5.13499309947978e-08
Cnn2	1.6345757913812e-48	-0.464676664945175	0.895	0.968	3.69806427042082e-44
Cd5	9.11090594380051e-18	-0.464520835870451	0.483	0.665	2.06125136072543e-13
Thada	2.76295471115122e-28	0.460996111141232	0.459	0.241	6.25090873850851e-24
Vim	4.30668498061088e-12	-0.452214712397232	0.559	0.708	9.74344410013405e-08
Tagln2	1.88467288840845e-30	0.451436499154076	0.879	0.735	4.26388394273527e-26
Ccnd2	1.07935661117131e-20	-0.449374949029324	0.354	0.591	2.44193639711397e-16
Lck	2.78136968015338e-49	-0.448039672089781	0.874	0.97	6.29257076437901e-45
Wdr1	1.00181884200452e-29	-0.447337645059118	0.483	0.744	2.26651494815103e-25
Cotl1	3.37474187605234e-26	-0.440577709175063	0.583	0.77	7.63501602038082e-22
Actr3	3.70852343889535e-39	-0.437707446988404	0.774	0.928	8.39016342815683e-35
Cyba	1.3527537100524e-26	-0.428831409855216	0.717	0.87	3.06046999362254e-22
Hsd11b1	1.6775766697653e-18	-0.422512644553318	0.152	0.371	3.79534945767701e-14
Stmn1	6.73865883898765e-35	0.41679342636021	0.373	0.152	1.52455417573257e-30
Anxa6	1.83121143240614e-18	-0.413994381201936	0.36	0.586	4.14293274467564e-14
Cd6	7.13518700463274e-16	-0.413425792133818	0.399	0.593	1.61426470792811e-11
Ddit4	2.24035117761347e-11	-0.408264913106508	0.181	0.335	9.59337050423271e-07
Myo6	1.026957155056 51e-92	0.398708499997714	0.139	0.013	2.32338786759986e-88
Tubb2a	1.14961501241061e-18	0.397890403850396	0.22	0.094	2.60088900407776e-14
Lgals9	9.33006131829477e-21	-0.39543513619987	0.417	0.65	2.11083307265101e-16
Phgdh	9.75269978483862e-15	-0.394139711844109	0.131	0.317	2.20645079932189e-10
Cmah	4.53518841576293e-24	0.393189742628354	0.412	0.214	1.02604102718221e-19
Tnfrsf18	4.69778617983537e-09	-0.388055472887437	0.226	0.36	0.000106282714532595
Csk	9.69291846348923e-19	-0.386757442987766	0.383	0.611	2.1929258731798e-14
Atp1b3	2.07437196418041e-28	0.38669644631235	0.924	0.798	4.69305913176176e-24
Slamf6	1.35072939002386e-25	0.382429357646829	0.475	0.25	3.05589017198999e-21
Ms4a4b	2.91826173410421e-40	0.381374997839917	0.997	0.946	6.60227534723736e-36
Actn1	9.13988861570004e-23	0.380385554120811	0.709	0.522	2.06780840041598e-18
Itgb2	1.28637240180695e-17	-0.378255296718157	0.417	0.622	2.91028892184805e-13
Ms4a6b	1.99796001412258e-32	0.377428724512779	0.958	0.843	4.52018473595093e-28
Sept9	4.39902779167389e-17	-0.376907401136682	0.402	0.598	9.952360475883e-13
Pim1	7.61327130700689e-25	0.37453689869038	0.493	0.271	1.72242650049724e-20
Itga4	5.60670183138518e-26	0.373977412337985	0.462	0.239	1.26846022233258e-21
Rflnb	9.26428221010244e-19	0.372019013549729	0.493	0.308	2.09595120721358e-14
Ccr7	1.29452851600619e-16	0.370711600516595	0.898	0.831	2.92874131461241e-12
Kif1b	5.71685531640964e-25	0.365564573756553	0.312	0.137	1.29338134678452e-20
Tnfaip8	6.00904254748848e-15	-0.363227787190466	0.102	0.286	1.35948578594379e-10
Ighm	7.80442836215577e-13	-0.361130985729172	0.543	0.688	1.76567387265412e-08
F2rl1	1.23506335654335e-21	0.35994400015675	0.294	0.134	2.79420733784369e-17

Cluster 12 (B Cell) Markers

	p_val	avg_logFC	pct.1	pct.2	p_val_adj
Cd74	0	4.97124343053672	1	0.125	0
H2-Aa	0	4.15908824512217	1	0.007	0
H2-Eb1	0	3.87296409542576	1	0.008	0
Cd79a	0	3.72705916012356	1	0.004	0
H2-Ab1	0	3.57799334954162	1	0.004	0
Ly6d	0	3.22993541482461	0.982	0.005	0
Cd79b	0	3.05318044257865	1	0.019	0
Iglc2	0	2.74405542594872	0.975	0	0
H2-DMb2	0	2.6483974902532	0.982	0.005	0
Iglc3	0	2.56422410208571	0.938	0.001	0
Fcmr	0	2.47340077138972	0.913	0.001	0
Ms4a1	0	2.39244180326594	0.956	0	0
Igkc	0	2.38242838347628	0.84	0.005	0
Iglv1	0	2.21320763668439	0.149	0	0
Ebf1	0	2.16015527726108	0.905	0	0
Napsa	0	2.03801386688929	0.88	0.005	0
Fcer2a	0	1.98227138427903	0.745	0	0
Unc93b1	0	1.97957039900849	0.891	0.042	0
Mef2c	0	1.88748826218786	0.833	0.001	0
H2-Ob	0	1.84402302664207	0.909	0.107	0
Bank1	0	1.83621218952368	0.815	0.011	0
H2-Oa	0	1.77537424435483	0.855	0.058	0
Tnfrsf13c	0	1.76120853787244	0.782	0.003	0
Ms4a4b	9.48611798644232e-134	-1.74093038010415	0.196	0.952	2.14613933325271e-129
Cd3e	5.91213162965141e-149	-1.71898253553403	0.222	0.992	1.33756065989234e-144
Cd19	0	1.71078339035625	0.804	0	0
Cd3d	5.44400509462939e-144	-1.67722212889718	0.207	0.983	1.23165171260895e-139
Cd3g	1.13414368436301e-139	-1.66919379040616	0.204	0.981	2.56588667150287e-135
Ly86	0	1.65850108965914	0.789	0.002	0
Irf8	0	1.65605323760484	0.775	0.028	0
Thy1	4.39631700566811e-106	-1.62710362115409	0.175	0.857	9.94622759362353e-102
Lat	8.65464323326871e-136	-1.60112226738056	0.204	0.967	1.95802648509471e-131
Blnk	0	1.58113664645876	0.735	0.001	0
Ctsh	0	1.5543537008242	0.764	0.004	0
Cd24a	0	1.5356985707215	0.618	0.004	0
H2-DMa	1.62731943069797e-232	1.52185717076194	0.916	0.229	3.68164748001109e-228
Serpinb1a	0	1.51158958130159	0.662	0.003	0
Igfbp4	1.39351557506422e-53	-1.50853660400872	0.091	0.603	3.1526896370253e-49
Lyn	0	1.49188299196913	0.731	0.005	0
Lef1	2.38178867756482e-100	-1.47536180366338	0.131	0.83	5.38855870412264e-96
Siglecg	0	1.45017143478085	0.655	0	0
Lck	6.37580524343663e-132	-1.44417675626916	0.302	0.974	1.4424621782751e-127
Hvcn1	8.60640381651633e-151	1.43543860156836	0.833	0.272	1.94711279944865e-146
Swap70	0	1.42911790448085	0.716	0.033	0
Ighd	0	1.42594004213458	0.669	0.004	0
Cd72	2.16798431602152e-239	1.42088979214628	0.695	0.11	4.9048477165671e-235
Skap1	1.09409566479742e-114	-1.41099908202927	0.164	0.89	2.47528203203768e-110
Blk	0	1.40548064693291	0.644	0.001	0
Cd247	2.14000848066123e-106	-1.38407823576412	0.145	0.852	4.84155518664798e-102
Serp1	1.19703876201964e-153	1.36762635457128	0.935	0.4	2.70818049519324e-149
Apoe	0	1.36046762714508	0.367	0.008	0
Cd83	0	1.33742372837462	0.604	0.042	0
Cd37	3.71586287571719e-146	1.29689730902982	0.989	0.773	8.40676817002257e-142
Tcf7	1.28404483186549e-75	-1.29547891867037	0.102	0.701	2.90502302761248e-71
Pkig	0	1.28967256601915	0.629	0.005	0
Saraf	6.82318659869968e-92	-1.26031309226277	0.175	0.807	1.54367773608982e-87
Ms4a6b	1.47537677458386e-90	-1.24262406627196	0.222	0.849	3.33789241481853e-86
Fcrla	0	1.20176909704629	0.589	0	0
Plac8	0	1.1993446208635	0.433	0.004	0
Ralgps2	4.60224933832951e-192	1.18461052194674	0.72	0.141	1.04121289030367e-187
Spib	0	1.1573684139344	0.52	0	0
Fyb	2.27887613443217e-74	-1.15461422056111	0.135	0.709	5.15572936653934e-70
Aldh2	4.07596072605214e-270	1.14806630142014	0.611	0.071	9.22145354662035e-266
Snn	0	1.14724934312696	0.582	0.028	0
Syk	0	1.13722814357909	0.531	0.001	0
Fxyd5	5.58864388539782e-119	-1.13622744307653	0.633	0.985	1.2643747926324e-114
Bcl11a	0	1.13271000883103	0.531	0.001	0
Vpreb3	0	1.12611188948534	0.465	0	0
Rgs10	5.52572862845532e-70	-1.12356909374212	0.156	0.713	1.25014084490173e-65

Cluster 13 (CD8) Markers

	p_val	avg_logFC	pct.1	pct.2	p_val_adj
Cd8b1	0	2.57953019337529	0.932	0.094	0
Cd8a	0	2.13331107130408	0.889	0.003	0
Nkg7	0	2.01850883819425	0.94	0.028	0
Ly6c2	0	1.71795410425291	0.376	0.008	0
Ccl5	4.81436358981236e-57	1.51752071292819	0.184	0.023	1.08920161855915e-52
Ctsw	2.56494260177304e-108	1.10933147910536	0.812	0.247	5.80292614225132e-104
Cd4	3.63042514379018e-53	-1.08675656382162	0.051	0.593	8.2134738453109e-49
Klrd1	0	1.07057916258504	0.632	0.052	0
Ly6c1	7.7371627660292e-23	-0.973363554430434	0.013	0.319	1.75045570418645e-18
Izumo1r	1.96772104437261e-14	-0.8842348323701	0.107	0.336	4.45177209078858e-10
Cd40lg	2.73129897765547e-30	-0.855571096809105	0.056	0.43	6.17929080704774e-26
Tspan32	2.90539334274388e-36	-0.795649913040802	0.291	0.673	6.57316189862375e-32
Epsti1	4.93736492389021e-50	0.787494869636583	0.778	0.377	1.11702944038092e-45
Dnajc15	5.26191660589939e-63	0.755255352605193	0.778	0.32	1.19045601291868e-58
Cxcr6	0	0.728789847320049	0.402	0.019	0
Cd5	1.30782843632097e-21	-0.723058172131574	0.462	0.664	2.95883105433255e-17
Igfbp4	1.42647254585058e-08	-0.694522634894815	0.521	0.599	0.000322725148773235
Plac8	0	0.685028689703923	0.308	0.005	0
Cd7	8.28038603787637e-60	0.661157865944343	0.466	0.117	1.87335453720915e-55
Dusp1	2.51506310865565e-10	-0.612320356963273	0.483	0.622	5.69007877702254e-06
Ass1	2.84795478000733e-21	-0.60255896834899	0.397	0.658	6.44321289428858e-17
Ly6a	1.03403334993946e-13	-0.586656319965581	0.329	0.538	2.33939705090304e-09
Trbv12-1	5.03674451902639e-15	0.586027966524323	0.12	0.031	1.13951307998453e-10
Cd28	1.10864029417141e-18	-0.567620740506073	0.269	0.518	2.5081878015334e-14
Cst7	6.90245696832614e-71	0.565626736521923	0.53	0.128	1.56161186451411e-66
Dapl1	3.53108163986697e-21	0.561344790709088	0.504	0.247	7.98871910203503e-17
Zbtb7b	1.67650732958909e-17	-0.519976755584746	0.021	0.271	3.79293018246235e-13
Ifi27l2a	5.1837094846428e-11	-0.519439316627716	0.598	0.723	1.17276243380559e-06
Klk8	1.45518199939548e-27	0.516696674368576	0.705	0.391	3.29220375543234e-23
Junb	1.85708429419917e-25	-0.515270184412167	0.94	0.975	4.20146750719621e-21
Ccr9	3.51973086252739e-255	0.504053840932802	0.239	0.009	7.96303910338196e-251
Cd81	4.9813108103828e-11	-0.501702787160885	0.009	0.171	1.12697175774101e-06
Tesc	2.71101494758234e-14	-0.493806141622312	0.115	0.336	6.13340021741028e-10
Rcn3	6.22426605667245e-92	0.482847738551041	0.286	0.035	1.40817795266158e-87
Selenop	2.1839785250947e-10	-0.482551373211312	0.38	0.532	4.94103301517425e-06
Ms4a4c	1.50381122643712e-40	0.464224934621379	0.346	0.091	3.40222251869134e-36
Glipr2	1.27131536131181e-32	0.458785797990136	0.547	0.216	2.87622387343183e-28
Tmem108	5.39179161410518e-43	0.429992567039832	0.372	0.097	1.21983893477516e-38
Wls	2.99043715974888e-27	0.413126268473996	0.44	0.167	6.76556503021586e-23
Jun	5.48153986115889e-11	-0.406418793204755	0.637	0.769	1.24014357818859e-06
Zfp36l1	8.87530793468131e-09	-0.406111673506665	0.624	0.727	0.00020079496671423
Lcn4	9.7482649788339e-203	0.400496348351877	0.205	0.009	2.20544746881138e-198
Rgcc	3.52810978264859e-15	0.399198988755242	0.585	0.339	7.98199557226418e-11
Cd226	3.66988454027994e-36	0.398850650137996	0.333	0.091	8.30274678392934e-32
Slc25a4	2.68886023843461e-21	0.397282835428269	0.641	0.324	6.08327740343446e-17
Cytip	9.96830585197289e-16	-0.394885513582259	0.774	0.865	2.25522951595035e-11
Atp1b1	3.7673724544517e-09	-0.391763482392306	0.171	0.337	8.52330344095152e-05
Ecm1	2.05764776445041e-09	-0.390056356122246	0.026	0.174	4.65522230229261e-05
Pdlim4	3.46017970479203e-10	-0.388002847172927	0.004	0.152	7.82831056412149e-06
Zyx	3.83735418983013e-13	0.37335516925037	0.645	0.404	8.6816301907168e-09
Cyb5a	3.61322452473618e-11	-0.372994489420591	0.491	0.611	8.17455916476313e-07
Ppp1r15a	3.87573399422831e-10	-0.365044980893209	0.671	0.747	8.76846058854213e-06
H3f3b	6.03449122818946e-24	-0.353365558992648	0.983	0.991	1.36524329546558e-19
Trat1	1.60507744702409e-08	-0.352184439453063	0.103	0.259	0.000363132721614731
Racgap1	2.66803774302983e-113	0.345541673774966	0.218	0.017	6.03616858983068e-109
Jaml	9.83771055003633e-79	0.335628669105505	0.231	0.026	2.22568363484022e-74
Gimap6	5.57936256770277e-11	-0.334994043068576	0.816	0.871	1.26227498731708e-06
Cd160	6.30455813567164e-85	0.317649695336491	0.167	0.013	1.42634323261435e-80
Itgae	3.13045179161861e-87	0.315380281762963	0.261	0.03	7.08233413335795e-83
Tpst2	1.07311383878251e-13	0.313899238570866	0.688	0.431	2.42781274886156e-09
Acp5	3.42225260787818e-13	0.310183166672815	0.765	0.515	7.7425043000636e-09
Pkm	8.58011396939393e-14	-0.309990170248385	0.868	0.89	1.94116498443568e-09
Ddx5	4.64163401515331e-18	-0.301848426078306	0.987	0.995	1.05012327958828e-13
Cd247	4.75775697454137e-10	-0.300762840761003	0.812	0.846	1.07639493792024e-05
AB124611	7.05954961647192e-14	0.300471320127887	0.474	0.246	1.59715250523061e-09
Fth1	8.79507900725742e-26	-0.297489623751579	0.996	0.999	1.98979867460192e-21
Fkbp1a	5.23876249717738e-10	-0.296532347357102	0.679	0.754	1.18521762736141e-05
Tagln2	1.0806019904953e-12	0.295664551281862	0.919	0.735	2.44475394329656e-08
Sidt1	2.96135154034621e-12	0.295549937572838	0.329	0.158	6.69976172487928e-08

Cluster 14 (APC) Markers

	p_val	avg_logFC	pct.1	pct.2	p_val_adj
Lyz2	0	3.49248321215359	0.671	0.004	0
Tyrobp	0	2.41406523583969	0.735	0.003	0
Apoe	0	2.35456286167661	0.624	0.008	0
Cd74	1.30205157702909e-126	2.35409060394745	0.724	0.129	2.9457614878706e-122
H2-Aa	0	2.32863982577023	0.524	0.012	0
Lyz1	0	2.09498660943422	0.265	0.001	0
H2-Eb1	0	2.07753624269958	0.459	0.014	0
H2-Ab1	0	1.88653511436576	0.371	0.01	0
Fcer1g	0	1.80001480794682	0.582	0.002	0
Cst3	1.26235826398201e-31	1.62764706011415	0.665	0.319	2.85595933643289e-27
Irf8	4.79950107412383e-146	1.61290992337472	0.388	0.032	1.08583912300978e-141
Cd209b	0	1.41338352165774	0.324	0.002	0
S100a6	1.1204562640309e-143	1.35995004210505	0.618	0.079	2.53492025174352e-139
Siglech	0	1.35848336049193	0.176	0	0
Ctsb	2.77847559548612e-26	1.35050623216961	0.729	0.463	6.2860231872278e-22
Psap	8.00170531560198e-12	1.28687453372746	0.824	0.748	1.81030581060179e-07
Grn	8.64528016561669e-58	1.2845886537977	0.347	0.059	1.95590818466912e-53
Gpx1	5.08862413153413e-34	1.27289025127827	0.935	0.796	1.15125032351828e-29
Fth1	1.63239868004594e-67	1.26919915440261	1	0.999	3.69313877373594e-63
Lgals3	0	1.23241730137238	0.553	0.013	0
Bst2	5.0613524670332e-10	1.23196483678755	0.588	0.407	1.14508038214159e-05
Ftl1	5.10450481776652e-86	1.23011895660544	1	0.983	1.1548431699715e-81
Ccl8	0	1.18844654380762	0.271	0.001	0
C1qa	0	1.1826991453358	0.371	0.001	0
Ctsh	0	1.15544484911831	0.335	0.009	0
C1qb	0	1.15171340495196	0.341	0.001	0
Timd4	0	1.1203364274416	0.353	0.001	0
Pltp	7.32908772731849e-266	1.10273732063716	0.171	0.003	1.65813280742853e-261
C1qc	0	1.07842214933786	0.359	0.001	0
Ctsl	6.97366486327861e-17	1.07426628397234	0.182	0.048	1.57772193866815e-12
Pld4	4.22767848881364e-277	1.05604576270138	0.182	0.003	9.56469981309197e-273
Ly6c2	8.98651054653798e-36	1.0540078325131	0.106	0.01	2.03310814604875e-31
Aif1	0	1.05118815292277	0.471	0.002	0
Fabp5	7.90625585424266e-62	1.04264479037773	0.306	0.044	1.78871132446386e-57
Plac8	3.48996135486997e-62	1.03844779262744	0.112	0.006	7.89568856925783e-58
Cd63	0	1.01393289998106	0.271	0.001	0
Spi1	0	1.01039804440786	0.465	0.005	0
Cfp	0	0.989715246958547	0.306	0.004	0
Alox5ap	2.9975228817193e-160	0.968443746525075	0.206	0.008	6.78159576760174e-156
Unc93b1	3.56496888832056e-78	0.964970256219186	0.353	0.047	8.06538561293644e-74
Igfbp4	2.09371519916898e-16	-0.962123771165913	0.306	0.6	4.73682126659989e-12
Tmem176b	6.72156203298207e-149	0.947471266416743	0.341	0.024	1.52068619434186e-144
Lgals1	1.13992015279531e-23	0.946949944504937	0.647	0.357	2.57895535368412e-19
EGFP	1.58305743607329e-08	0.944167168050657	0.182	0.072	0.00035815094337222
Ctsz	1.11324489351178e-35	0.930745653379077	0.524	0.185	2.51860524708104e-31
Mt1	0	0.913634913380808	0.276	0.003	0
Marcksl1	2.24086055390982e-57	0.913191664950659	0.347	0.058	5.06972291716558e-53
Nr1h3	0	0.912320639941594	0.282	0.003	0
Cd68	0	0.908771485779179	0.365	0.008	0
Pla2g2d	0	0.832122059727227	0.294	0	0
Msrb1	2.6146477426301e-21	0.802519575382566	0.441	0.177	5.91537905292634e-17
Gngt2	1.10265456802865e-51	0.800089200081592	0.512	0.131	2.49464569470802e-47
Tmem176a	9.55276162234677e-101	0.792546882273141	0.229	0.016	2.16121678943973e-96
Fscn1	0	0.786344363214862	0.165	0.002	0
Ehd1	5.00481248534905e-32	0.783697722293948	0.288	0.066	1.13228877668537e-27
Selenop	4.9492370276882e-10	0.774484318525585	0.676	0.53	1.11971538514418e-05
Hmox1	3.17788422912192e-270	0.750863570126207	0.265	0.008	7.18964527996542e-266
Prg3	0	0.749361872790441	0.188	0	0
Dhrs1	3.42402543972019e-38	0.739846237478568	0.341	0.079	7.74651515482296e-34
Litaf	1.82989368569352e-115	0.732063016665463	0.347	0.032	4.13995147451303e-111
Il18	0	0.729357627374572	0.259	0.003	0
Vim	1.07949821352957e-16	0.728694221345372	0.859	0.706	2.4422567582893e-12
Lef1	8.0713415242892e-29	-0.727627749395465	0.447	0.826	1.82606030645519e-24
Syngr2	6.86647050048911e-13	0.725573765970035	0.494	0.271	1.55347028603066e-08
Il4i1	7.31077708606228e-276	0.724074383798498	0.176	0.003	1.65399020795073e-271
Marco	0	0.714685437300811	0.212	0.001	0
Cd209d	0	0.703491002794696	0.182	0	0
Ly86	1.7107767269415 2e-209	0.70225133476226	0.218	0.007	3.87046126703249e-205
Plbd1	0	0.699652062995391	0.229	0.001	0

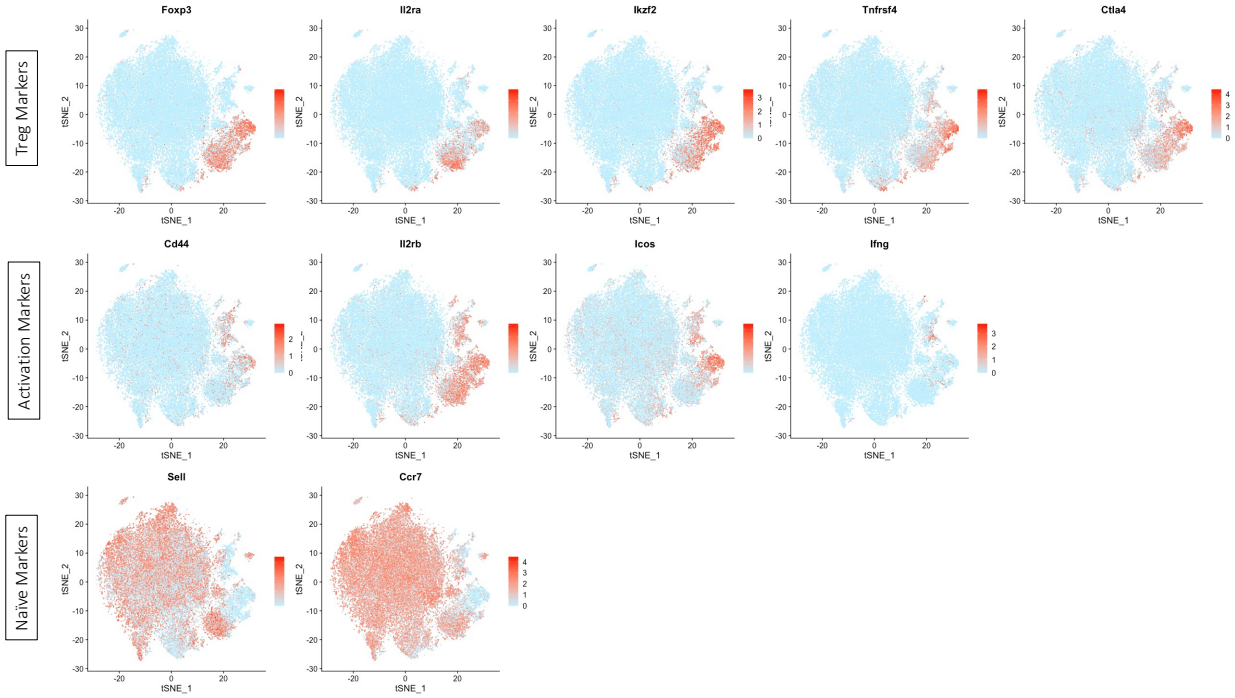
Treg Markers
Foxp3
Il2ra
Ikzf2
Tnfrsf4
Ctla4
Activation Markers
Cd44
Il2rb
Icos
Ifng
Naïve Markers
Sell
Ccr7
tSNE_1
tSNE_2

Appendix C – List of Genes that Were Enriched in Pathway Analysis of PHD2 KD Tregs

Genes in the IL-2-STAT5 Hallmark signalling pathway enriched in PHD2 Tregs vs. other Foxp3^{+} Tregs

	Entrez	Symbol
1	16178	Il1r2
2	22163	Tnfrsf4
3	54167	Icos
4	18619	Penk
5	12477	Ctla4
6	12773	Ccr4
7	12520	Cd81
8	16407	Itgae
9	53314	Batf
10	21942	Tnfrsf9
11	12977	Csf1
12	21936	Tnfrsf18
13	12522	Cd83
14	12332	Capg
15	19883	Rora
16	21938	Tnfrsf1b
17	13011	Cst7
18	22779	Ikzf2
19	17873	Gadd45b
20	12367	Casp3
21	12505	Cd44
22	18186	Nrp1
23	20893	Bhlhe40
24	20947	Swap70

Genes in the apical surface Hallmark signalling pathway enriched in PHD2 Tregs vs. other Active Tregs

	Entrez
Hspb1	15507
Gstm5	14866

Genes in the UV response Hallmark signalling pathway negatively enriched in PHD2 Tregs vs. other Active Tregs

	Entrez
Junb	16477
H2-Q4	15015
H2-Q7	15018
Dnaja1	15502

HALLMARK_APICAL_SURFACE

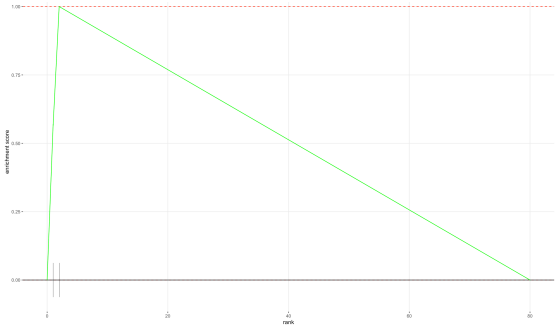

HALLMARK_UV_RESPONSE_UP